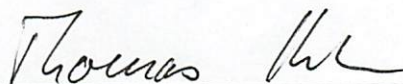


SYNTHESIS OF SPHINGOSINE ANALOGUES BY DIASTEREOSPECIFIC
AMINATION OF ENANTIOPURE TRANS-GAMMA, DELTA-UNSATURATED-
BETA-HYDROXYESTERS

By

Zhipeng Dai

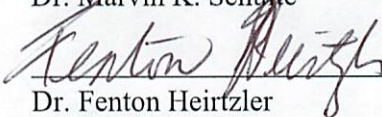
RECOMMENDED:



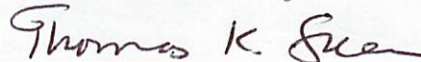
Dr. Thomas B. Kuhn



Dr. Marvin K. Schulte



Dr. Fenton Heirtzler

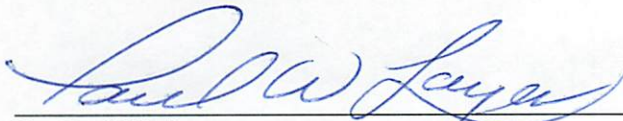


Dr. Thomas K. Green, Advisory Committee Chair

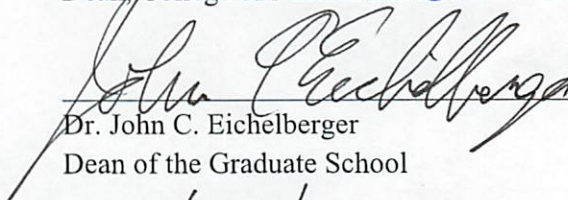


Dr. William R. Simpson
Chair, Department of Chemistry and Biochemistry

APPROVED:



Dr. Paul W. Layer
Dean, College of Natural Science and Mathematics



Dr. John C. Eichelberger
Dean of the Graduate School

11/28/13

Date

SYNTHESIS OF SPHINGOSINE ANALOGUES BY DIASTEREOSPECIFIC
AMINATION OF ENANTIOPURE TRANS-GAMMA, DELTA-UNSATURATED-
BETA-HYDROXYESTERS

A
DISSERTATION

Presented to the Faculty
of the University of Alaska Fairbanks

in Partial Fulfillment of the Requirements
for the degree of

DOCTOR OF PHILOSOPHY

By

Zhipeng Dai, B.S.

Fairbanks, Alaska

December 2013

Abstract

Sphingolipids play critical roles in signal transduction, intercellular membrane trafficking and cell growth. As bioactive sphingolipids, ceramide and sphingosine have been implicated in activating anti-proliferative and apoptotic responses in various cancer cells. Conversely, metabolic conversion of ceramide into sphingosine 1-phosphate, ceramide 1-phosphate and glucosylceramide regulates cell proliferation and suppresses programmed cell death. Many anticancer drugs and stress-induced agonists have been developed to increase endogenous ceramide levels. Sphingosine/ceramide analogues reportedly enhance antitumor activity and have been proposed as a potential new class of chemotherapeutic agents. Among these, sphingosines with aromatic substituents in the side chain often exhibit stronger biological activity compared to natural sphingosines. While a large number of synthetic pathways to sphingosine analogues have been described in the literature, very few pathways provide analogues with high stereospecificity. This dissertation describes a novel synthetic pathway to aromatic sphingosines which is highly stereospecific, provides good yields, uses commonly available reagents, and is versatile in terms of its potential to provide a large family of sphingosine analogues for future research.

The entry into the synthetic pathway toward sphingosine analogues involves first the enantiospecific synthesis of *trans*- γ , δ -unsaturated β -hydroxyesters using biocatalytic reduction of *trans*- γ , δ -unsaturated- β -ketoesters with commercially available ketoreductases. With the advantages of compatibility with carbon-carbon double bonds,

high enantioselectivity, broader substrate acceptance, mild environmentally-friendly reaction conditions and easy separation, the biocatalytic reduction was found to be superior compared to other more traditional chemical methods. Indeed, both (*R*) and (*S*)-enantiomers of *trans*- γ , δ -unsaturated β -hydroxyesters are synthesized by one or more ketoreductases in excellent stereochemical purity and high yield. The enantiopure *trans*- γ , δ -unsaturated β -hydroxyesters were used to prepare *erthyro*-sphingosine analogues with aromatic substituents in the side chain. The strategy is based on the diastereospecific amination of *trans*- γ , δ -unsaturated β -hydroxyesters to introduce the amino group and establish anti *N*-Boc- α -hydrazino- β -hydroxyesters. Proper *E1cB* non-reductive elimination is essential for the successful cleavage of N-N bond of the hydrazino group. No racemization is detected during the entire course of the synthetic pathway. A total novel synthetic route of sphingosine analogues was thus accomplished with stereochemically pure intermediates and products.

Table of Contents

Signature Page.....	i
Title Page	iii
Abstract.....	v
Table of Contents.....	vii
List of Figures.....	xv
List of Tables.....	xxiii
List of Schemes.....	xxv
List of Appendices.....	xxvii
Acknowledgements.....	xxix
Chapter 1 Introduction.....	1
1.1. Biological significance of ceramide, sphingosine and sphingosine 1-phosphate	1
1.2. Structure-activity relationship between sphingolipid metabolites and enzymes	6
1.2.1. C3-Hydroxyl group	7
1.2.2. C2-Amino group.....	7
1.2.3. <i>trans</i> -Configured C4-C5 double bond.....	8
1.2.4. Stereoisomers	8
1.2.5. Aliphatic tail positively interacts with hydrophobic area.....	9
1.3. Current approaches to synthesize sphingosine and its analogues	10

1.4. Aromatic sphingosine derivatives	19
1.5. Summary of research aims	22
Reference.....	25
Chapter 2 Stereoselective Synthesis of Aryl γ , δ -unsaturated β -hydroxyesters by Ketoreductases.....	33
2.1. Introduction	33
2.2. Experimental	36
2.2.1. Materials	36
2.2.2. Instrument.....	37
2.2.3. Synthesis of γ , δ -unsaturated β -keto ethyl esters 2A-2F.....	38
2.2.4. Synthesis of racemic γ , δ -unsaturated β -hydroxyesters 3A-3F	39
2.2.5. Stereoselectivity of enzymatic formation of β -hydroxyesters 3A-3F using NADH system (enzyme 1-5).....	39
2.2.6. Stereoselectivity of enzymatic formation of β -hydroxyesters 3A-3F using NADPH system (enzyme 6-24).....	39
2.2.7. Synthesis of MTPA ester of γ , δ -unsaturated β -hydroxyesters.....	40
2.2.8. Procedure of Mukaiyama Aldol condensation based synthesis of <i>trans</i> - γ , δ - unsaturated β -hydroxyester	41
2.2.9. Procedure of Me-CBS-BH ₃ catalyzed synthesis of <i>trans</i> - γ , δ -unsaturated β - hydroxy ester	42
2.3. Results and discussion.....	42

2.3.1. Preparation of γ , δ -unsaturated β -keto ethyl esters 2A-2F	42
2.3.2. Stereoselectivity of enzymatic formation of β -hydroxyesters 3A-3F	43
2.3.4. Mukaiyama Aldol condensation based synthesis of <i>trans</i> - γ , δ -unsaturated β -hydroxy Ester	51
2.3.5. Me-CBS-BH ₃ catalyzed synthesis of <i>trans</i> - γ , δ -unsaturated β -hydroxyester ..	53
2.4. Summary of formation of aryl γ , δ -unsaturated β -hydroxyesters.....	54
2.5. Physical Data.....	55
2.5.1. Physical Data and NMR Spectra of γ , δ -unsaturated β -ketoesters 2A – 2F	55
2.5.1.1. (E)-ethyl 3-oxo-5-phenylpent-4-enoate (2A).....	55
2.5.1.2. (E)-ethyl 3-oxo-5-(p-tolyl)pent-4-enoate (2B).	56
2.5.1.3. (E)-ethyl 5-(4-chlorophenyl)-3-oxopent-4-enoate (2C).....	57
2.5.1.4. (E)-ethyl 5-(4-nitrophenyl)-3-oxopent-4-enoate (2D)	57
2.5.1.5. (E)-ethyl 5-(4-butylphenyl)-3-oxopent-4-enoate (2E).....	58
2.5.1.6. (E)-ethyl 3-oxo-6-phenylhex-4-enoate (2F)	58
2.5.2. Physical Data and NMR spectra of γ , δ -unsaturated β -hydroxyesters 3A-3F .	59
2.5.2.1. (E)-ethyl 3-hydroxy-5-phenylpent-4-enoate (3A)	59
2.5.2.2. (E)-ethyl 3-hydroxy-5-(p-tolyl)pent-4-enoate (3B)	60
2.5.2.3. (E)-ethyl 5-(4-chlorophenyl)3-hydroxypent-4-enoate (3C).....	60
2.5.2.4. (E)-ethyl 3-hydroxy-5-(4-nitrophenyl)pent-4-enoate (3D).....	61

2.5.2.5. (E)-ethyl 5-(4-butylphenyl)-3-hydroxypent-4-enoate (3E).....	61
Reference.....	63
Appendix A, Supplementary for Chapter 2	69
A.1. Determination of absolute configuration of β -hydroxyesters.....	103
Chapter 3 A Total New Synthesis of Ceramide and Sphingosine Analogues.....	121
3.1. Introduction.....	121
3.2. Results and discussion.....	125
3.2.1. Anti N-Boc- α -hydrazino- β -hydroxyesters (4).....	126
3.2.2. Anti 2-hydrazino 1, 3-diol (5).....	132
3.2.3. Non-reductive eliminative cleavage of the hydrazine N-N bonds.....	137
3.2.4. Deprotection of 2-Bocamino-1,3 diol ketals (8) to provide target products.	143
3.3. Summary of the novel synthetic route.....	145
3.4. General methods.....	147
3.4.1. Materials.....	147
3.4.2. Instruments.....	147
3.4.3. Diastereospecific formation of <i>anti</i> N-Boc- α -hydrazino- β -hydroxyesters (4).....	148
3.4.3.1. Ethyl (4E)-2-[1,2-bis(tert-butoxycarbonyl)hydrazino]-2,4,5-trideoxy-5-phenyl-D-erythro-pent-4-enonate (4A).....	149

3.4.3.2. Ethyl (4E)-2-[1,2-bis(tert-butoxycarbonyl)hydrazino]-2,4,5-trideoxy-5-phenyl-D-erythro-pent-4-enonate (4B).....	149
3.4.3.3. Ethyl (4E)-2-[1,2-bis(tert-butoxycarbonyl)hydrazino]-5-(4-chlorophenyl)-2,4,5-trideoxy-D-erythro-pent-4-enonate (4C).....	150
3.4.3.4. Ethyl (4E)-2-[1,2-bis(tert-butoxycarbonyl)hydrazino]-5-(4-butylphenyl)-2,4,5-trideoxypent-4-enonate (4E)	151
3.4.4. Synthesis of <i>anti</i> 2-di-tert-butoxycarbonyl hydrazino 1, 3-diol (5).....	152
3.4.4.1. (4E)-2-[1,2-bis(tert-butoxycarbonyl)hydrazino]-2,4,5-trideoxy-5-phenyl-D-erythro-pent-4-enitol (5A).	152
3.4.4.2. (4E)-2-[1,2-bis(tert-butoxycarbonyl)hydrazino]-2,4,5-trideoxy-5-(4-methylphenyl)-D-erythro-pent-4-enitol (5B).	153
3.4.4.3. (4E)-2-[1,2-bis(tert-butoxycarbonyl)hydrazino]-5-(4-chlorophenyl)-2,4,5-trideoxy-D-erythro-pent-4-enitol (5C).	153
3.4.4.5. (1E)-4-[1,2-bis(tert-butoxycarbonyl)hydrazino]-1-(4-butylphenyl)-1,2,4-trideoxypent-1-enitol (5E).	154
3.4.5. Synthesis of <i>anti</i> 2-di- <i>tert</i> -butoxycarbonyl hydrazino 1, 3-diol ketal (6).....	155
3.4.5.1. (1E)-4-[1,2-bis(tert-butoxycarbonyl)hydrazino]-1,2,4-trideoxy-3,5-O-(1-methylethylidene)-1-phenylpent-1-enitol (6A).	155
3.4.5.2. (1E)-4-[1,2-bis(tert-butoxycarbonyl)hydrazino]-1,2,4-trideoxy-3,5-O-(1-methylethylidene)-1-(4-methylphenyl)pent-1-enitol (6B).....	156
3.4.5.3. (4E)-2-[1,2-bis(tert-butoxycarbonyl)hydrazino]-5-(4-chlorophenyl)-2,4,5-trideoxy-1,3-O-(1-methylethylidene)-D-erythro-pent-4-enitol (6C).	157
3.4.5.4. (1E)-4-[1,2-bis(tert-butoxycarbonyl)hydrazino]-1-(4-butylphenyl)-1,2,4-trideoxy-3,5-O-(1-methylethylidene)pent-1-enitol (6E).....	157
3.4.6. Synthesis <i>anti</i> 2-alkylhydrazino 1, 3-diol ketal (7)	158

3.4.6.1. (1E)-4-[1,2-bis(tert-butoxycarbonyl)-2-(2-methoxy-2-oxoethyl)hydrazino]-1,2,4-trideoxy-3,5-O-(1-methylethylidene)-1-phenyl-D-erythro-pent—enitol (7A).....	159
3.4.6.2. (1E)-4-[1,2-bis(tert-butoxycarbonyl)-2-(2-methoxy-2oxoethyl)hydrazino]-1,2,4-trideoxy-3,5-O-(1-methylethylidene)-1-(4-methylphenyl)pent-1-enitol (7B).....	160
3.4.6.3. (1E)-4-[1,2-bis(tert-butoxycarbonyl)-2-(2-methoxy-2oxoethyl)hydrazino]- 1-(4-chlorophenyl)-1,2,4-trideoxy-3,5-O-(1-methylethylidene)pent-1-enitol (7C).....	161
3.4.6.4. (1E)-4-[1,2-bis(tert-butoxycarbonyl)-2-(2-methoxy-2-oxoethyl)hydrazino]-1-(4-butylphenyl)-1,2,4-trideoxy-3,5-O-(1-methylethylidene)pent-1-enitol (7E).....	162
3.4.7. Synthesis of <i>anti</i> 2-BocAmino 1, 3-diol ketal (8)	163
3.4.7.1. (1E)-4-[(tert-butoxycarbonyl)amino]-1,2,4-trideoxy-3,5-O-(1-methylethylidene)-1-phenylpent-1-enitol (8A).....	163
3.4.7.2. (1E)-4-[(tert-butoxycarbonyl)amino]-1,2,4-trideoxy-3,5-O-(1-methylethylidene)-1-(4-methylphenyl)pent-1-enitol (8B).....	164
3.4.7.3. (1E)-4-[(tert-butoxycarbonyl)amino]-1-(4-methylphenyl)-1,2,4-trideoxy-3,5-O-(1-methylethylidene)pent-1-enitol (8C).....	164
3.4.7.4. (1E)-4-[(tert-butoxycarbonyl)amino]-1-(4-butylphenyl)-1,2,4-trideoxy-3,5-O-(1-methylethylidene)pent-1-enitol (8E).....	165
3.4.8. Direct synthesis of <i>anti</i> 2-BocAmino 1,3-diol ketal (8)	166
3.4.9. <i>trans</i> -4,5-Unsaturated <i>anti</i> 2-BocAmino 1,3-diol (9).....	166
3.4.9.1. (1E)-4-[(tert-butoxycarbonyl)amino]-1,2,4-trideoxy-1-phenylpent-1-enitol (9A).....	167
3.4.9.2. (1E)-4-[(tert-butoxycarbonyl)amino]-1,2,4-trideoxy-1-(4-methylphenyl)pent-1-enitol (9B).....	167

3.4.9.3. (1E)-4-[(tert-butoxycarbonyl)amino]-1-(4-chlorophenyl)-1,2,4-trideoxypent-1-enitol (9C).	168
3.4.9.4. (1E)-4-[(tert-butoxycarbonyl)amino]-1-(4-butylphenyl)-1,2,4-trideoxypent-1-enitol (9E).	168
Reference.....	171
Appendix B, Supplementary for Chapter 3	177
Chapter 4 Conclusion.....	231
4.1. Overview	231
4.2. Conclusions on KREDs induced reduction of aryl γ , δ -unsaturated- β -ketoesters.	231
4.3. Conclusion of a novel and effective synthesis of erythro aromatic sphingosine analogues.....	233
4.4. Final remarks.....	234
Appendix C Atropisomers of Serotonin Dimer	237
C.1 Abstract.....	237
C.2. Introduction	238
C.3. Results and Discussion	240
C.3.1. Synthesis and NMR studies of DHBT	240
C.3.2. Atropisomers of DHBT	246
C.4. Summary of atropisomers of DHBT	250
C.5. Experimental.....	251

C.5.1. Materials	251
C.5.2. NMR Spectroscopy.....	251
C.5.3. Chiral Capillary Electrophoresis.....	252
C.5.4. Synthesis and Purification.....	252
C.5.4.1. 5,5'-dihydroxy-4, 4'-bitryptamine (DHBT)·2HCl.....	252
C.5.4.2. Boc-protected 5-HT.....	254
C.6. Calculations	256
C.7. Conclusion on atropisomers of DHBT	257
Reference.....	259

List of Figures

Figure 1.1. General structure of sphingolipids.....	1
Figure 1.2. Structure of existing aromatic sphingosine analogues.	20
Figure A2.1. ^1H NMR spectrum of 2A in CDCl_3	69
Figure A2.2. ^{13}C NMR spectrum of 2A in CDCl_3	70
Figure A2.3. gCOSY spectrum of 2A in CDCl_3	71
Figure A2.4. ^1H NMR spectrum of 2B in CDCl_3	72
Figure A2.5. ^{13}C NMR spectrum of 2B in CDCl_3	73
Figure A2.6. gCOSY spectrum of 2B in CDCl_3	74
Figure A2.7. ^1H NMR spectrum of 2C in CDCl_3	75
Figure A2.8. ^{13}C NMR spectrum of 2C in CDCl_3	76
Figure A2.9. gCOSY spectrum of 2C in CDCl_3	77
Figure A2.10. ^1H NMR spectrum of 2D in CDCl_3	78
Figure A2.11. ^{13}C NMR spectrum of 2D in CDCl_3	79
Figure A2.12. gCOSY spectrum of 2D in CDCl_3	80
Figure A2.13. ^1H NMR spectrum of 2E in CDCl_3	81
Figure A2.14. ^{13}C NMR spectrum of 2E in CDCl_3	82
Figure A2.15. gCOSY spectrum of 2E in CDCl_3	83
Figure A2.16. ^1H NMR spectrum of 2F in CDCl_3	84
Figure A2.17. ^{13}C NMR spectrum of 2F in CDCl_3	85
Figure A2.18. gCOSY spectrum of 2F in CDCl_3	86
Figure A2.19. ^1H NMR spectrum of 3A in CDCl_3	87

Figure A2.20. ^{13}C NMR spectrum of 3A in CDCl_3	88
Figure A2.21. gCOSY spectrum of 3A in CDCl_3	89
Figure A2.22. ^1H NMR spectrum of 3B in CDCl_3	90
Figure A2.23. ^{13}C NMR spectrum of 3B in CDCl_3	91
Figure A2.24. gCOSY spectrum of 3B in CDCl_3	92
Figure A2.25. ^1H NMR spectrum of 3C in CDCl_3	93
Figure A2.26. ^{13}C NMR spectrum of 3C in CDCl_3	94
Figure A2.27. ^1H NMR spectrum of 3D in CDCl_3	95
Figure A2.28. ^{13}C NMR spectrum of 3D in CDCl_3	96
Figure A2.29. gCOSY spectrum of 3D in CDCl_3	97
Figure A2.30. ^1H NMR spectrum of 3E in CDCl_3	98
Figure A2.31. ^{13}C NMR spectrum of 3E in CDCl_3	99
Figure A2.32. gCOSY spectrum of 3E in CDCl_3	100
Figure A2.33. ^1H NMR spectrum of olefinic and methylene hydrogens in 3F and 3F'. 101	
Figure A2.34. Ultraviolet absorption spectrum of ethyl (5E)-3-hydroxy-6-phenylhex-5-enoate 3F'.	102
Figure A2.35. Ultraviolet absorption spectrum of ethyl (4E)-3-hydroxy-6-phenylhex-4-enoate 3F.....	102
Figure A2.36. Structure of (a) (<i>R</i>)-3C-(<i>S</i>)-MTPA ester and (b) (<i>S</i>)-3C-(<i>S</i>)-MTPA ester and their hyperchem models at the bottom.....	104
Figure A2.37. ^1H NMR spectra of olefinic protons H_a (H_a') and H_b (H_b') in CDCl_3	105
Figure A2.38. ^1H NMR spectra of (<i>S</i>)-MTPA ester of 3A in CDCl_3	106
Figure A2.39. ^1H NMR spectra of (<i>S</i>)-MTPA ester of 3B in CDCl_3	107

Figure A2.40. ¹ H NMR spectra of (<i>S</i>)-MTPA ester of 3C in CDCl ₃	108
Figure A2.41. ¹ H NMR spectra of (<i>S</i>)-MTPA ester of 3D in CDCl ₃	109
Figure A2.42. ¹ H NMR spectra of (<i>S</i>)-MTPA ester spectra of 3E in CDCl ₃	110
Figure A2.43. Stacked ¹ H NMR spectra of crude enzymatic product 3E in CDCl ₃	111
Figure A2.44. Chiral HPLC chromatograph of 3A.....	112
Figure A2.45. Chiral HPLC chromatograph of 3B.....	113
Figure A2.46. Chiral HPLC chromatograph of 3C.....	114
Figure A2.47. Chiral HPLC chromatograph of 3D.....	115
Figure A2.48. Chiral HPLC chromatograph of 3E.....	116
Figure A2.49. CE Electropherogram for 3C.....	117
Figure A2.50. ¹ H NMR spectra of methyl (3 <i>S</i> , 4 <i>E</i>)-3-hydroxy-5-phenylpent-4-enoate made from Mukaiyama aldol condensation.....	118
Figure A2.51. CE Electropherogram for <i>trans</i> γ , δ -unsaturated β -ketoester made from Mukaiyama Aldol condensation and Me-CBS-BH ₃ catalyst.....	119
Figure 3.1. Structure of BLM-258, (2 <i>R</i> , 3 <i>S</i> , 4 <i>E</i>)- <i>N</i> -methyl-5-(4'-pentylphenyl)-2-aminopent-4-ene-1,3-diol).....	123
Figure 3.2. Structure of <i>trans</i> - γ , δ -unsaturated β -hydroxyesters.....	124
Figure 3.3. Basic Structural Feature of Sphingosine derivatives.....	125
Figure 3.4. Methyl (4 <i>E</i>)-2-[1,2-bis(<i>tert</i> -butoxycarbonyl)hydrazino]-2,4,5-trideoxy-5-phenyl- <i>D</i> -erythro-pent-4-enonate (4A).....	130
Figure 3.5. ¹ H NMR spectrum of methyl (4 <i>E</i>)-2-[1,2-bis(<i>tert</i> -butoxycarbonyl)hydrazino]-2,4,5-trideoxy-5-phenyl- <i>D</i> -erythro-pent-4-enonate (4A).....	131
Figure 3.6. ¹ H NMR spectrum of (4 <i>E</i>)-2-[1,2-bis(<i>tert</i> -butoxycarbonyl)hydrazino]-2,4,5-trideoxy-5-phenyl- <i>D</i> -erythro-pent-4-enitol (5A).....	136
Figure 3.7. ¹ H NMR spectrum of (7C) in CDCl ₃ by a Bruker 600 MHz spectroscopy..	141

Figure 3.8. Stacked ^1H NMR spectra of olefin and aromatic hydrogen of 7C in DMSO- d_6 at variant temperatures.....	143
Figure B3.1. ^1H NMR spectrum of Ethyl (4E)-2-[1,2-bis(<i>tert</i> -butoxycarbonyl)hydrazino]-2,4,5-trideoxy-5-phenyl-D- <i>erythro</i> -pent-4-enonate (4A)	177
Figure B3.2. ^{13}C NMR spectrum of Ethyl (4E)-2-[1,2-bis(<i>tert</i> -butoxycarbonyl)hydrazino] -2,4,5-trideoxy-5-phenyl-D- <i>erythro</i> -pent-4-enonate (4A)	178
Figure B3.3. ^1H NMR spectrum of Ethyl (4E)-2-[1,2-bis(<i>tert</i> -butoxycarbonyl)hydrazino] -2,4,5-trideoxy-5-(4-methylphenyl)-D- <i>erythro</i> -pent-4-enonate (4B).....	179
Figure B3.4. ^{13}C NMR spectrum of Ethyl (4E)-2-[1,2-bis(<i>tert</i> -butoxycarbonyl)hydrazino] -2,4,5-trideoxy-5-(4-methylphenyl)-D- <i>erythro</i> -pent-4-enonate (4B).....	180
Figure B3.5. ^1H NMR spectrum of ethyl (4E)-2-[1,2-bis(<i>tert</i> -butoxycarbonyl)hydrazino]-5-(4-chlorophenyl)-2,4,5-trideoxy-D- <i>erythro</i> -pent-4-enonate (4C).	181
Figure B3.6. ^{13}C NMR spectrum of ethyl (4E)-2-[1,2-bis(<i>tert</i> -butoxycarbonyl)hydrazino]-5-(4-chlorophenyl)-2,4,5-trideoxy-D- <i>erythro</i> -pent-4-enonate (4C)	182
Figure B3.7. ^1H NMR spectrum of ethyl (4E)-2-[1,2-bis(<i>tert</i> -butoxycarbonyl)hydrazino]-5-(4-butylphenyl)-2,4,5-trideoxypent-4-enonate (4E)	183
Figure B3.8. ^{13}C NMR spectrum of ethyl (4E)-2-[1,2-bis(<i>tert</i> -butoxycarbonyl)hydrazino]-5-(4-butylphenyl)-2,4,5-trideoxypent-4-enonate (4E)	184
Figure B3.9. ^1H NMR spectrum of (4E)-2-[1,2-bis(<i>tert</i> -butoxycarbonyl)hydrazino]-2,4,5-trideoxy-5-phenyl-D- <i>erythro</i> -pent-4-enitol (5A).....	185
Figure B3.10. ^{13}C NMR spectrum of (4E)-2-[1,2-bis(<i>tert</i> -butoxycarbonyl)hydrazino]-2,4,5-trideoxy-5-phenyl-D- <i>erythro</i> -pent-4-enitol (5A)	186
Figure B3.11. ^1H NMR spectrum of (4E)-2-[1,2-bis(<i>tert</i> -butoxycarbonyl)hydrazino]-2,4,5-trideoxy-5-(4-methylphenyl)-D- <i>erythro</i> -pent-4-enitol (5B).....	187
Figure B3.12. ^{13}C NMR spectrum of (4E)-2-[1,2-bis(<i>tert</i> -butoxycarbonyl)hydrazino]-2,4,5-trideoxy-5-(4-methylphenyl)-D- <i>erythro</i> -pent-4-enitol (5B).	188
Figure B3.13. ^1H NMR spectrum of (4E)-2-[1,2-bis(<i>tert</i> -butoxycarbonyl)hydrazino]-5-(4-chlorophenyl)-2,4,5-trideoxy-D- <i>erythro</i> -pent-4-enitol (5C).....	189

Figure B3.14. ^{13}C NMR spectrum of (4 <i>E</i>)-2-[1,2-bis(<i>tert</i> -butoxycarbonyl)hydrazino]-5-(4-chlorophenyl)-2,4,5-trideoxy- <i>D</i> -erythro-pent-4-enitol (5C).....	190
Figure B3.15. ^1H NMR spectrum of (<i>IE</i>)-4-[1,2-bis(<i>tert</i> -butoxycarbonyl)hydrazino]-1-(4-butylphenyl)-1,2,4-trideoxypent-1-enitol (5E).....	191
Figure B3.16. ^{13}C NMR spectrum of (<i>IE</i>)-4-[1,2-bis(<i>tert</i> -butoxycarbonyl)hydrazino]-1-(4-butylphenyl)-1,2,4-trideoxypent-1-enitol (5E).....	192
Figure B3.17. ^1H NMR spectrum of (<i>IE</i>)-4-[1,2-bis(<i>tert</i> -butoxycarbonyl)hydrazino]-1,2,4-trideoxy-3,5- <i>O</i> -(1-methylethylidene)-1-phenylpent-1-enitol (6A).....	193
Figure B3.18. ^{13}C NMR spectrum of (<i>IE</i>)-4-[1,2-bis(<i>tert</i> -butoxycarbonyl)hydrazino]-1,2,4-trideoxy-3,5- <i>O</i> -(1-methylethylidene)-1-phenylpent-1-enitol (6A).....	194
Figure B3.19. ^1H NMR spectrum of (<i>IE</i>)-4-[1,2-bis(<i>tert</i> -butoxycarbonyl)hydrazino]-1,2,4-trideoxy-3,5- <i>O</i> -(1-methylethylidene)-1-(4-methylphenyl)pent-1-enitol (6B).....	195
Figure B3.20. ^{13}C NMR spectrum of (<i>IE</i>)-4-[1,2-bis(<i>tert</i> -butoxycarbonyl)hydrazino]-1,2,4-trideoxy-3,5- <i>O</i> -(1-methylethylidene)-1-(4-methylphenyl)pent-1-enitol (6B).....	196
Figure B3.21. ^1H NMR spectrum of (4 <i>E</i>)-2-[1,2-bis(<i>tert</i> -butoxycarbonyl)hydrazino]-5-(4-chlorophenyl)-2,4,5-trideoxy-1,3- <i>O</i> -(1-methylethylidene)- <i>D</i> -erythro-pent-4-enitol (6C).....	197
Figure B3.22. ^{13}C NMR spectrum of (4 <i>E</i>)-2-[1,2-bis(<i>tert</i> -butoxycarbonyl)hydrazino]-5-(4-chlorophenyl)-2,4,5-trideoxy-1,3- <i>O</i> -(1-methylethylidene)- <i>D</i> -erythro-pent-4-enitol (6C).....	198
Figure B3.23. ^1H NMR spectrum of (<i>IE</i>)-4-[1,2-bis(<i>tert</i> -butoxycarbonyl)hydrazino]-1-(4-butylphenyl)-1,2,4-trideoxy-3,5- <i>O</i> -(1-methylethylidene)pent-1-enitol (6E).....	199
Figure B3.24. ^{13}C NMR spectrum of (<i>IE</i>)-4-[1,2-bis(<i>tert</i> -butoxycarbonyl)hydrazino]-1-(4-butylphenyl)-1,2,4-trideoxy-3,5- <i>O</i> -(1-methylethylidene)pent-1-enitol (6E).....	200
Figure B3.25. ^1H NMR spectrum of (<i>IE</i>)-4-[1,2-bis(<i>tert</i> -butoxycarbonyl)-2-(2-methoxy-2-oxoethyl)hydrazino]-1,2,4-trideoxy-3,5- <i>O</i> -(1-methylethylidene)-1-phenyl- <i>D</i> -erythro-pent-enitol (7A).....	201
Figure B3.26. ^{13}C NMR spectrum of (<i>IE</i>)-4-[1,2-bis(<i>tert</i> -butoxycarbonyl)-2-(2-methoxy-2-oxoethyl)hydrazino]-1,2,4-trideoxy-3,5- <i>O</i> -(1-methylethylidene)-1-phenyl- <i>D</i> -erythro-pent-enitol (7A).....	202

Figure B3.27. ¹ H NMR spectrum of (<i>1E</i>)-4-[1,2-bis(<i>tert</i> -butoxycarbonyl)-2-(2-methoxy-2oxoethyl)hydrazino]-1,2,4-trideoxy-3,5- <i>O</i> -(1-methylethylidene)-1-(4-methylphenyl)pent-1-enitol (7B).....	203
Figure B3.28. ¹³ C NMR spectrum of (<i>1E</i>)-4-[1,2-bis(<i>tert</i> -butoxycarbonyl)-2-(2-methoxy-2oxoethyl)hydrazino]-1,2,4-trideoxy-3,5- <i>O</i> -(1-methylethylidene)-1-(4-methylphenyl) pent-1-enitol (7B).....	204
Figure B3.29. ¹ H NMR spectrum of (<i>1E</i>)-4-[1,2-bis(<i>tert</i> -butoxycarbonyl)-2-(2-methoxy-2oxoethyl)hydrazino]- 1-(4-chlorophenyl)-1,2,4-trideoxy-3,5- <i>O</i> -(1-methylethylidene) pent-1-enitol (7C) on a 600 MHz Bruker spectroscopy.....	205
Figure B3.30. ¹³ C NMR spectrum of (<i>1E</i>)-4-[1,2-bis(<i>tert</i> -butoxycarbonyl)-2-(2-methoxy-2oxoethyl)hydrazino]- 1-(4-chlorophenyl)-1,2,4-trideoxy-3,5- <i>O</i> -(1-methylethylidene) pent-1-enitol (7C) on a 600 MHz Bruker spectroscopy.....	206
Figure B3.31. ¹ H NMR spectrum of (<i>1E</i>)-4-[1,2-bis(<i>tert</i> -butoxycarbonyl)-2-(2-methoxy-2-oxoethyl)hydrazino]-1-(4-butylphenyl)-1,2,4-trideoxy-3,5- <i>O</i> -(1-methylethylidene)pent-1-enitol (7E)	207
Figure B3.32. ¹³ C NMR spectrum of (<i>1E</i>)-4-[1,2-bis(<i>tert</i> -butoxycarbonyl)-2-(2-methoxy-2-oxoethyl)hydrazino]-1-(4-butylphenyl)-1,2,4-trideoxy-3,5- <i>O</i> -(1-methylethylidene) pent-1-enitol (7E).....	208
Figure B3.33. ¹ H NMR spectrum of (<i>1E</i>)-4-[(<i>tert</i> -butoxycarbonyl)amino]-1,2,4-trideoxy-3,5- <i>O</i> -(1-methylethylidene)-1-phenylpent-1-enitol (8A).....	209
Figure B3.34. ¹³ C NMR spectrum of (<i>1E</i>)-4-[(<i>tert</i> -butoxycarbonyl)amino]-1,2,4-trideoxy-3,5- <i>O</i> -(1-methylethylidene)-1-phenylpent-1-enitol (8A).....	210
Figure B3.35. ¹ H NMR spectrum of (<i>1E</i>)-4-[(<i>tert</i> -butoxycarbonyl)amino]-1,2,4-trideoxy-3,5- <i>O</i> -(1-methylethylidene)-1-(4-methylphenyl)pent-1-enitol (8B).....	211
Figure B3.36. ¹³ C NMR spectrum of (<i>1E</i>)-4-[(<i>tert</i> -butoxycarbonyl)amino]-1,2,4-trideoxy-3,5- <i>O</i> -(1-methylethylidene)-1-(4-methylphenyl)pent-1-enitol (8B).....	212
Figure B3.37. ¹ H NMR spectrum of (<i>1E</i>)-4-[(<i>tert</i> -butoxycarbonyl)amino]-1-(4-methylphenyl)-1,2,4-trideoxy-3,5- <i>O</i> -(1-methylethylidene)pent-1-enitol (8C).	213
Figure B3.38. ¹³ C NMR spectrum of (<i>1E</i>)-4-[(<i>tert</i> -butoxycarbonyl)amino]-1-(4-methylphenyl)-1,2,4-trideoxy-3,5- <i>O</i> -(1-methylethylidene)pent-1-enitol (8C).....	214
Figure B3.39. ¹ H NMR spectrum of (<i>1E</i>)-4-[(<i>tert</i> -butoxycarbonyl)amino]-1-(4-butylphenyl)-1,2,4-trideoxy-3,5- <i>O</i> -(1-methylethylidene)pent-1-enitol (8E).	215

Figure B3.40. ^{13}C NMR spectrum of (1 <i>E</i>)-4-[(<i>tert</i> -butoxycarbonyl)amino]-1-(4-butylphenyl)-1,2,4-trideoxy-3,5- <i>O</i> -(1-methylethylidene)pent-1-enitol (8E).....	216
Figure B3.41. ^1H NMR spectrum of (1 <i>E</i>)-4-[(<i>tert</i> -butoxycarbonyl)amino]-1,2,4-trideoxy-1-phenylpent-1-enitol (9A)	217
Figure B3.42. ^{13}C NMR spectrum of (1 <i>E</i>)-4-[(<i>tert</i> -butoxycarbonyl)amino]-1,2,4-trideoxy-1-phenylpent-1-enitol (9A)	218
Figure B3.43. ^1H NMR spectrum of (1 <i>E</i>)-4-[(<i>tert</i> -butoxycarbonyl)amino]-1,2,4-trideoxy-1-(4-methylphenyl)pent-1-enitol (9B).....	219
Figure B3.44. ^{13}C NMR spectrum of (1 <i>E</i>)-4-[(<i>tert</i> -butoxycarbonyl)amino]-1,2,4-trideoxy-1-(4-methylphenyl)pent-1-enitol (9B).....	220
Figure B3.45. ^1H NMR spectrum of (1 <i>E</i>)-4-[(<i>tert</i> -butoxycarbonyl)amino]-1-(4-chlorophenyl)-1,2,4-trideoxypent-1-enitol (9C)	221
Figure B3.46. ^{13}C NMR spectrum of (1 <i>E</i>)-4-[(<i>tert</i> -butoxycarbonyl)amino]-1-(4-chlorophenyl)-1,2,4-trideoxypent-1-enitol (9C)	222
Figure B3.47. ^1H NMR spectrum (1 <i>E</i>)-4-[(<i>tert</i> -butoxycarbonyl)amino]-1-(4-butylphenyl)-1,2,4-trideoxypent-1-enitol (9E).....	223
Figure B3.48. ^{13}C NMR spectrum of (1 <i>E</i>)-4-[(<i>tert</i> -butoxycarbonyl)amino]-1-(4-butylphenyl)-1,2,4-trideoxypent-1-enitol (9E).....	224
Figure B3.49. Chiral HPLC chromatograph of 9A.....	225
Figure B3.50. Chiral HPLC chromatograph of 8B and 9B.....	226
Figure B3.51. Chiral HPLC chromatograph of 8C and 9C.....	227
Figure B3.52. Chiral HPLC chromatograph of 8E	228
Figure B3.53. Chiral HPLC chromatograph of 9E	229
Figure C1. a. Schematic of 5-hydroxytryptamine (Serotonin) showing numbering scheme used in this work; b. DHBT; c. Boc-protected 5-HT; d. 5-Hydroxyindole	239
Figure C2. ^1H NMR spectra of 5-HT neutralized by 1.0 equivalent of NaOH then reacted with 1.25 equivalents of $\text{CuCl}_2 \cdot 2\text{H}_2\text{O}$	241

Figure C3. Effect of various amounts of base added on the conversion of 5-HT to DHBT after 1 hour of reaction time as monitored by ^1H NMR spectroscopy.....	242
Figure C4. ^1H NMR spectra of Boc-protected 5-HT in the presence of 1.25 equivalents of $\text{CuCl}_2 \cdot 2\text{H}_2\text{O}$	244
Figure C5. ^1H NMR spectra of 5-Hydroxyindole in the presence of 1.25 equivalents of $\text{CuCl}_2 \cdot 2\text{H}_2\text{O}$	245
Figure C6. Computational simulations of DHBT where the dihedral C4-C5-C5'-C4' was restrained.	247
Figure C7. Atropisomers of DHBT attributed to slow rotation about 4-4' carbon-carbon bond.	248
Figure C8. Electropherogram for 5-HT and DHBT atropisomers.....	249
Figure C9. ^1H NMR spectrum of upfield region of 5, 5'-dihydroxy-4, 4'-bitryptamine (DHBT) (lower spectrum) and simulated spectrum using chemical shifts (δ) and coupling constants (J).	250
Figure C10. ^1H NMR spectrum of 5, 5'-dihydroxy-4, 4'-bitryptamine (DHBT)	253
Figure C11. ^{13}C NMR spectrum of 5, 5'-dihydroxy-4, 4'-bitryptamine (DHBT).....	254
Figure C12. ^1H NMR spectrum of Boc-protected 5-HT.....	255
Figure C13. ^{13}C NMR spectrum of Boc-protected 5-HT.....	256

List of Tables

Table 2.1. Stereocontrolled reduction of γ , δ -unsaturated β -ketoesters to γ , δ -unsaturated β -hydroxyesters by twenty-four Codex [®] ketoreductases.....	49
Table 2.2. Isolated yields of γ , δ -unsaturated- β -hydroxyesters 3 using ketoreductases which provide both good yield and high enantioselectivity.....	50
Table 3.1. Reduction of <i>anti</i> <i>N</i> -Boc- α -hydrazino- β -hydroxyesters 4 by excess NaBH ₄	135
Table 3.2. Configuration, diastereoisomeric excesses and isolated yields of all intermediates making from corresponding racemic, enantiomeric excess and enantiopure pure <i>trans</i> - γ , δ -unsaturated β -hydroxyesters.	145

List of Schemes

Scheme 1.1. Pathway of sphingolipid metabolism.	3
Scheme 1.2. Newman's synthetic route to sphingosine.....	12
Scheme 1.3. Herold's synthetic route to sphingosine.	14
Scheme 1.4. Koshinen's synthetic route to sphingosine.....	15
Scheme 1.5. Dondoni's synthetic route to sphingosine.	16
Scheme 1.6. Murakami's synthetic route to sphingosine.	17
Scheme 1.7. Chum's synthetic route to sphingosine.	17
Scheme 1.8. Liebeskind's cross-coupling synthetic route starting from N-Boc-L-serine 23.	18
Scheme 1.9. The overview for the stereospecific synthesis of sphingosine analogues in the dissertation.	23
Scheme 2.1. Synthesis of γ , δ -unsaturated- β -hydroxyesters from appropriate aldehydes and 4-(diethoxyphosphinyl)-3-oxobutanoate in the presence of two equivalents of n-BuLi.	43
Scheme 2.2. Enzymatic reduction of γ , δ -unsaturated β -ketoesters with NAD(P)H- dependent Codex [®] ketoreductases.	44
Scheme 2.3. Enzymatic reduction of 2F to 3F and rearranged product 3F'.	48
Scheme 2.4. Aldol condensation between <i>trans</i> -cinnamaldehyde and silyl ketene acetal.....	52
Scheme 2.5. Preparation of titanium catalyst from 2-amino-2'-hydroxy-1,1'- binaphthyl, Ti(O ⁱ Pr) ₄ and 3,5- <i>di-tert</i> -butylsalicylic acid.	52
Scheme 2.6. Preparation of Ketene Silyl Acetyl.....	52
Scheme 2.7. Preparation of Me-CBS-BH ₃ catalyst from methyl oxazaborolidine and borane-methyl sulfide complex (BMS).	53

Scheme 2.8. Me-CBS-BH ₃ catalyst catalyzed reduction of <i>trans</i> γ , δ -unsaturated β -ketoester.....	54
Scheme A2.1. Synthesis of diastereomeric pair (<i>R</i>)-3C-(<i>S</i>)-MTPA ester and (<i>S</i>)-3C-(<i>S</i>)-MTPA ester from racemic β -hydroxyester (<i>RS</i>)-3C and <i>R</i> -(-)-MTPA-Cl 5R.	104
Scheme 3.1. General reaction scheme for the stereospecific synthesis of ceramide and Sphingosine derivatives from <i>trans</i> - γ , δ -unsaturated β -(<i>S</i>)-hydroxyesters <i>S</i> -3A and <i>S</i> -3E.....	126
Scheme 3.2. Chelated zinc enolates of β -hydroxyesters 3.....	128
Scheme 3.3. Restricted rotation in carbamate. N-lone electron pair delocalization (a and b). $R_1 \neq R_2$	129
Scheme 3.4. A possible ring intermediate between <i>anti</i> N-Boc- α -hydrazino- β -hydroxyesters 4 and trimethoxy borane.....	133
Scheme 3.5. Ketalization of <i>anti</i> 2-di- <i>tert</i> -butoxycarbonyl hydrazino 1,3-diol ketals (6).....	139
Scheme 3.6. <i>ElcB</i> non-reductive cleavage of N-N bonds into carbamates (8).	140
Scheme 3.7. <i>ElcB</i> elimination of N-N bonds in <i>anti</i> 2- <i>N</i> -alkylated-di- <i>tert</i> -butoxycarbonyl hydrazino 1, 3-diol ketals (7) to obtain (8).....	141

List of Appendices

Appendix A, Supplementary for Chapter 2	69
Appendix B, Supplementary for Chapter 3.....	177
Appendix C, Atropisomers of Serotonin Dimer.....	237

Acknowledgements

I would like to express my deepest gratitude to my thesis advisor, Dr. Tom Green, for his excellent guidance, patience, enthusiasm, and immense knowledge. As an advisor, friend and mentor in my Ph.D. study and research, his guidance will benefit all of my life. I would like to thank the Department of Chemistry and Biochemistry and the Institute of Arctic Biology for providing me with an excellent research atmosphere, faculty support and financial support. A large portion of this research was supported in part by funding through UAF office of Intellectual Property and Commercialization (Innovation Seed Award) and Institute of Arctic Biology.

I would like to thank members of Green's Research Lab, for valuable insights and direct contributions. I thank Dr. Carl Murphy, for his help on NMR technique. Special thanks go to Michael Jaramillo and Daniel Kirschner, for helping and giving their best suggestions.

I am especially indebted to Dr. Tom Kuhn, Dr. Marvin Schulte and Dr. Kelly Drew for helping me to develop my background in biochemistry and neurochemistry. And I am thankful Dr. Fenton Heirtzler, and Dr. Tom Clausen, for their insightful comments in organic chemistry.

I also thank my parents, two elder brothers, for supporting me spiritually throughout my life.

Finally, I thank my wife, Dr. Xiaoyu Shi. I could not have imagined finishing my dissertation without her motivation, sweet caring and unrequited support.

Chapter 1

Introduction

1.1. Biological significance of ceramide, sphingosine and sphingosine 1-phosphate

As the fourth largest class of membrane lipids, sphingolipids (SP) play critical roles in signal transduction, intercellular membrane trafficking and cell growth and survival (Hannun, Luberto et al. 2001, van Meer and Lisman 2002, Sigal, McDermott et al. 2005). Sphingolipids are found in essentially all animals, plants, and fungi, as well as some prokaryotic organisms and viruses. They are mostly located in membranes, and are also major constituents of lipoproteins (Merrill, Wang et al. 2007). Sphingolipids, as shown in **Figure 1.1**, have one polar head group and two nonpolar tails including one molecule of the long-chain amino sphingoid base (such as sphingosine or its derivatives) and one molecule of a long-chain fatty acid (Hannun and Obeid 2008).

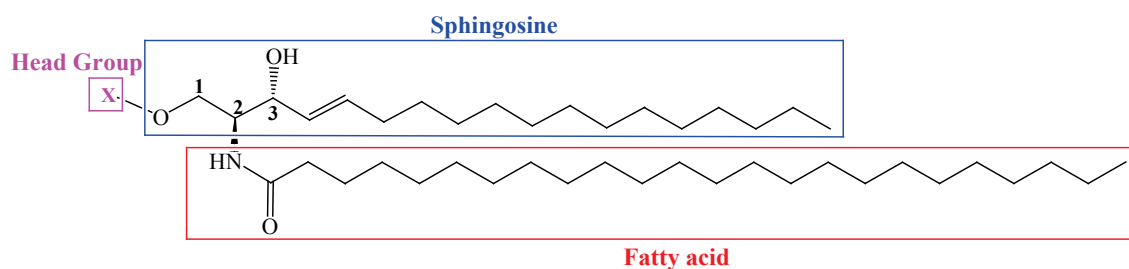
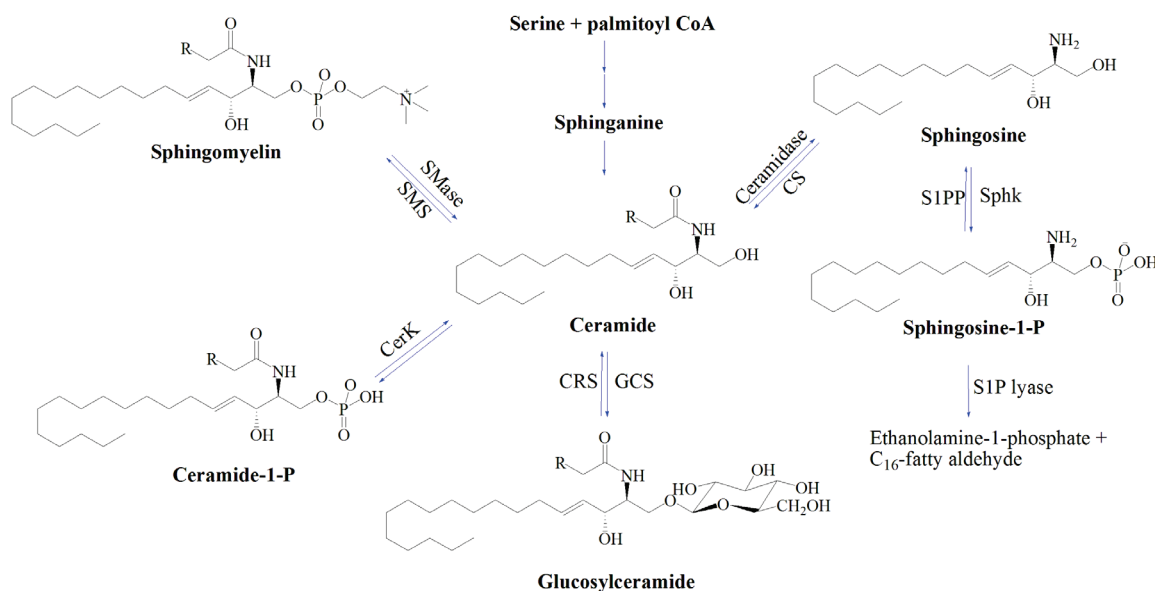


Figure 1.1. General structure of sphingolipids.

Sphingolipids metabolism, as shown in **Scheme 1.1**, involves several intermediate metabolites, many of which have distinctive biological activities (Pyne and Pyne 2000,

Merrill 2002, Spiegel and Milstien 2003, Ogretmen and Hannun 2004, Hannun and Obeid 2008, Wymann and Schneider 2008). The reviews typically describe the *de novo* biosynthesis of SP beginning with condensation of L-serine and palmitoyl-CoA by serine palmitoyltransferase at the cytoplasmic face of the endoplasmic reticulum (ER). After formation in ER, ceramide (Cer) is translocated into Golgi apparatus, where it is converted to sphingomyelin (SM) by sphingomyelin synthase on the lumen side of the Golgi. Cer is also converted to glucosylceramide (GlcCer) mediated by glucosylceramide synthase (GCS) on the cytosolic surface of the Golgi. Cer can also be phosphorylated by ceramide kinase (CerK) into ceramide-1-phosphate (C1P). After formation, SM is translocated into the plasma membrane, where it can be hydrolyzed back into Cer, and then catalyzed by acid and neutral sphingomyelinase (SMase). Cer can be broken down by one of many ceramidases (CDase), leading to the formation of SP in endosome. SP is then phosphorylated to sphingosine 1-phosphate (S1P) by one of two sphingosine kinases (SK1 and SK2), or acylated back to pro-apoptotic C16-ceramide (R is C₁₄H₂₉ in **Scheme 1.1**) via ceramide synthase (CS) in the mitochondria to lead to downstream activation of caspases and apoptosis (Pyne and Pyne 2000, Kroesen, Pettus et al. 2001, Spiegel and Milstien 2003).



Scheme 1.1. Pathway of sphingolipid metabolism.

Cer has been involved in regulation of anti-proliferative and apoptotic responses in various cancer cells, and proposed as a potential new class of chemotherapeutic agent (Hannun and Obeid 2002, Ogretmen and Hannun 2004, Reynolds, Maurer et al. 2004). However, its metabolites GlcCer, C1P and S1P promote cell proliferation, as opposed to apoptosis, which result in the development of a multidrug resistance in many cancer cells (Ogretmen and Hannun 2004, Reynolds, Maurer et al. 2004). Approaches to elevate tumor Cer levels have been reviewed by Radin (Radin 2003). This includes (1) introducing exogenous Cer or analogues to mimic Cer and produce apoptosis; (2) accelerating *de novo* synthesis of Cer; (3) stimulating the hydrolysis of SM and GlcCer back into Cer; (4) inhibiting the conversion of Cer to GlcCer, C1P, SM and S1P by blocking relevant enzymes; and (5) elevating Cer level in tumor by radiation. The interrelated network of Cer and its metabolites suggest that blocking or stimulating one or

two of the pathways in Cer metabolism is very likely to fail in anti-tumor treatment. Because, although elevated Cer levels produce apoptosis, the conversion of Cer to other metabolites leads to cell proliferation. While some tumor cells will undergo apoptosis, other tumor cells will adapt and find alternative pathways and ultimately proliferate (Radin 2003). Thus multiple pathways will need to be controlled using many different agents.

Sphingosine, the backbone of sphingolipids, has also been indicated to have significant biological activity. For example, sphingosine is an inhibitor of extracellular signal-regulated kinase signaling in airway smooth muscle cells (Tolan, Conway et al. 1996) and it may also inhibit protein kinase C to suppress the insulin-like effects of growth hormone in rat adipocytes (Smal and Demeyts 1989).

S1P has been reported to act as an extracellular mediator and intercellular second messenger, and therefore has become a target in drug development (Pyne and Pyne 2000, Spiegel and Milstien 2002, Huwiler and Pfeischieter 2008, Pyne and Pyne 2010). S1P formed intracellularly from SP by SK is implicated in various stages of cancer pathogenesis, including an anti-apoptotic phenotype, metastasis and escape from senescence (Ogretmen and Hannun 2004). Therefore, SK inhibitors have been proposed as potential anti-cancer agents (Watson, Tonelli et al. 2013). For example, a selective SK1 inhibitor *BLM-258* reported by Paugh et al. could integrate multiple molecular therapeutic targets in human leukemia (Paugh, Paugh et al. 2008). Also, inhibition of SK1 has been reported to reduce gastric and mammary adenocarcinoma tumor growth in

mice (French, Schrecengost et al. 2003). Sphingosine analogues such as DMS (*N, N*-dimethylsphingosine) (Yatomi, Ruan et al. 1996, Edsall, Van Brocklyn et al. 1998) and sphingamine (*D, L*-threo-dihydrosphingosine) (Ahn, Chang et al. 2006, Ahn and Schroeder 2010) have been developed to serve as pharmacological inhibitors of SK. FTY720 (fingolimod) directly inhibits SK1 activity and is reported to decrease metastasis in a breast cancer mouse model (Pyne, Bittman et al. 2011). Antoon et al. reported a selective SK2 inhibitor ABC294640 which has therapeutic potential in the treatment of chemo and endocrine therapy resistant human breast cancer (Antoon, White et al. 2011).

S1P could also be translocated into the extracellular side of the cell, where it functions as a ligand and binds to five S1P specific G-protein-coupled receptors (GPCRs) S1PR₁₋₅ of the endothelial differentiation gene (EDG) family (Rosen and Goetzl 2005, Kim, Takabe et al. 2009, Pyne and Pyne 2010). The binding of S1P with its receptors could promote downstream regulation and activation of SK to synthesize more S1P in intracellular side of the cell (Taha, Hannun et al. 2006). S1P- S1PR₁₋₅ regulatory systems could therefore be novel targets for cancer research (Rosen and Goetzl 2005, Rivera, Proia et al. 2008). Many synthetic chemical modulators of S1P receptors have been reported by Marsolais and Rosen (Marsolais and Rosen 2009, Marsolais, Yagi et al. 2009).

The Cer-SP-S1P rheostat model was first proposed by Cuvillier (Cuvillier, Pirianov et al. 1996), which is based on the fact that ceramide/SP and S1P elicit opposing cellular responses. For example, ceramide and sphingosine are involved in the regulation of anti-

proliferative and apoptotic responses in various cancer cells (Hannun and Obeid 2002, Ogretmen and Hannun 2004), while S1P leads to cell proliferation, inflammation and is referred to as a tumor-promoting lipid (Spiegel and Milstien 2003, Milstien and Spiegel 2006, Wymann and Schneider 2008, Pyne and Pyne 2010). The Cer-SP-S1P rheostat model predicts that the balance between ceramide and S1P may determine the physiological fate of the cell. The key evidence thereof is that ceramide induced cell apoptosis is suppressed by exogenous increase of S1P or sphingosine kinase activated endogenous increase of S1P (Cuvillier, Pirianov et al. 1996, Pyne and Pyne 2000).

Current articles should be consulted for more details related to sphingolipids metabolism (Divecha and Irvine 1995, Kolesnick, Goni et al. 2000, Pyne and Pyne 2000, Shayman 2000, Hannun and Obeid 2002, Merrill 2002, van Meer and Lisman 2002, Spiegel and Milstien 2003, Ogretmen and Hannun 2004, Rosen and Goetzl 2005, Taha, Hannun et al. 2006, Rivera, Proia et al. 2008, Ader, Malavaud et al. 2009, Fyrst and Saba 2010, Pyne and Pyne 2010).

1.2. Structure-activity relationship between sphingolipid metabolites and enzymes

The structure-activity relationship (SAR) relates the effect of the functional groups and their structural modification in the drug to its biological activity. SAR is a widely employed approach in both pharmaceutical research and the drug design (McKinney, Richard et al. 2000, Hajduk, Huth et al. 2005). SAR of sphingosine analogues on ceramidase and S1P analogues on sphingosine 1-phosphate receptor have been

investigated, respectively, by Usta et al. and Lim et al. (Usta, Bawab et al. 2001, Lim, Park et al. 2004). The critical SARs of analogues with enzymes are described below.

1.2.1. C3-Hydroxyl group

The C3 hydroxyl group plays a very important role in the interaction and recognition of sphingosine analogues with ceramidase. When C3-hydroxyl group was methylated, the potency of D-erythro-sphingosine as an inhibitor decreased severely. Moreover, (2S)-3-keto-sphingosine showed significant loss of inhibition to ceramidase in comparison to D-*erthyro*-sphingosine. These findings suggest the C3-hydroxyl group plays a critical role in the specific binding of sphingosine analogues to ceramidase (Usta, Bawab et al. 2001).

1.2.2. C2-Amino group

N-methylation of the C2-NH of D-*erthyro*-ceramide caused loss of interaction of ceramide with ceramidase. Also, N-methylation of sphingosine attenuated inhibition by sphingosine, and N,N-dimethylation of sphingosine resulted in nearly complete loss of activity. Since N-methylated ceramide and N,N-dimethyl sphingosine both lack an N-H bond, the results indicate that the hydrogen donor capacity on the C2-amino group of either ceramide or sphingosine is essential for interaction with ceramidase (Usta, Bawab et al. 2001).

1.2.3. *trans*-Configured C4-C5 double bond

In the binding of ceramide/sphingosine analogues with ceramidase, the C4-C5 double bond plays a significant role. Reduction of the C4-C5 double bond in ceramide decreased significantly its activity as a substrate (Usta, Bawab et al. 2001). In the binding affinity study of S1P analogues with S1P receptor, 4,5-dihydro-S1P showed less affinity than S1P itself. This finding shows that the double bond somehow plays an important role in the binding S1P analogues with S1P receptor (Hajduk, Huth et al. 2005).

In comparison to *trans*-configured C4-C5 double bond, *cis*-*D-erythro*-ceramide did not exhibit any interaction with ceramidase. Also, the 4,5-*cis* isomer of *D-erythro*-sphingosine was only a weak inhibitor of the enzyme. The preferential requirement for the *trans* double bond is probably a consequence of a steric effect, since the *cis* double bond introduces a kink in the hydrophobic chain, preventing ceramide and sphingosine from fitting properly into the catalytic site.

1.2.4. Stereoisomers

Lim et al. studied that the interaction of S1P stereoisomers with S1P receptors. They found *D-erythro* forms of S1P have higher affinities than the other stereoisomers. The results suggest that *D-erythro* forms of S1P are very important for the specific binding to EDG/S1P receptors (Lim, Oh et al. 2003). Usta et al. claimed that all stereoisomers of both ceramide interacted with ceramidase with high affinity. However, only *D-erythro* forms of ceramide functioned as a substrate (Usta, Bawab et al. 2001), suggesting that the

D-erythro form retains a unique configuration for catalysis but not for binding. Similarly, stereochemistry had no impact on the ability of sphingosine analogues to inhibit the enzyme, consistent with the conclusion that interaction with ceramidase is not stereospecific.

1.2.5. Aliphatic tail positively interacts with hydrophobic area.

Lim studied the effect of the aliphatic tail of S1P analogues on the interaction with S1P receptors. S1P analogue with *m*-alkylphenyl group instead of the aliphatic tail was found to have no impact on the binding affinity with S1P receptors. This finding together suggests that the aliphatic tail of S1P analogues positively interact with the hydrophobic area of S1P receptors, which is consistent with their computational model study (Lim, Park et al. 2004).

In sphingosine structure based drugs design, the above findings provide the basis for the modification of the sphingolipid metabolites and determine how these changes may affect biological activity. Further modifications could focus on introduction of substituents into C1, C2, C4 and C5 positions of sphingosine, which could affect the potency, selectivity, duration of action, toxicity and stability of the sphingosine analogues.

1.3. Current approaches to synthesize sphingosine and its analogues

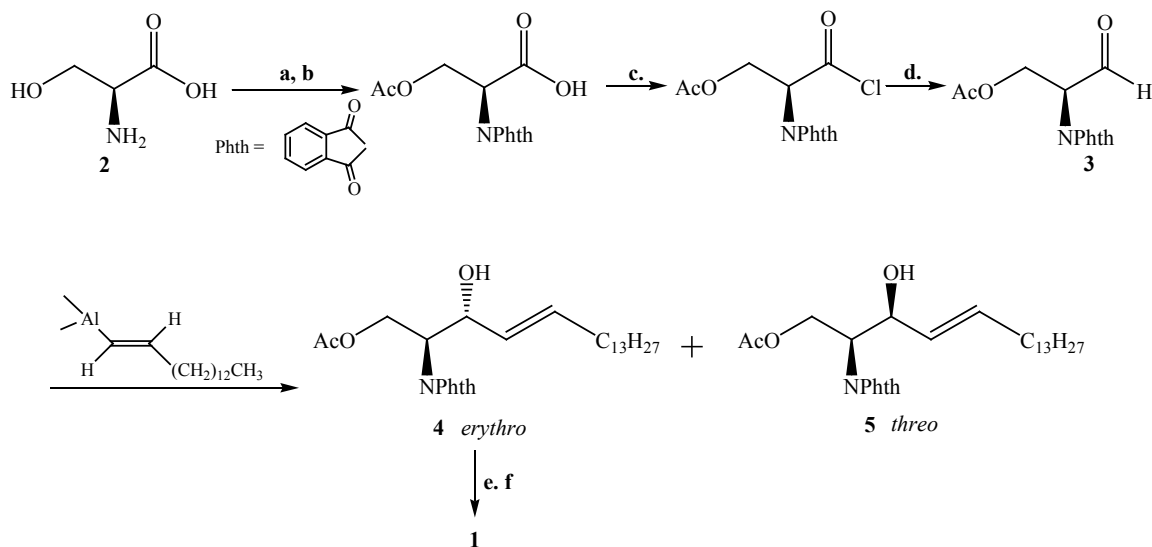
Since the first preparation of sphingosine in 1953 by Shapiro and Segal (Shapiro and Segal 1954), more than 70 sphingosine syntheses have been developed. The most significant approaches were thoroughly reviewed by Devant in 1992 (Devant 1992) and Koskinen and Koskinen in 1998 (Koskinen and Koskinen 1998). This dissertation distinguishes different approaches to sphingosine synthesis depending on the starting materials and key reaction steps. The first synthetic strategy towards sphingosine was published by Shapiro et al.. They utilized a modification of the Japp-Klingemann reaction between alkyl-substituted ethyl acetoacetate and phenyl diazonium salt in the presence of ammonium chloride. *Erythro* and *threo* intermediates with a ratio of 3:2 were generated and the overall yield of (-)-(D)-*erythro*-sphingosine was 10%. A strategy published in 1957 by Grob and Gadiant started with the condensation between nitroethanol and hexadecynal (Grob and Gadiant 1957). The strategies for the formation of *trans* double bond in the sphingosine backbone include Wittig olefination between protected sugar derivatives and triphenylphosphonium ylide (Gigg and Gigg 1966, Gigg, Gigg and Warren al. 1966, Reist and Christie 1970, Schmidt and Zimmermann 1986, S Yadav, Vidyanand et al. 1993, Wild and Schmidt 1994, Chaudhari, Ajish Kumar et al. 2005), Horner-Wadsworth-Emmons olefination (Gargano and Lees 2001, Lee, Kim and Chung 2002, Lee, Lim and Park 2002, Lu and Bittman 2005), and other methods (He, Byun et al. 1999, van den Berg, Korevaar et al. 2002, Rai and Basu 2004, Singh and Han 2007, Yang and Liebeskind 2007). Some strategies employ asymmetric epoxidation (Bernet and Vasella 1983, Roush and Adam 1985, Julina, Herzig et al. 1986, Shibuya, Kawashima et

al. 1989, Takano, Iwabuchi et al. 1991, Olofsson and Somfai 2003, Torrsell and Somfai 2004, Moreno, Murruzzu et al. 2011), other epoxidation (van den Berg, Korevaar et al. 2004), and aldol reactions as key steps using titanium enolate (Solladie-Cavallo and Koessler 1994, Solladié-Cavallo and Nsenda 1998, Cai, Ling et al. 2006) and Sn(II) catalyst (Kobayashi, Hayashi et al. 1994). Yet other approaches have also been reported (Nakamura and Shiozaki 2001, Milne, Jarowicki et al. 2002, Disadee and Ishikawa 2005, Kim, Lee et al. 2006, Llaveria, Díaz et al. 2008, Morales-Serna, Llaveria et al. 2008).

One of the most popular and reliable strategies for the synthesis of sphingosine, with the specific introduction of the C1-C3 chiral motif, employs protected serine derivatives as the source of chirality. This approach will be discussed and reviewed in this dissertation in detail in chronological order.

In 1973, Newman first reported the stereoselective synthesis of sphingosine using L-serine as the chiral center, as shown in **Scheme 1.2** (Newman 1973). In this strategy, the amino and hydroxyl groups of L-serine were sequentially protected, followed by conversion of carboxyl group to the acid chloride. The acid chloride was then hydrogenated to aldehyde **3**. Aldehyde **3** then reacted with *trans*-pentadecenyldiisobutylalane to form *D-erythro-O*-acetyl-*N*-phthaloylsphingosine **4** and its *D-threo* isomer **5** in a ratio of 79:21. The isomers were separated by partition chromatography. After removal of the protecting groups, *D-erythro*-sphingosine was synthesized. However, this strategy lacks diastereoselectivity in introducing the side

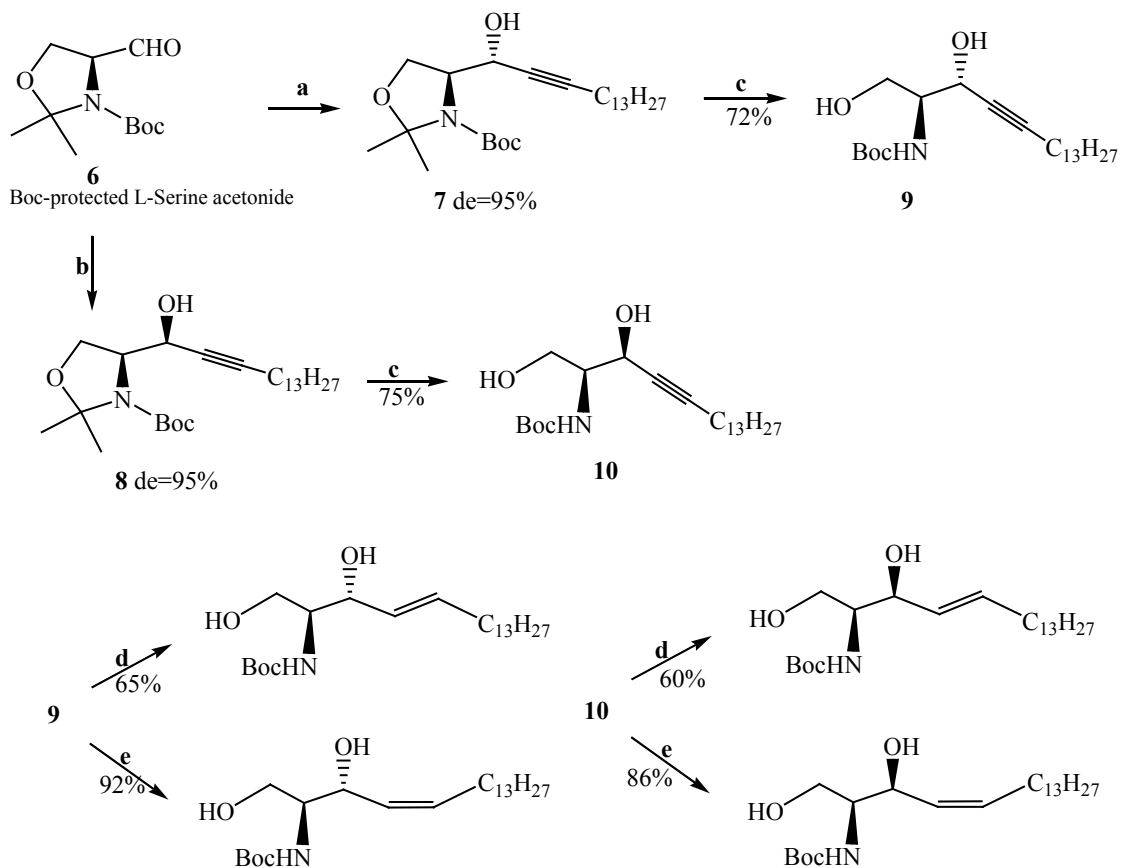
chain via alkylation (Tkaczuk and Thornton 1981, Mori and Funaki 1985, Boutin and Rapoport 1986).



Scheme 1.2. Newman's synthetic route to sphingosine. a) PhthNCO₂Et, Na₂CO₃; b) Ac₂O; c) SOCl₂, C₆H₅N; d) H₂, C₆H₅N, 40 °C, 1.5 h; e) MeOH, H⁺; f) NH₂NH₂-EtOH.

In 1984, Garner (Garner 1984, Garner and Park 1987) succeeded in preparing a configurationally stable Boc-protected serine acetonide aldehyde **6**, which has been widely employed as a chiral building block for the synthesis of natural products bearing the 2-amino-1,3-diol subunit (Liang, Andersch et al. 2001). In 1988, Herold (Herold 1988), Nimkar *et al.* (Nimkar, Menaldino et al. 1988), Radunz *et al.* (Radunz, Devant et al. 1988) and Garner *et al.* (Garner, Park et al. 1988) all started with enantiopure Boc-protected serine acetonide aldehyde (Garner's aldehyde) **6** to introduce the chiral centers. In these four publications, the most versatile synthetic scheme is that by Herold (Herold 1988), shown in **Scheme 1.3**. In this strategy, Boc-protected serine aldehyde was

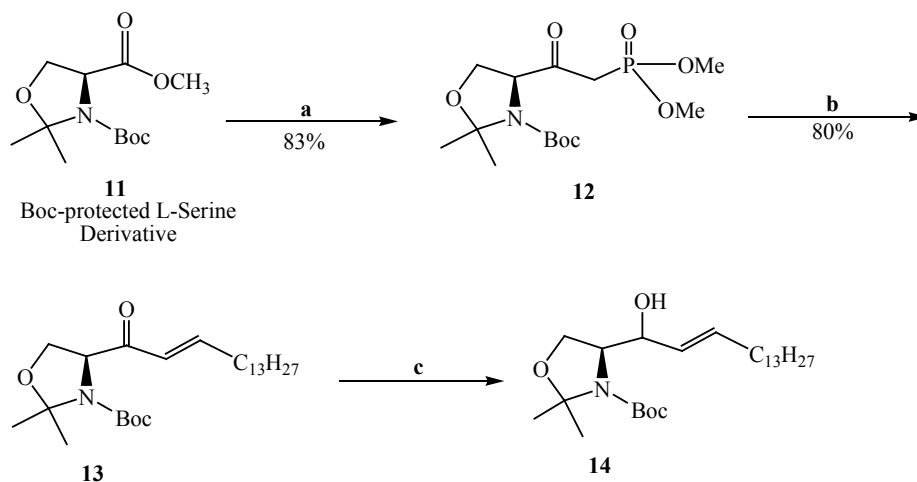
alkylated diastereoselectively by 1-pentadecynyllithium to provide either *erythro* **7** or *threo* **8** using selective reaction conditions with 95% d.e., respectively, followed by deketalization and sodium bis(2-methoxyethoxy)-aluminumhydride (Red-Al) induced reduction of the triple bond to afford a variety of pure *N*-Boc-protected sphingosine isomers. Four possible isomers of sphingosine (including the *Z*-isomer) were obtained by this strategy (Herold 1988). The *N*-Boc-protected form of sphingosine prevents oxidation of sphingosine in the presence of oxygen. The overall yield reported by Herold is 25%. In 1999, Overmeire et al. (Van Overmeire, Boldin et al. 1999) applied this strategy to synthesize ceramide analogues containing a C₇ side chain and a phenyl group substituted for the C₁₃ residue. This compound reverses the inhibitory function of FB₁ toxin on axonal growth in hippocampal neurons.



Scheme 1.3. Herold's synthetic route to sphingosine. a) 1-Pentadecynyllithium, THF, -78 °C; b) 1-Pentadecynyllithium, THF, -78 °C, ZnBr₂/Et₂O; c) Amberlyst 15/MeOH; d) Red-Al/Et₂O; e) H₂/Lindlar catalyst/EtOAc.

In 1990, Koshinen and Krische (Koskinen and Krische 1990) started with Boc-protected serine derivative **11** and employed Horner-Wadsworth-Emmons olefination to synthesize sphingosine, shown in **Scheme 1.4**. A β -ketophosphonate **12** was formed by reacting Boc-protected serine derivative **11** with the lithium compound derived from dimethyl methylphosphonate and n-butyl lithium in hexanes. Horner-Wadsworth-Emmons reaction of **12** with aliphatic aldehyde tetradecanal gave the *trans*-configured

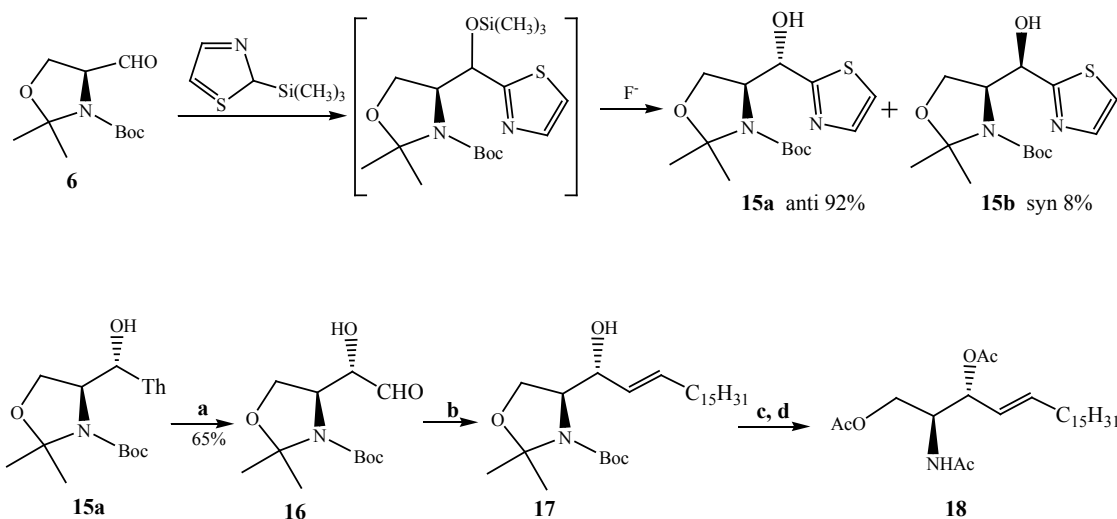
enone **13** formation of sphingosine. Then enone **13** was stereoselectively reduced to desired enol **14** by L-selectride, followed by deprotection of the amino and hydroxyl functions to afford sphingosine. Although this modified Horner-Wadsworth-Emmons reaction on a serine-derived ketophosphonate provided a mild protocol to produce the C4-C5 *trans* alkene, the author did not report the diastereomeric excess. Poor diastereomeric excess was reported by Chung and Lee for the reduction of enone to enol using L-selectride (Chung and Lee 1999).



Scheme 1.4. Koshinen's synthetic route to sphingosine. a) $(\text{MeO})_2\text{P}(=\text{O})\text{-CH}_2\text{-Li}^+$, THF; b) $\text{C}_{13}\text{H}_{27}\text{CHO}$, K_2CO_3 , CH_3CN ; c) L-selectride, THF.

In 1988 and 1990, Dondoni et al. (Dondoni, Fantin et al. 1988, Dondoni, Fantin et al. 1990) reacted 2-(trimethylsilyl)thiazole to Boc-protected Garner aldehyde **6**, **Scheme 1.5**, followed by *in situ* desilylation of the resulting intermediate with tetrabutylammonium fluoride, to stereoselectively give chiral building block *anti*-**15a** and *syn*-**15b** with 84% d.e.. Deblocking of the thiazole ring in **15a** by formyl using NaBH_4 provided aldehyde **16**.

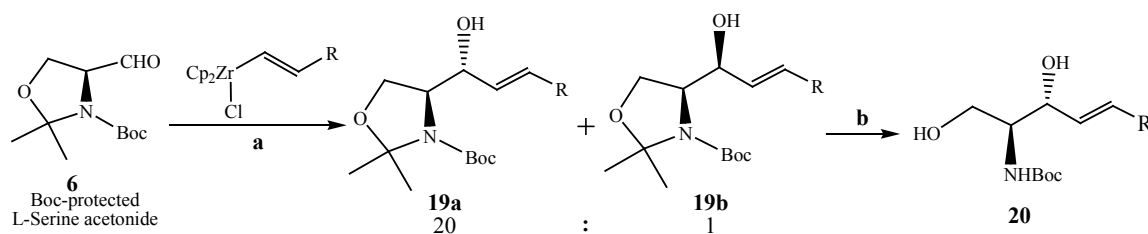
Aldehyde **6** was subjected to Wittig reaction using *n*-hexadecanilydene-triphenylphosphorane to form *trans*-configured olefin **17** and alkyl chain. After deprotection of **17** with trifluoroacetic acid-water (98:2 mixture) and acetylation of the crude reaction mixture, triacetyl-*C*₂₀-*D*-*erythro*-sphingosine **18** was afforded.



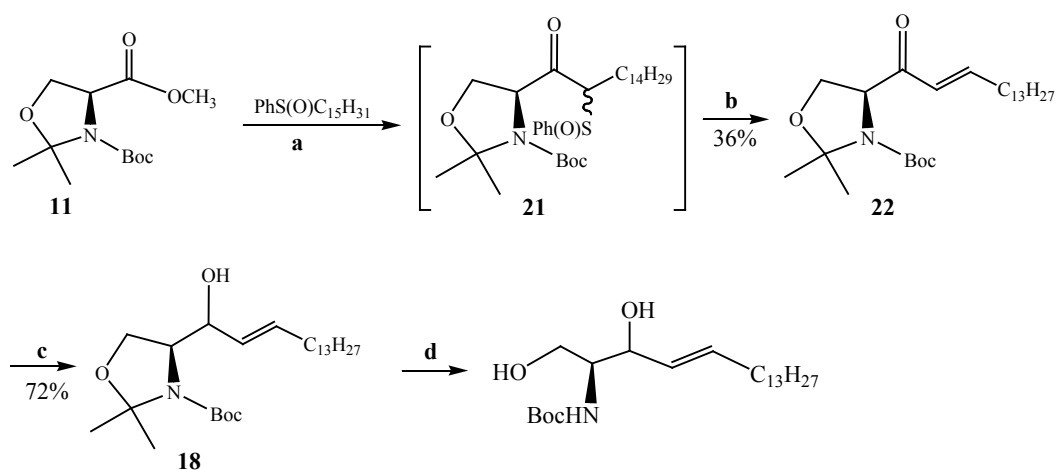
Scheme 1.5. Dondoni's synthetic route to sphingosine. Th = 2-thiazolyl; Bn = benzyl; Ac = acetyl. a) NaBH₄/MeOH, -10 °C; b) *n*-C₁₆H₃₃P⁺Ph₃Br⁻/PhLi, Et₂O-Toluene, -30 °C; c) CF₃CO₂H/H₂O; d) Ac₂O-pyridine.

In 2002, Murakami and Furusawa (Murakami and Furusawa 2002) treated aldehyde **6** with 1-alkenyl-zirconocene chloride in the presence of ZnBr₂ in THF to give the natural erythro isomers **19a** with 90% d.e., **Scheme 1.6**. Using this strategy, derivatives with a short chain and aromatic in place of the C₁₃ chain could also be synthesized (Murakami and Furusawa 2002, Murakami, Furusawa et al. 2005). In the same year, Chum et al. reacted sulfoxide to L-serine methyl ester derivative **20** to form sulfoxide intermediate **21**, which was refluxed in CCl₄ to afford **22**, **Scheme 1.7** (Chun, Li et al. 2002). The author

claimed reduction of **22** by NaBH₄ and CeCl₃ in MeOH gave diastereoselectively alcohol **18**, which then could be hydrolyzed by 1 M HCl in dioxane at 100 °C to sphingosine or its derivatives. However, the author did not report the diastereomeric excess of alcohol **18** (Chun, Li et al. 2002).

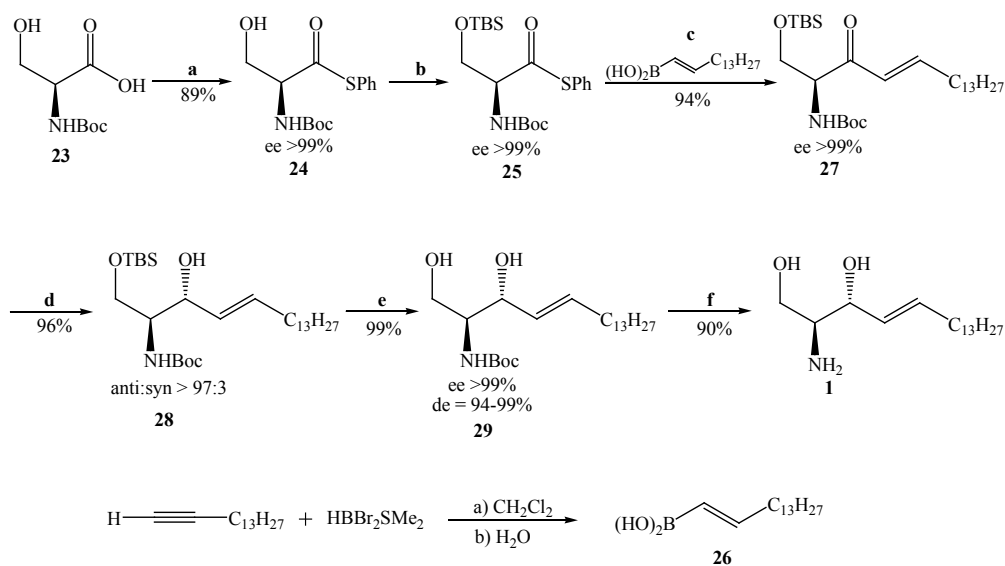


Scheme 1.6. Murakami's synthetic route to sphingosine. R = n-C₁₃H₂₇ or Ph; Cp = cyclopentadienyl; a) 25-50 mol% ZnBr₂; b) aq. AcOH, 50 °C.



Scheme 1.7. Chum's synthetic route to sphingosine. a) LDA, -78 °C, rt.; b) CCl₄, reflux; c) NaBH₄, CeCl₃, MeOH, -15 °C; d) 1 M HCl, dioxane, 100 °C.

In 2007, Yang and Liebeskind improved the L-serine based approach, which provided the highest stereoselectivity and yield among current strategies (Yang and Liebeskind 2007). In their approach (**Scheme 1.8**), they started with *N*-Boc-L-serine **23** to make *N*-Boc-*O*-TBS serine thiophenyl ester **25**. Compound **25** underwent a palladium-catalyzed copper(I)-mediated coupling with *E*-1-pentadecenyl boronic acid **26** to provide enone **27** with high enantiopurity (e.e. >99%). No *E/Z* isomerization of unsaturated ketone was observed. In turn, compound **26** was prepared by hydroboration of 1-pentadecyne with $\text{HBBr}_2 \cdot \text{SMe}_2$ followed by hydrolysis in ice-water. Enone **27** was diastereoselectively reduced by $\text{LiAl}(\text{tert-butoxy})_3\text{H}$ at -78°C , to give alcohol **28** with > 94% diastereomeric purity, followed by a simple recrystallization and final *N*-deprotection with TFA to give (-)-*D*-erythro-sphingosine **1**.



Scheme 1.8. Liebeskind's cross-coupling synthetic route starting from *N*-Boc-L-serine **23**. a). PhSH, HOBT, DCC, EtOAc; b) TBSCl, NMM, DMAP, DMF; c) 2.5 mol% $\text{Pd}_2(\text{dba})_3$, *E*-1-pentadecenyl boronic acid **26**, 20 mol% $\text{P}(\text{OEt})_3$, 1.5 equiv. CuTC ; d) $\text{LiAl}(\text{O-}t\text{-Bu})_3\text{H}$, -78°C ; e) 1 M HCl; f) TFA.

1.4. Aromatic sphingosine derivatives

Recently, many sphingosine derivatives have been developed to enhance ceramide levels in anti-cancer treatment. For example, many anticancer drugs and stress-induced agonists have been employed to increase endogenous Cer levels through *de novo* synthesis of Cer or the hydrolysis of SM. In addition, treating cancer cells *in vitro* with more easily dispersed short-chain Cers (C2 to C8-Cer) almost always produces apoptosis and cell-cycle arrest, and those exogenous Cers compete metabolically with natural Cers and their metabolites (Radin 2003). In other examples, DMS (*N, N*-dimethylsphingosine) (Yatomi, Ruan et al. 1996, Edsall, Van Brocklyn et al. 1998) and sphingamine (*D, L*-threo-dihydrosphingosine) (Ahn, Chang et al. 2006, Ahn and Schroeder 2010) have been developed and serve as pharmacological inhibitors of SK. FTY720 (fingolimod) has also been studied to directly inhibit SK1 activity, reduce tumor metastasis and increase apoptosis (Lim, Tonelli et al. 2011).

Sphingosine/ceramide analogues reportedly enhance antitumor activity and have been proposed as a potential new class of chemotherapeutic agents (Moreno, Murruzzu et al. 2011). Sphingosine with aromatic substituents in the side chain have been developed and evaluated to have stronger biological activities (Lim, Park et al. 2004). Overmeire et al. synthesized and evaluated the biological activities of several aromatic ceramide analogues **30**, which were able to reverse fumonisin B1 (FB1) inhibited ceramide synthesis (Van Overmeire, Boldin et al. 2000). Chandrasekhar et al. prepared compound **31**, which serves as a stronger sphingosine kinase inhibitor relative to the corresponding parent compounds and is an intermediate in the synthesis of (-)-Codonopsinine which has

antibiotic and hypotensive activity (Chandrasekhar, Saritha et al. 2006). Murakami et al. made aromatic sphingosine derivatives **32**, which have been suggested as EDG/S1P receptor (Endothelial Differentiation Gene family of sphingosine 1-phosphate receptors) inhibitors and block S1P mediated Ca^{2+} increase (Murakami, Furusawa et al. 2005). In the same year, Kim et al. produced sphingosine analog **SG-12**, which possesses an aromatic ring in place of the unsaturated C_{14} and lacks the C4-C5 *trans* double bond. **SG-12** exhibited specific inhibitory effects against sphingosine kinase 2 (Kim, Kim et al. 2005).

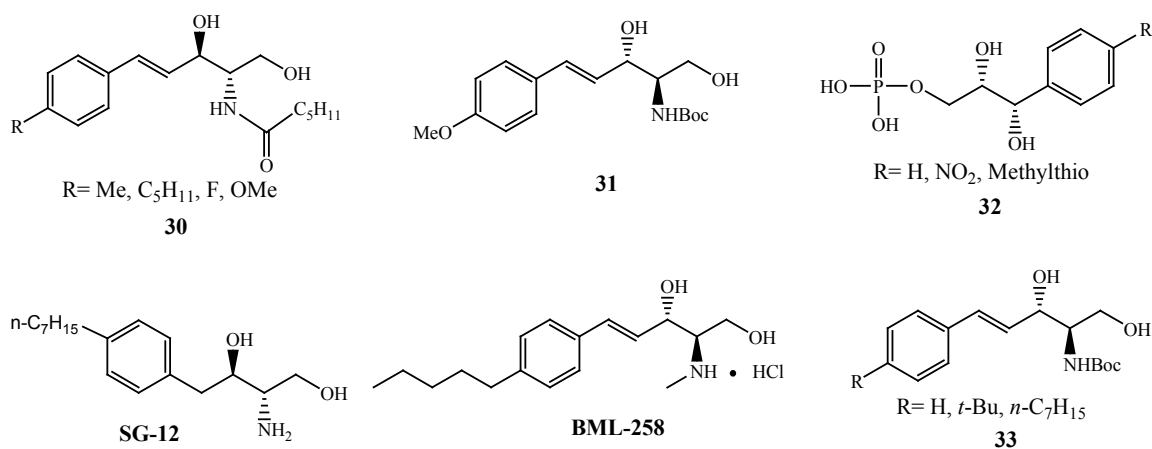


Figure 1.2. Structure of existing aromatic sphingosine analogues.

A synthesis of *BML-258* was the subject of a patent by Zipkin (Zipkin, Spiegel et al. 2010) utilizing Garner aldehyde **6** based strategies, **Scheme 1.3**. *BML-258* is a water soluble sphingosine analogue, which is evaluated as an SK1 selective inhibitor and shown to be efficacious both *in vitro* and *in vivo* (Paugh, Paugh et al. 2008, Pyne,

Bittman et al. 2011). In 2011, several aromatic sphingosine analogs **33** were synthesized by Moreno et al. (Moreno, Murruzzu et al. 2011)

To summarize, many approaches to synthesize sphingosine and its analogs have been published with good to high stereoselectivity. Among these methods, the L-serine based approach is the most commonly employed, since L-serine bears an amino group attached to the C-2 chiral center and has C-1 hydroxyl functionality. The enantiopure serine aldehyde **6** (Garner aldehyde), which is prepared through an efficient and short synthesis from L-serine, is diastereoselectively alkylated by 1-alkynyllithium compound to introduce a second chiral center (with OH attached to C-3). Sphingosine analogues are then produced by reduction of the triple bond to a double bond. However, the reaction of the Garner aldehyde is not diastereospecific when adding alkenyl- or alkynyllithium reagent to introduce the second chiral center. Rather, a mixture of *threo* and *erythro* products results, which require chiral separation. In most cases, *threo* isomer possesses a polarity similar to that of *erythro* isomer on TLC, and consequently is difficult to be separated by silica gel chromatography. What is more, the α stereocenter of the amino acid derivatives is racemized under both acidic and basic conditions. To overcome the potential configurational liability of the Garner aldehyde, Liebeskind utilized palladium-catalyzed copper(I)-mediated cross-coupling of the thiophenyl ester of *N*-Boc-*O*-TBS L-serine with *E*-1-pentadecenyl boronic acid and obtained high enantio- and diastereopurity with only traces of diastereomers detected (Yang and Liebeskind 2007). Other approaches provide less opportunity to introduce substituents into the C-1, C-2, C-4 and C-5 positions of sphingosine, which may change the affinity of sphingosine analogs for

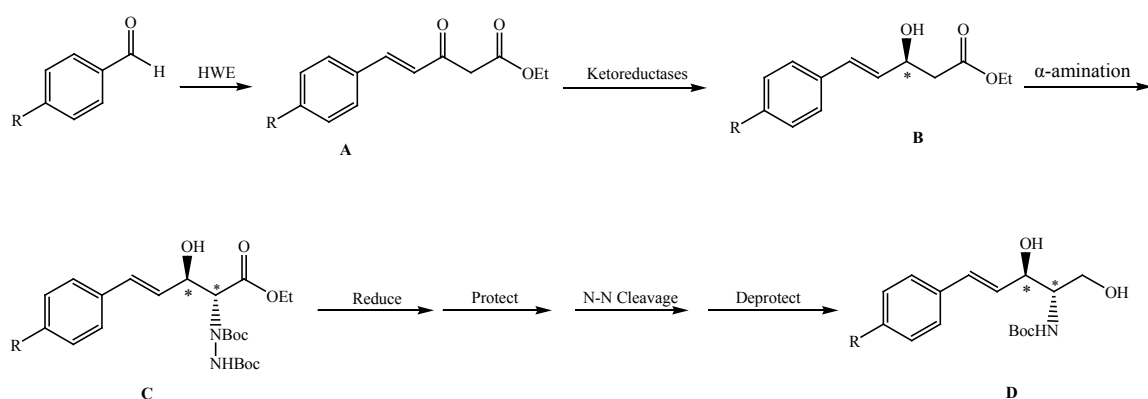
enzymes in the sphingolipid metabolism pathway and as a result affect endogenous levels of ceramide and S1P. For example, in the L-serine based approach in **Scheme 1.3**, the ability to introduce functional groups onto the double bond (C-4 and C5) is limited. This limitation arises from the reduction of the triple bond to produce exclusively the *trans* disubstituted double bond. This limitation also exists in Liebeskind's cross-coupling strategy, where *E*-1-pentadecenyl boronic acid was prepared by hydroboration of 1-pentadecyne with $\text{HBBr}_2 \cdot \text{SMe}_2$ to produce the *trans* alkene **26**.

1.5. Summary of research aims

The aim of this research is to develop a novel and effective scheme to sphingosine analogues that meet to following requirements. First, the synthetic route should be highly stereospecific, so that purification or resolution of stereoisomers is not required. Second, the synthesis should employ common and selective inexpensive reagents that provide high yields of intermediates. The synthetic route should also be scalable to provide gram quantities of sphingosine analogues. And finally the synthetic route should also offer an opportunity to introduce modified groups into the C-1, C-2, C-4 and C-5 positions.

Unlike the L-serine based synthetic routes, this research sought to prepare the fundamental stereochemical framework of a *trans* double bond and two stereocenters starting first with formation of a enantiomerically-pure chiral alcohol with a *trans* double bond. Once synthesized, the chiral alcohol was reacted to introduce the N as the second chiral center.

As shown in **Scheme 1.9**, the key entry point of this research was the synthesis of a family of aryl *trans*- γ , δ -unsaturated- β -ketoesters **A** with the stereospecific formation of a *trans* double bond using the Horner-Wadsworth-Emmons olefination. Once in hand, the *trans*- γ , δ -unsaturated- β -ketoesters were asymmetrically reduced to enantiopure *trans*- γ , δ -unsaturated- β -hydroxyesters **B** through the use of commercially available ketoreductases. Diastereospecific α -amination then introduced the second chiral center bearing the amino group in the form of hydrazine **C**, which was followed by cleavage of the N-N bond of the hydrazino by *E1cB* non-reductive elimination to yield the aromatic sphingosine derivative **D**.



Scheme 1.9. The overview for the stereospecific synthesis of sphingosine analogues in the dissertation.

Another aim of this research is development of a preparative scale synthesis of a dimer of serotonin (5-HT) 5,5'-dihydroxy-4,4'-bitryptamine (DHBT). This research is trying to resolve atropisomers of DHBT by chiral capillary electrophoresis, which need to be considered when evaluating possible neurodegenerative roles of DHBT in biological

systems. This research is not the part of the main focus of this dissertation and will be included as Appendix C.

Reference

Ader, I., Malavaud, B. and Cuvillier, O. (2009). When the sphingosine kinase 1/sphingosine 1-phosphate pathway meets hypoxia signaling: new targets for cancer therapy. *Cancer Res.* 9: 3723-3726.

Ahn, E.H., Chang, C.-C. and Schroeder, J.J. (2006). Evaluation of sphinganine and sphingosine as human breast cancer chemotherapeutic and chemopreventive agents. *Exp. Bio. Med.* 10: 1664-1672.

Ahn, E.H. and Schroeder, J.J. (2010). Induction of apoptosis by sphingosine, sphinganine, and C2-ceramide in human colon cancer cells, but not by C2-dihydroceramide. *Anticancer Res.* 7: 2881-2884.

Antoon, J.W., White, M.D., Slaughter, E.M., Driver, J.L., Khalili, H.S., Elliott, S., Smith, C.D., Burow, M.E. and Beckman, B.S. (2011). Targeting NF kappa B mediated breast cancer chemoresistance through selective inhibition of sphingosine kinase-2. *Cancer Biol. Ther.* 7: 678-689.

Bernet, B. and Vasella, A. (1983). Enantioselective synthesis of D-erythro-sphingosine. *Tetrahedron Lett.* 49: 5491-5494.

Boutin, R.H. and Rapoport, H. (1986). α -Amino acid derivatives as chiral educts for asymmetric products. Synthesis of sphingosine from α' -amino- α,β -ynones. *J. Org. Chem.* 26: 5320-5327.

Cai, Y., Ling, C.-C. and Bundle, D.R. (2006). A general, efficient and stereospecific route to sphingosine, sphinganines, phytosphingosines and their analogs. *Org. Biomol. Chem.* 6: 1140-1146.

Chandrasekhar, S., Saritha, B., Jagadeshwar, V. and Prakash, S.J. (2006). Practical and highly stereoselective approaches to the total synthesis of (-)-codonopsinine. *Tetrahedron: Asymmetry* 9: 1380-1386.

Chaudhari, V.D., Ajish Kumar, K.S. and Dhavale, D.D. (2005). An efficient synthesis of D-erythro- and D-threo-Sphingosine from D-Glucose: olefin cross-metathesis approach. *Org. Lett.* 26: 5805-5807.

Chun, J., Li, G., Byun, H.-S. and Bittman, R. (2002). A concise route to D-erythro-sphingosine from N-Boc-l-serine derivatives via sulfoxide or sulfone intermediates. *Tetrahedron Lett.* 3: 375-377.

Chung, S.-K. and Lee, J.-M. (1999). Stereoselective synthesis of β -amino alcohols: practical preparation of all four stereoisomers of N-PMB-protected sphingosine from l- and d-serine. *Tetrahedron: Asymmetry* 8: 1441-1444.

Cuvillier, O., Pirianov, G., Kleuser, B., Vanek, P.G., Coso, O.A., Gutkind, J.S. and Spiegel, S. (1996). Suppression of ceramide-mediated programmed cell death by sphingosine-1-phosphate. *Nature* 6585: 800-803.

Devant, R.M. (1992). Kontakte 11.

Disadee, W. and Ishikawa, T. (2005). Chirality transfer from guanidinium ylides to 3-alkenyl (or 3-Alkynyl) aziridine-2-carboxylates and application to the syntheses of (2R,3S)-3-hydroxyleucinate and D-erythro-sphingosine. *J. Org. Chem.* 23: 9399-9406.

Divecha, N. and Irvine, R.F. (1995). Phospholipid signaling. *Cell* 2: 269-278.

Dondoni, A., Fantin, G., Fogagnolo, M. and Medici, A. (1988). Stereoselective mono- and bis-homologation of L-serinal via 2-trimethylsilylthiazole addition. The thiazole route to amino L-sugars and D-erythro-sphingosines. *J. Chem. Soc., Chem. Commun.* 1: 10-12.

Dondoni, A., Fantin, G., Fogagnolo, M. and Pedrini, P. (1990). Stereochemistry associated with the addition of 2-(trimethylsilyl)thiazole to differentially protected α -amino aldehydes. Applications toward the synthesis of amino sugars and sphingosines. *J. Org. Chem.* 5: 1439-1446.

Dondoni, A., Fantin, G., Fogagnolo, M. and Pedrini, P. (1990). Stereochemistry associated with the addition of 2-(trimethylsilyl)thiazole to differentially protected α -amino aldehydes. Applications toward the synthesis of amino sugars and sphingosines. *J. Org. Chem.* 5: 1439-1446.

Edsall, L.C., Van Brocklyn, J.R., Cuvillier, O., Kleuser, B. and Spiegel, S. (1998). N,N-Dimethylsphingosine is a potent competitive inhibitor of sphingosine kinase but not of protein kinase C: modulation of cellular levels of sphingosine 1-phosphate and ceramide. *Biochemistry* 37: 12892-12898.

French, K.J., Schrecengost, R.S., Lee, B.D., Zhuang, Y., Smith, S.N., Eberly, J.L., Yun, J.K. and Smith, C.D. (2003). Discovery and evaluation of inhibitors of human sphingosine kinase. *Cancer Res.* 18: 5962-5969.

Fyrst, H. and Saba, J.D. (2010). An update on sphingosine-1-phosphate and other sphingolipid mediators. *Nat. Chem. Biol.* 7: 489-497.

Gargano, J.M. and Lees, W.J. (2001). Synthesis of an orthogonally protected D-(+)-erythro-sphingosine. *Tetrahedron Lett.* 34: 5845-5847.

Garner, P. (1984). Stereocontrolled addition to a penaldic acid equivalent: an asymmetric of threo- β -hydroxy-L-glutamic acid. *Tetrahedron Lett.* 51: 5855-5858.

Garner, P. and Park, J.M. (1987). The synthesis and configurational stability of differentially protected .beta.-hydroxy- α -amino aldehydes. *J. Org. Chem.* 12: 2361-2364.

Garner, P., Park, J.M. and Malecki, E. (1988). A stereodivergent synthesis of D-erythro-sphingosine and D-threo-sphingosine from L-serine. *J. Org. Chem.* 18: 4395-4398.

Gigg, J. and Gigg, R. (1966). A synthesis of phytosphingosines from D-galactose. *J. Chem. Soc. Perkin I*: 1876-1879.

Gigg, J., Gigg, R. and Warren, C.D. (1966). A synthesis of phytosphingosines from D-glucosamine. *J. Chem. Soc. Perkin I*: 1872-1876.

Grob, C.A. and Gadiant, F. (1957). Die synthese des sphingosins und seiner stereoisomeren. *Helv. Chim. Acta* 5: 1145-1157.

- Hajduk, P.J., Huth, J.R. and Fesik, S.W. (2005). Druggability indices for protein targets derived from NMR-based screening data. *J. Med. Chem.* 7: 2518-2525.
- Hannun, Y.A., Luberto, C. and Argraves, K.M. (2001). Enzymes of sphingolipid metabolism: From modular to integrative signaling. *Biochemistry* 16: 4893-4903.
- Hannun, Y.A. and Obeid, L.M. (2002). The ceramide-centric universe of lipid-mediated cell regulation: Stress encounters of the lipid kind. *J. Biol. Chem.* 29: 25847-25850.
- Hannun, Y.A. and Obeid, L.M. (2008). Principles of bioactive lipid signalling: lessons from sphingolipids. *Nat. Rev. Mol. Cell Biol.* 2: 139-150.
- He, L., Byun, H.-S., Smit, J., Wilschut, J. and Bittman, R. (1999). Enantioselective Synthesis of a novel trans double bond ceramide analogue via catalytic asymmetric dihydroxylation of an enyne. The role of the trans double bond of ceramide in the fusion of semliki forest virus with target membranes. *J. Am. Chem. Soc.* 16: 3897-3903.
- Herold, P. (1988). Synthesis of D-erythro-sphingosine and D-threo-sphingosine derivatives from L-serine. *Helv. Chim. Acta* 2: 354-362.
- Huwiler, A. and Pfeischifter, J. (2008). New players on the center stage: Sphingosine 1-phosphate and its receptors as drug targets. *Biochem. Pharmacol.* 10: 1893-1900.
- Julina, R., Herzig, T., Bernet, B. and Vasella, A. (1986). Enantioselective synthesis of D-erythro-sphingosine and of ceramide. *Helv. Chim. Acta* 2: 368-373.
- Liang, X., Andersch, J. and Bols, M. (2001). Garner's aldehyde. *J. Chem. Soc., Perkin Trans. 1* 18: 2136-2157.
- Lim, H.-S., Oh, Y.-S., Suh, P.-G. and Chung, S.-K. (2003). Syntheses of sphingosine-1-phosphate stereoisomers and analogues and Their interaction with EDG receptors. *Bioorg. Med. Chem. Lett.* 2: 237-240.
- Lim, H.-S., Park, J.-J., Ko, K., Lee, M.-H. and Chung, S.-K. (2004). Syntheses of sphingosine-1-phosphate analogues and their interaction with EDG/S1P receptors. *Bioorg. Med. Chem. Lett.* 10: 2499-2503.
- Lim, K.G., Tonelli, F., Li, Z.G., Lu, X.Q., Bittman, R., Pyne, S. and Pyne, N.J. (2011). FTY720 Analogues as Sphingosine Kinase 1 Inhibitors enzyme inhibition kinetics, allosterism, proteasomal degradation, and actin rearrangement in MCF-7 breast cancer cells. *J. Biol. Chem.* 21: 18633-18640.
- Lu, X. and Bittman, R. (2005). Efficient and versatile synthesis of (2S,3R)-sphingosine and its 2-azido-3-O-benzylsphingosine analogue. *Tetrahedron Lett.* 11: 1873-1875.
- Kim, J.-W., Kim, Y.-W., Inagaki, Y., Hwang, Y.-A., Mitsutake, S., Ryu, Y.-W., Lee, W.K., Ha, H.-J., Park, C.-S. and Igarashi, Y. (2005). Synthesis and evaluation of sphingoid analogs as inhibitors of sphingosine kinases. *Bioorg. Med. Chem.* 10: 3475-3485.
- Kim, R.H., Takabe, K., Milstien, S. and Spiegel, S. (2009). Export and functions of sphingosine-1-phosphate. *Biochim. Biophys. Acta-Mol. Cell Biol. Lipids* 7: 692-696.

- Kim, S., Lee, S., Lee, T., Ko, H. and Kim, D. (2006). Efficient synthesis of D-erythro-sphingosine and D-erythro-azidosphingosine from d-ribo-phytosphingosine via a cyclic sulfate intermediate. *J. Org. Chem.* 22: 8661-8664.
- Kobayashi, S., Hayashi, T. and Kawasuji, T. (1994). Enantioselective syntheses of D-erythro-sphingosine and phytosphingosine from simple achiral aldehydes using catalytic asymmetric aldol reactions as key steps. *Tetrahedron Lett.* 51: 9573-9576.
- Kolesnick, R.N., Goñi, F.M. and Alonso, A. (2000). Compartmentalization of ceramide signaling: physical foundations and biological effects. *J. Cell. Physiol.* 3: 285-300.
- Koskinen, A.M.P. and Krische, M.J. (1990). γ -amino- β -keto phosphonates in synthesis- synthesis of the sphingosine skeleton. *Synlett* 11: 665-666.
- Koskinen, P.M. and Koskinen, A.M.P. (1998). Sphingosine, an enigmatic lipid: A review of recent literature syntheses. *Synth.-Stuttgart* 8: 1075-1091.
- Kroesen, B.J., Pettus, B., Luberto, C., Busman, M., Sietsma, H., de Leij, L. and Hannun, Y.A. (2001). Induction of apoptosis through B-cell receptor cross-linking occurs via de novo generated C16-ceramide and involves mitochondria. *J. Biol. Chem.* 17: 13606-13614.
- Lee, H.K., Kim, E.-K. and Pak, C.S. (2002). Facile transformation of 2-azetidiones to unsaturated ketones: application to the formal synthesis of sphingosine and phytosphingosine. *Tetrahedron Lett.* 52: 9641-9644.
- Lee, J.-M., Lim, H.-S. and Chung, S.-K. (2002). A short and efficient stereoselective synthesis of all four diastereomers of sphingosine. *Tetrahedron: Asymmetry* 4: 343-347.
- Lim, H.-S., Park, J.-J., Ko, K., Lee, M.-H. and Chung, S.-K. (2004). Syntheses of sphingosine-1-phosphate analogues and their interaction with EDG/S1P receptors. *Bioorg. Med. Chem. Lett.* 10: 2499-2503.
- Llaveria, J., Díaz, Y., Matheu, M.I. and Castellón, S. (2008). An efficient and general enantioselective synthesis of sphingosine, phytosphingosine, and 4-substituted derivatives. *Org. Lett.* 1: 205-208.
- Marsolais, D. and Rosen, H. (2009). Chemical modulators of sphingosine-1-phosphate receptors as barrier-oriented therapeutic molecules. *Nat. Rev. Drug Discovery.* 4: 297-307.
- McKinney, J.D., Richard, A., Waller, C., Newman, M.C. and Gerberick, F. (2000). The practice of structure activity relationships (SAR) in toxicology. *Toxicol. Sci.* 1: 8-17.
- Merrill, A.H. (2002). De novo sphingolipid biosynthesis: A necessary, but dangerous, pathway. *J. Biol. Chem.* 29: 25843-25846.
- Merrill, A.H., Wang, M.D., Park, M. and Sullards, M.C. (2007). (Glyco)sphingolipidology: an amazing challenge and opportunity for systems biology. *Trends Biochem. Sci.* 10: 457-468.
- Milne, J.E., Jarowicki, K., Kocienski, P.J. and Alonso, J. (2002). Synthesis of D-erythro-sphingosine and D-erythro-ceramide. *Chem. Commun.* 5: 426-427.

- Milstien, S. and Spiegel, S. (2006). Targeting sphingosine-1-phosphate: A novel avenue for cancer therapeutics. *Cancer Cell* 3: 148-150.
- Morales-Serna, J.A., Llaveria, J., Diaz, Y., Matheu, M.I. and Castillon, S. (2008). Asymmetric sulfur ylide based enantioselective synthesis of D-erythro-sphingosine. *Org. Biomol. Chem.* 24: 4502-4504.
- Moreno, M., Murruzzu, C. and Riera, A. (2011). Enantioselective synthesis of sphingadienines and Aaromatic ceramide analogs. *Org. Lett.* 19: 5184-5187.
- Mori, K. and Funaki, Y. (1985). Synthesis of (4E,8E,2S,3R,2'R-N-2'-hydroxyhexadecanoyl-1-O- β -D-glucopyranosyl-9-methyl-4,8-sphingadienine, the fruiting-inducing cerebroside in a basidiomycete schizophyllum commune. *Tetrahedron* 12: 2379-2386.
- Murakami, T. and Furusawa, K. (2002). Efficient stereodivergent synthesis of erythro- and threo-sphingosines: unprecedented reversal of the stereochemistry in the addition. *Tetrahedron* 45: 9257-9263.
- Murakami, T., Furusawa, K., Tamai, T., Yoshikai, K. and Nishikawa, M. (2005). Synthesis and biological properties of novel sphingosine derivatives. *Bioorg. Med. Chem. Lett.* 4: 1115-1119.
- Nakamura, T. and Shiozaki, M. (2001). Stereoselective synthesis of D-erythro-sphingosine and l-lyxo-phytosphingosine. *Tetrahedron* 44: 9087-9092.
- Newman, H. (1973). Stereoselective synthesis of D-erythro-sphingosine. *J. Am. Chem. Soc.* 12: 4098-4099.
- Nimkar, S., Menaldino, D., Merrill, A.H. and Liotta, D. (1988). A stereoselective synthesis of sphingosine, a protein kinase c inhibitor. *Tetrahedron Lett.* 25: 3037-3040.
- Ogretmen, B. and Hannun, Y.A. (2004). Biologically active sphingolipids in cancer pathogenesis and treatment. *Nat. Rev. Cancer* 8: 604-616.
- Olofsson, B. and Somfai, P. (2003). Divergent Synthesis of D-erythro-sphingosine, l-threo-sphingosine, and their regioisomers. *J. Org. Chem.* 6: 2514-2517.
- Paugh, S.W., Paugh, B.S., Rahmani, M., Kapitonov, D., Almenara, J.A., Kordula, T., Milstien, S., Adams, J.K., Zipkin, R.E., Grant, S. and Spiegel, S. (2008). A selective sphingosine kinase 1 inhibitor integrates multiple molecular therapeutic targets in human leukemia. *Blood* 4: 1382-1391.
- Pyne, N.J. and Pyne, S. (2010). Sphingosine 1-phosphate and cancer. *Nat. Rev. Cancer* 7: 489-503.
- Pyne, S., Bittman, R. and Pyne, N.J. (2011). Sphingosine kinase inhibitors and cancer: seeking the golden sword of hercules. *Cancer Res.* 21: 6576-6582.
- Pyne, S. and Pyne, N.J. (2000). Sphingosine 1-phosphate signalling in mammalian cells. *Biochem. J.* 385-402.

Radin, N.S. (2003). Killing tumours by ceramide-induced apoptosis: a critique of available drugs. *Biochem. J.* 243-256.

Radunz, H.-E., Devant, R.M. and Eiermann, V. (1988). Eine effiziente und stereoselektive Synthese von D-erythro-sphingosin. *Liebigs Ann. Chem.* 11: 1103-1105.

Rai, A.N. and Basu, A. (2004). Sphingolipid synthesis via olefin cross metathesis: preparation of a differentially protected building block and application to the synthesis of D-erythro-ceramide. *Org. Lett.* 17: 2861-2863.

Reist, E. and Christie, P. (1970). Synthesis of trans- and cis-Sphingosine. *J. Org. Chem.* 12: 4127-4130.

Reynolds, C.P., Maurer, B.J. and Kolesnick, R.N. (2004). Ceramide synthesis and metabolism as a target for cancer therapy. *Cancer Lett.* 2: 169-180.

Rivera, J., Proia, R.L. and Olivera, A. (2008). The alliance of sphingosine-1-phosphate and its receptors in immunity. *Nat. Rev. Immunol.* 10: 753-763.

Rosen, H. and Goetzl, E.J. (2005). Sphingosine 1-phosphate and its receptors: an autocrine and paracrine network. *Nat. Rev. Immunol.* 7: 560-570.

Roush, W.R. and Adam, M.A. (1985). Directed openings of 2,3-epoxy alcohols via reactions with isocyanates: synthesis of (+)-erythro-dihydrosphingosine. *J. Org. Chem.* 20: 3752-3757.

S Yadav, J., Vidyanand, D. and Rajagopal, D. (1993). Stereoselective synthesis of D(+)-erythro and L(-)-threo sphingosines from carbohydrates. *Tetrahedron Lett.* 7: 1191-1194.

Schmidt, R.R. and Zimmermann, P. (1986). Synthesis of D-erythro-sphingosines. *Tetrahedron Lett.* 4: 481-484.

Shapiro, D. and Segal, K. (1954). The synthesis of sphingosine. *J. Am. Chem. Soc.* 22: 5894-5895.

Shibuya, H., Kawashima, K., Ikeda, M. and Kitagawa, I. (1989). Synthesis of two pairs of enantiomeric C18-sphingosines. *Tetrahedron Lett.* 51: 7205-7208.

Sigal, Y.J., McDermott, M.I. and Morris, A.J. (2005). Integral membrane lipid phosphatases/phosphotransferases: common structure and diverse functions. *Biochem. J.* 281-293.

Singh, O.V. and Han, H. (2007). Stereoselective synthesis of trans-olefins by the copper-mediated SN2' reaction of vinyl oxazines with Grignard reagents. Asymmetric synthesis of D-threo-sphingosines. *Tetrahedron Lett.* 13: 2345-2348.

Smal, J. and Demeys, P. (1989). Sphingosine, an inhibitor of protein kinase-C, suppresses the insulin-like effects of growth-hormone in rat adipocytes. *Proc. Natl. Acad. Sci. U. S. A.* 12: 4705-4709.

Solladié-Cavallo, A. and Nsenda, T. (1998). A four-step synthesis of erythro-m-chloro-3-hydroxytyrosine ethyl ester enantiomerically pure. *Tetrahedron Lett.* 15: 2191-2194.

- Solladie-Cavallo, A. and Koessler, J.L. (1994). A four-Step diastereoselective synthesis of D-erythro-sphingosine by an enantioselective aldol reaction using a titanium enolate derived from a chiral iminoglycinate. *J. Org. Chem.* 11: 3240-3242.
- Spiegel, S. and Milstien, S. (2002). Sphingosine 1-phosphate, a key cell signaling molecule. *J. Biol. Chem.* 29: 25851-25854.
- Spiegel, S. and Milstien, S. (2003). Sphingosine-1-phosphate: an enigmatic signalling lipid. *Nat. Rev. Mol. Cell Biol.* 5: 397-407.
- Shayman, J.A. (2000). Sphingolipids. *Kidney Int.* 1: 11-26.
- Taha, T.A., Hannun, Y.A. and Obeid, L.M. (2006). Sphingosine kinase: Biochemical and cellular regulation and role in disease. *J. Biochem. Mol. Biol.* 2: 113-131.
- Takano, S., Iwabuchi, Y. and Ogasawara, K. (1991). An enantio- and stereo-controlled synthesis of L-erythro- and D-threo-C18-sphingosines via the anomalous version of the katsuki-sharpless asymmetric epoxidation reaction. *J. Chem. Soc., Chem. Commun.* 12: 820-821.
- Tkaczuk, P. and Thornton, E.R. (1981). Useful syntheses of erythro- and threo-N-oleoyl-D-sphingosines (ceramides) and galactosylceramides (cerebrosides) from L-serine. *J. Org. Chem.* 22: 4393-4398.
- Tolan, D., Conway, A.M., Steele, L., Pyne, S. and Pyne, N.J. (1996). The identification of DL-threo dihydrosphingosine and sphingosine as novel inhibitors of extracellular signal-regulated kinase signalling in airway smooth muscle. *Br. J. Pharmacol.* 2: 185-186.
- Torsell, S. and Somfai, P. (2004). A practical synthesis of d-erythro-sphingosine using a cross-metathesis approach. *Org. Biomol. Chem.* 11: 1643-1646.
- Usta, J., Bawab, S.E., Roddy, P., Szulc, Z.M., Hannun, Y.A. and Bielawska, A. (2001). Structural requirements of ceramide and sphingosine based inhibitors of mitochondrial ceramidase. *Biochemistry* 32: 9657-9668.
- van den Berg, R.J.B.H.N., Korevaar, C.G.N., Overkleeft, H.S., van der Marel, G.A. and van Boom, J.H. (2004). Effective, high-Yielding, and stereospecific total synthesis of D-erythro-(2R,3S)-sphingosine from D-ribo-(2S,3S,4R)-phytosphingosine. *J. Org. Chem.* 17: 5699-5704.
- van den Berg, R.J.B.H.N., Korevaar, C.G.N., van der Marel, G.A., Overkleeft, H.S. and van Boom, J.H. (2002). A simple and low cost synthesis of D-erythro-sphingosine and D-erythro-azidosphingosine from D-ribo-phytosphingosine: glycosphingolipid precursors. *Tetrahedron Lett.* 46: 8409-8412.
- van Meer, G. and Lisman, Q. (2002). Sphingolipid transport: rafts and translocators. *J. Biol. Chem.* 29: 25855-25858.
- Van Overmeire, I., Boldin, S.A., Dumont, F., Van Calenbergh, S., Slegers, G., De Keukeleire, D., Futerman, A.H. and Herdewijn, P. (1999). Effect of aromatic short-chain analogues of ceramide on axonal growth in hippocampal neurons. *J. Med. Chem.* 14: 2697-2705.

Van Overmeire, I., Boldin, S.A., Venkataraman, K., Zisling, R., De Jonghe, S., Van Calenbergh, S., De Keukeleire, D., Futerman, A.H. and Herdewijn, P. (2000). Synthesis and biological evaluation of ceramide analogues with substituted aromatic rings or an allylic fluoride in the sphingoid moiety. *J. Med. Chem.* 22: 4189-4199.

Watson, D.G., Tonelli, F., Alossaimi, M., Williamson, L., Chan, E., Gorshkova, I., Berdyshev, E., Bittman, R., Pyne, N.J. and Pyne, S. (2013). The roles of sphingosine kinases 1 and 2 in regulating the Warburg effect in prostate cancer cells. *Cell Signal* 4: 1011-1017.

Wild, R. and Schmidt, R.R. (1994). Sphingosine and phytosphingosine from D-threose synthesis of a 4-keto-ceramide. *Tetrahedron: Asymmetry* 11: 2195-2208.

Wymann, M.P. and Schneider, R. (2008). Lipid signalling in disease. *Nat. Rev. Mol. Cell Biol.* 2: 162-176.

Yang, H. and Liebeskind, L.S. (2007). A concise and scalable synthesis of high enantiopurity (-)-D-erythro-sphingosine using peptidyl thiol ester-boronic acid cross-coupling. *Org. Lett.* 16: 2993-2995.

Yatomi, Y., Ruan, F., Megidish, T., Toyokuni, T., Hakomori, S.-i. and Igarashi, Y. (1996). N,N-dimethylsphingosine inhibition of sphingosine kinase and sphingosine 1-phosphate activity in human platelets. *Biochem.* 2: 626-633.

Zipkin, R.E., Spiegel, S. and Adams, J.K. (2010). Novel sphingosine kinase type 1 inhibitors, compositions and processes for using same. US. 12387228.

Chapter 2

Stereoselective Synthesis of Aryl γ, δ -unsaturated β -hydroxyesters by Ketoreductases¹

2.1. Introduction

Enantiomerically pure γ, δ -unsaturated- β -hydroxyesters and their derivatives are important chiral building blocks for synthesis of many biologically active compounds, pharmaceutical products and their intermediates, such as (-)-CP₂-Disorazole C₁ (Hopkins, Schmitz et al. 2011), turnagainolides A and B (Li, Carr et al. 2011), epothilone (Reiff, Nair et al. 2004), and Seimatopolide A (Schmidt, Kunz et al. 2012). Many traditional methods have been employed to make β -hydroxyesters asymmetrically, for example, (1) enantioselective Mukaiyama aldol addition between aldehyde and methyl (ethyl) acetate *O*-Silyl enolates with a chiral Ti(IV) complexes as catalyst (Smrčina, Lorenc et al. 1991, Carreira, Singer et al. 1994, Mukaiyama 2004); (2) enantioselective ruthenium-catalyzed hydrogenation of saturated α -ketoesters (Rimoldi, Pellizzoni et al. 2011), β -ketoesters (Taber and Silverberg 1991, Greck, Bischoff et al. 1993, Genêt, Pfister et al. 1994, Genêt, Pinel et al. 1994, Burk, Harper et al. 1995, Girard, Greck et al. 1996, Zhang, Qian et al. 2000, Zhou, Tang et al. 2002, Hu, Ngo et al. 2004, Seashore-Ludlow, Saint-Dizier et al. 2012) and α, β -unsaturated carbonyls (Ohkuma, Koizumi et al. 1998, Arai, Azuma et al.

¹ Zhipeng Dai, Kate Guillemette, and Thomas K. Green. (2013). *Journal of Molecular Catalysis B: Enzymatic*. 97: 264-269

2008); and (3) chiral oxazaborolidine-catalyzed reduction of prochiral ketones, cyclic and acyclic α , and β -enones (Corey, Bakshi et al. 1987, Corey, Bakshi and Shibata et al. 1987, Mathre, Thompson et al. 1993, Corey and Helal 1998, Kawanami, Murao et al. 2003).

All of these methods, while potentially providing high enantioselectivity, have disadvantages. The Mukaiyama aldol methods often require an expensive chiral ligand (e.g. BINAP) and multiple steps to make the catalyst (Smrčina, Lorenc et al. 1991). While ruthenium-catalyzed hydrogenation has been shown to selectively reduce the carbonyl of β -ketoesters chemoselectively in the presence of a nonconjugated carbon-carbon double bond (Taber and Silverberg 1991, Greck, Ferreira et al. 1996), we and others (Ma, Li et al. 2012) have found that partial hydrogenation of the double bond of conjugated γ , δ -unsaturated- β -ketoesters often occurs, and is difficult to control. Recently, Ma et al. published a Ru-catalyzed hydrogenation of γ -halo- γ , δ -unsaturated- β -ketoesters in up to 97% e.e. (Ma, Li et al. 2012), where halogen at the γ -position is needed to protect the γ , δ -carbon-carbon double bond with further organometallic transformation required to remove the vinyl halide moiety. The enantioselectivity of chiral oxazaborolidines catalysts are sensitive to moisture and temperature and must be conducted under strictly anhydrous conditions and typically at low temperature (-20 °C and below). Also, the use of $\text{BH}_3\cdot\text{THF}$ (or $\text{BH}_3\cdot\text{Me}_2\text{S}$) is often incompatible with carbon-carbon double bonds. Although these chemical methods using chiral auxiliaries are frequently used, other limitations remain in many cases. The limitation arises from the incompatibility of catalytic conditions with a number of functionalities (Genêt, Pinel et al. 1994, Akutagawa 1995, Schmidt 2004) and the catalytic behavior (enantiomeric purity and productivity)

being sensitive to even slight modifications in the substances due to the change of steric and electronic properties.

With the advantages of high enantioselectivity, broader substrate acceptance, mild and environmental friendly reaction conditions, tolerance of organic solvents and easy separation, biocatalysts using whole cells and isolated enzymes have received increasing interest toward the production of optically pure β -hydroxyesters and their derivatives (Kaluzna, Matsuda et al. 2004, Zhu, Yang et al. 2006, Kalaitzakis, Kambourakis et al. 2007, Matsuda, Yamanaka et al. 2009, Turner 2009, Huisman, Liang et al. 2010). For instances, the asymmetric reduction of α - and/or β -ketoesters was evaluated by means of whole cells of *Candida parapsilosis* ATCC 7330 (on the reduction alkyl 2-oxo-4-arylbutanoates) (Baskar, Pandian et al. 2004), the recombinant *Escherichia Coli* (for the synthesis of 3-hydroxybutyrate) (Schroer, Mackfeld et al. 2007), *Chlorella strains* (toward the reduction of α -ketoesters) (Ishihara, Yamaguchi et al. 2000), yeast (reduction of α - and β -ketoesters) (Kaluzna, Matsuda et al. 2004, Rimoldi, Cesarotti et al. 2011), carbonyl reductase from *Candila magnolia* (Zhu, Yang et al. 2006), nicotinamide-dependent ketoreductases (reduction of β -ketoesters with alkyl substituents at α - or β -position) (Kambourakis and Rozzell 2004, Zhu, Mukherjee et al. 2006), and NADPH-dependent ketoreductases (toward the reduction of α -alkyl- β -ketoesters) (Kalaitzakis, Rozzell et al. 2005). What is more, *Candida parapsilosis* ATCC 7330-induced deracemisation of unsaturated aryl β -hydroxyesters to a single enantiomer has also been reported (Padhi and Chadha 2005, Saravanan, Selvakumar et al. 2012).

This chapter describes the synthesis of a series of aryl *trans*- γ , δ -unsaturated- β -hydroxyesters from aryl *trans*- γ , δ -unsaturated- β -ketoesters via the action of twenty-four isolated NAD(P)H dependent ketoreductases from Codexis. Either enantiomer of γ , δ -unsaturated β -hydroxyesters can be synthesized with high enantioselectivity (>99% e.e.) and chemoselectivity (no olefin reduction) in good to excellent yield in one step by one or more enzymes. Additionally, conversions and purifications were achieved economically, safely and readily under the enzymatic reaction condition used.

Contribution: Kate Guillemette contributed to KRED reduction of γ , δ -unsaturated β -ketoester **2C**.

2.2. Experimental

2.2.1. Materials

All chemicals were purchased from Sigma-Aldrich Chemical Company unless otherwise noted. Methylene chloride was distilled from CaCl_2 and stored over 4 Å molecular sieves. Spectroscopy grade chloroform was used for all optical rotation measurements. Cyclodextrins used for capillary electrophoresis, heptakis(2,3-di-O-methyl-6-O-sulfobutyl) cyclomaltoheptaose, sodium salt (NaSBDM- β -CD) and heptakis(2, 3-di-O-ethyl-6-O-sulfopropyl) cyclomaltoheptaose potassium salt (KSPDE- β -CD), were synthesized according to procedures reported in the literature (Kirschner, Jaramillo et al. 2008). Codex[®] KRED screening kit was purchased from Codexis, Inc. Both reconstituted KRED Recycle Mix N (containing 250 mM potassium phosphate, 2 mM

magnesium sulfate, 1.1 mM NADP⁺, 1.1 mM NAD⁺, 80 mM D-glucose, 10 U/mL glucose dehydrogenase, pH 7.0) and reconstituted KRED Recycle Mix P (containing 125 mM potassium phosphate, 1.25 mM magnesium sulfate, 1.0 mM NADP⁺, pH 7.0) are available from Codexis, Inc.. Aluminum coated silica gel WF_{254s} plates were used to monitor reactions products and flash chromatography eluents. Column chromatography was performed with silica gel SiliaFlash®P60 (40-60 μm, 230-400 mesh).

2.2.2. Instrument

¹H and ¹³C NMR spectra were recorded in CDCl₃ solution with a Varian 300 MHz instrument (300 MHz for ¹H NMR, 75 MHz for ¹³C NMR). Chemical shifts are reported in ppm relative to TMS as internal standard. HPLC was performed on Agilent 1100 series with isocratic pump and UV-visible detector. A Phenomenex® Lux 3 μ cellulose-1 column (50 x 4.60 mm) was used for the chiral separation at 23 °C. The mobile phase consisted of hexanes and isopropanol in the ratio of 90:10, and flow rate of 0.5 mL/min. Optical rotations were measured on Krüss P3000 polarimeter operating at the sodium D line 589 nm and reported as follows: $[\alpha_{589}^{23}]$, concentration (g/100ml), and solvent. Capillary electrophoresis was performed with an Agilent 3D Capillary Electrophoresis System using bare fused silica capillary (purchased from Polymicro Technologies, L.L.C.) (50 μm i.d., 32.5 cm total length, 24.0 cm to detector) under reverse polarity (-10 or -15 kV), and detection was by UV absorbance at 254 nm. Prior to first use, the capillary was primed for 2 min with 1 M NaOH solution and then for 2 min with 0.1 M NaOH solution.

For each use, the capillary was preconditioned for 1 min using background electrolyte (BGE). BGE was either 5.0 mM NaSBDM- β -CD or 5.0 mM KSPDE- β -CD as a chiral selector in 25 mM tris buffer, pH 2.5. Samples (diluted 10 fold into 90:10 v/v deionized water/acetone solvent) were injected into the capillary under 50.0 mbar pressures for 3 seconds. At the end of each run, the capillary was post-conditioned with 0.1 M NaOH solution for 1 min and then with deionized water for 1 min.

2.2.3. Synthesis of γ , δ -unsaturated β -keto ethyl esters 2A-2F

(*E*)-Ethyl 4-(diethoxyphosphinyl)-3-oxobutanoate (2.234 g, 6.6 mmol), prepared according to the literature (Moorhoff 2003), in 20 mL anhydrous THF was reacted with 2.0 equivalents of *n*-BuLi (6.0 mL, 13.2 mmol, 2.2 M in hexanes) at 0 °C. After gas formation ceased, stirring was continued for 1 h at room temperature. One equivalent of aldehyde (6.0 mmol) was added over 10 min, and the reaction mixture was stirred at room temperature for another 2.5 h. After completion, the reaction was quenched by adding 15 mL of saturated NH₄Cl. The reaction mixture was concentrated under vacuum at 50 - 60 °C. The residue was extracted by CH₂Cl₂ (3 x 15 mL), the combined organic extracts were washed with saturated NaCl (2 x 15 mL), and then dried with anhydrous Na₂SO₄. The organic solvent was removed under vacuum at 30 °C. Product was isolated by column chromatography on silica gel using 10:1 CH₂Cl₂/EtOAc eluent and verified by ¹H and ¹³C NMR spectroscopy.

2.2.4. Synthesis of racemic γ , δ -unsaturated β -hydroxyesters 3A-3F

In a round bottom flask β -ketoester (1 mmol) was dissolved in 5 mL ethanol. In portion, cautiously and intermittently, 0.4 equivalent of NaBH₄ (15 mg, 0.4 mmol) was added and the mixture was stirred for 30 min at room temperature. The reaction mixture was concentrated under vacuum at 60 °C. The product was isolated by column chromatography on silica gel using 10:1 CH₂Cl₂/EtOAc eluent and verified by ¹H and ¹³C NMR spectroscopy.

2.2.5. Stereoselectivity of enzymatic formation of β -hydroxyesters 3A-3F using NADH system (enzyme 1-5)

Into a solution of β -ketoester (25 μ mol) in 50 μ L methanol, was added KRED Mix N (57.4 mg in 1.0 mL deionized H₂O) and 1.0 mg ketoreductase. The mixture was shaken at 32 \pm 1 °C. After 24 h, the reaction was extracted by EtOAc (2 x 1 mL). The combined organic extract was dried over anhydrous Na₂SO₄ and was subjected to chiral HPLC or CE analysis, and ¹H NMR spectroscopy.

2.2.6. Stereoselectivity of enzymatic formation of β -hydroxyesters 3A-3F using NADPH system (enzyme 6-24)

Into a solution of β -ketoester (25 μ mol) in 400 μ L isopropanol and 50 μ L methanol, was added KRED Mix P (29.1 mg in 1.0 mL deionized H₂O) and 1.0 mg ketoreductase. The mixture was stirred at 32 \pm 1 °C. After 24 h, the reaction was extracted by EtOAc (2

x 1 mL). The combined organic extract was dried over anhydrous Na₂SO₄ and was subjected to chiral HPLC or CE analysis, and ¹H NMR spectroscopy. For β-ketoesters **2A-2E** except **2D**, the reactions were scaled up by a factor of 20 or 100 using enzymes that yielded high conversions and e.e., and all products were isolated by column chromatography on silica gel using 10:1 CH₂Cl₂/EtOAc eluent and verified by ¹H and ¹³C NMR spectroscopy.

2.2.7. Synthesis of MTPA ester of γ, δ-unsaturated β-hydroxyesters (Hoye, Jeffrey et al. 2007)

Into a solution of 64 μmol β-hydroxy ester (racemic or made by enzyme **8** KRED-P1-B05 or enzyme **23** KRED-P3-G09) and dry pyridine (16 μL, 200 μmol, 3.1 equiv.) in 1.0 mL anhydrous CH₂Cl₂, was added the (*R*)-(-)-α-Methoxy-α-(trifluoromethyl) phenylacetyl chloride [*R*-(-)-MTPA-Cl] (23 μL, 120 μmol, 1.9 equiv.). The reaction mixture was stirred at ambient temperature till the reaction was completed as monitored by TLC plate (eluent: 10:1= CH₂Cl₂: EtOAc) (usually 3 h). After completion, the reaction was quenched by 2 mL H₂O, extracted by EtOAc (2 x 5 mL). The combined organic layer was dried over anhydrous Na₂SO₄ and the solvent was removed under vacuum. The product MTPA ester of γ,δ-unsaturated β-hydroxyesters was isolated by column chromatography on silica gel using 10:1 CH₂Cl₂/EtOAc eluent. (*S*)-MTPA ester spectra are included in Supporting Information.

2.2.8. Procedure of Mukaiyama Aldol condensation based synthesis of *trans*- γ , δ -unsaturated β -hydroxyester

5% Ti catalyst (0.109 mmol) was dissolved in 5.0 mL anhydrous Et₂O, and the solution was cooled to -78 °C. *Trans*-cinnamaldehyde (288.1 mg, 2.18 mmol) in 1.0 mL anhydrous Et₂O and 2.0 equiv. of silyl ketene acetyl (382.6 mg, 2.616 mmol) in 1.0 mL anhydrous Et₂O were added sequentially. The reaction mixture was warmed to -10±1°C, and the reaction mixture was stirred for another 5 h. After the reaction was completed, the reaction was quenched by saturated aqueous NaHCO₃ solution. The organic layer was washed with a saturated aqueous NaCl solution, dried over anhydrous Na₂SO₄ and concentrated under vacuum. The residue was taken up in THF and treated with 2.0 to 3.0 equiv. of Bu₄NF for 10 min, and then partitioned between Et₂O and 1 M aqueous HCl. The organic layer was washed with a 5% aqueous NaHCO₃ solution, saturated aqueous brine, dried over anhydrous Na₂SO₄ and concentrated under vacuum. Flash chromatography on silica gel using 10:1 CH₂Cl₂/hexane to remove the catalyst ligand followed by 10:1 CH₂Cl₂/EtOAc afforded the aldol adduct as slightly yellow oil. The ¹H NMR spectrum of methyl (3*S*, 4*E*)-3-hydroxy-5-phenylpent-4-enoate is shown in **Figure A2.50**.

2.2.9. Procedure of Me-CBS-BH₃ catalyzed synthesis of *trans*- γ , δ -unsaturated β -hydroxy ester

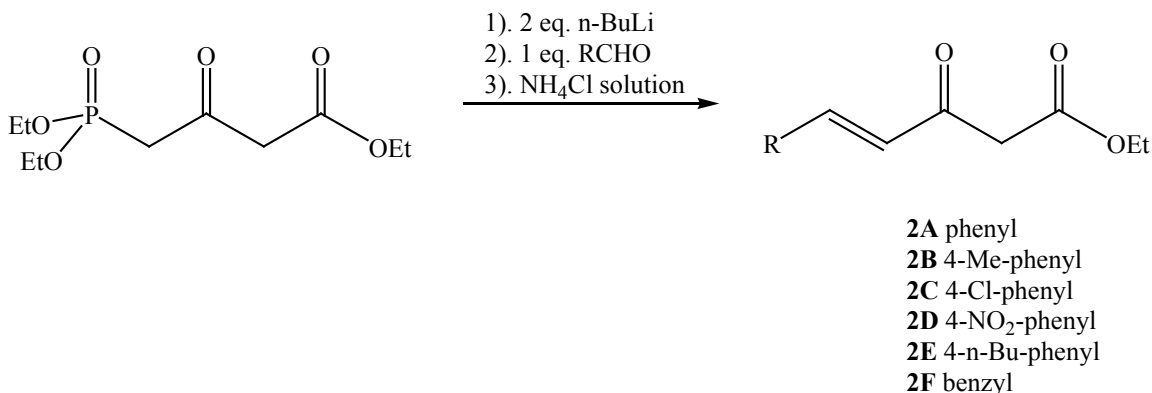
Into 0.025 mmol of Me-CBS-borane (8 mg) and 1.2 equivalents of BH₃-Me₂S (0.03 mmol, 0.03 ml, 1M in THF) in 0.5 ml anhydrous THF under N₂ at -20 °C, a solution of ethyl (4E)-5-(4-methylphenyl)-3-oxopent-4-enoate (55 mg, 0.25 mmol) in 0.5 ml anhydrous THF was added over 20 min. After the completion of addition, the reaction was quenched by adding 5 ml of methanol, and then diluted with 20 ml H₂O. The reaction mixture was extracted by EtOAc (3 x 15 ml). The combined organic phase was washed with water, saturated aqueous brine and dried over MgSO₄. Purification was carried by column chromatography on silica gel using 10:1 CH₂Cl₂/EtOAc. Isolated yield%: 50%. The ¹H NMR spectrum of methyl (3S, 4E)-3-hydroxy-5-phenylpent-4-enoate is shown in **Figure A2.51**.

2.3. Results and discussion

2.3.1. Preparation of γ , δ -unsaturated β -keto ethyl esters 2A-2F

By optimizing previously reported procedures (Svendsen and Boll 1973, Bodalski, Pietrusiewicz et al. 1980, Vandengoorbergh and Vandergen 1980, Moorhoff and Schneider 1987, du Pisani, Schneider et al. 2002), synthesis of *trans*- γ , δ -unsaturated β -keto ethyl esters **2A-F**, shown in **Scheme 2.1**, was accomplished via the condensation of appropriate aldehydes with the anion from 4-(diethoxyphosphinyl)-3-oxobutanoate (Moorhoff 2003) by two equivalents of n-BuLi at room temperature. No *Z*-configured

olefins were detected by ^1H NMR (*E*-olefins have a coupling constant with a value of 15 Hz in ^1H NMR spectrometry). The condensation afforded yields of 75% - 90% for **2A-E**, but the keto ester **2F** was formed in only 15% yield when phenylacetaldehyde **1F** was used under the same reaction condition. The low yield could possibly be attributed to the α -hydrogen of phenylacetaldehyde, which is activated by the phenyl and formyl groups and easily deprotonated under basic conditions. This deprotonation could possible lead to an intermolecular aldol condensation, although this product are not isolated and identified.

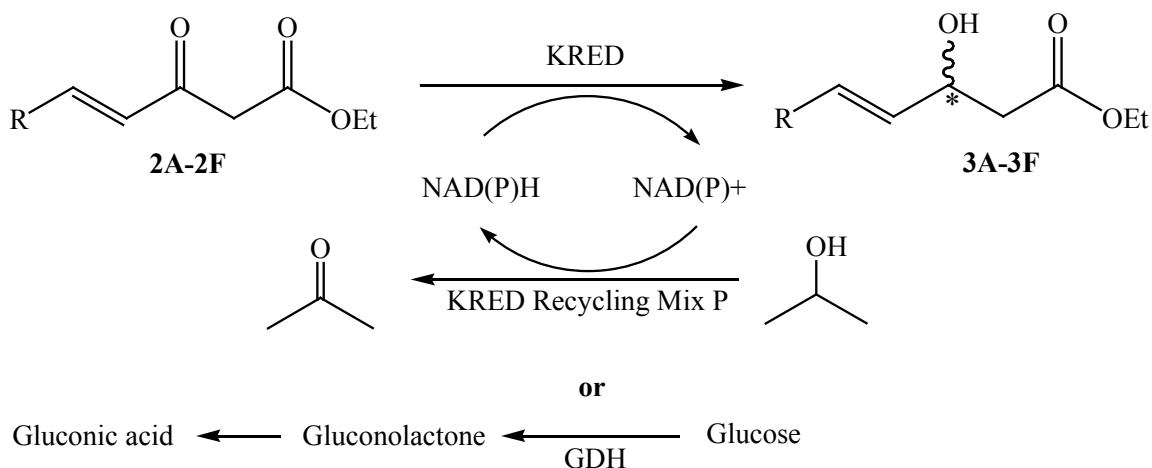


Scheme 2.1. Synthesis of γ , δ -unsaturated- β -hydroxyesters from appropriate aldehydes and 4-(diethoxyphosphinyl)-3-oxobutanoate in the presence of two equivalents of n-BuLi.

2.3.2. Stereoselectivity of enzymatic formation of β -hydroxyesters **3A-3F**

The five *para*-substituted phenyl (**2A-E**) and one benzyl (**2F**) *trans*- γ , δ -unsaturated β -keto esters were selected as substrates to evaluate the stereoselectivity of twenty-four isolated ketoreductases listed in **Table 2.1** from the Codex[®] ketoreductase screening kit which includes five wild type KREDs **1-5** and nineteen engineered KREDs **6-24**. All KREDs reactions used the NADPH recycling system except enzyme **4** (KRED-NADH-

101) and **5** (KRED-NADH-110) which used NADH instead of NADPH, as shown in **Scheme 2.2**. For engineered KREDs **6-24** which have high tolerance to high concentrations of isopropanol (IPA), IPA was used to assist in dissolving poorly water soluble substances and served to recycle NADPH cofactor from NADP⁺, and the reconstituted KRED recycle Mix P used as the reaction medium. However, for wild type KREDs **1-5**, the reconstituted KRED recycle Mix N containing D-glucose/glucose dehydrogenase (GDH) and NAD(P)⁺ was used to provide a cofactor recycle system. In each case, methanol was used as co-solvent to enhance the solubility of β -keto esters, but the amount of co-solvent was no more than 5% of the total volume of reaction solution as recommended in the protocol provided by Codexis.



Scheme 2.2. Enzymatic reduction of γ,δ -unsaturated β -ketoesters with NAD(P)H-dependent Codex[®] ketoreductases.

In the protocol provided by the Codex[®], 1-4 mg of KREDs was recommended to reduce 1 mmol of substance. Instead, in our experiment 40 mg/mmol ratio of KREDs

relative to unsaturated β -keto esters was used to perform all the microscale reactions (using 25 μ mol of unsaturated β -keto esters) shown in **Table 2.1**. All reactions were carried out at 30-32 °C. Approximate yields for the microscale reactions were determined by integration of the vinyl hydrogen regions of the ^1H NMR spectra of the crude mixtures, which also served to establish whether the double bond was reduced to other byproducts. There was no evidence of double bond reduction in any reaction. When conversion of β -keto esters was greater than 3%, only the presence of unreacted β -keto esters and product β -hydroxy ester was observed in the spectrum (See example spectra in **Figure A2.43**).

To determine the absolute configuration of β -hydroxy esters, the reductions of β -keto esters with enzyme **8** and **23**, which provide >99% ee of R and S isomers, respectively, were scaled by a factor of 10 (0.25 mmol) by using the same relative ratio of enzyme to β -keto esters as the microscale reaction. The Mosher ester method was then used to determine the absolute configuration of each enantiopure β -hydroxy ester from enzyme **8** or **23** by comparison with the racemic mixture (**Figure A2.37-A2.42**) (Hoye, Jeffrey et al. 2007). Optical rotations of both enantiomers of aryl γ , δ -unsaturated β -hydroxy esters **3** except **3D** were also measured (**Table 2**). Comparing the signs of measured values of **3A** with those of known literature values, the absolute configurations of β -hydroxy esters were further confirmed (Carreira, Singer et al. 1994, Padhi and Chadha 2005). The percent enantiomeric excess (% e.e.) was determined by either chiral HPLC or chiral capillary electrophoresis using a charged cyclodextrin as chiral selector (**Figure A2.44-A2.49**).

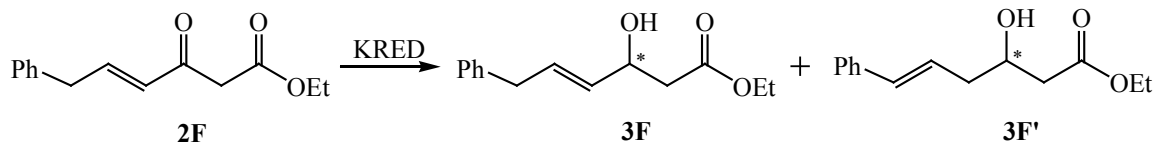
The data reported in **Table 2.1** present the results of the reduction of γ , δ -unsaturated β -keto esters under the action of twenty-four KREDs **1-24**. With exceptions of eight enzymes (P1-A04, P1-C01, P1-H08, P1-H10, P2-D03, P2-D12, P2-H07 and P2-D11) which have no (or very weak) effect on the conversion of β -keto esters and two enzymes (P1-B10 and P1-B12) which provide low to medium enantiomeric excess of the desired β -hydroxy esters, most enzymes showed activity and excellent stereoselectivity for the reduction of β -keto esters **2A-2F** toward β -hydroxy esters **3A-3F**. We do not discern any trends, either in terms of e.e. or conversion, as the substituent on the aromatic rings changes from weakly electron-donating (**2B** and **2E**, alkyl) to strongly electron-withdrawing (**2D**, nitro).

Both (*R*) and (*S*) enantiomers of each β -hydroxy ester were produced impressively in optically pure form (>99% e.e.) by a number of KREDs. (*S*)-enantiomers β -hydroxy esters were made from four enzymes (130, NADH-101, P3-G09 and P3-H12) while (*R*)-enantiomers can be accessed using nine enzymes (101, 119, P1-B02, P1-B05, P2-B02, P2-C02, P2-C11, P2-D11 and P2-G03). For each β -keto esters, at least one enzyme could be used to catalyze the formation of the corresponding (*S*)-enantiomer and several enzymes could be used to produce the corresponding (*R*)-enantiomer, both with excellent stereoselectivity and good conversion. For example, in the formation of (*S*)-**3A**, three out of four enzymes (NADH-101, P3-G09 and P3-H12) had low conversion with over 99% enantiomeric excess. However, enzyme **3** (**130**) could catalyze formation of (*S*)-**3A** with both excellent stereoselectivity (>99%) and conversion (84%). Seven out of nine enzymes catalyzed the formation of (*R*)-**3A** with over 99% e.e. and 83-99% conversion.

Impressively, the ^1H NMR spectra of several crude products (e.g. those from enzyme 8) showed no impurities, and were essentially identical to the spectrum of the “purified” product.

For β -keto esters **2A** – **E** except **2D**, the reactions were scaled up by a factor of 20 or 100 using chosen ketoreductases, as shown in **Table 2.2**. The product γ , δ -unsaturated β -hydroxy esters **3** were isolated by chromatography on silica gel using 10:1 $\text{CH}_2\text{Cl}_2/\text{EtOAc}$. Isolated yields were slightly lower compared to NMR yields in **Table 2.1**. The same optical purity was obtained in all scaled reactions, compared to the one obtained from crude product as shown in **Table 2.1**.

In the case of β -keto ester **2F**, 1,3-hydrogen rearrangement occurred to a small extent when some ketoreductases were used, which produced not only ethyl (4E)-3-hydroxy-6-phenylhex-4-enoate **3F**, but also ethyl (5E)-3-hydroxy-6-phenylhex-5-enoate **3F'**, as shown in **Scheme 2.3**. In the rearrangement process, the hydrogen was transferred without formation of the Z-isomer. Evidence of 1,3-hydrogen rearrangement comes from the HPLC ultraviolet absorption spectra of **3F** and **3F'** which show different absorption maxima (λ_{max}) for **3F** and **3F'**. Indeed, a λ_{max} at 250 nm is observed in the UV spectrum of **3F'** while a λ_{max} of 206 nm is the spectrum of **3F** (**Figure A2.34 and A2.35**). Further conclusive evidence for allylic rearrangement was obtained by examination of the ^1H NMR spectra of the crude products (**Figure A2.33**).



Scheme 2.3. Enzymatic reduction of **2F** to **3F** and rearranged product **3F'**.

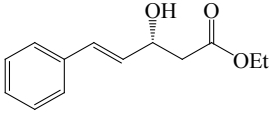
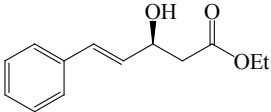
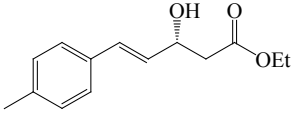
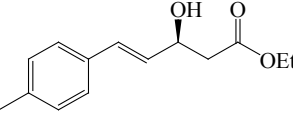
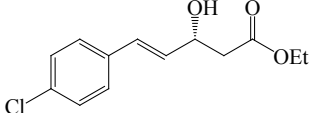
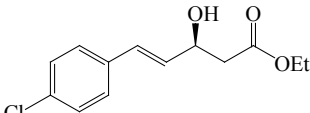
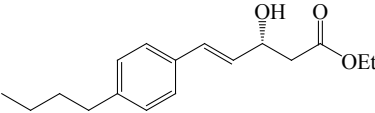
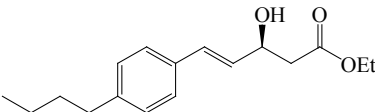
The pathway for the formation of **3F'** is not clear. Double bond migration of **2F** may occur prior to enzymatic reduction to **3F'**. Alternatively, **2F** may be enzymatically reduced to **3F**, followed by isomerization to **3F'**. Current literature is lacking on the mechanistic aspects of this process and further studies will be required. Nevertheless, product (*R*)-**3F** can be obtained in pure form with high e.e. and conversion (Enzymes 5 and 20) but further optimization is required for obtaining pure (*S*)-**3F** with high yield and conversion.

Table 2.1. Stereocontrolled reduction of γ , δ -unsaturated β -ketoesters to γ , δ -unsaturated β -hydroxyesters by twenty-four Codex[®] ketoreductases.

	KRED	3A		3B		3C		3D		3E		3F		3F'	
		e.e. ^{a,b} %	Conv. ^c (%)	e.e. ^{a,b} %	Conv. ^c (%)	e.e. ^b %	Conv. ^c (%)	e.e. ^{a,b} %	Conv. ^c (%)	e.e. ^a %	Conv. ^c (%)	e.e. ^a %	Conv. ^c (%)	e.e. ^a %	Conv. ^c (%)
1	101	>99	92	>99	67	>99	77	>99	62	>99	49	91	>99	-	-
2	119	>99	94	>99	96	94	95	>99	24	>99	87	96	>99	-	-
3	130	->99	84	->99	84	-93	85	->99	6	->99	74	-85	81	-	-
4	NADH-101	>99	w	->99	w	-	-	<3	<3	-	-	->99	50	-	-
5	NADH-110	>99	94	>99	75	>99	66	>99	13	>99	8	>99	>99	-	-
6	P1-A04	-	-	-	-	-	-	-	-	-	-	-	-	-	-
7	P1-B02	84	88	90	90	>99	>99	>99	86	54	87	98	97	8	3
8	P1-B05	>99	>99	>99	79	>99	>99	>99	92	>99	>99	82	89	90	11
9	P1-B10	53	28	84	13	68	40	72	<3	-	-	52	<3	-68	<3
10	P1-B12	49	31	45	28	50	<3	>99	<3	-	-	38	<3	-76	<3
11	P1-C01	90	<3	-	-	-	-	-	-	-	-	-	-	-	-
12	P1-H08	98	<3	95	8	40	<3	54	<3	-	-	-	-	-	-
13	P1-H10	-	-	-	-	-	-	-	-	-	-	48	<3	14	<3
14	P2-B02	>99	>99	>99	>99	>99	>99	96	96	>99	>99	>99	97	95	3
15	P2-C02	>99	93	>99	>99	>99	>99	25	90	>99	>99	>99	98	>99	2
16	P2-C11	>99	96	>99	93	>99	>99	>99	96	>99	98	>99	94	>99	6
17	P2-D03	94	<3	-	-	80	<3	-	-	-	-	-	-	-	-
18	P2-D11	96	33	>99	10	92	<3	-	-	-	-	-	-	-	-
19	P2-D12	95	<3	96	<3	82	<3	-	-	-	-	-	-	-46	<3
20	P2-G03	>99	94	>99	97	>99	>99	>99	81	>99	>99	>99	>99	-	-
21	P2-H07	-	-	-	-	-	-	-	-	-	-	-	-	-	-
22	P3-B03	-	-	-	-	-	-	-	-	-	-	-	-	-	-
23	P3-G09	->99	15	->99	38	->99	>99	->99	73	->99	40	->99	43	->99	9
24	P3-H12	->99	8	->99	<3	->99	20	->99	43	->99	15	-90	62	21	31

- a. The percent e.e. was measured by chiral HPLC. The positive e.e. value indicates that (*R*)-enantiomer is the major product, while negative e.e. value indicates that (*S*)-enantiomer is the major product. In each case, the racemic mixture was prepared for calibration. Absolute configuration of stereogenic C-3 was identified by ¹H NMR analysis of corresponding MTPA ester. (Hoye, Jeffrey et al. 2007)
- b. The percent e.e. was determined by CE using charged β -CD as a chiral selector.
- c. The conversion was obtained by ¹H NMR integration using *d*-chloroform as a solvent. When <3% conversion is reported, the presence of byproducts made the measurement uncertain, although a small amount of product is detected. If no value is given, the product was not detected by either HPLC, CE, ¹H NMR spectroscopy or TLC.

Table 2.2. Isolated yields of γ , δ -unsaturated- β -hydroxyesters **3** using ketoreductases which provide both good yield and high enantioselectivity.

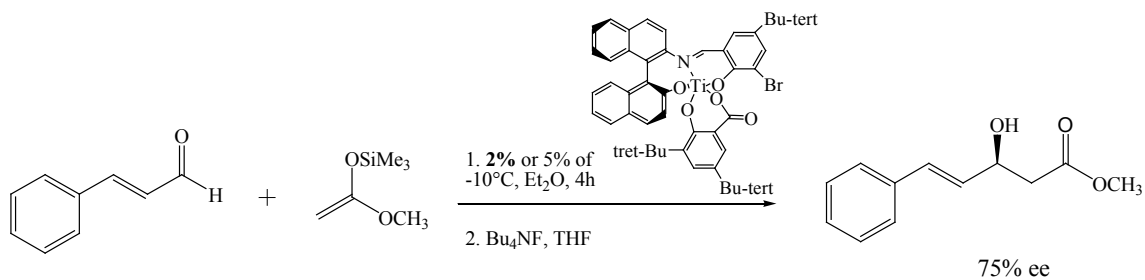
#	Substance	KRED	Isolated Yield (%)	e.e. ^a (%)	$[\alpha]_{589}^{23}$
3A		P2-B02	90	>99	+14° (c 0.57, CHCl ₃) lit. +13.6° (Carreira, Singer et al. 1994)
		130	70	->99	-16° (c 0.34, CHCl ₃) lit. -2.6° (Padhi and Chadha 2005), -6.8° (Saravanan, Selvakumar et al. 2012)
3B		P1-B05	79	>99	+20° (c 0.10, CHCl ₃)
		130	75	->99	-15° (c 0.33, CHCl ₃)
3C		P2-C11	85	>99	+15° (c 0.13, CHCl ₃)
		P3-G09	81	->99	-16° (c 0.16, CHCl ₃)
3E		P1-B05	77	>99	+20° (c 0.10, CHCl ₃)
		130	64	->99	-11° (c 0.55, CHCl ₃)

a. The percent e.e. was measured by chiral HPLC.

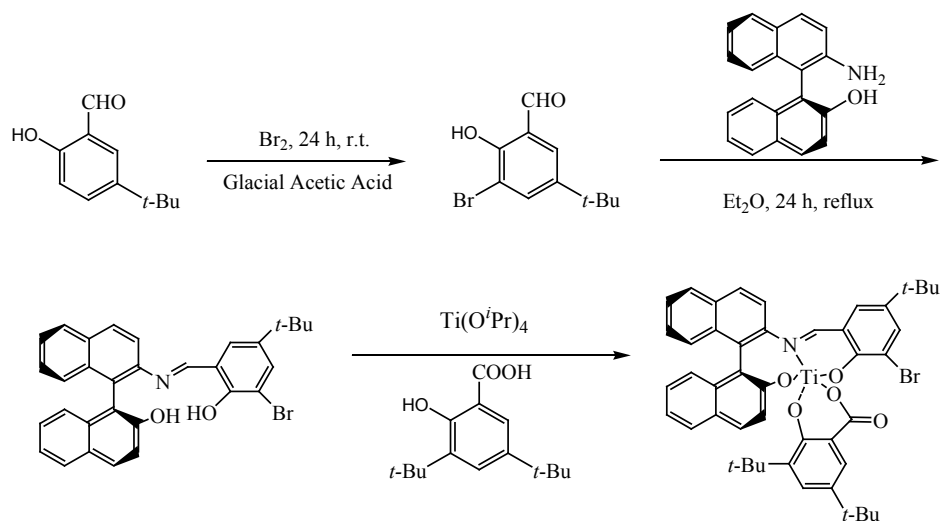
Besides KREDs induced reduction of *trans*- γ , δ -unsaturated β -ketoesters, this dissertation research also describes the synthesis of *trans*- γ , δ -unsaturated β -hydroxyesters via Mukaiyama aldol condensation and the reduction of *trans*- γ , δ -unsaturated β -ketoesters by Me-CBS-BH₃ catalyst.

2.3.4. Mukaiyama Aldol condensation based synthesis of *trans*- γ , δ -unsaturated β -hydroxy Ester

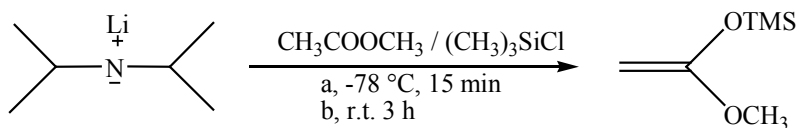
Carreira *et al.* established an enantioselective aldol addition reaction with methyl and ethyl acetate *O*-silyl enolate, catalyzed by a chiral tridentate chelated titanium (IV) catalyst and reported excellent e.e. (95-97%) and 72-98% yields (Carreira, Singer et al. 1994). The aldol condensation between *trans*-cinnamaldehyde and silyl ketene acetal is shown in **Scheme 2.4**. The condensation was catalyzed by Ti(IV) catalyst prepared from Ti(O^{*i*}Pr)₄ and tridentate ligands (**Scheme 2.5**. more detail for preparation of the catalyst the reader should see the reference by Carreira (Carreira, Singer et al. 1994)). Silyl ketene acetal is not commercially available and was prepared by the reaction between methyl acetate ester, LDA and chlorotrimethylsilane, followed by distillation (**Scheme 2.6**) (Oisaki, Suto et al. 2003). Mukaiyama aldol reaction provides *trans*- γ , δ -unsaturated β -hydroxy ester 80% yield and 75% e.e.



Scheme 2.4. Aldol condensation between *trans*-cinnamaldehyde and silyl ketene acetal.



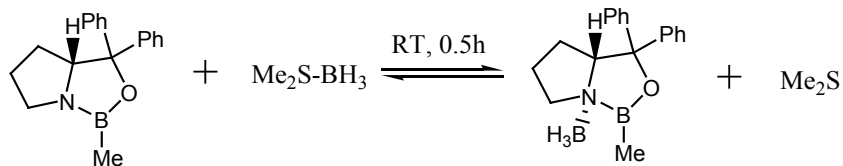
Scheme 2.5. Preparation of titanium catalyst from 2-amino-2'-hydroxy-1,1'-binaphthyl, $\text{Ti}(\text{O}^i\text{Pr})_4$ and 3,5-*di-tert*-butylsalicylic acid.



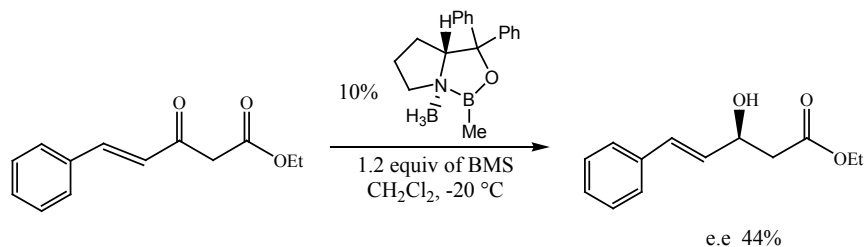
Scheme 2.6. Preparation of Ketene Silyl Acetyl.

2.3.5. Me-CBS-BH₃ catalyzed synthesis of *trans*- γ , δ -unsaturated β -hydroxyester

Corey and co-workers developed the chiral oxazaborolidine-catalyzed reduction of prochiral ketones, cyclic and acyclic α , β -enones (Corey, Bakshi et al. 1987, Corey, Bakshi and Shibata et al. 1987, Mathre, Thompson et al. 1993, Corey and Helal 1998, Kawanami, Murao et al. 2003). Owing to the stability of oxazaborolidine catalyst and use of BH₃·THF (or BH₃·Me₂S) which is obviously incompatible with C-C double bonds, the Me-CBS catalyst system produced a saturated byproduct and relatively lower e.e. when we used γ , δ -unsaturated β -ketoesters as substrates. **Scheme 2.8** shows the reduction of ethyl (4*E*)-3-oxo-5-phenylpent-4-enoate (**2A**) by 1.2 equivalent of borane-methyl sulfide complex (BMS) in the presence of 10% of methyl oxazaborolidine-borane complex (Me-CBS-BH₃) (**Scheme 2.7**), formed by reacting Me-CBS with BMS at -20 °C. The *trans*- γ , δ -unsaturated β -hydroxy ester was formed with 50% yield, but only 44% e.e. was obtained according to either chiral HPLC analysis or capillary electrophoresis with anionic β -cyclodextrins as chiral selector.



Scheme 2.7. Preparation of Me-CBS-BH₃ catalyst from methyl oxazaborolidine and borane-methyl sulfide complex (BMS).



Scheme 2.8. Me-CBS-BH₃ catalyst catalyzed reduction of *trans* γ , δ -unsaturated β -ketoester.

2.4. Summary of formation of aryl γ , δ -unsaturated β -hydroxyesters

Twenty four NAD(P)H-dependent ketoreductases were evaluated for the reduction of *trans*- γ , δ -unsaturated β -keto esters to their corresponding β -hydroxy esters. These ketoreductases includes five wild type enzymes and nineteen engineered enzymes. Five *para*-substituted phenyl and one benzyl γ , δ -unsaturated β -keto esters were selected as substrates, which were prepared via Horner-Wadsworth-Emmons olefination. For each β -keto esters, 40 mg/mmol ratio of KREDs relative to ester was used with a reaction time of 24 h at 32 ± 1 °C. All products were successfully characterized by NMR spectroscopy for percent yield, and chiral HPLC or capillary electrophoresis with anionic β -cyclodextrins for enantiomeric excess. At least one enzyme catalyzed the formation of the corresponding (*S*)-enantiomer of γ , δ -unsaturated β -hydroxyesters and several enzymes afforded the corresponding (*R*)-enantiomer, both in excellent stereoselectivity (>99%) and with good to excellent conversion for at least one ketoreductase. The scaled reaction with chosen enzyme shows that the isolated yields are very close to the conversion monitored by NMR spectroscopy and with same optical purity (>99%).

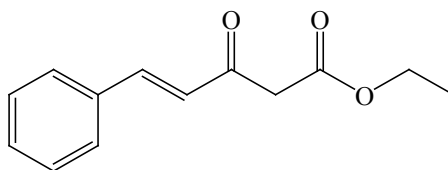
The practical synthesis of γ , δ -unsaturated β -hydroxyesters have also been performed by using traditional chemical methods, including Mukaiyama aldol condensation between *trans*-cinnamaldehyde and silyl ketene acetal, as well as Me-CBS-Borane catalyzed reduction of γ , δ -unsaturated β -ketoxyester. Both chemical methods provided good isolated yield of the product, however poor enantioselectivity were obtained under each case.

These results suggest that Codexis ketoreductases offer potential for large scale synthesis of either enantiomer of aryl γ , δ -unsaturated- β -hydroxyesters with excellent stereoselectivity.

2.5. Physical Data

2.5.1. Physical Data and NMR Spectra of γ , δ -unsaturated β -ketoesters 2A – 2F

2.5.1.1. (*E*)-ethyl 3-oxo-5-phenylpent-4-enoate (2A).

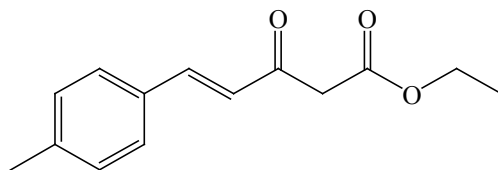


2A (*E*)-ethyl 3-oxo-5-phenylpent-4-enoate

A slightly yellow solid; Isolated yield (%): 85%. ^1H NMR (300 MHz, CDCl_3): δ 12.00 (dd, $J = 3\text{Hz}$, 0.8H), 7.60 (d, $J = 15\text{ Hz}$, 1H), 7.31-7.55 (m, 10 H), 6.80 (d, $J = 15$, 1H), 6.43 (dd, $J = 3, 15\text{ Hz}$, 0.8H), 5.17 (s, 0.8H), 4.18-4.26 (m, $J = 9\text{Hz}$, 3.6H), 3.70 (s, 2H),

1.31 (t, $J = 9$ Hz, 2.4H), 1.28 (t, $J = 9$ Hz, 3H); ^{13}C NMR (75 MHz, CDCl_3): δ 192.0, 172.8, 169.2, 167.4, 144.6, 136.7, 135.3, 134.0, 130.9, 129.3, 129.0, 128.8, 128.5, 127.6, 125.2, 121.9, 91.9, 61.4, 60.2, 47.6, 14.3, 14.1

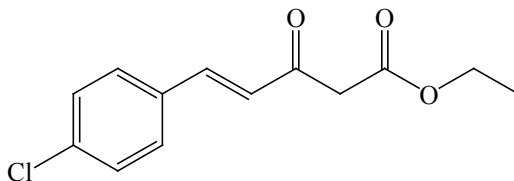
2.5.1.2. (*E*)-ethyl 3-oxo-5-(*p*-tolyl)pent-4-enoate (2B).



2B (*E*)-ethyl 3-oxo-5-(*p*-tolyl)pent-4-enoate

Slightly yellow solid; Isolated yield (%): 88%. ^1H NMR (300 MHz, CDCl_3): δ 12.01 (d, $J = 3$ Hz, 0.7H), 7.53 (d, $J = 15$ Hz, 1H), 7.13-7.44 (m, 4H), 7.13-7.19 (m, 3.5H), 6.74 (d, $J = 15$, 1H), 6.47 (dd, $J = 3, 15$ Hz, 0.7H), 5.12 (s, 0.7H), 4.16-4.24 (m, $J = 9$ Hz, 3.4H), 3.67 (s, 2H), 2.35 (s, 3H), 2.33 (s, 1.4H), 1.23-1.29 (m, $J = 9$ Hz, 5H); ^{13}C NMR (75 MHz, CDCl_3): δ 192.02, 172.89, 169.47, 167.47, 144.67, 141.52, 139.59, 136.75, 132.58, 131.33, 129.75, 129.55, 128.55, 127.55, 124.31, 120.82, 91.52, 72.62, 61.36, 60.16, 47.47, 21.52, 21.38, 14.30, 14.15

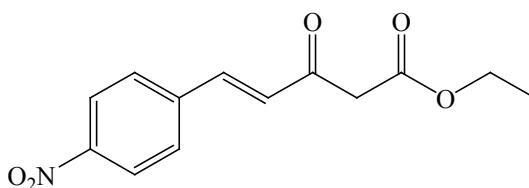
2.5.1.3. (*E*)-ethyl 5-(4-chlorophenyl)-3-oxopent-4-enoate (2C).



2C (*E*)-ethyl 5-(4-Chlorophenyl)-3-oxopent-4-enoate

Slightly yellow solid; Isolated yield (%): 90%. ^1H NMR (300 MHz, CDCl_3): δ 11.98 (dd, $J = 3\text{ Hz}$, 1H), 7.30-7.56 (m, 10H), 6.78 (d, $J = 15\text{ Hz}$, 1H), 6.40 (dd, $J = 3, 15\text{ Hz}$, 1H), 5.16 (s, 1H), 4.22 (m, $J = 6\text{ Hz}$, 4H), 3.68 (s, 2H), 1.31 (t, $J = 6\text{ Hz}$, 3H), 1.28 (t, $J = 6\text{ Hz}$, 3H); ^{13}C NMR (75 MHz, CDCl_3): δ 191.93, 172.98, 168.98, 167.50, 143.22, 137.10, 135.50, 135.31, 134.11, 132.81, 129.87, 129.53, 129.27, 128.93, 125.77, 122.67, 92.55, 61.71, 60.54, 48.00, 14.51, 14.36

2.5.1.4. (*E*)-ethyl 5-(4-nitrophenyl)-3-oxopent-4-enoate (2D)

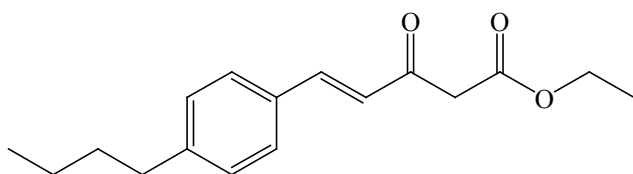


2D (*E*)-ethyl 5-(4-nitrophenyl)-3-oxopent-4-enoate

Slightly yellow solid; Isolated yield (%): 78%. ^1H NMR (300 MHz, CDCl_3): δ 11.95 (dd, $J = 3\text{ Hz}$, 1H), 8.23 (m, $J = 3, 9, 15\text{ Hz}$, 2.1H), 7.63 (m, $J = 3, 9, 15\text{ Hz}$, 2.12H), 7.46 (d, $J = 15\text{ Hz}$, 1H), 6.95 (d, $J = 15, 0.04\text{ Hz}$), 6.56 (dd, $J = 3, 15\text{ Hz}$), 5.25 (s, 1H), 4.26 (q, $J = 6\text{ Hz}$, 2H), 4.20 (q, $J = 6\text{ Hz}$, 0.8H), 3.72 (s, 0.08H), 1.33 (t, $J = 6\text{ Hz}$, 3H), 1.30 (t, $J = 6\text{ Hz}$,

0.12H); ^{13}C NMR (75 MHz, CDCl_3): δ 191.45, 172.52, 167.66, 167.05, 148.76, 147.77, 141.68, 141.17, 140.24, 133.82, 129.07, 128.49, 128.04, 126.15, 124.21, 124.14, 93.98, 61.64, 60.58, 47.98, 14.25, 14.13

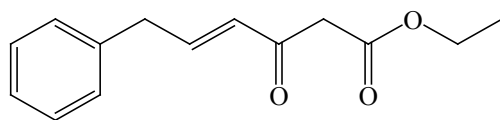
2.5.1.5. (*E*)-ethyl 5-(4-butylphenyl)-3-oxopent-4-enoate (2E)



2E (*E*)-ethyl 5-(4-butylphenyl)-3-oxopent-4-enoate

Slightly yellow solid; Isolated yield (%): 85%. ^1H NMR (300 MHz, CDCl_3): δ 12.0 (d, J = 3 Hz, 0.6H), 7.58 (d, J = 15 Hz, 1H), 7.39-7.49 (m, 3.8H), 7.17-7.23 (m, 3.2H), 6.76 (d, J = 15 Hz, 1H), 6.40 (dd, J = 3, 15 Hz, 0.6 H), 5.15 (s, 0.6H), 4.21 (m, J = 6 Hz, 3.2H), 3.69 (s, 2H), 2.60 (m, 3.2H), 1.55-1.65 (m, 3.2H), 1.21-1.41 (m, 8H), 0.93 (t, J = 6, 4.8H); ^{13}C NMR (75 MHz, CDCl_3): δ 192.03, 172.90, 169.49, 167.48, 146.59, 144.78, 144.67, 136.80, 132.81, 131.52, 129.13, 128.91, 128.58, 127.56, 124.32, 120.86, 90.51, 61.42, 60.17, 47.61, 35.62, 35.52, 33.45, 33.34, 22.34, 22.32, 14.31, 14.14, 13.94, 13.92

2.5.1.6. (*E*)-ethyl 3-oxo-6-phenylhex-4-enoate (2F)

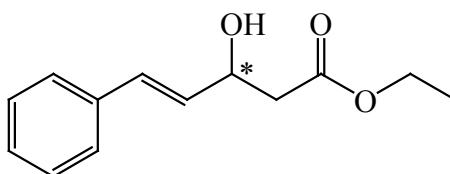


2F (*E*)-ethyl 3-oxo-6-phenylhex-4-enoate

Slightly yellow oil; Isolated yield (%): 15%. ^1H NMR (300 MHz, CDCl_3): δ 11.88 (d, $J = 3\text{Hz}$, 0.8H), 7.15-7.35 (m, 9H), 6.99 (dt, $J = 9, 15\text{ Hz}$, 1H), 6.80 (dt, $J = 9, 15\text{ Hz}$, 0.8H), 6.15 (dt, $J = 3, 15\text{ Hz}$, 1H), 5.80 (dq, $J = 3, 15\text{ Hz}$, 0.8H), 4.99 (s, 1H), 4.13 – 4.23 (m, $J = 6\text{Hz}$, 3.4H), 3.57 (s, 2H), 3.50-3.57 (dq, $J = 3, 6\text{ Hz}$, 3.6H), 1.28 (t, $J = 6\text{ Hz}$, 2.4H), 1.24 (t, $J = 6\text{ Hz}$, 3H) 192.13, 172.90, 169.12, 167.32, 147.78, 138.97, 138.49, 137.21, 130.34, 128.80, 128.79, 128.75, 128.61, 126.87, 126.49, 125.37, 90.66, 61.37, 60.10, 46.98, 38.80, 38.77, 14.27, 14.06

2.5.2. Physical Data and NMR spectra of γ , δ -unsaturated β -hydroxyesters 3A-3F

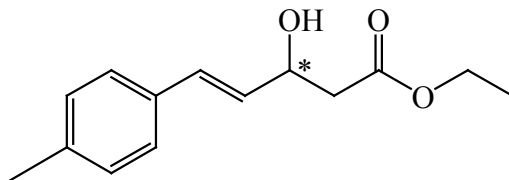
2.5.2.1. (*E*)-ethyl 3-hydroxy-5-phenylpent-4-enoate (3A)



3A (*E*)-ethyl 3-hydroxy-5-phenylpent-4-enoate

Slightly yellow oil; **R-3A**: $[\alpha_{589}^{23}] +14^\circ$ ($c = 0.57$, CHCl_3), lit. $+13.6^\circ$ (Carreira, Singer et al. 1994); **S-3A**: $[\alpha_{589}^{23}] -16^\circ$ ($c = 0.34$, CHCl_3), lit. -2.6° (Padhi and Chadha 2005), -6.8° (Saravanan, Selvakumar et al. 2012); ^1H NMR (300 MHz, CDCl_3): δ 7.22-7.39 (m, 5H), 6.65 (d, $J = 15\text{ Hz}$, 1H), 6.25 (dd, $J = 6, 15\text{ Hz}$, 1H), 4.73 (m, $J = 3, 6\text{ Hz}$, 1H), 4.20 (q, $J = 6\text{ Hz}$, 2H), 3.15 (br, 1H), 2.56-2.70 (m, 2H), 1.27 (t, $J = 6\text{ Hz}$, 3H); ^{13}C NMR (75 MHz, CDCl_3): δ 172.23, 135.42, 130.73, 129.94, 128.57, 127.79, 126.53, 68.87, 60.85, 41.51, 14.18

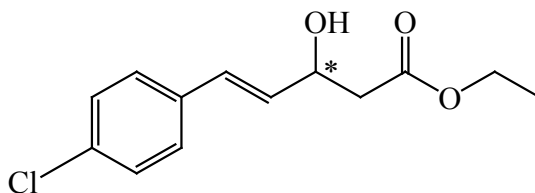
2.5.2.2. (*E*)-ethyl 3-hydroxy-5-(*p*-tolyl)pent-4-enoate (**3B**)



3B (*E*)-ethyl 3-hydroxy-5-(*p*-tolyl)pent-4-enoate

Slightly yellow oil; **R-3B**: $[\alpha_{589}^{23}] + 20^\circ$ ($c = 0.1$, CHCl_3); **S-3B**: $[\alpha_{589}^{23}] - 15^\circ$ ($c = 0.33$, CHCl_3), lit. -2.6° (Padhi and Chadha 2005), -6.8° (Saravanan, Selvakumar et al. 2012); $^1\text{H NMR}$ (300 MHz, CDCl_3): δ 7.26 (d, $J = 7$ Hz, 2H), 7.11 (d, $J = 7$ Hz, 2H), 6.61 (d, $J = 15$ Hz, 1H), 6.17 (dd, $J = 6, 15$ Hz, 1H), 4.70 (m, $J = 3, 6$ Hz, 1H), 4.18 (q, $J = 6$ Hz, 2H), 3.10 (d, $J = 6$ Hz, 1H), 2.54-2.69 (m, 2H), 2.33 (s, 3H), 1.27 (t, $J = 6$ Hz, 3H); $^{13}\text{C NMR}$ (75 MHz, CDCl_3): δ 172.29, 137.65, 133.61, 130.68, 129.25, 128.89, 126.44, 68.98, 60.82, 41.57, 21.19, 14.18

2.5.2.3. (*E*)-ethyl 5-(4-chlorophenyl)3-hydroxypent-4-enoate (**3C**)

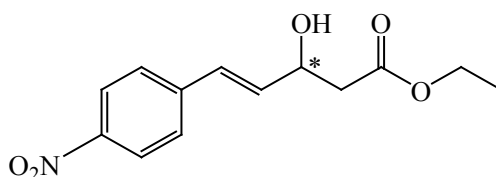


3C (*E*)-ethyl 5-(4-chlorophenyl)3-hydroxypent-4-enoate

Slightly yellow oil; **R-3C**: $[\alpha_{589}^{23}] + 15^\circ$ ($c = 0.13$, CHCl_3); **S-3C**: $[\alpha_{589}^{23}] - 16^\circ$ ($c = 0.16$, CHCl_3); $^1\text{H NMR}$ (300 MHz, CDCl_3): δ 7.27 (br, 4H), 6.60 (d, $J = 15$ Hz, 1H), 6.19 (dd, $J = 6, 15$ Hz, 1H), 4.71 (q, $J = 6$ Hz, 1H), 4.18 (q, $J = 6$ Hz, 2H), 3.31 (br, 1H), 2.25-2.69

(m, 2H), 1.26 (t, $J = 6$ Hz, 1H); ^{13}C NMR (75 MHz, CDCl_3): δ 172.14, 134.94, 133.35, 130.64, 129.40, 128.70, 127.72, 68.66, 60.89, 41.44, 14.17

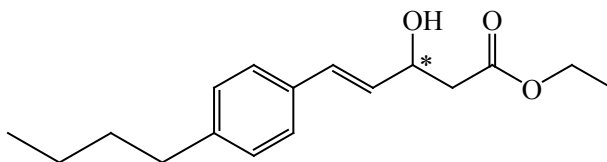
2.5.2.4. (*E*)-ethyl 3-hydroxy-5-(4-nitrophenyl)pent-4-enoate (**3D**)



3D (*E*)-ethyl 3-hydroxy-5-(4-nitrophenyl)pent-4-enoate

Slightly yellow oil; ^1H NMR (300 MHz, CDCl_3): δ 8.17 (dt, $J = 2, 7$ Hz, 2H), 7.50 (dt, $J = 2, 7$ Hz, 2H), 6.76 (d, $J = 15$ Hz, 1H), 6.42 (dd, $J = 6, 15$ Hz, 1H), 4.75-4.82 (m, 1H), 4.20 (q, $J = 6$ Hz, 2H), 3.27 (br, 1H), 2.58-2.75 (m, 2H), 1.29 (t, $J = 6$ Hz, 3H); ^{13}C NMR (75 MHz, CDCl_3): δ 172.06, 146.97, 142.99, 134.83, 128.35, 127.03, 123.96, 68.26, 61.03, 41.11, 14.15

2.5.2.5. (*E*)-ethyl 5-(4-butylphenyl)-3-hydroxypent-4-enoate (**3E**)



3E (*E*)-ethyl 5-(4-butylphenyl)-3-hydroxypent-4-enoate

Slightly yellow oil; **R-3E**: $[\alpha_{589}^{23}] + 20^\circ$ (c = 0.1, CHCl₃); **S-3E**: $[\alpha_{589}^{23}] - 11^\circ$ (c = 0.55, CHCl₃); ¹H NMR (300 MHz, CDCl₃): δ 7.28 (d, *J* = 7 Hz, 2H), 7.12 (d, *J* = 7 Hz, 2H), 6.62 (d, *J* = 15 Hz, 1H), 6.17 (dd, *J* = 6, 15 Hz, 1H), 4.70 (m, *J* = 6 Hz, 1H), 4.17 (q, *J* = 6 Hz, 2H), 3.15 (br, 1H), 2.56-2.67 (m, 4H), 1.53-1.63 (m, 2H), 1.28-1.40 (m, 2H), 1.26 (t, *J* = 6 Hz, 3H), 0.92 (t, *J* = 6 Hz, 3H); ¹³C NMR (75 MHz, CDCl₃): δ 172.22, 142.71, 133.85, 130.68, 129.00, 128.63, 126.44, 69.00, 60.81, 41.63, 35.36, 33.56, 22.33, 14.18, 13.95

Reference

Akutagawa, S. (1995). Asymmetric synthesis by metal BINAP catalysts. *Appl. Catal., A* 2: 171-207.

Arai, N., Azuma, K., Nii, N. and Ohkuma, T. (2008). Highly Enantioselective hydrogenation of aryl vinyl ketones to allylic alcohols catalyzed by the Tol-Binap/Dmapen ruthenium(II) complex. *Angew. Chem., Int. Ed.* 39: 7457-7460.

Baskar, B., Pandian, N.G., Priya, K. and Chadha, A. (2004). Asymmetric reduction of alkyl 2-oxo-4-arylbutanoates and -but-3-enoates by *Candida parapsilosis* ATCC 7330: assignment of the absolute configuration of ethyl 2-hydroxy-4-(p-methylphenyl)but-3-enoate by ¹H NMR. *Tetrahedron: Asymmetry* 24: 3961-3966.

Bodalski, R., Pietrusiewicz, K.M., Monkiewicz, J. and Koszuk, J. (1980). A new efficient synthesis of substituted Nazarov reagents - a Wittig-Horner-Emmons approach. *Tetrahedron Lett.* 23: 2287-2290.

Burk, M.J., Harper, T.G.P. and Kalberg, C.S. (1995). Highly enantioselective hydrogenation of β -Keto Esters under Mild Conditions. *J. Am. Chem. Soc.* 15: 4423-4424.

Carreira, E.M., Singer, R.A. and Lee, W.S. (1994). Catalytic, enantioselective aldol additions with methyl and ethyl-acetate O-silyl enolates - a chiral tridentate chelate as a Ligand for titanium(IV). *J. Am. Chem. Soc.* 19: 8837-8838.

Corey, E.J., Bakshi, R.K. and Shibata, S. (1987). Highly enantioselective borane reduction of ketones catalyzed by chiral oxazaborolidines. Mechanism and synthetic implications. *J. Am. Chem. Soc.* 18: 5551-5553.

Corey, E.J., Bakshi, R.K., Shibata, S., Chen, C.P. and Singh, V.K. (1987). A stable and easily prepared catalyst for the enantioselective reduction of ketones. Applications to multistep syntheses. *J. Am. Chem. Soc.* 25: 7925-7926.

Corey, E.J. and Helal, C.J. (1998). Reduction of carbonyl compounds with chiral oxazaborolidine catalysts: a new paradigm for enantioselective catalysis and a powerful new synthetic method. *Angew. Chem., Int. Ed.* 15: 1986-2012.

du Pisani, C., Schneider, D.F. and Venter, P.C.R. (2002). Ethyl 4-(diethoxyphosphinyl)-3-oxobutanoate: Selective synthesis of β -keto phosphonates. *Synth. Commun.* 2: 305-314.

Genêt, J.P., Pfister, X., Ratovelomanana-Vidal, V., Pinel, C. and Laffitte, J.A. (1994). Dynamic kinetic resolution of cyclic [β]-ketoesters with preformed or prepared in situ chiral diphosphine-ruthenium (II) catalysts. *Tetrahedron Lett.* 26: 4559-4562.

Genêt, J.P., Pinel, C., Ratovelomanana-Vidal, V., Mallart, S., Pfister, X., Bischoff, L., De Andrade, M.C.C., Darses, S., Galopin, C. and Laffitte, J.A. (1994). Enantioselective

hydrogenation reactions with a full set of preformed and prepared in situ chiral diphosphine-ruthenium (II) catalysts. *Tetrahedron: Asymmetry* 4: 675-690.

Girard, A., Greck, C., Ferroud, D. and Genêt, J.P. (1996). Syntheses of the syn and anti α -amino- β -hydroxy acids of vancomycin: (2S, 3R) and (2R, 3R) p-chloro-3-hydroxytyrosines. *Tetrahedron Lett.* 44: 7967-7970.

Greck, C., Bischoff, L., Ferreira, F., Pinel, C., Piveteau, E. and Genet, J.P. (1993). Asymmetric-Synthesis of Anti N-Boc- α -Hydrazino- β -Hydroxyesters from β -Ketoesters by Sequential Catalytic-Hydrogenation and Electrophilic Amination. *Synlett* 7: 475-477.

Greck, C., Ferreira, F. and Genet, J.P. (1996). Synthesis of both enantiomers of trans 3-hydroxypipicolinic acid. *Tetrahedron Lett.* 12: 2031-2034.

Hopkins, C.D., Schmitz, J.C., Chu, E. and Wipf, P. (2011). Total Synthesis of (-)-CP2-Disorazole C1. *Org. Lett.* 15: 4088-4091.

Hoye, T.R., Jeffrey, C.S. and Shao, F. (2007). Mosher ester analysis for the determination of absolute configuration of stereogenic (chiral) carbinol carbons. *Nature Protocols* 10: 2451-2458.

Hu, A., Ngo, H.L. and Lin, W. (2004). Remarkable 4,4'-substituent effects on binap: highly enantioselective Ru catalysts for asymmetric hydrogenation of β -aryl ketoesters and their immobilization in room-temperature ionic liquids. *Angew. Chem., Int. Ed.* 19: 2501-2504.

Huisman, G.W., Liang, J. and Krebber, A. (2010). Practical chiral alcohol manufacture using ketoreductases. *Curr. Opin. Chem. Biol.* 2: 122-129.

Ishihara, K., Yamaguchi, H., Adachi, N., Hamada, H. and Nakajima, N. (2000). Stereocontrolled reduction of α - and beta-Keto esters with Micro Green Algae, *Chlorella* Strains. *Biosci., Biotechnol., Biochem.* 10: 2099-2103.

Kalaitzakis, D., Kambourakis, S., Rozzell, D.J. and Smonou, I. (2007). Stereoselective chemoenzymatic synthesis of sitophilate: a natural pheromone. *Tetrahedron: Asymmetry* 20: 2418-2426.

Kalaitzakis, D., Rozzell, J.D., Kambourakis, S. and Smonou, I. (2005). Highly Stereoselective Reductions of α -Alkyl-1,3-diketones and α -Alkyl- β -keto Esters Catalyzed by Isolated NADPH-Dependent Ketoreductases. *Org. Lett.* 22: 4799-4801.

Kaluzna, I.A., Matsuda, T., Sewell, A.K. and Stewart, J.D. (2004). Systematic Investigation of *Saccharomyces cerevisiae* Enzymes Catalyzing Carbonyl Reductions. *J. Am. Chem. Soc.* 40: 12827-12832.

- Kambourakis, S. and Rozzell, J.D. (2004). Ketoreductases in the synthesis of valuable chiral intermediates: application in the synthesis of α -hydroxy β -amino and β -hydroxy γ -amino acids. *Tetrahedron* 3: 663-669.
- Kawanami, Y., Murao, S., Ohga, T. and Kobayashi, N. (2003). Practical enantioselective reduction of ketones using oxazaborolidine catalyst generated in situ from chiral lactam alcohol and borane. *Tetrahedron* 42: 8411-8414.
- Kirschner, D., Jaramillo, M., Green, T., Hapiot, F., Leclercq, L., Bricout, H. and Monflier, E. (2008). Fine tuning of sulfoalkylated cyclodextrin structures to improve their mass-transfer properties in an aqueous biphasic hydroformylation reaction. *J. Mol. Catal. A: Chem.* 1-2: 11-20.
- Li, D., Carr, G., Zhang, Y., Williams, D.E., Amlani, A., Bottriell, H., Mui, A.L.F. and Andersen, R.J. (2011). Turnagainolides A and B, cyclic depsipeptides produced in culture by a *Bacillus* sp.: isolation, structure elucidation, and synthesis. *J. Nat. Prod.* 5: 1093-1099.
- Ma, X., Li, W., Li, X., Tao, X., Fan, W., Xie, X., Ayad, T., Ratovelomanana-Vidal, V. and Zhang, Z. (2012). Ru-catalyzed highly chemo- and enantioselective hydrogenation of γ -halo- γ,δ -unsaturated- β -keto esters under neutral conditions. *Chem. Commun.* 43: 5352-5354.
- Mathre, D.J., Thompson, A.S., Douglas, A.W., Hoogsteen, K., Carroll, J.D., Corley, E.G. and Grabowski, E.J.J. (1993). A practical process for the preparation of tetrahydro-1-methyl-3,3-diphenyl-1H,3H-pyrrolo[1,2-c][1,3,2]oxazaborole-borane. A highly enantioselective stoichiometric and catalytic reducing agent. *J. Org. Chem.* 10: 2880-2888.
- Matsuda, T., Yamanaka, R. and Nakamura, K. (2009). Recent progress in biocatalysis for asymmetric oxidation and reduction. *Tetrahedron: Asymmetry* 5: 513-557.
- Moorhoff, C.M. (2003). An efficient separation method for enol phosphate and corresponding β -ketophosphonate from their mixtures under aqueous conditions. *Synth. Commun.* 12: 2069-2086.
- Moorhoff, C.M. and Schneider, D.F. (1987). Comments on the reaction of ethyl 4-(diethoxyphosphinyl)-3-oxobutanoate and related phosphonate esters with enals. *Tetrahedron Lett.* 5: 559-562.
- Mukaiyama, T. (2004). The directed aldol reaction. *Organic Reactions*, John Wiley & Sons, Inc.
- Ohkuma, T., Koizumi, M., Doucet, H., Pham, T., Kozawa, M., Murata, K., Katayama, E., Yokozawa, T., Ikariya, T. and Noyori, R. (1998). Asymmetric hydrogenation of alkenyl, cyclopropyl, and aryl ketones. $\text{RuCl}_2(\text{xylbinap})(1,2\text{-diamine})$ as a precatalyst exhibiting a wide scope. *J. Am. Chem. Soc.* 120: 13529-13530.

Oisaki, K., Suto, Y., Kanai, M. and Shibasaki, M. (2003). A new method for the catalytic aldol reaction to ketones. *J. Am. Chem. Soc.* 19: 5644-5645.

Padhi, S.K. and Chadha, A. (2005). Deracemisation of aromatic β -hydroxy esters using immobilised whole cells of *Candida parapsilosis* ATCC 7330 and determination of absolute configuration by ^1H NMR. *Tetrahedron: Asymmetry* 16: 2790-2798.

Reiff, E.A., Nair, S.K., Narayan Reddy, B.S., Inagaki, J., Henri, J.T., Greiner, J.F. and Georg, G.I. (2004). Practical syntheses of the C12-C21 epothilone subunit via catalytic asymmetric reductions: Itsuno-Corey oxazaborolidine reduction and asymmetric Noyori hydrogenation. *Tetrahedron Lett.* 30: 5845-5847.

Rimoldi, I., Cesarotti, E., Zerla, D., Molinari, F., Albanese, D., Castellano, C. and Gandolfi, R. (2011). 3-(Hydroxy(phenyl)methyl)azetidin-2-ones obtained via catalytic asymmetric hydrogenation or by biotransformation. *Tetrahedron: Asymmetry* 5: 597-602.

Rimoldi, I., Pellizzoni, M., Facchetti, G., Molinari, F., Zerla, D. and Gandolfi, R. (2011). Chemo- and biocatalytic strategies to obtain phenylisoserine, a lateral chain of Taxol by asymmetric reduction. *Tetrahedron: Asymmetry* 24: 2110-2116.

Saravanan, T., Selvakumar, R., Doble, M. and Chadha, A. (2012). Stereochemical preference of *Candida parapsilosis* ATCC 7330 mediated deracemization: E- versus Z-aryl secondary alcohols. *Tetrahedron: Asymmetry* 18-19: 1360-1368.

Schmidt, B. (2004). Ruthenium-catalyzed olefin metathesis double-bond isomerization sequence. *J. Org. Chem.* 22: 7672-7687.

Schmidt, B., Kunz, O. and Petersen, M.H. (2012). Total syntheses of naturally occurring Seimatopolide A and its enantiomer from chiral pool starting materials using a bidirectional strategy. *J. Org. Chem.* 23: 10897-10906.

Schroer, K., Mackfeld, U., Tan, I.A.W., Wandrey, C., Heuser, F., Bringer-Meyer, S., Weckbecker, A., Hummel, W., Daubmann, T., Pfaller, R., Liese, A. and Lütz, S. (2007). Continuous asymmetric ketone reduction processes with recombinant *Escherichia coli*. *J. Biotechnol.* 4: 438-444.

Seashore-Ludlow, B., Saint-Dizier, F. and Somfai, P. (2012). Asymmetric transfer hydrogenation coupled with dynamic kinetic resolution in water: synthesis of anti- β -Hydroxy- α -amino acid derivatives. *Org. Lett.* 24: 6334-6337.

Smrčina, M., Lorenc, M., Hanuš, V. and Kočovský, P. (1991). A facile synthesis of 2-amino-2'-hydroxyl-1,1'-binaphthyl and 2,2'-diamino-1,1'-binaphthyl by oxidative coupling using copper (II) chloride. *Synlett* 4: 231-232.

Svendsen, A. and Boll, P.M. (1973). Naturally occurring lactones and lactames-V: Halogenated β -keto esters as starting materials for the synthesis of tetrionic acids. *Tetrahedron* 24: 4251-4258.

Taber, D.F. and Silverberg, L.J. (1991). Enantioselective reduction of β -keto esters. *Tetrahedron Lett.* 34: 4227-4230.

Turner, N.J. (2009). Directed evolution drives the next generation of biocatalysts. *Nat. Chem. Biol.* 8: 568-574.

Vandengoerbergh, J.A.M. and Vandergen, A. (1980). Ethyl 4-diphenylphosphinoyl-2-oxobutanoate - a convenient reagent for the synthesis of γ -unsaturated, δ -unsaturated β -Ketoesters. *Tetrahedron Lett.* 37: 3621-3624.

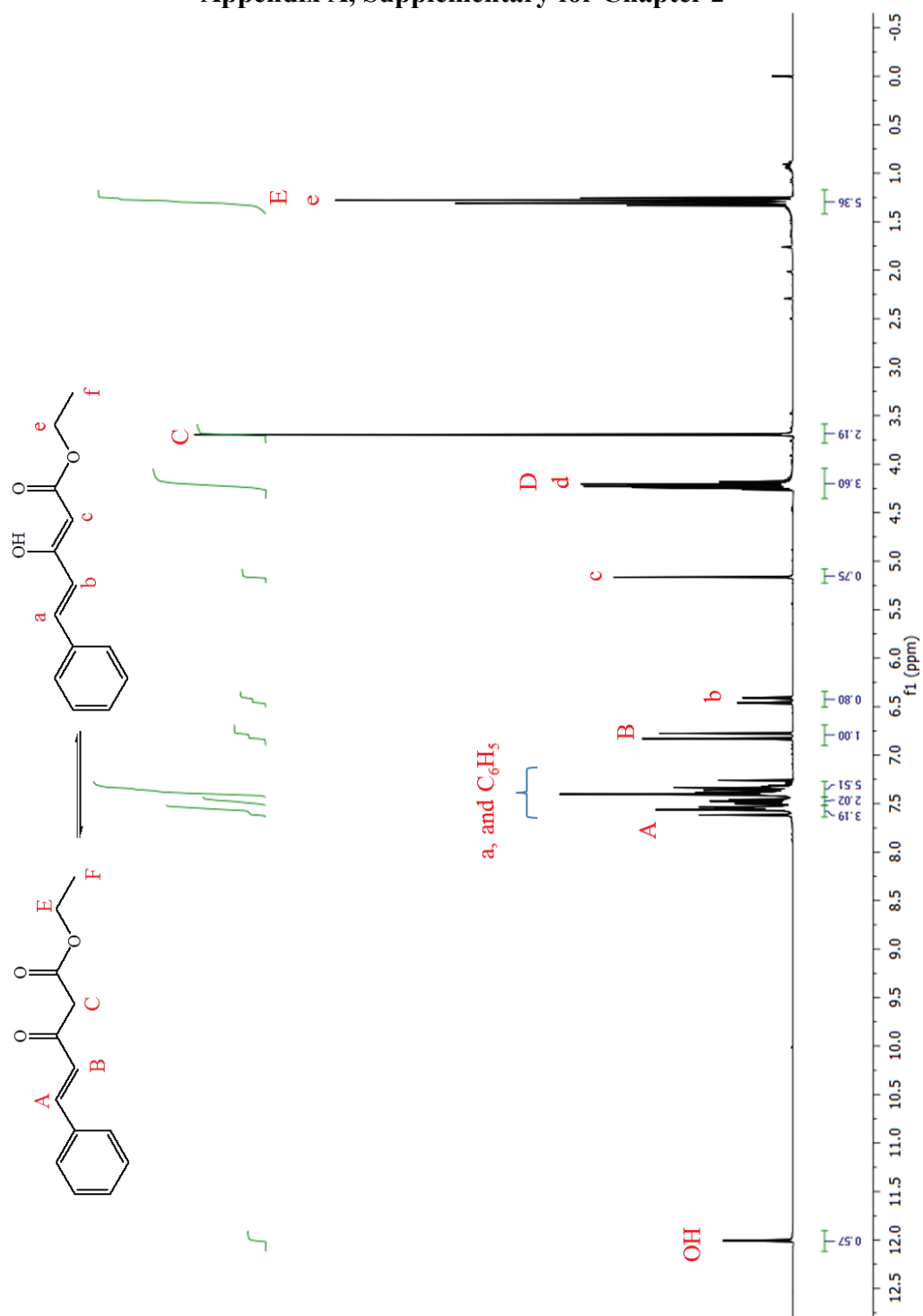
Zhang, Z., Qian, H., Longmire, J. and Zhang, X. (2000). Synthesis of chiral bisphosphines with tunable bite angles and their applications in asymmetric hydrogenation of β -ketoesters. *J. Org. Chem.* 19: 6223-6226.

Zhou, Y.-G., Tang, W., Wang, W.-B., Li, W. and Zhang, X. (2002). Highly Effective Chiral Ortho-Substituted BINAPO Ligands (o-BINAPO): Applications in Ru-catalyzed asymmetric hydrogenations of β -aryl-substituted β -(acylamino)acrylates and β -keto esters. *J. Am. Chem. Soc.* 18: 4952-4953.

Zhu, D., Mukherjee, C., Rozzell, J.D., Kambourakis, S. and Hua, L. (2006). A recombinant ketoreductase tool-box. Assessing the substrate selectivity and stereoselectivity toward the reduction of β -ketoesters. *Tetrahedron* 5: 901-905.

Zhu, D., Yang, Y. and Hua, L. (2006). Stereoselective enzymatic synthesis of chiral alcohols with the use of a carbonyl reductase from *Candida magnoliae* with anti-prelog enantioselectivity. *J. Org. Chem.* 11: 4202-4205.

Appendix A, Supplementary for Chapter 2

**Figure A2.1.** ^1H NMR spectrum of **2A** in CDCl_3 .

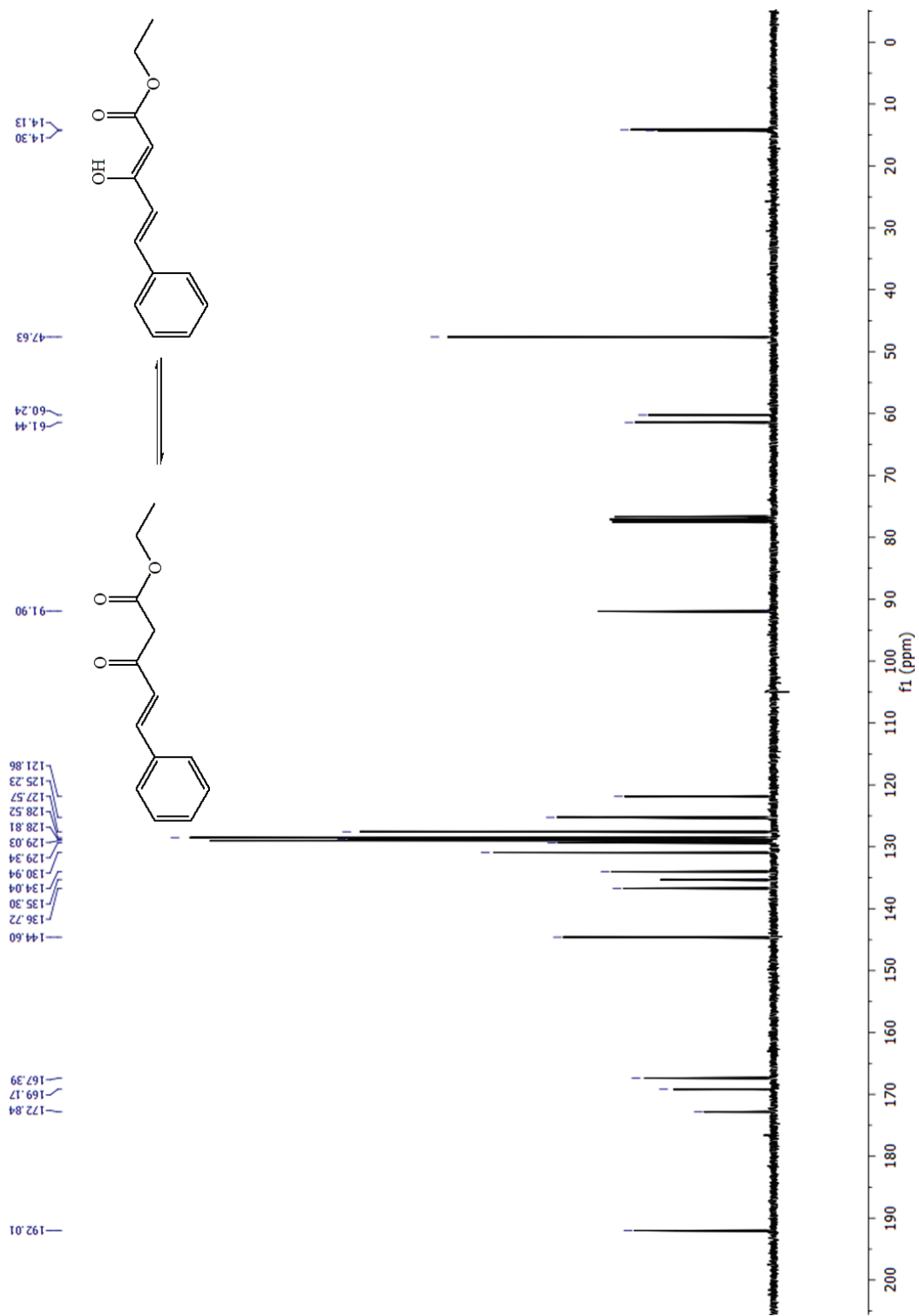


Figure A2.2. ^{13}C NMR spectrum of **2A** in CDCl_3 .

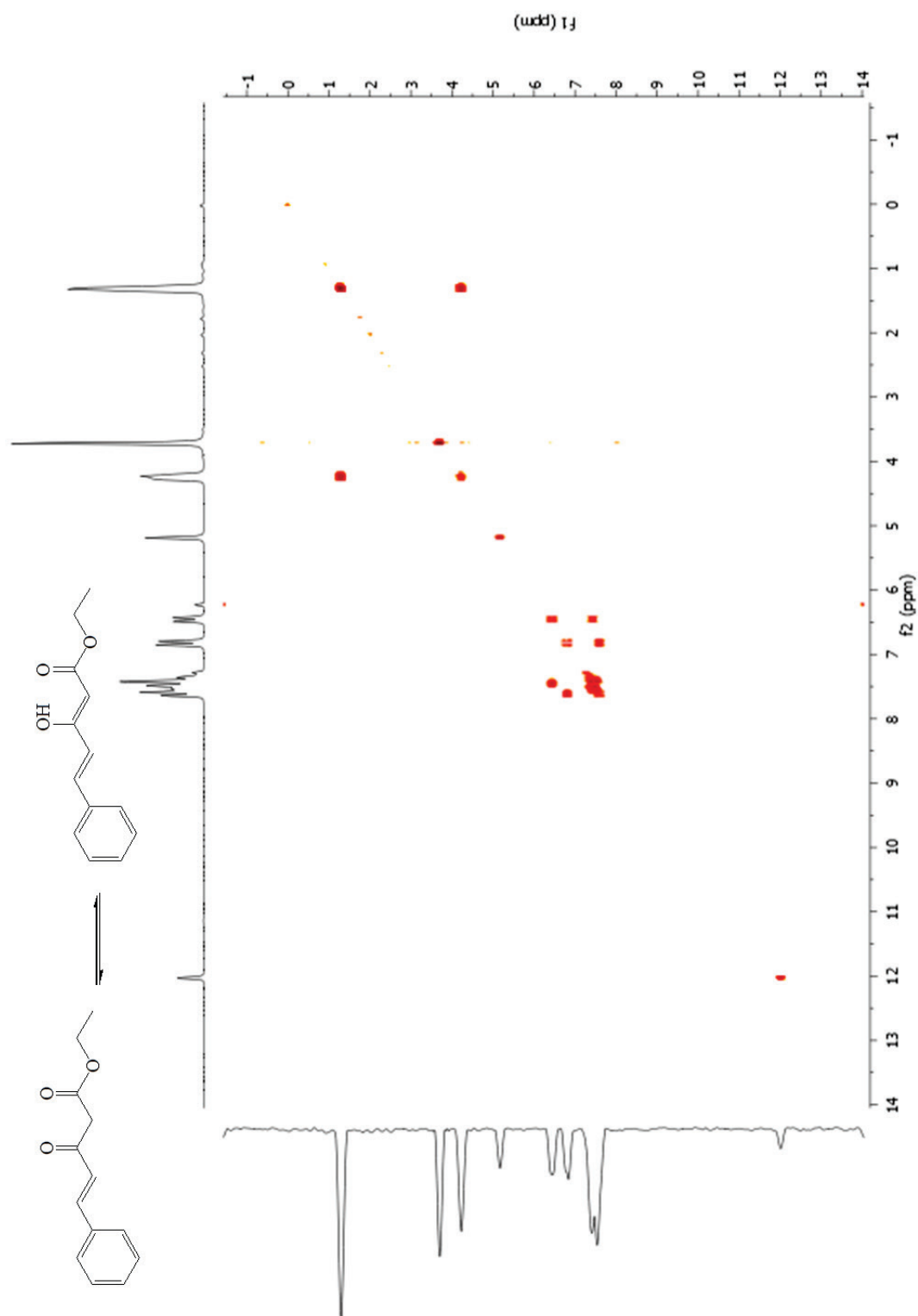


Figure A2.3. gCOSY spectrum of 2A in CDCl₃.

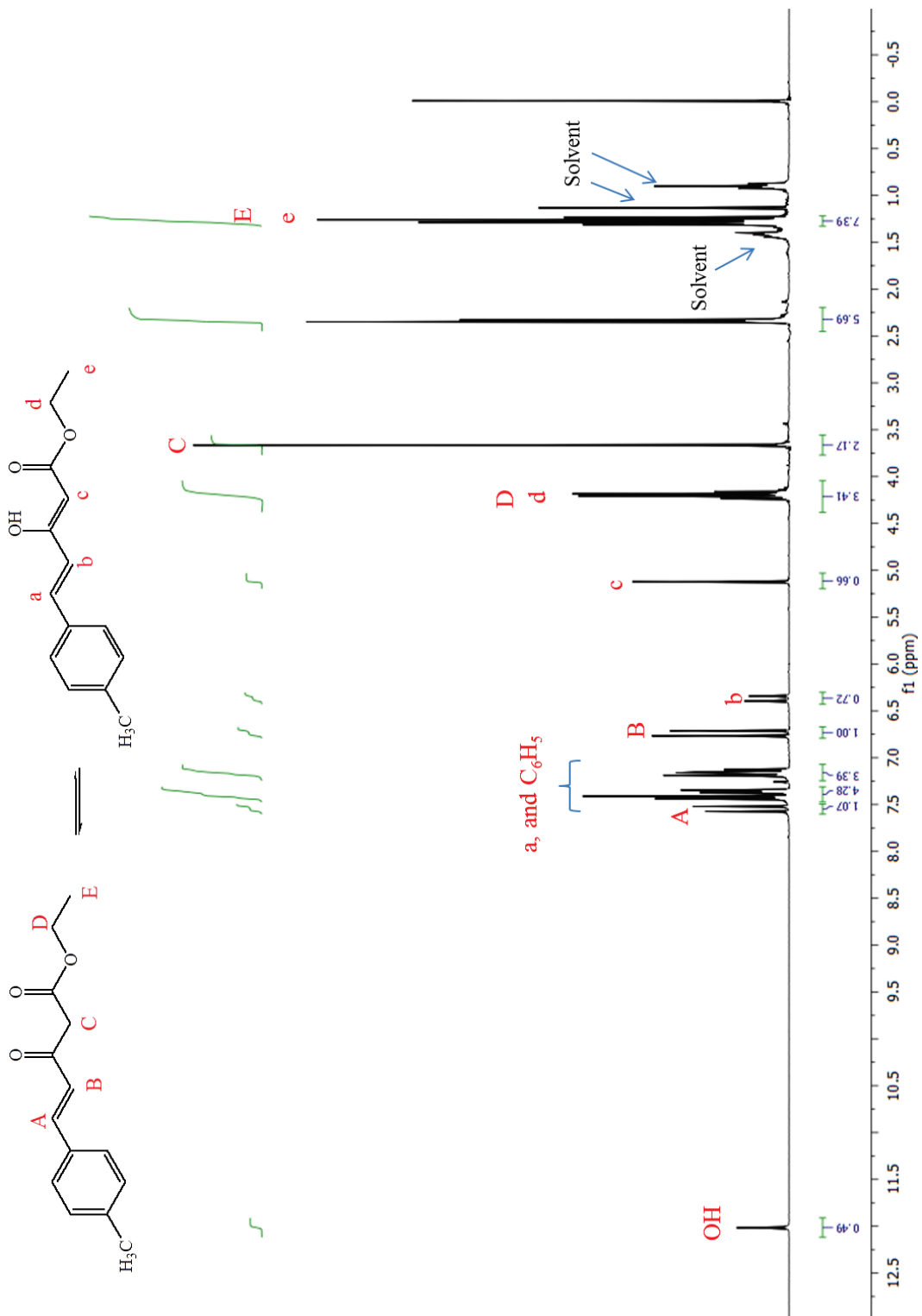


Figure A2.4. ^1H NMR spectrum of **2B** in CDCl_3 .

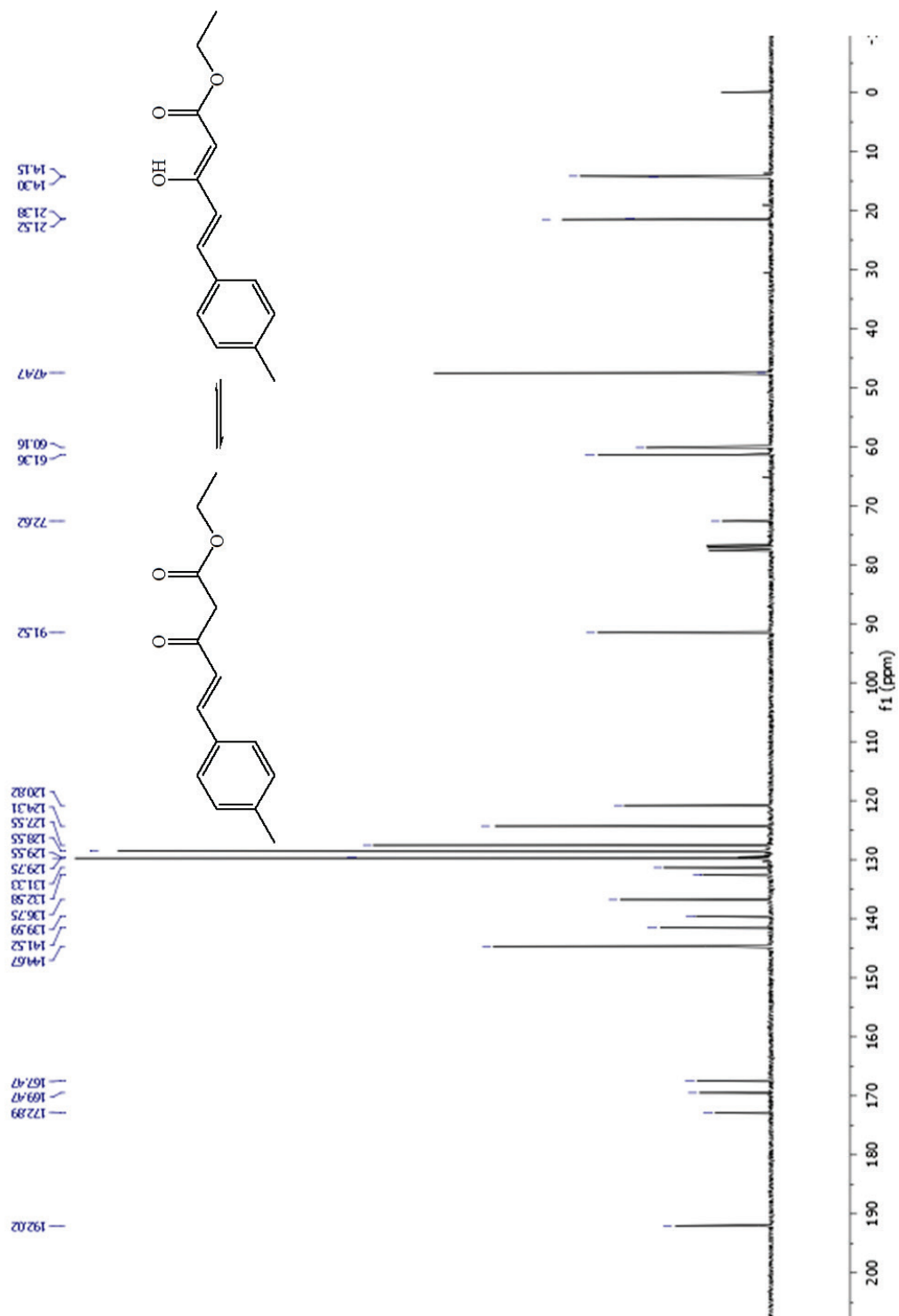


Figure A2.5. ^{13}C NMR spectrum of **2B** in CDCl_3 .

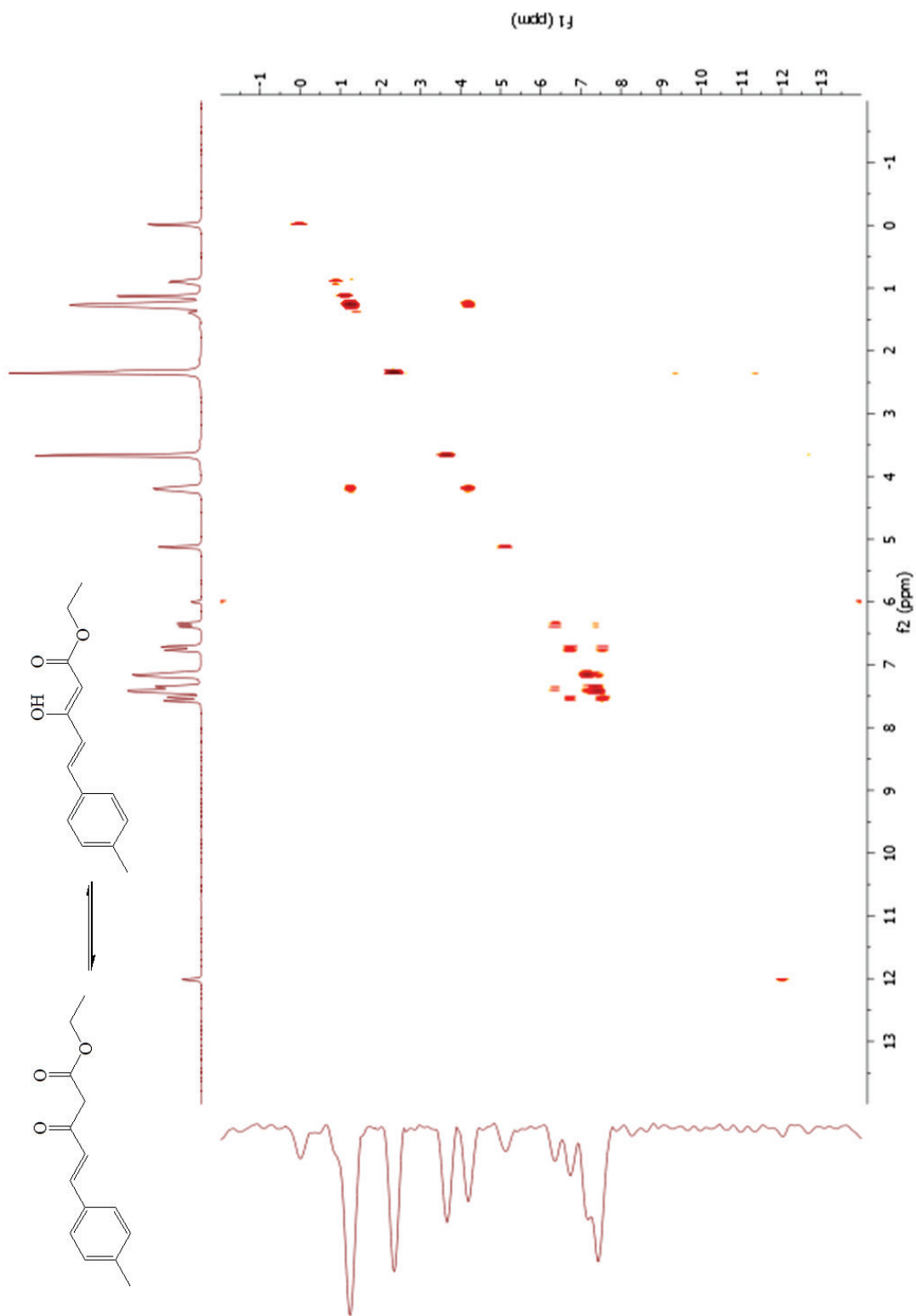


Figure A2.6. gCOSY spectrum of **2B** in CDCl_3 .

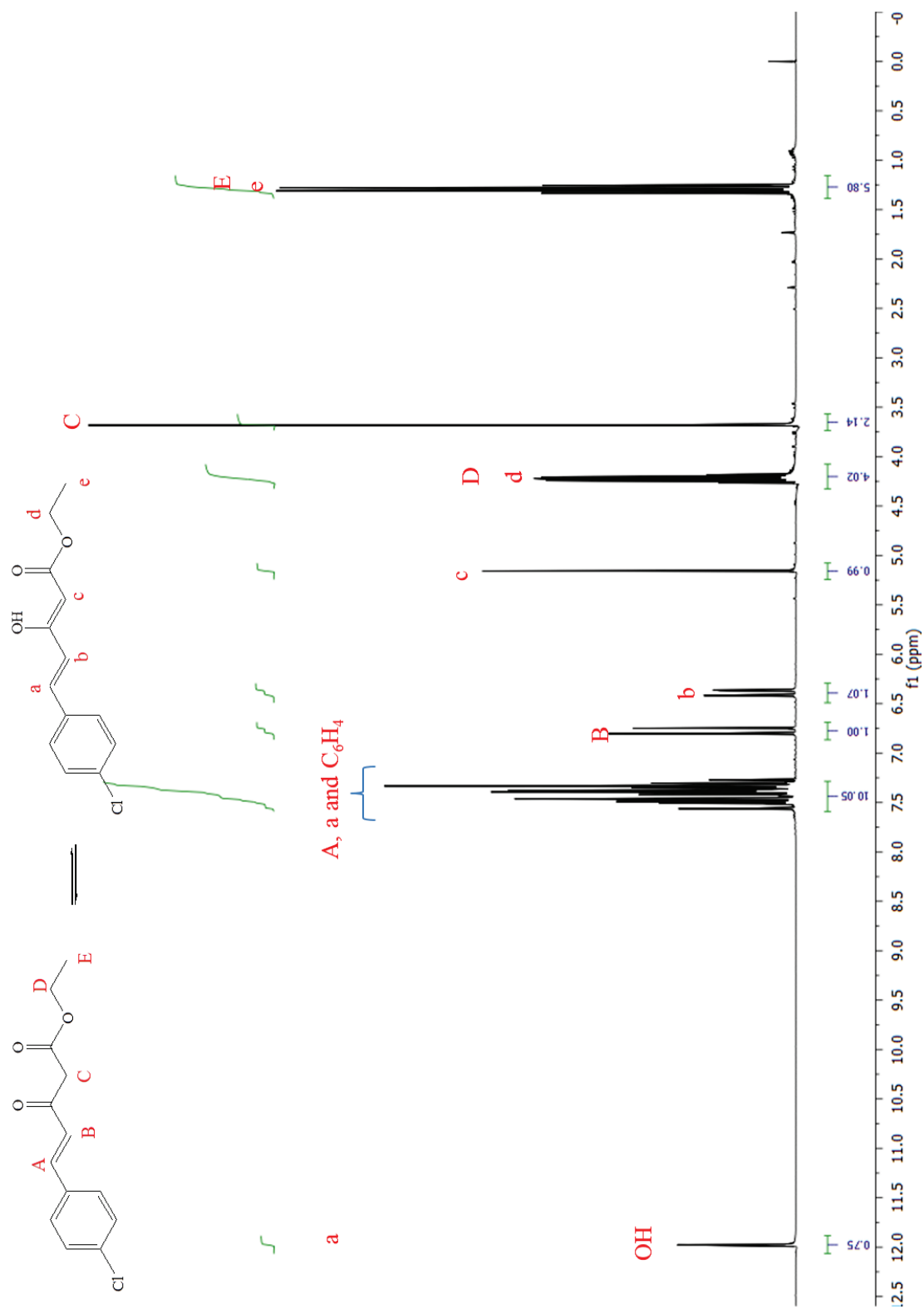


Figure A2.7. ^1H NMR spectrum of **2C** in CDCl_3 .

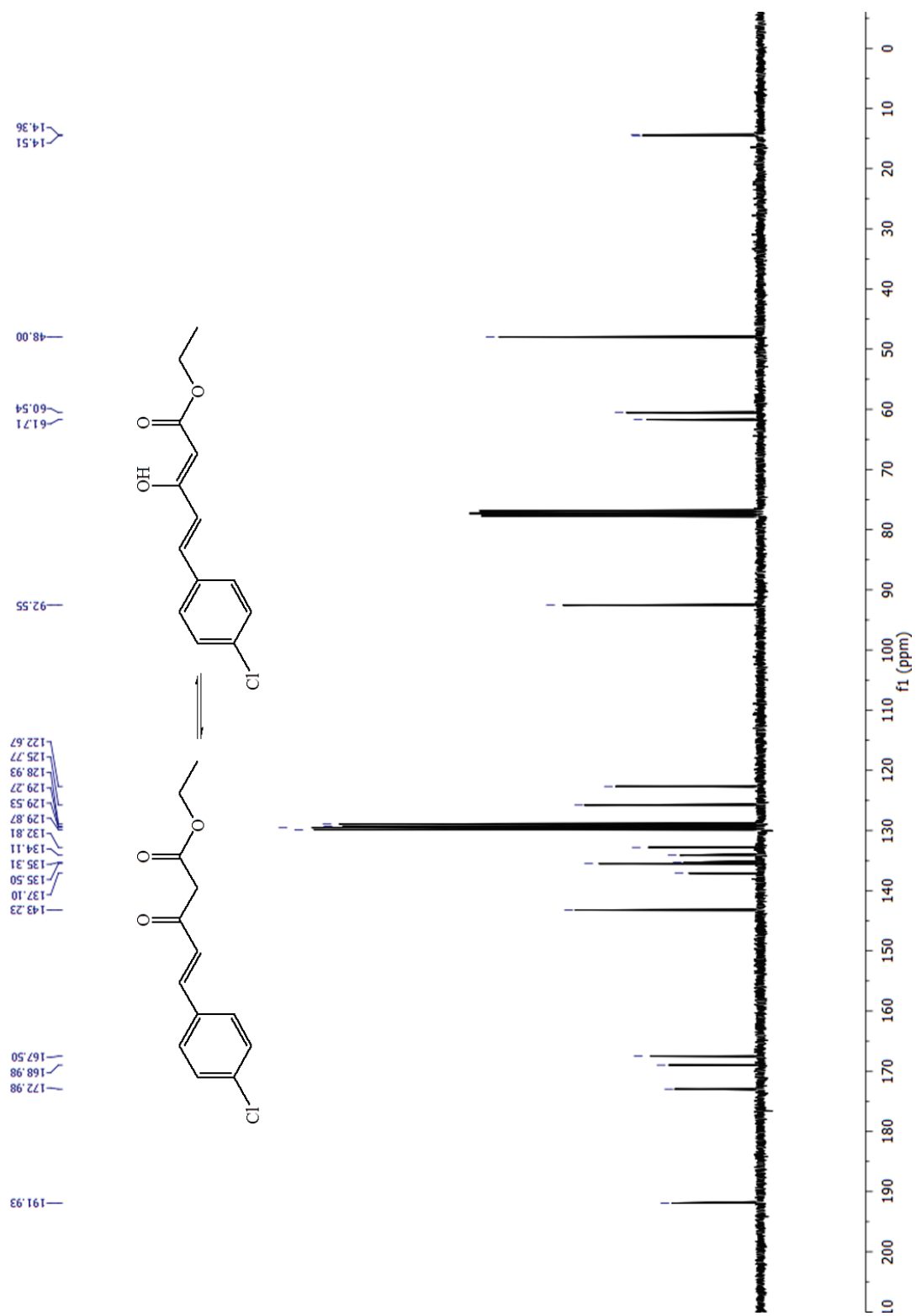


Figure A2.8. ^{13}C NMR spectrum of **2C** in CDCl_3 .

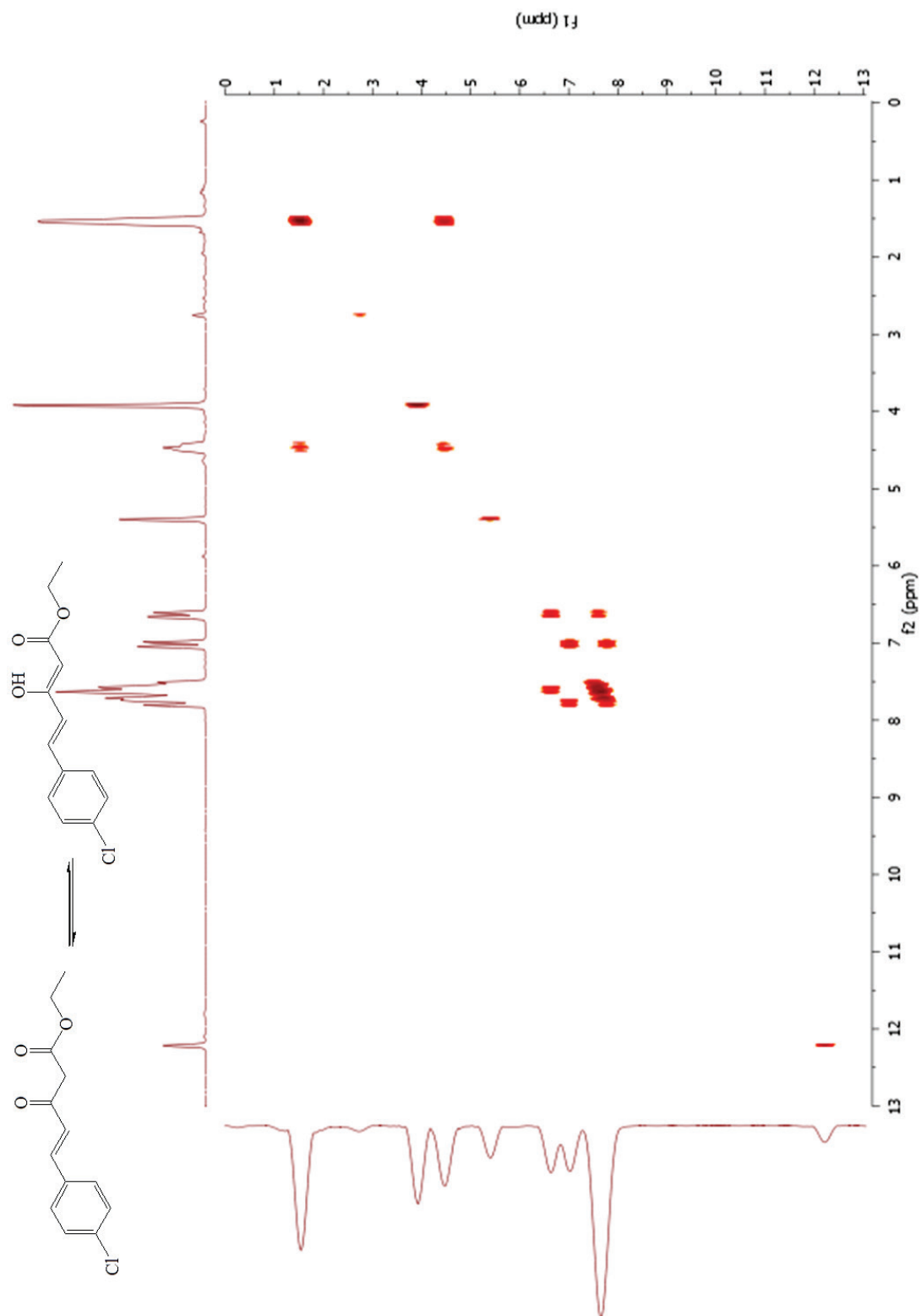


Figure A2.9. gCOSY spectrum of 2C in CDCl_3 .

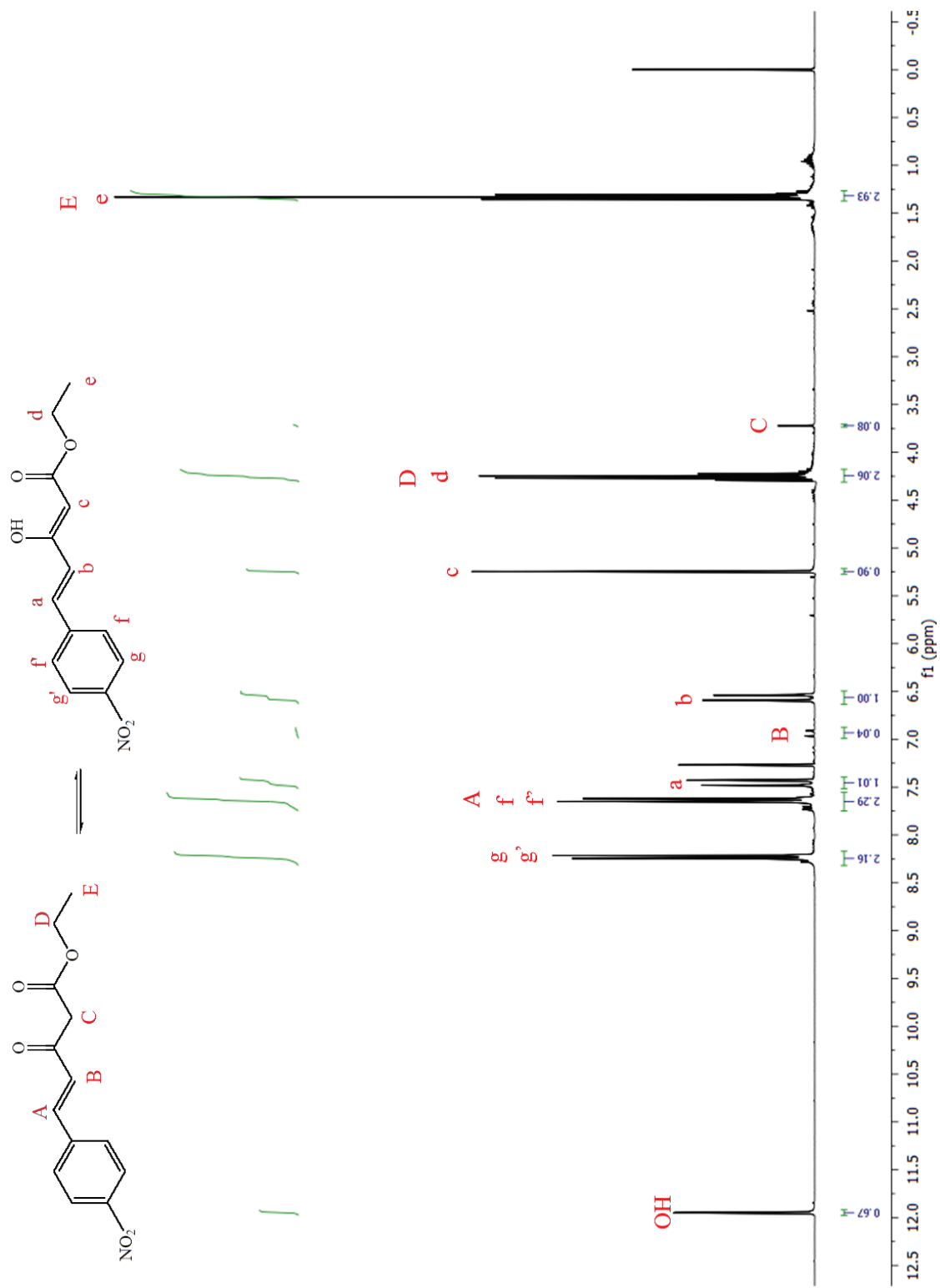


Figure A2.10. ^1H NMR spectrum of 2D in CDCl_3 .

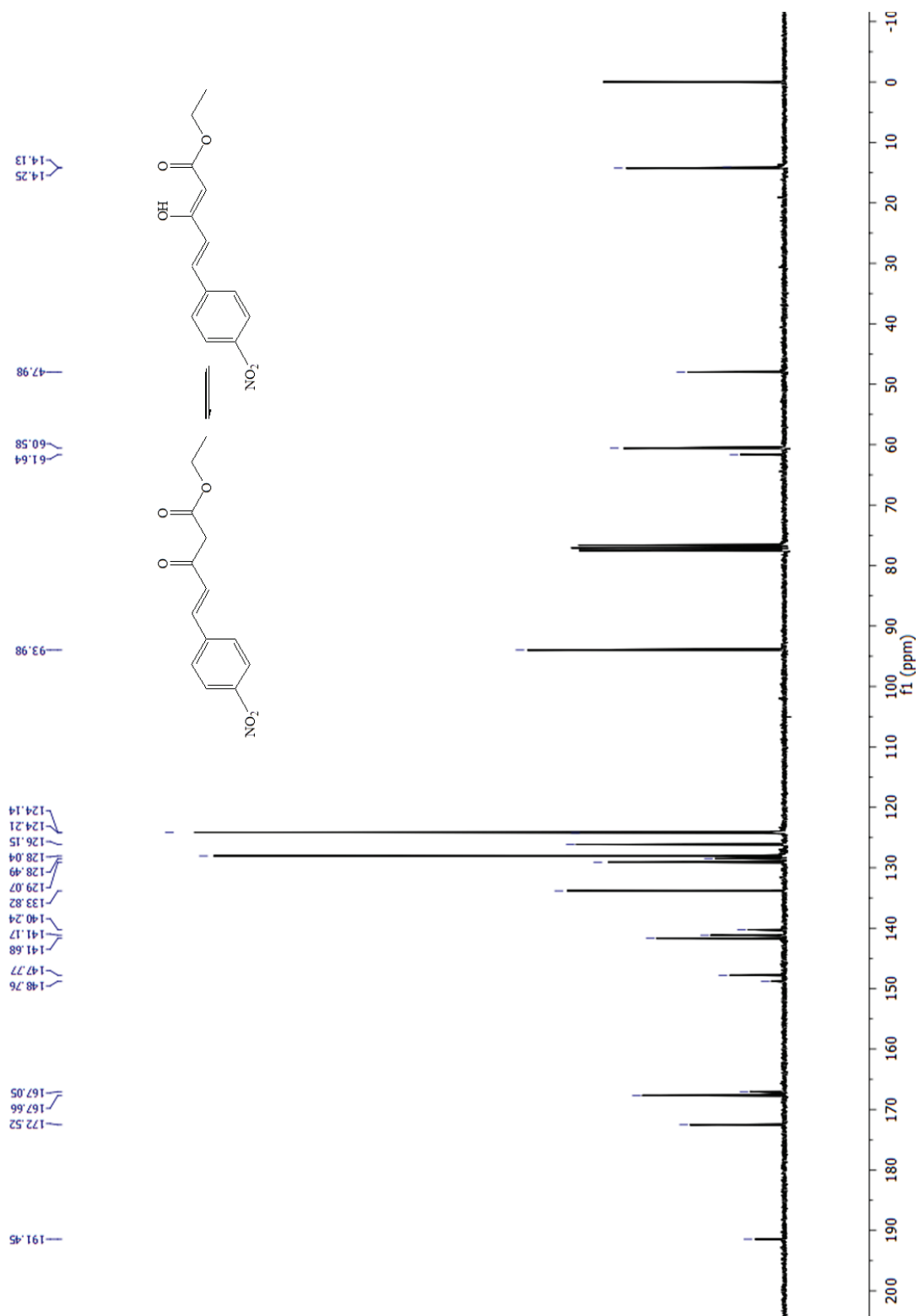


Figure A2.11. ^{13}C NMR spectrum of **2D** in CDCl_3 .

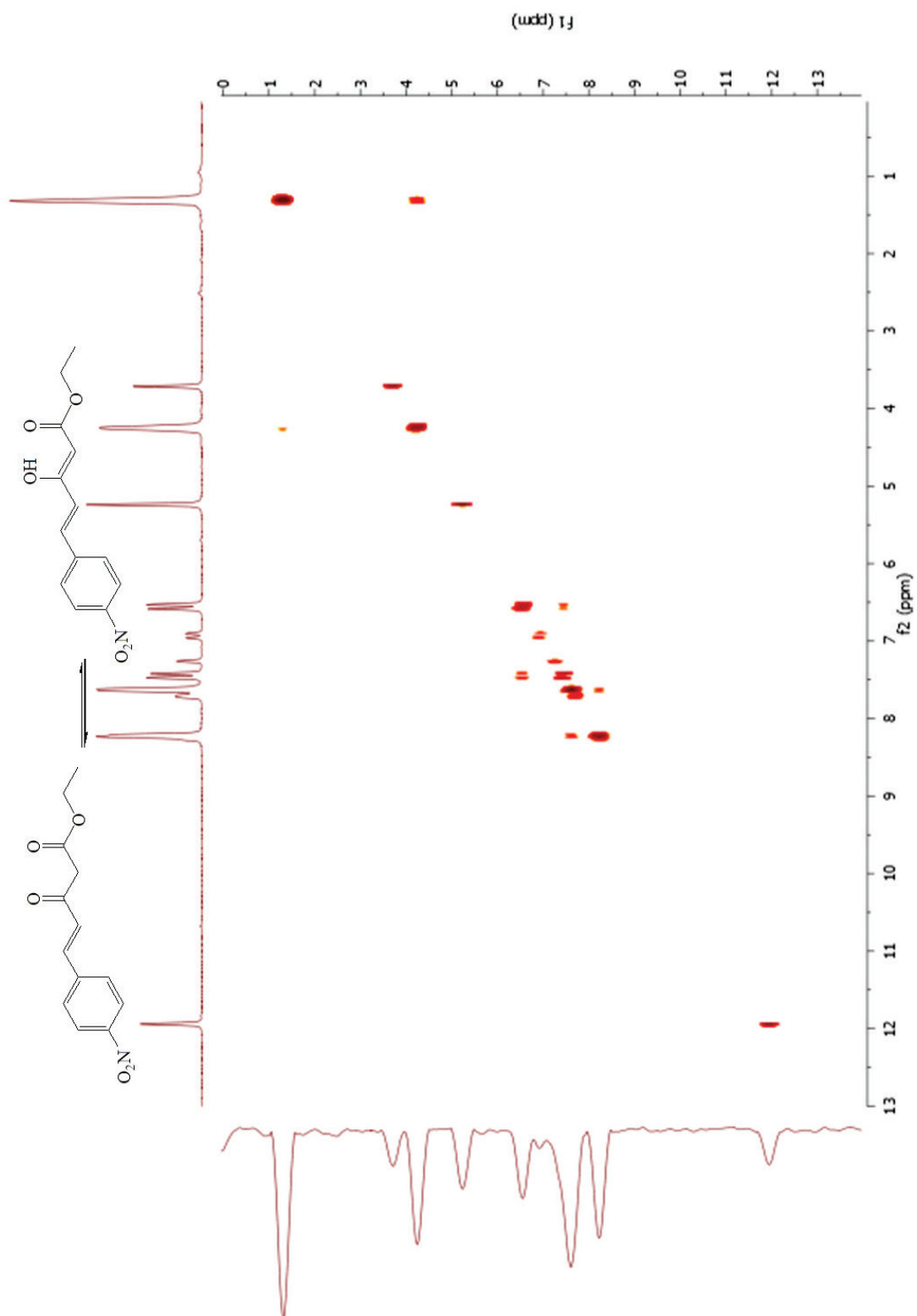


Figure A2.12. gCOSY spectrum of **2D** in CDCl_3 .

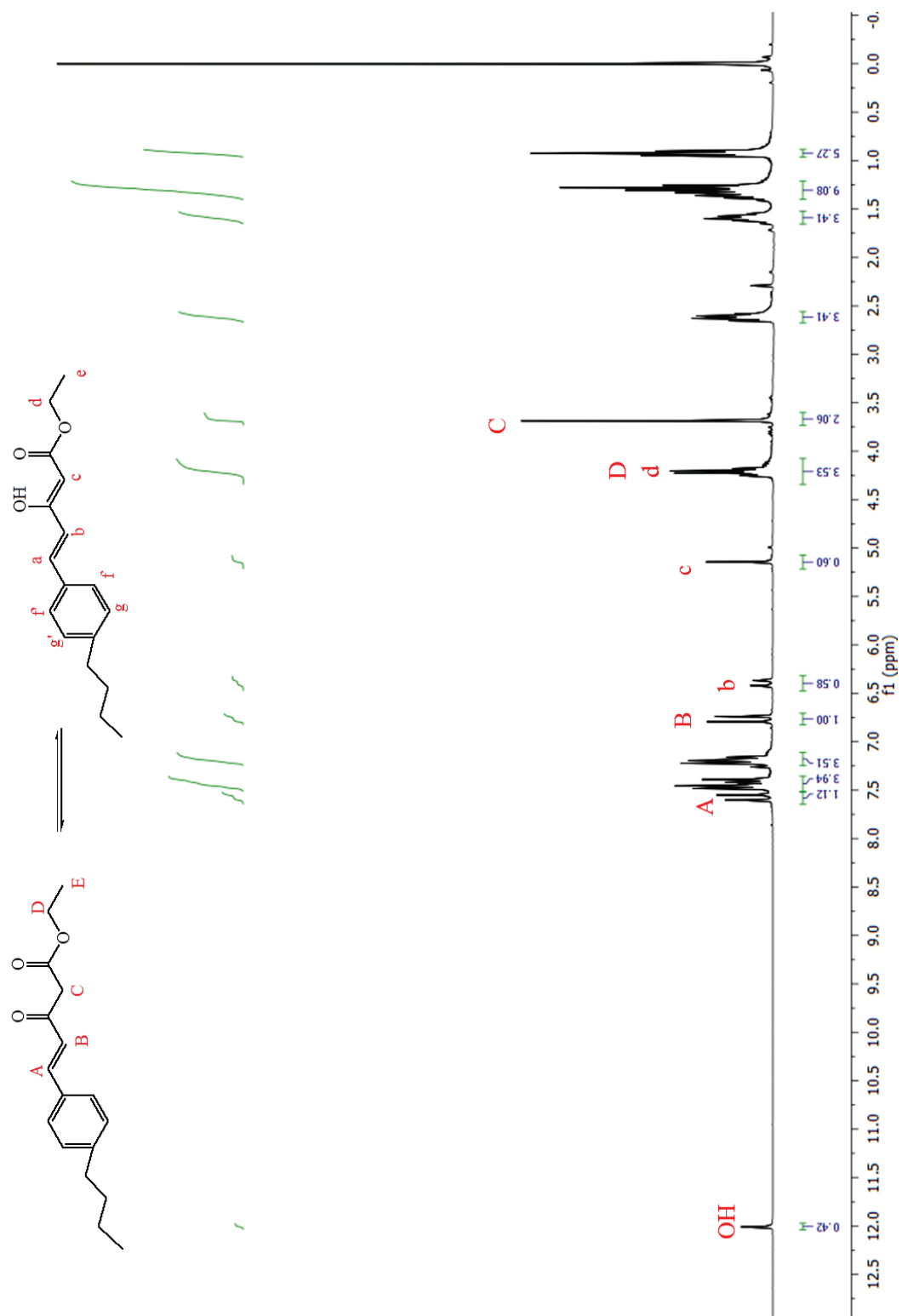
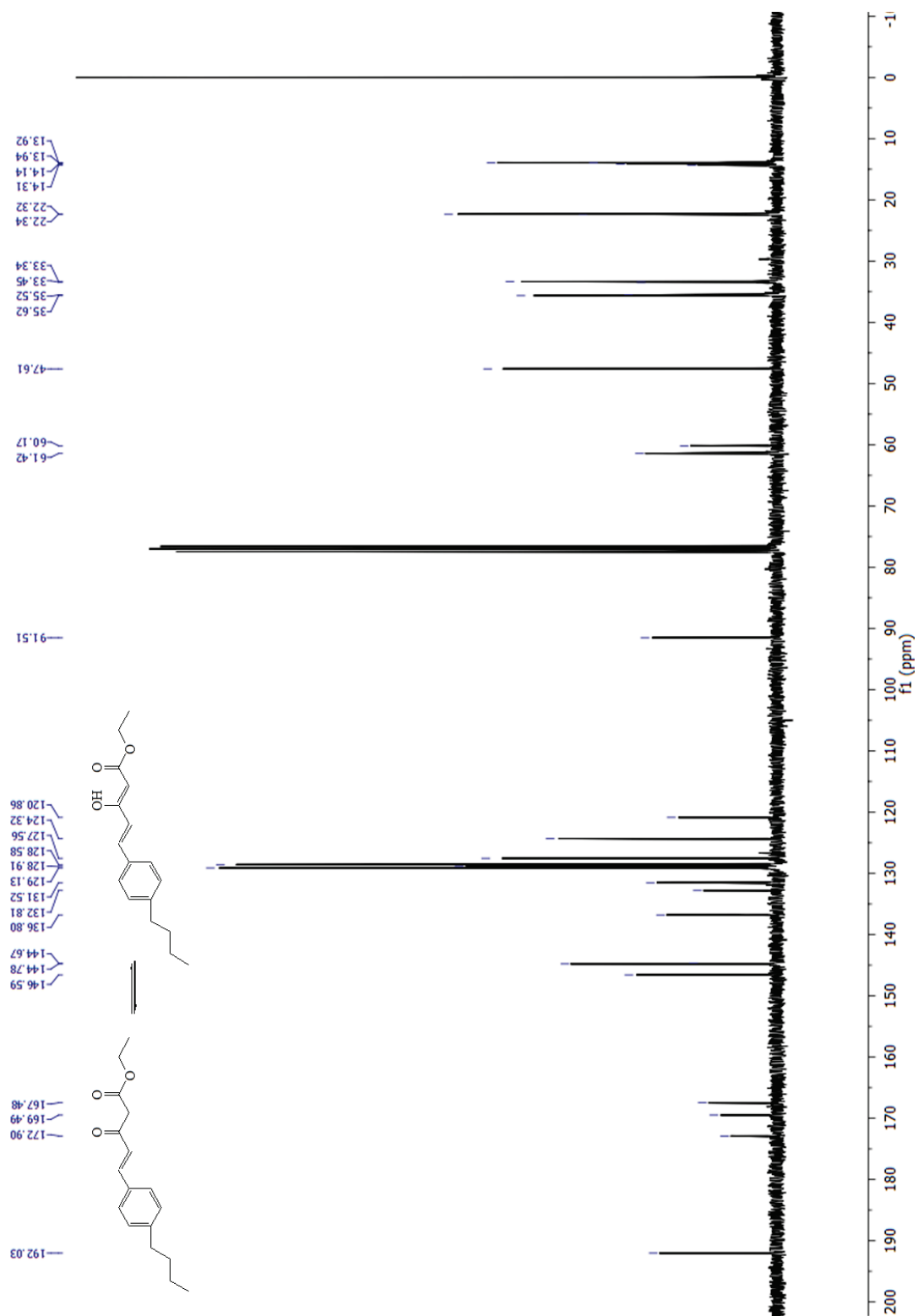


Figure A2.13. ^1H NMR spectrum of **2E** in CDCl_3 .



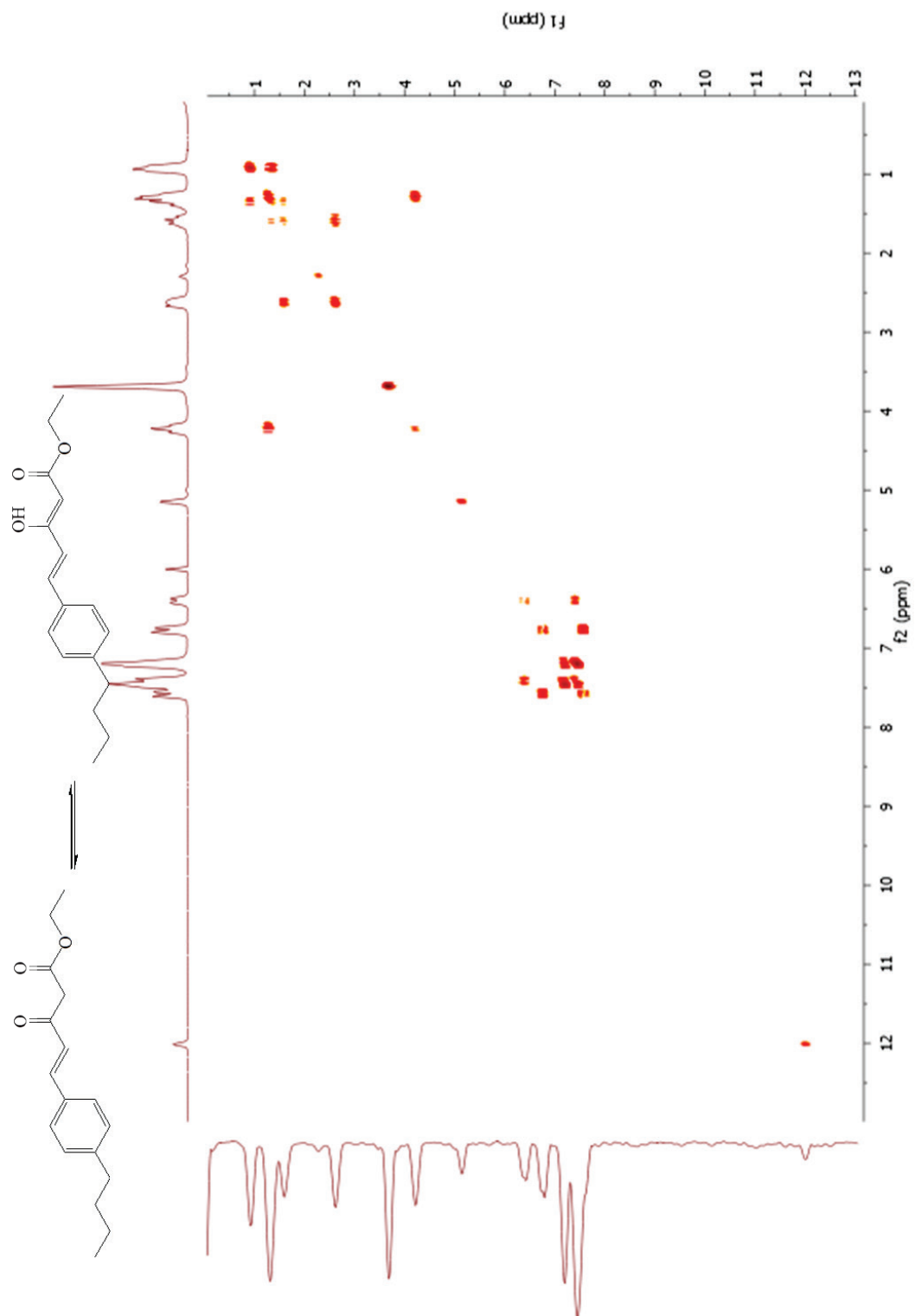


Figure A2.15. gCOSY spectrum of **2E** in CDCl_3 .

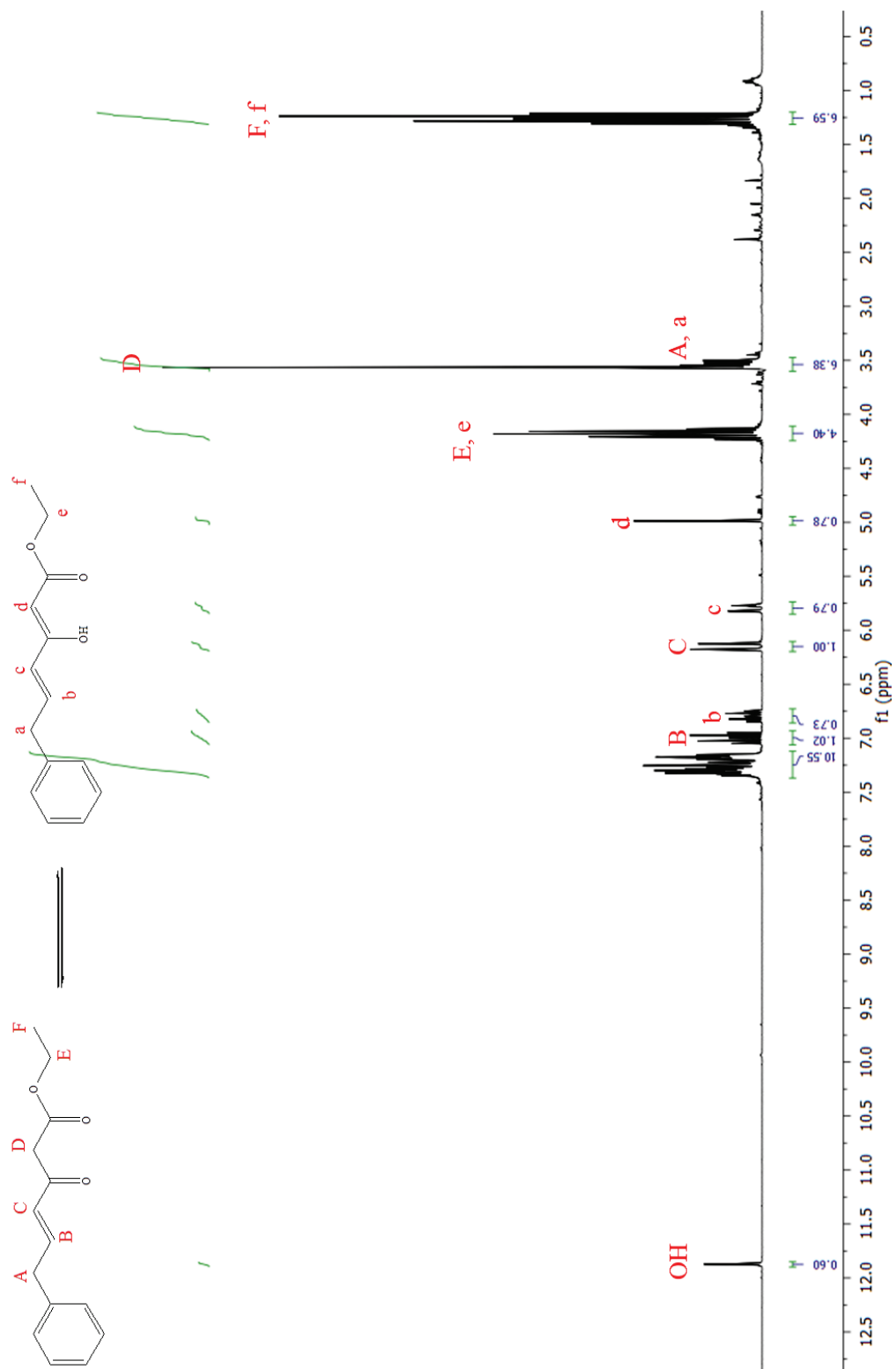


Figure A2.16. ^1H NMR spectrum of 2F in CDCl_3 .

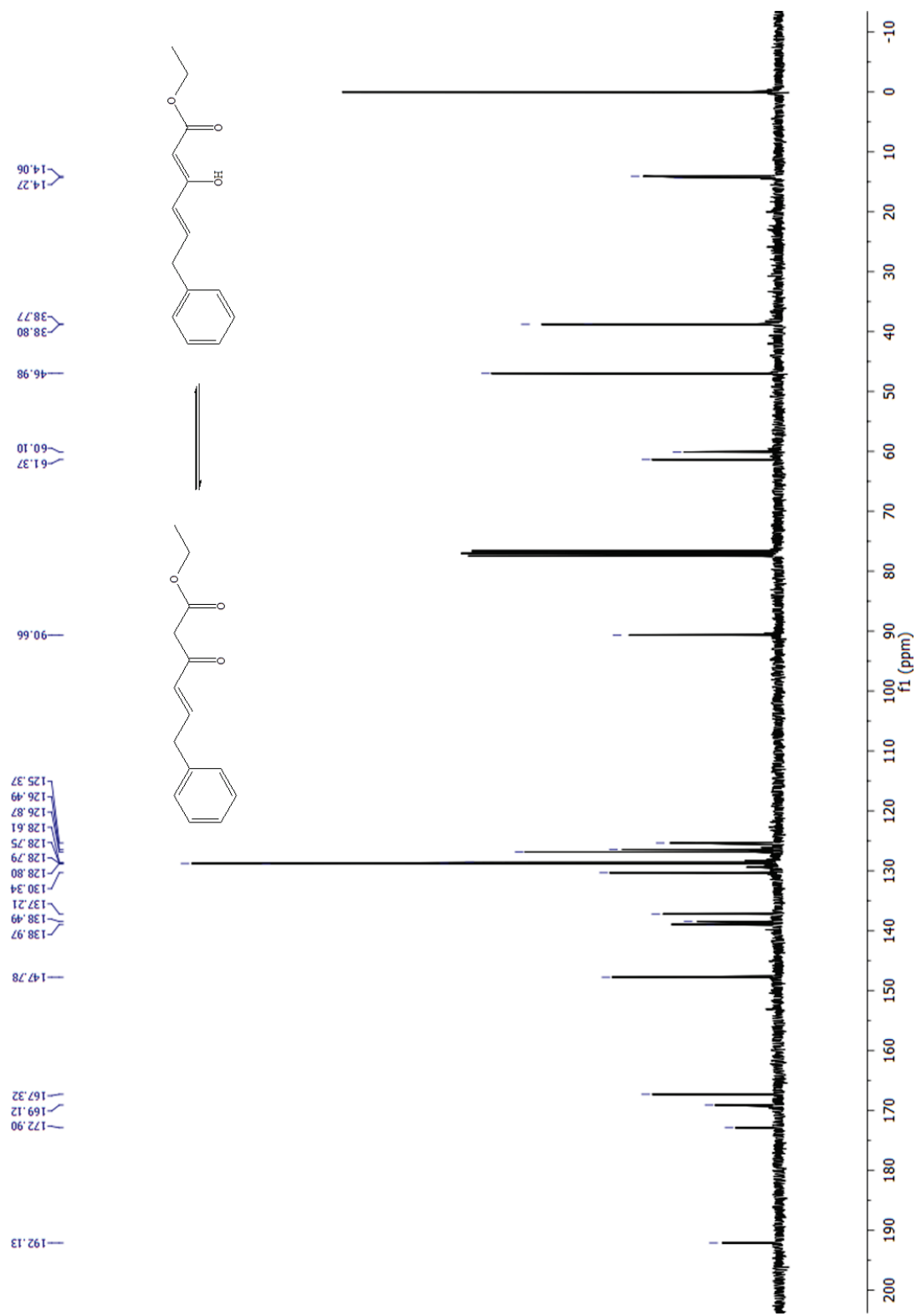


Figure A2.17. ^{13}C NMR spectrum of 2F in CDCl_3 .

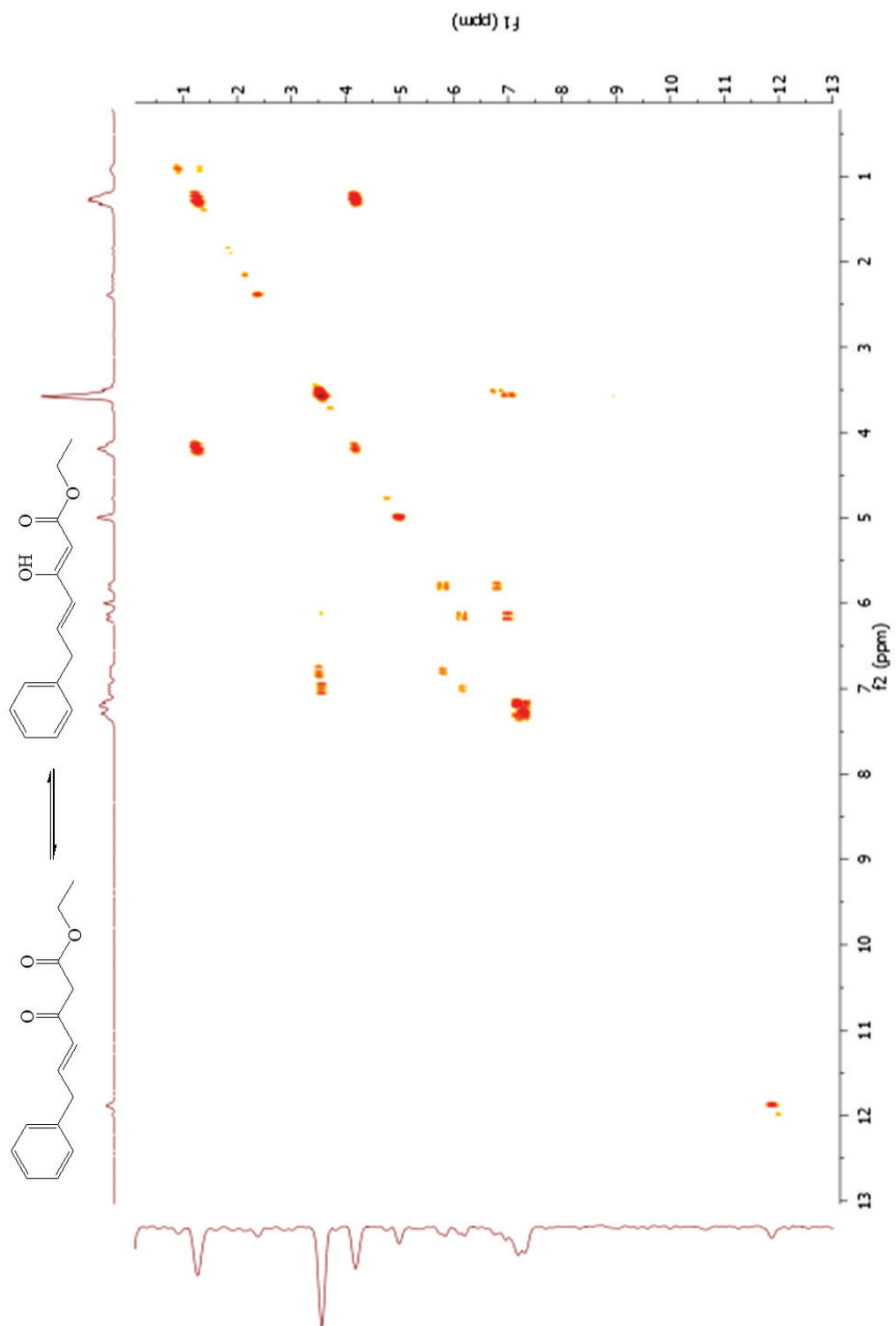


Figure A2.18. gCOSY spectrum of **2F** in CDCl_3 .

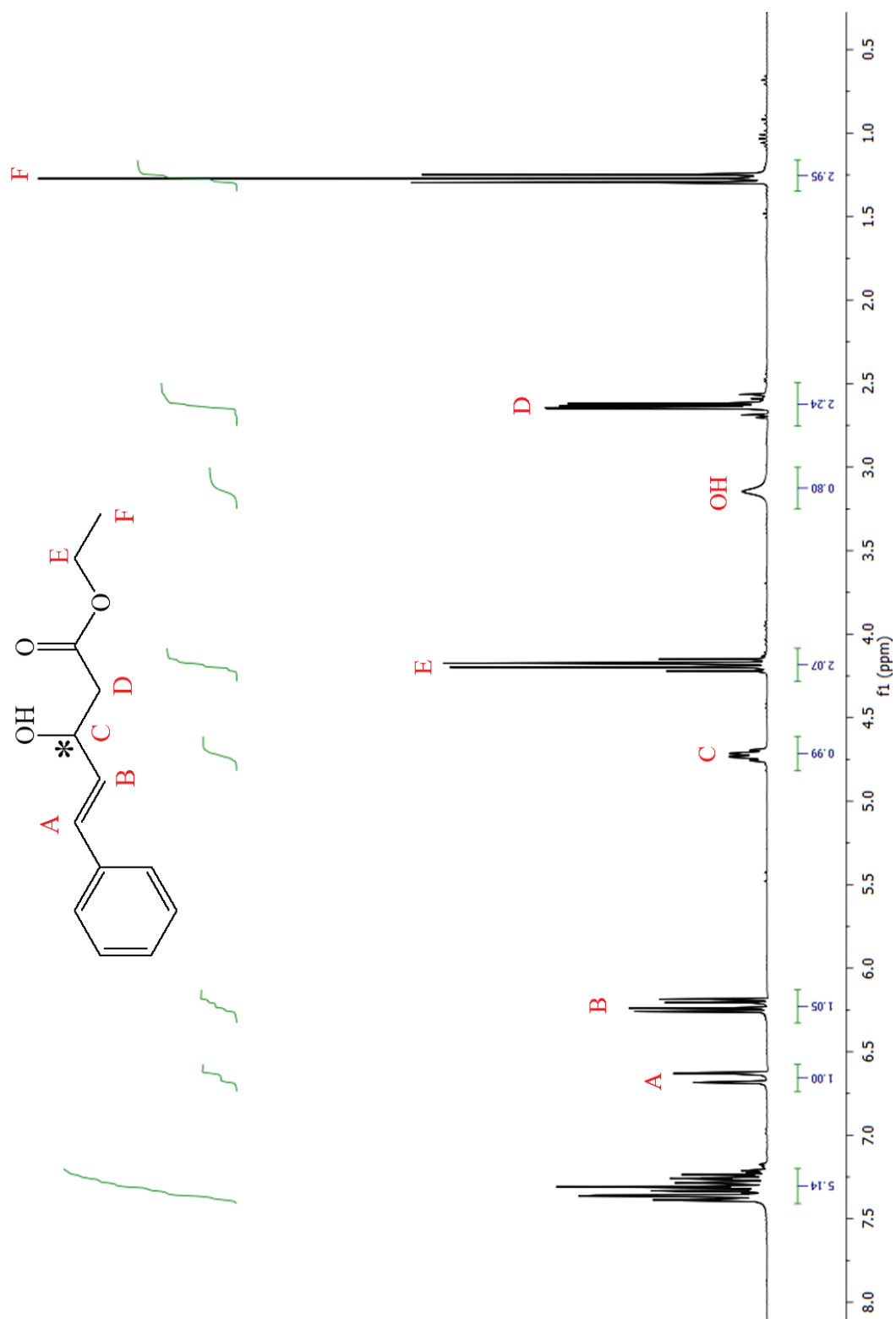


Figure A2.19. ^1H NMR spectrum of **3A** in CDCl_3 .

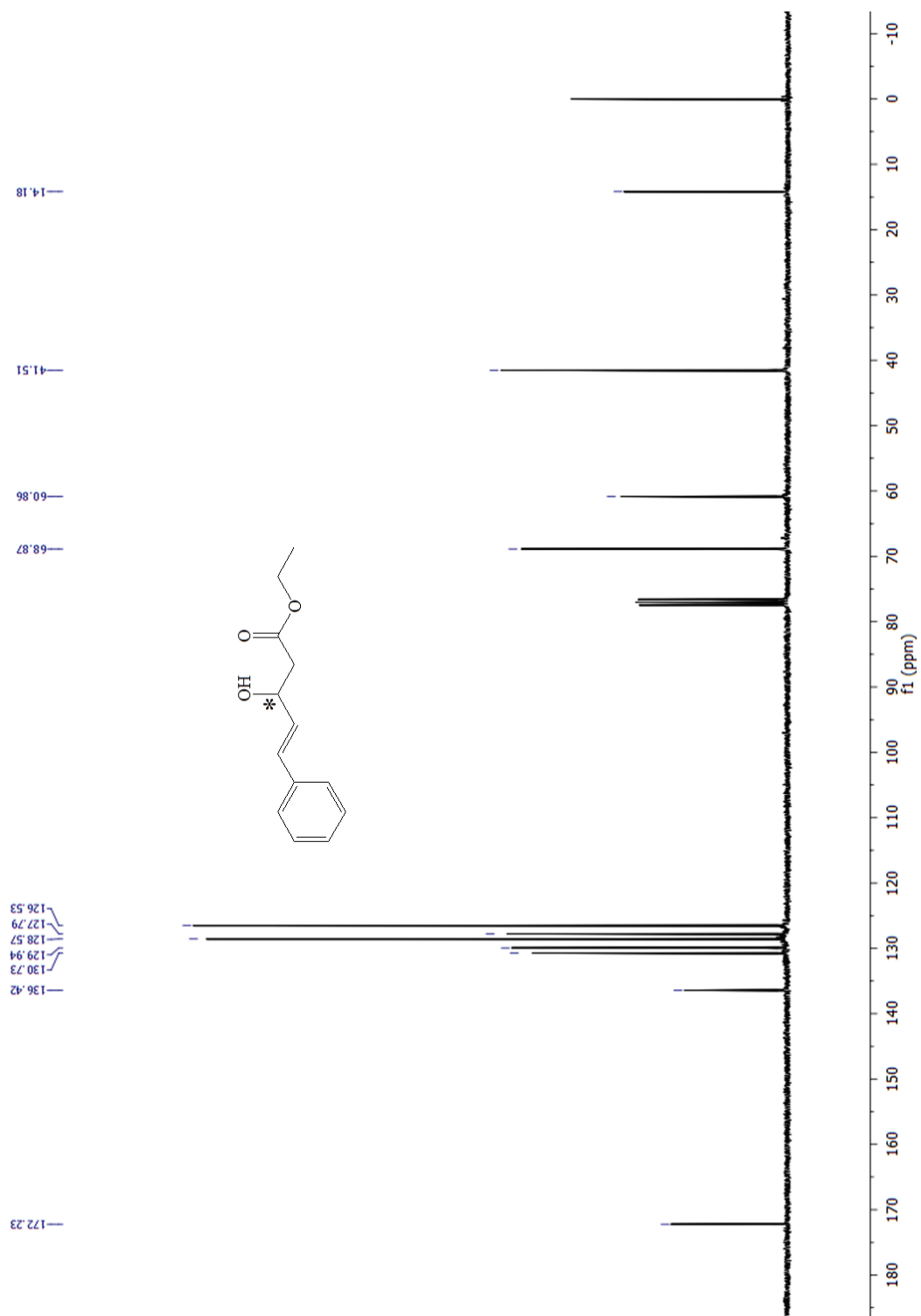


Figure A2.20. ^{13}C NMR spectrum of 3A in CDCl_3 .

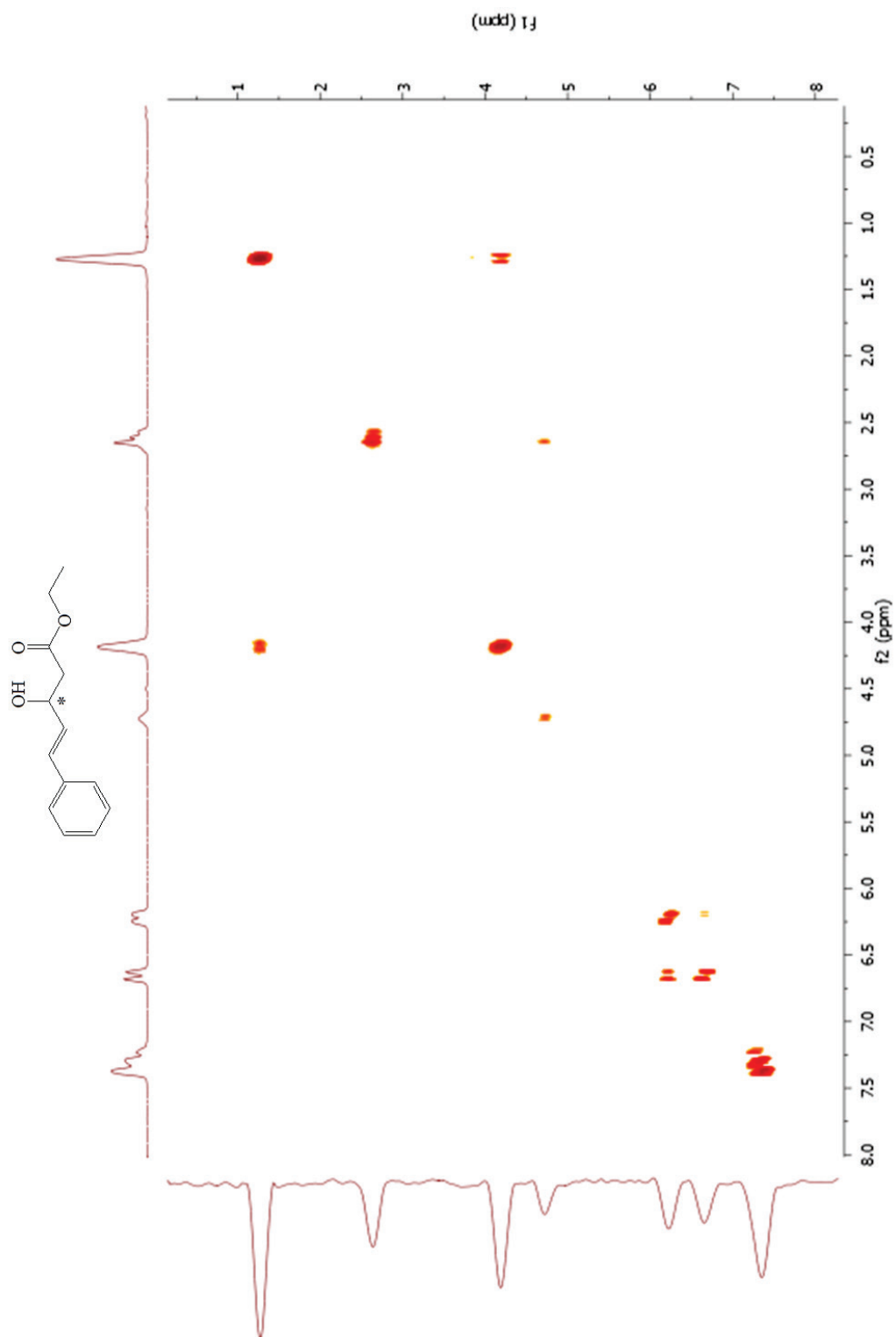


Figure A2.21. gCOSY spectrum of **3A** in CDCl₃.

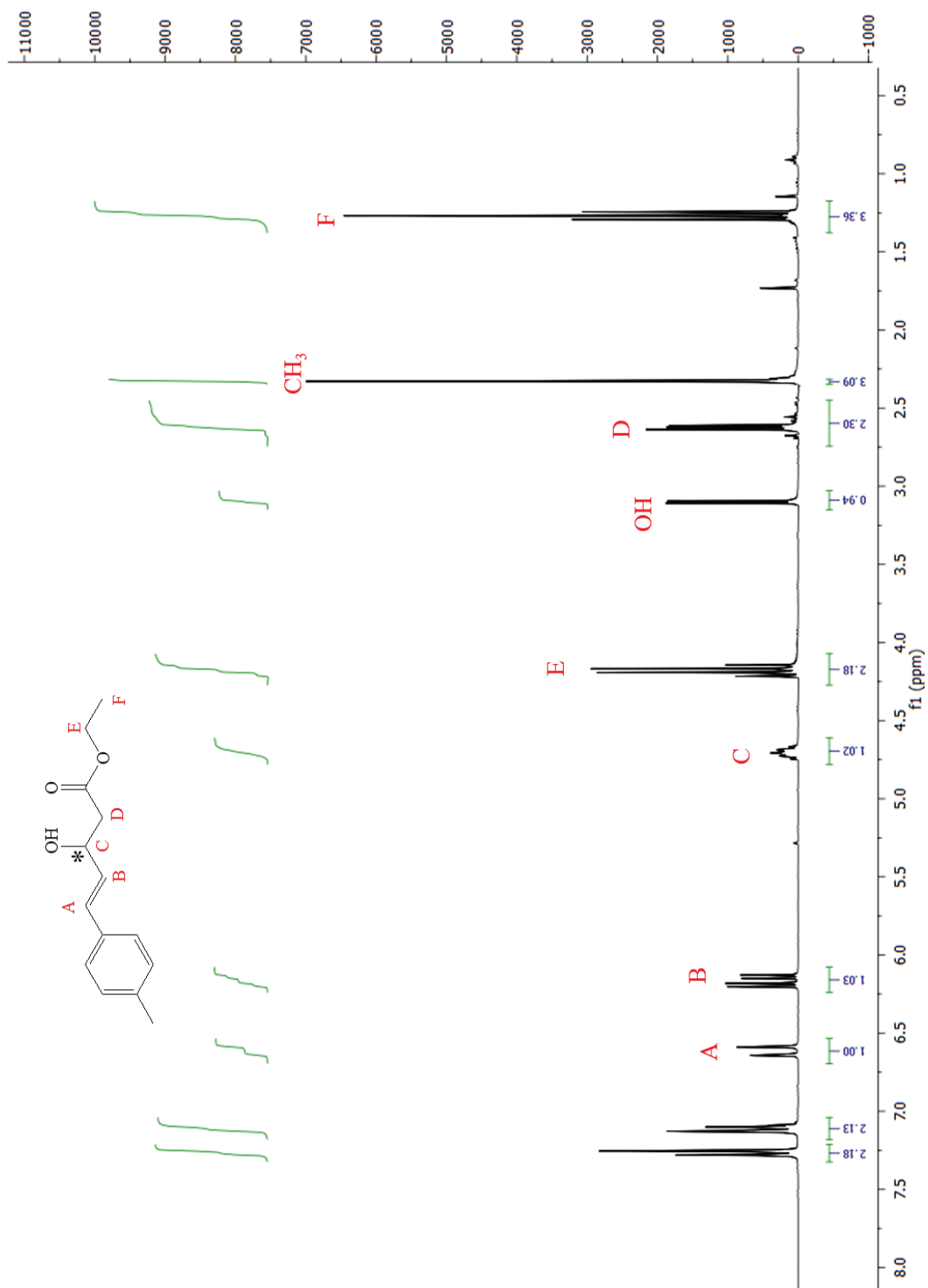


Figure A2.22. ^1H NMR spectrum of **3B** in CDCl_3 .

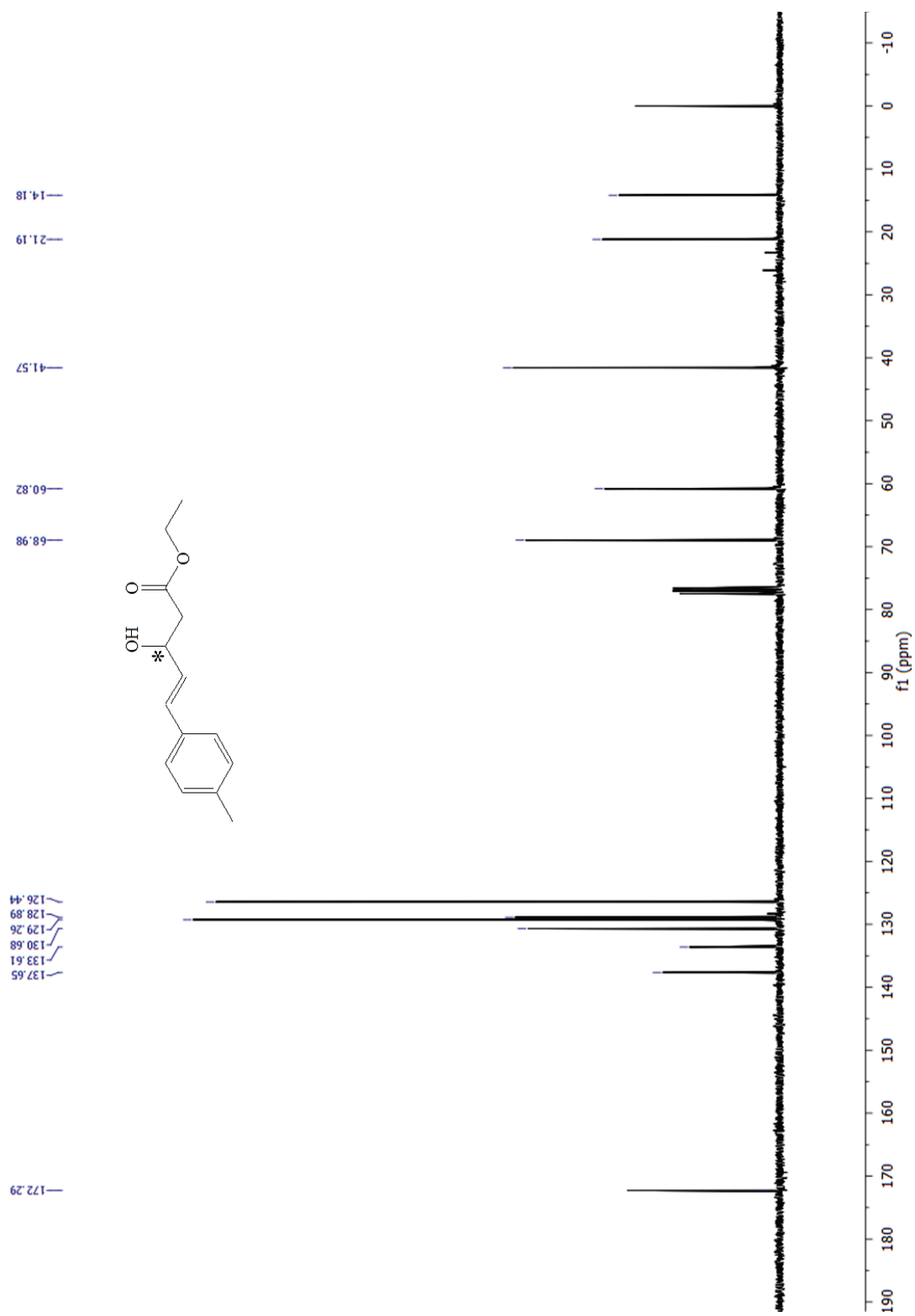


Figure A2.23. ^{13}C NMR spectrum of **3B** in CDCl_3 .

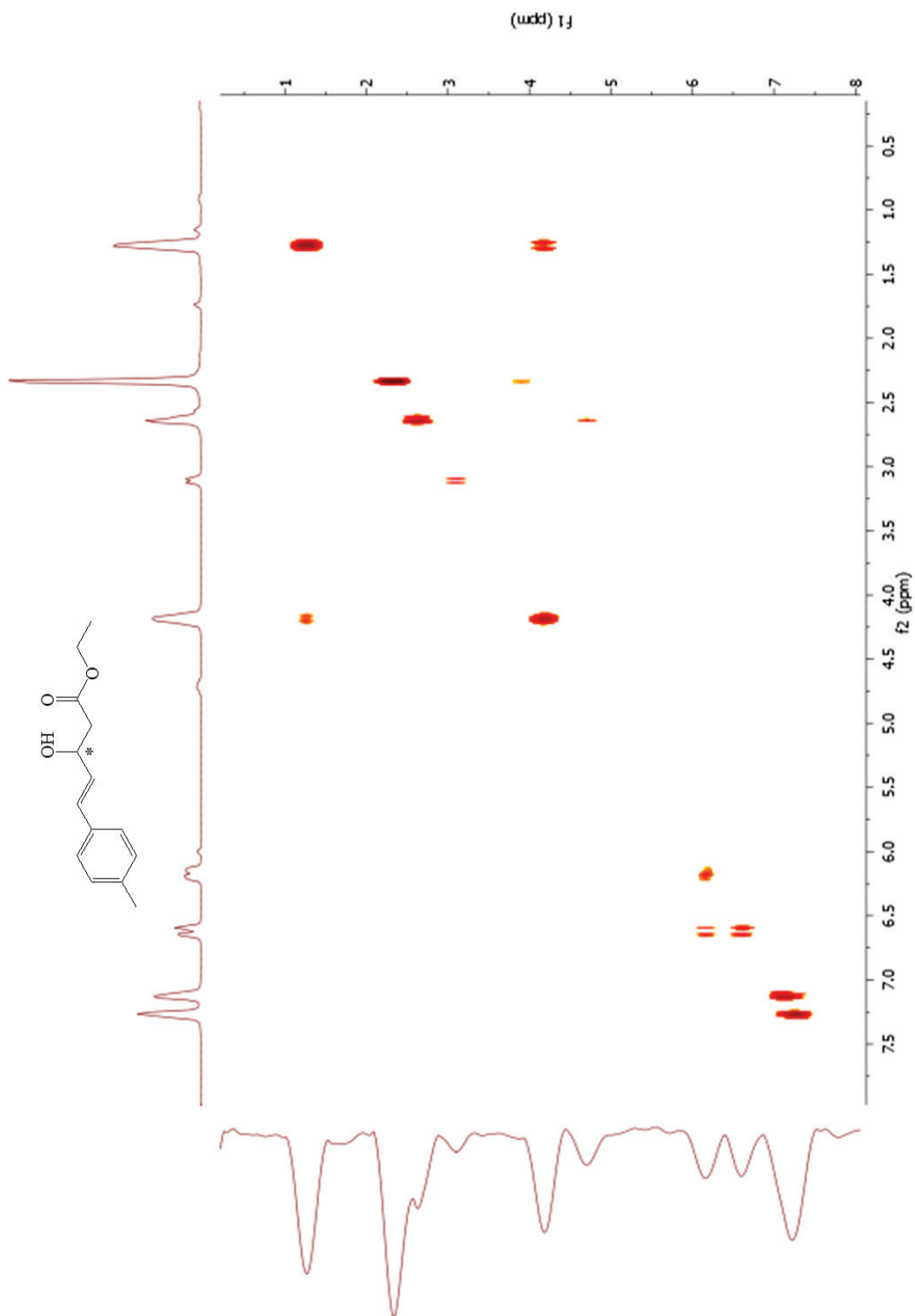


Figure A2.24. gCOSY spectrum of **3B** in CDCl_3 .

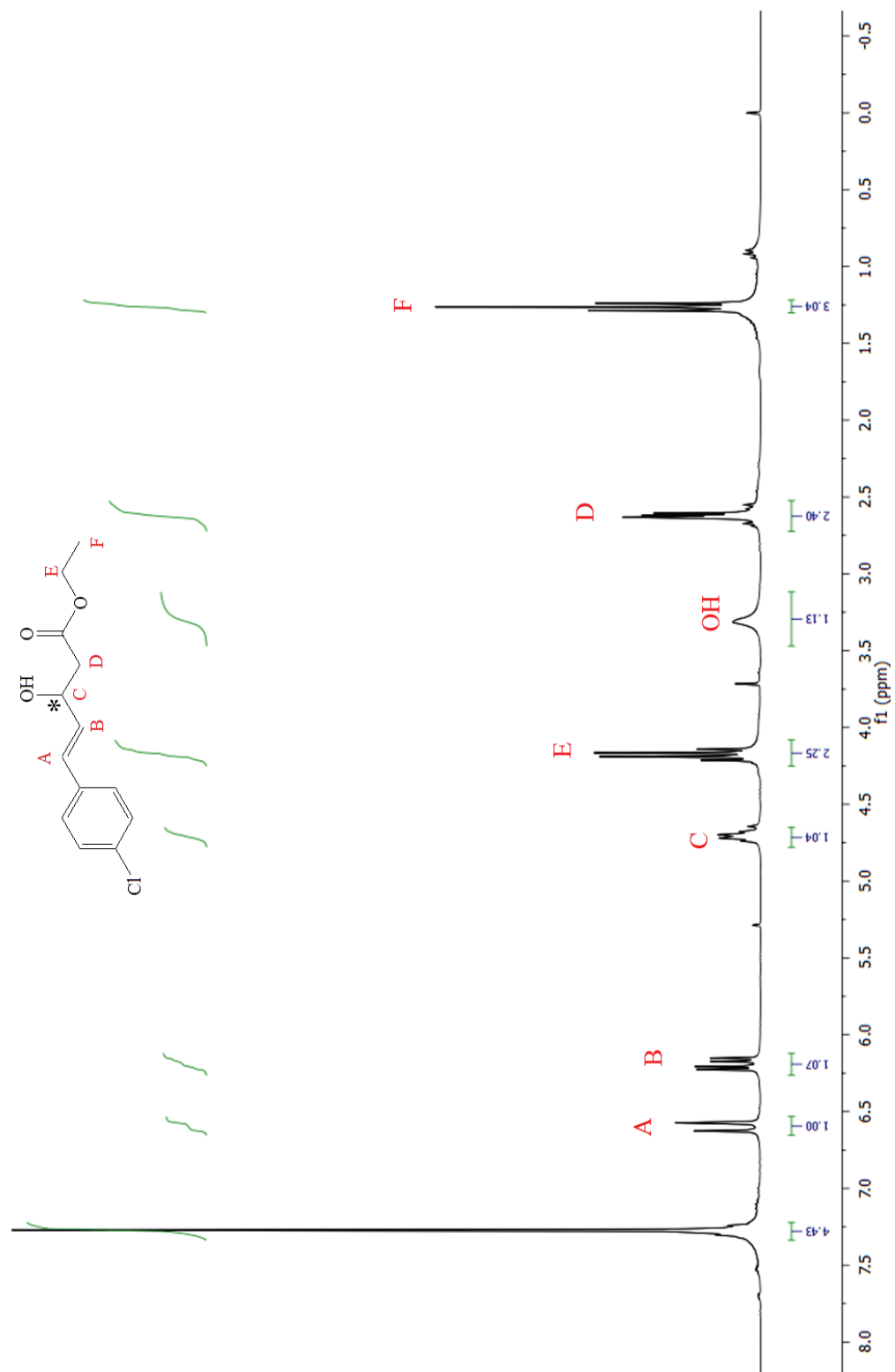


Figure A2.25. ^1H NMR spectrum of **3C** in CDCl_3 .

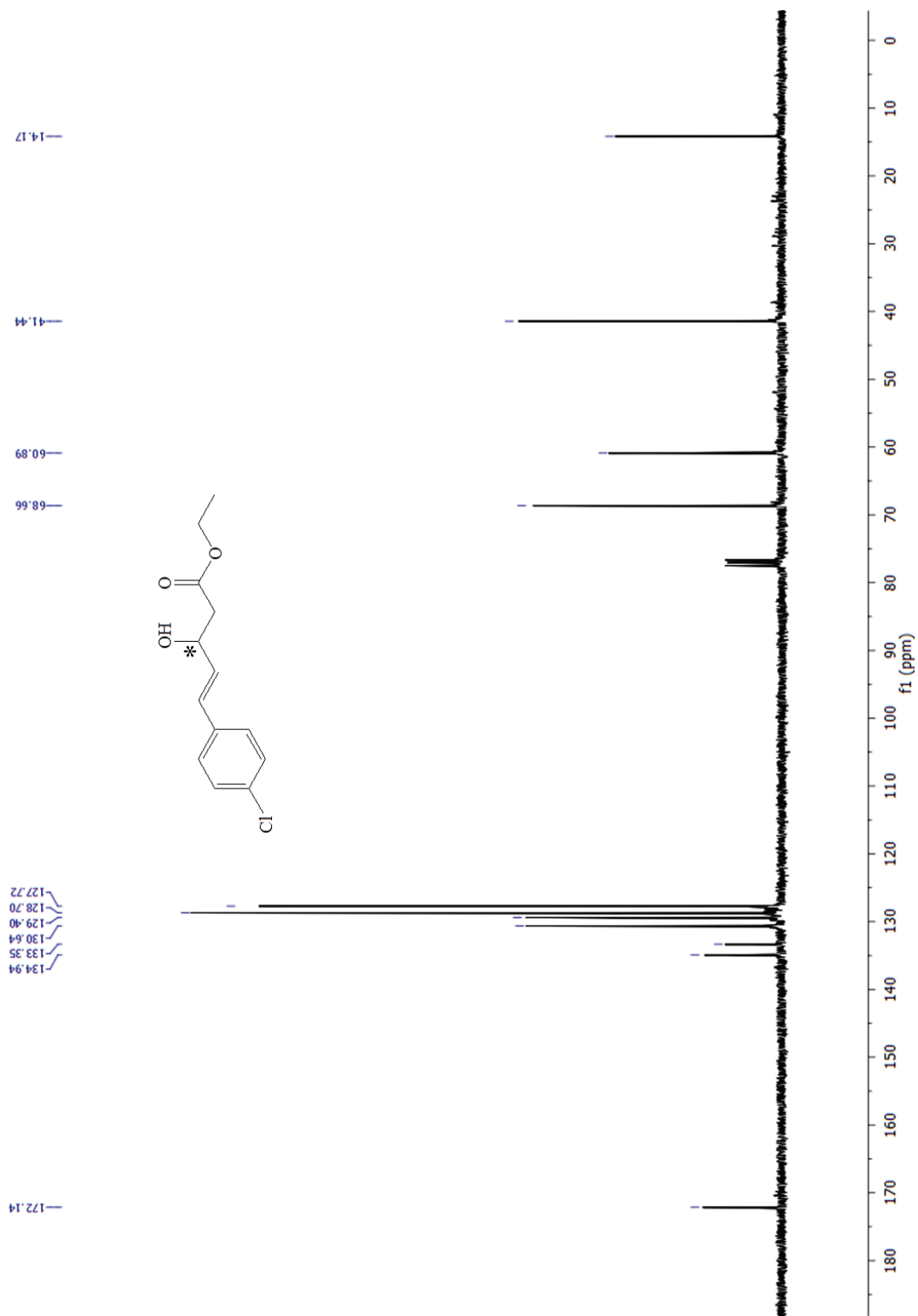


Figure A2.26. ^{13}C NMR spectrum of **3C** in CDCl_3 .

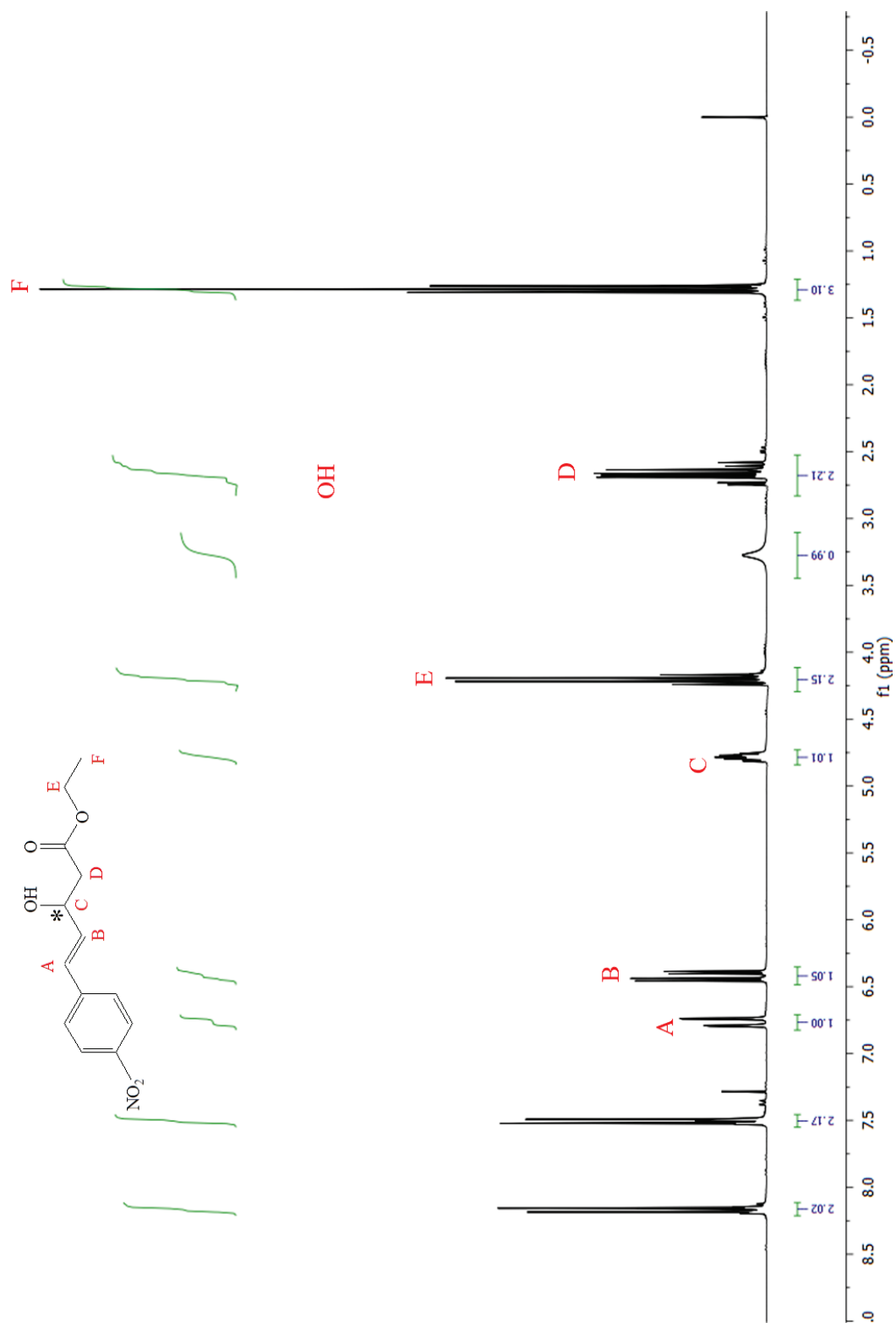


Figure A2.27. ^1H NMR spectrum of **3D** in CDCl_3 .

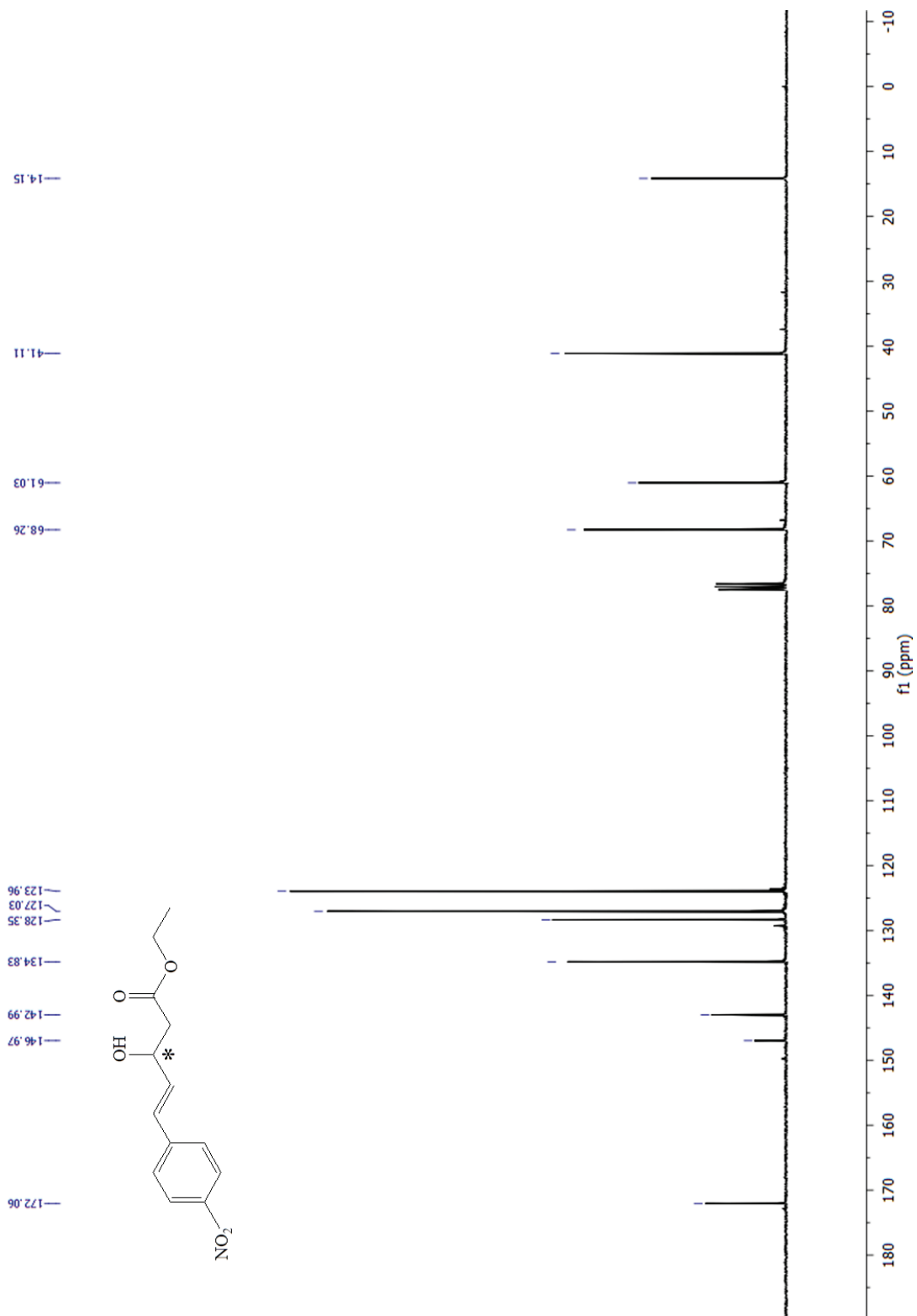


Figure A2.28. ^{13}C NMR spectrum of **3D** in CDCl_3 .

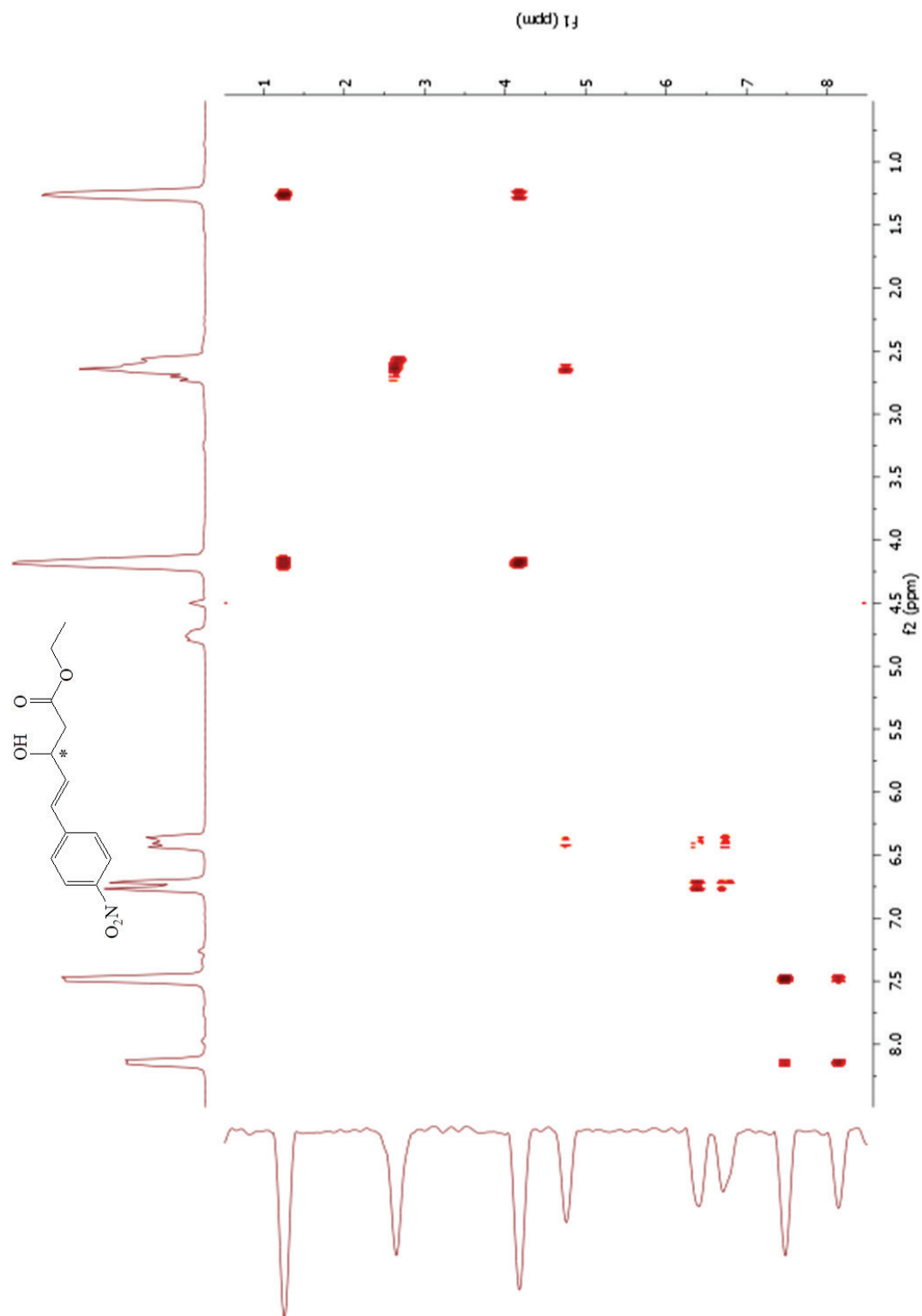


Figure A2.29. gCOSY spectrum of **3D** in CDCl₃.

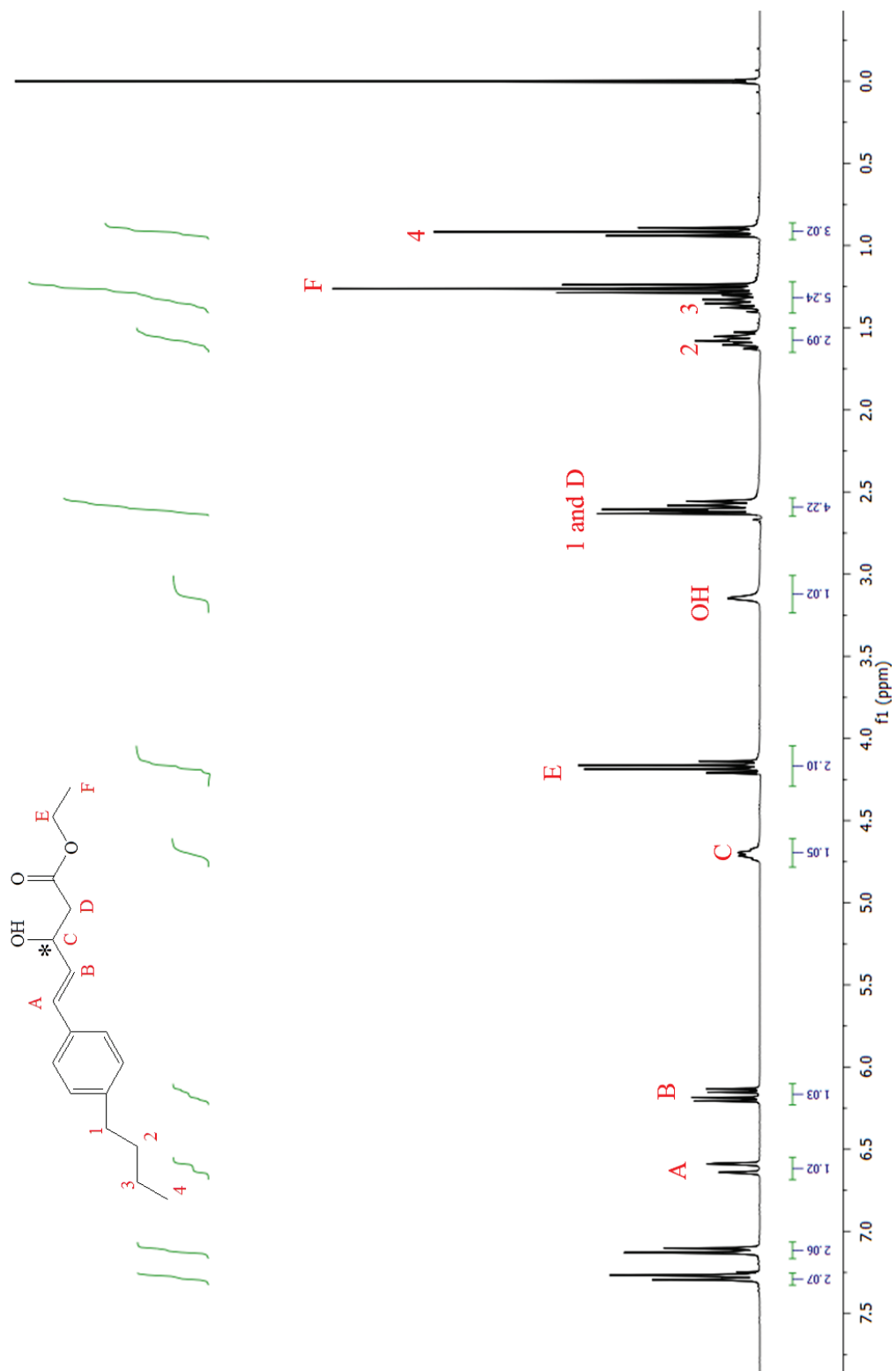


Figure A2.30. ^1H NMR spectrum of **3E** in CDCl_3 .

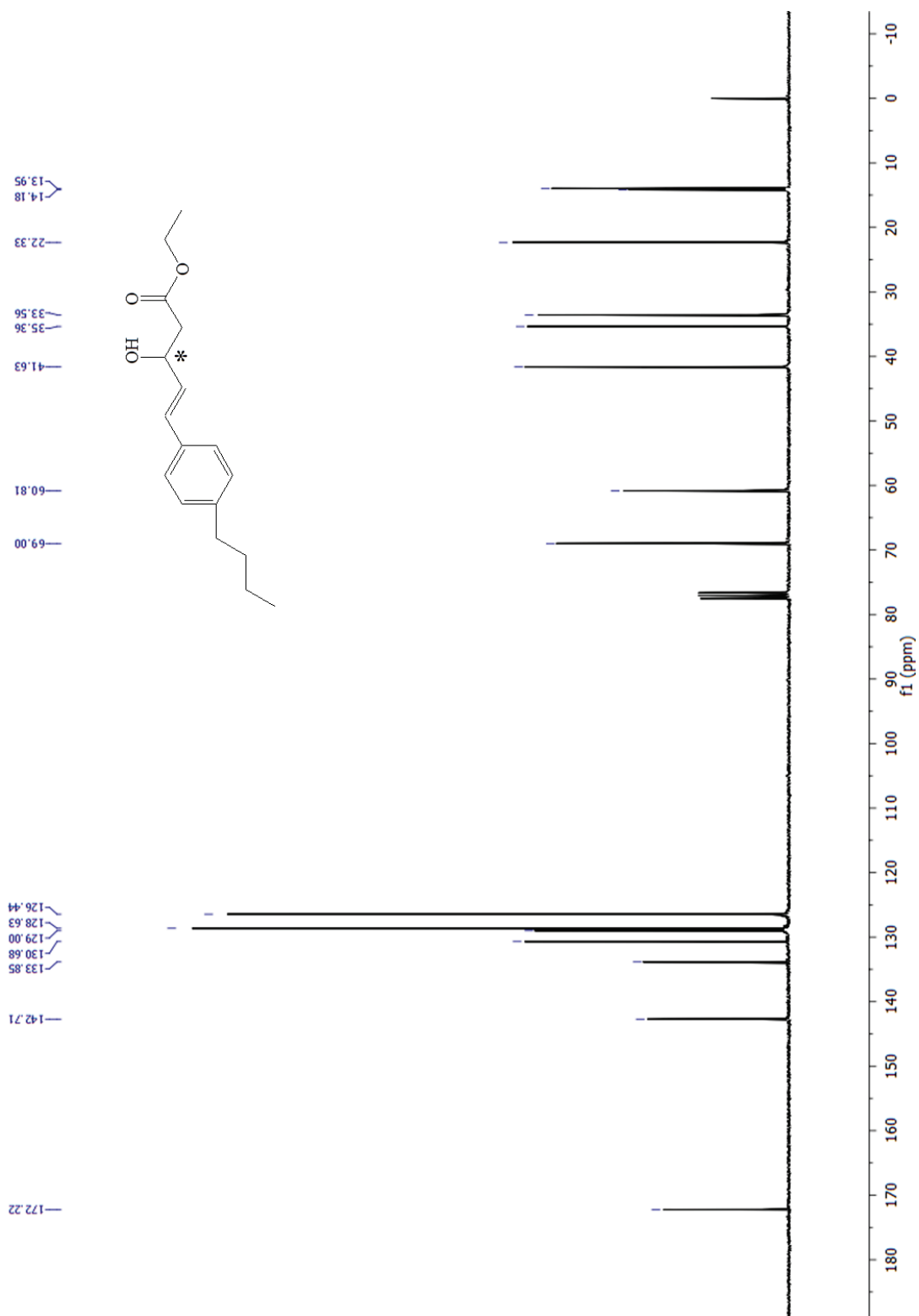


Figure A2.31. ^{13}C NMR spectrum of **3E** in CDCl_3 .

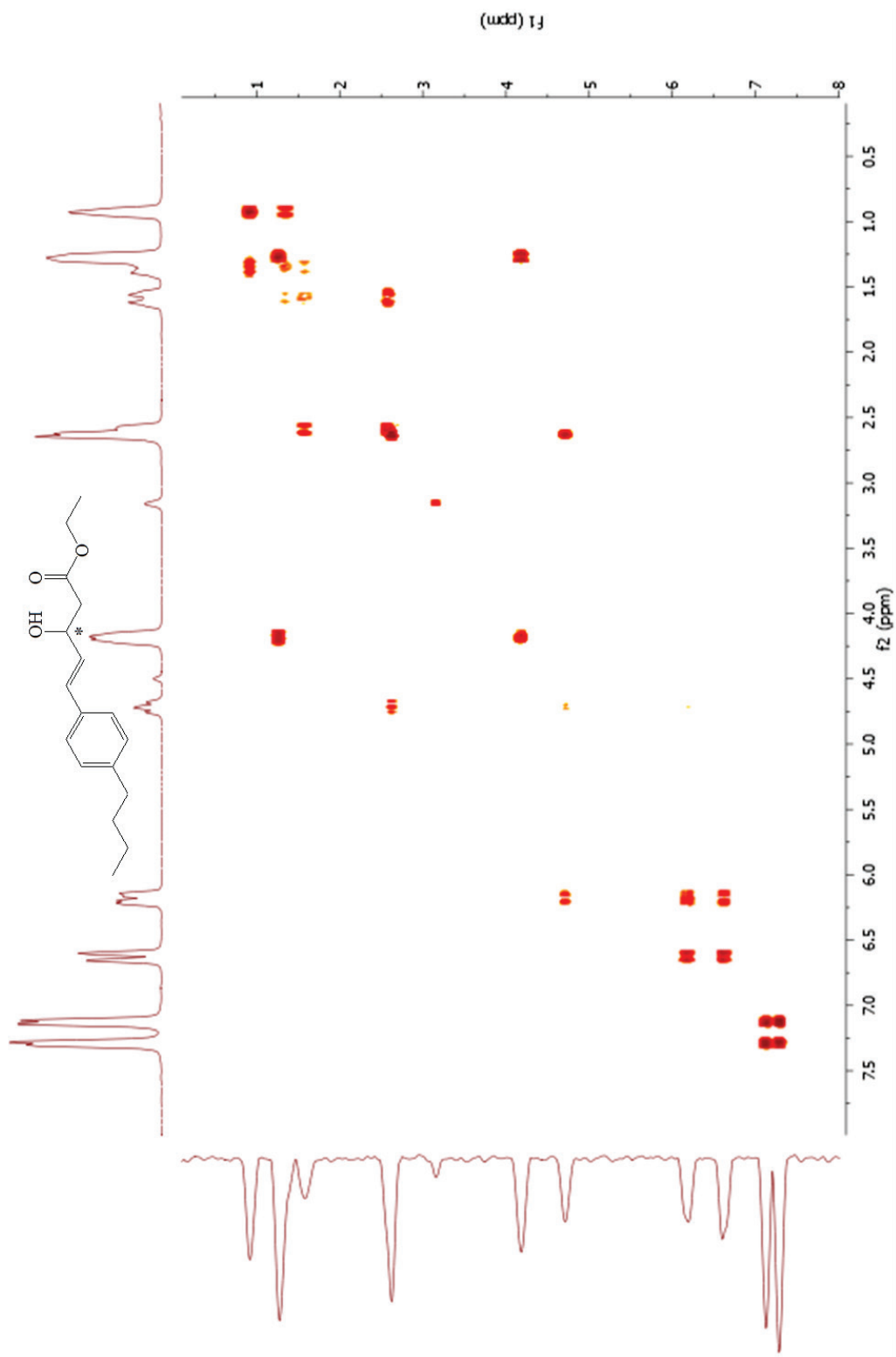


Figure A2.32. gCOSY spectrum of **3E** in CDCl_3 .

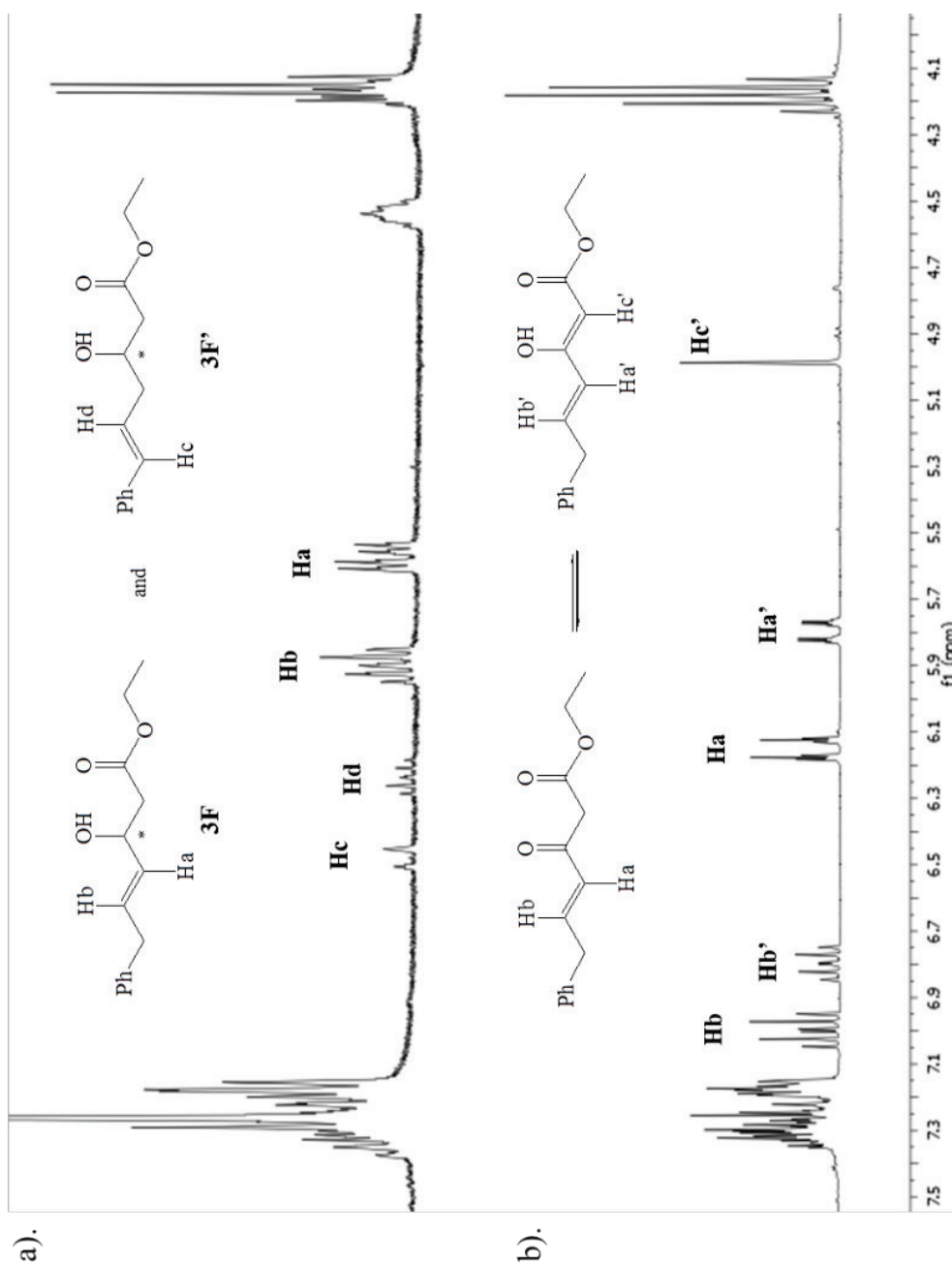


Figure A2.33. ^1H NMR spectrum of olefinic and methylene hydrogens in **3F** and **3F'**. a): purified enzymatic products **3F** and **3F'** from β -ketoester **2F** reduced by enzyme **23** (KRED-P3-G09). ^1H NMR of olefinic protons in **3F** and **3F'** made from enzyme **23** (KRED-P3-G09) are displayed. Hc (d, $J=15$ Hz) and Hd (dt, $J=9, 15$ Hz) resonance at 6.48 and 6.25 ppm were assigned as olefinic protons of **3F'** while Ha (d, $J=15$ Hz) and Hb (dt, $J=9, 15$ Hz) resonance at 5.57 and 5.90 ppm belong to olefinic protons of **3F**, which confirmed the allylic rearrangement. b): β -ketoester **2F** in keto-enol form.

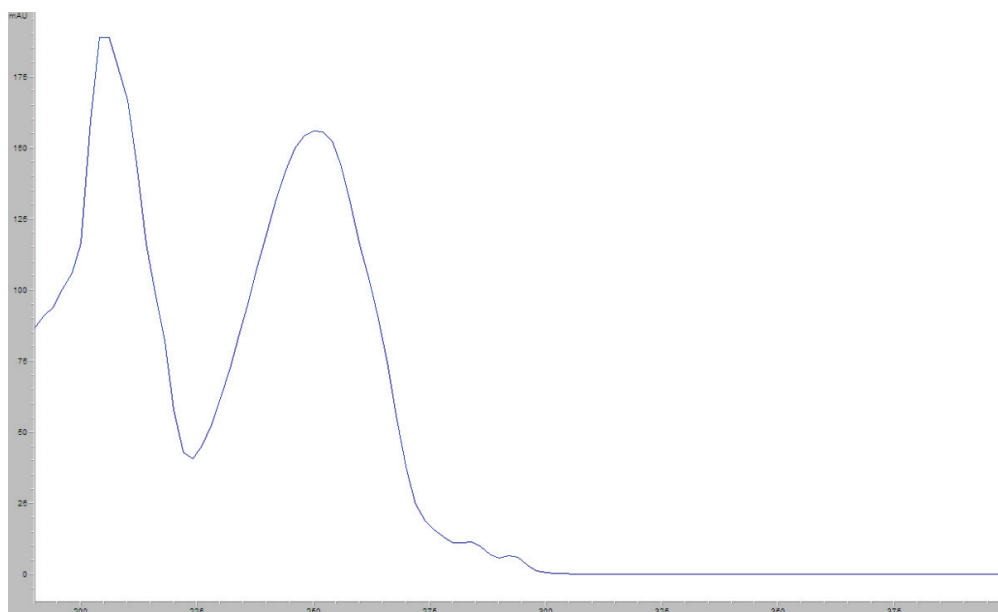


Figure A2.34. Ultraviolet absorption spectrum of ethyl (5E)-3-hydroxy-6-phenylhex-5-enoate **3F'**.

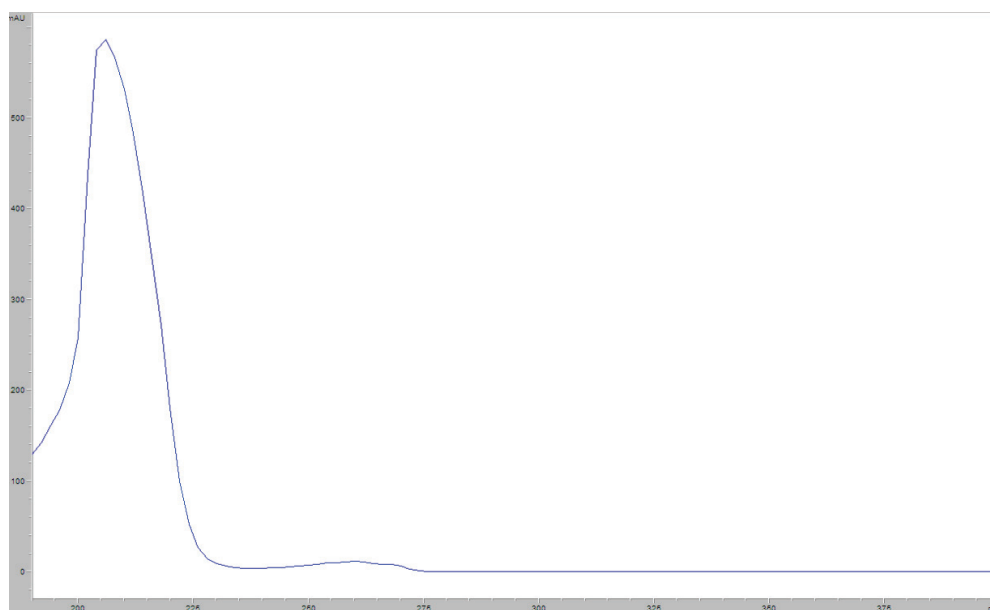
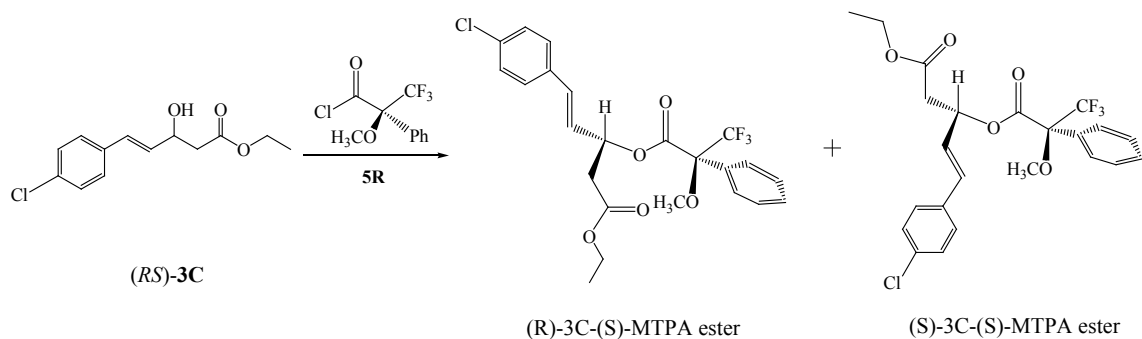


Figure A2.35. Ultraviolet absorption spectrum of ethyl (4E)-3-hydroxy-6-phenylhex-4-enoate **3F**.

A.1. Determination of absolute configuration of β -hydroxyesters

The absolute configuration of γ , δ -unsaturated β -hydroxyesters was assigned according to Mosher ester technique (Hoye, Jeffrey et al. 2007). In this report, the absolute configuration assignment of **3C** is discussed in detail as a reference. Racemic β -hydroxyester (*RS*)-**3C** (made from the reduction of β -ketoester **2C** by NaBH₄) reacted with *R*-(-)-MTPA-Cl **5R** (*R*-(-)- α -methoxyl- α -trifluoromethylphenylacetyl chloride) to form a mixture of diastereomeric pair (*R*)-**3C**-(*S*)-MTPA ester and (*S*)-**3C**-(*S*)-MTPA ester, as shown in **Scheme A2.1**. Relying on the fact that the underlined atoms in C(H)-O-C(=O)-C-CF₃ substructure (**Figure 2.1**, highlighted in red) are coplanar (Hoye, Jeffrey et al. 2007), the olefinic protons H_a and H_b are in the shielding region of the MTPA phenyl moiety in (*R*)-**3C**-(*S*)-MTPA ester (**Figure A2.36a**), while H_{a'} and H_{b'} are in the less shield region of MTPA phenyl moiety in (*S*)-**3C**-(*S*)-MTPA ester (**Figure A2.36b**). Considering that the protons in diastereomers show different arrays of chemical shifts in ¹H NMR spectra, more shielded protons H_a and H_b display in the upfield region relative to less shielded protons H_{a'} and H_{b'}, as shown in **Figure A2.37a**. Therefore, H_a at 6.6 ppm and H_b at 6.0 ppm belong to the diastereomer (*R*)-**3C**-(*S*)-MTPA ester, and the corresponding β -hydroxyester has a configuration of '*R*'.



Scheme A2.1. Synthesis of diastereomeric pair (R) -3C-(S)-MTPA ester and (S) -3C-(S)-MTPA ester from racemic β -hydroxyester (RS) -3C and R -(-)-MTPA-Cl **5R**.

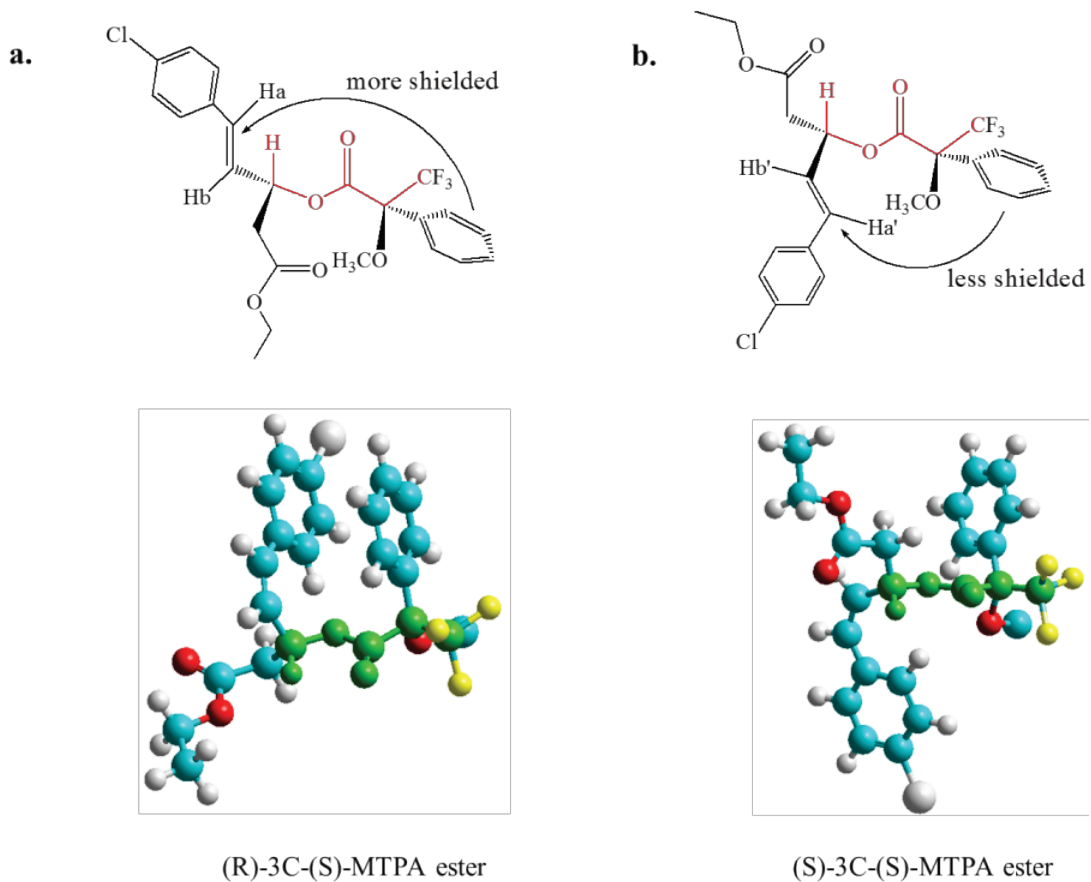


Figure A2.36. Structure of (a) (R) -3C-(S)-MTPA ester and (b) (S) -3C-(S)-MTPA ester and their hyperchem models at the bottom.

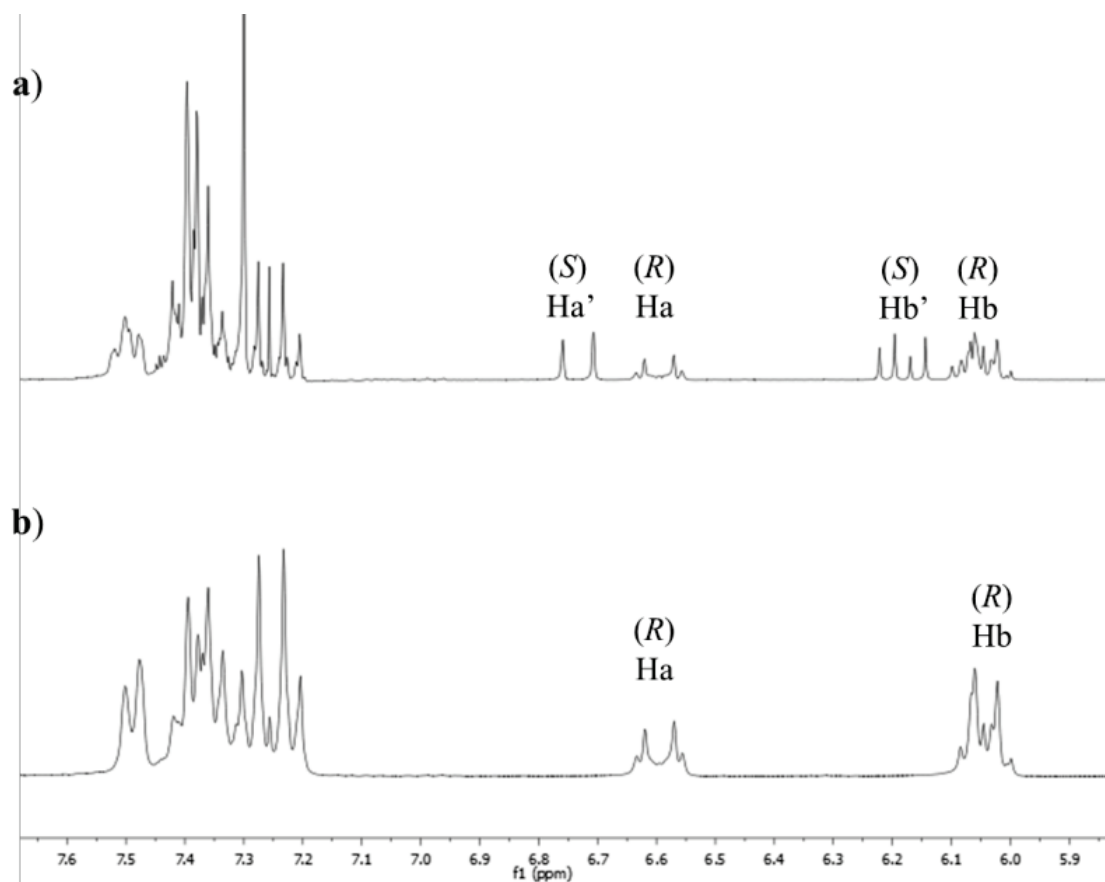


Figure A2.37. ^1H NMR spectra of olefinic protons H_a ($\text{H}_{a'}$) and H_b ($\text{H}_{b'}$) in CDCl_3 . (a) diastereomers (R) - 3C - (S) -MTPA ester and (S) - 3C - (S) -MTPA ester, (b) (R) - 3C - (S) -MTPA ester.

The absolute configuration of the unknown β -hydroxyester **3C** (>99% e.e. made with enzyme **8**) also reacted with R -(-)-MTPA-Cl **5R** to form (?) 3C - (S) -MTPA ester. By comparing the ^1H NMR spectrum of (?) 3C - (S) -MTPA ester with that of diastereomers (R) - 3C - (S) -MTPA ester and (S) - 3C - (S) -MTPA ester, the absolute configuration of β -hydroxyester **3C** was determined as “ R ” in the case of enzyme **8**. After the absolute configuration of β -hydroxyester from one enzymatic reaction was assigned, the absolute

configuration and e.e.% of other enzymatic reaction products β -hydroxyesters from the same β -ketoesters could also be confirmed by comparing the retention times on chiral HPLC and/or CE analysis.

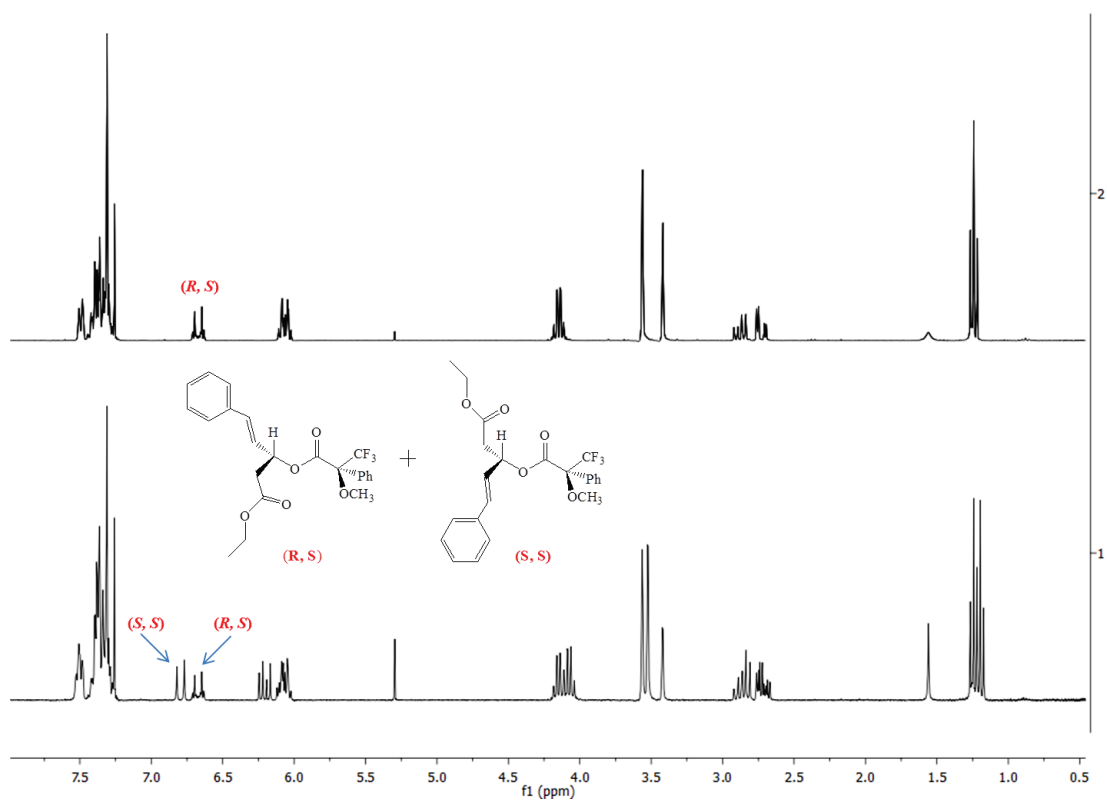


Figure A2.38. ¹H NMR spectra of (S)-MTPA ester of **3A** in CDCl₃. Top: (S)-MTPA ester of **3A** made by enzyme 8 (KRED-P1-B05); Bottom: (S)-MTPA ester of Racemic-**3A**.

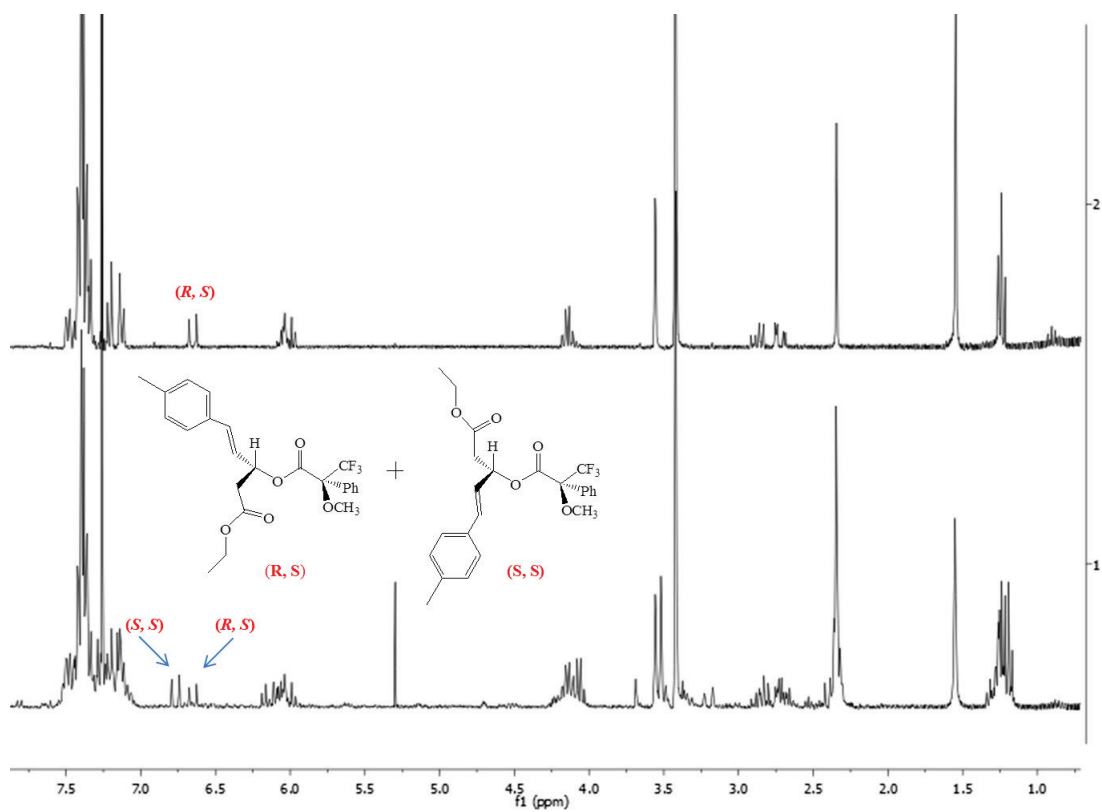


Figure A2.39. ^1H NMR spectra of (*S*)-MTPA ester of **3B** in CDCl_3 . Top: (*S*)-MTPA ester of **3B** made by enzyme 8 (KRED-P1-B05); Bottom: (*S*)-MTPA ester of Racemic-**3B**.

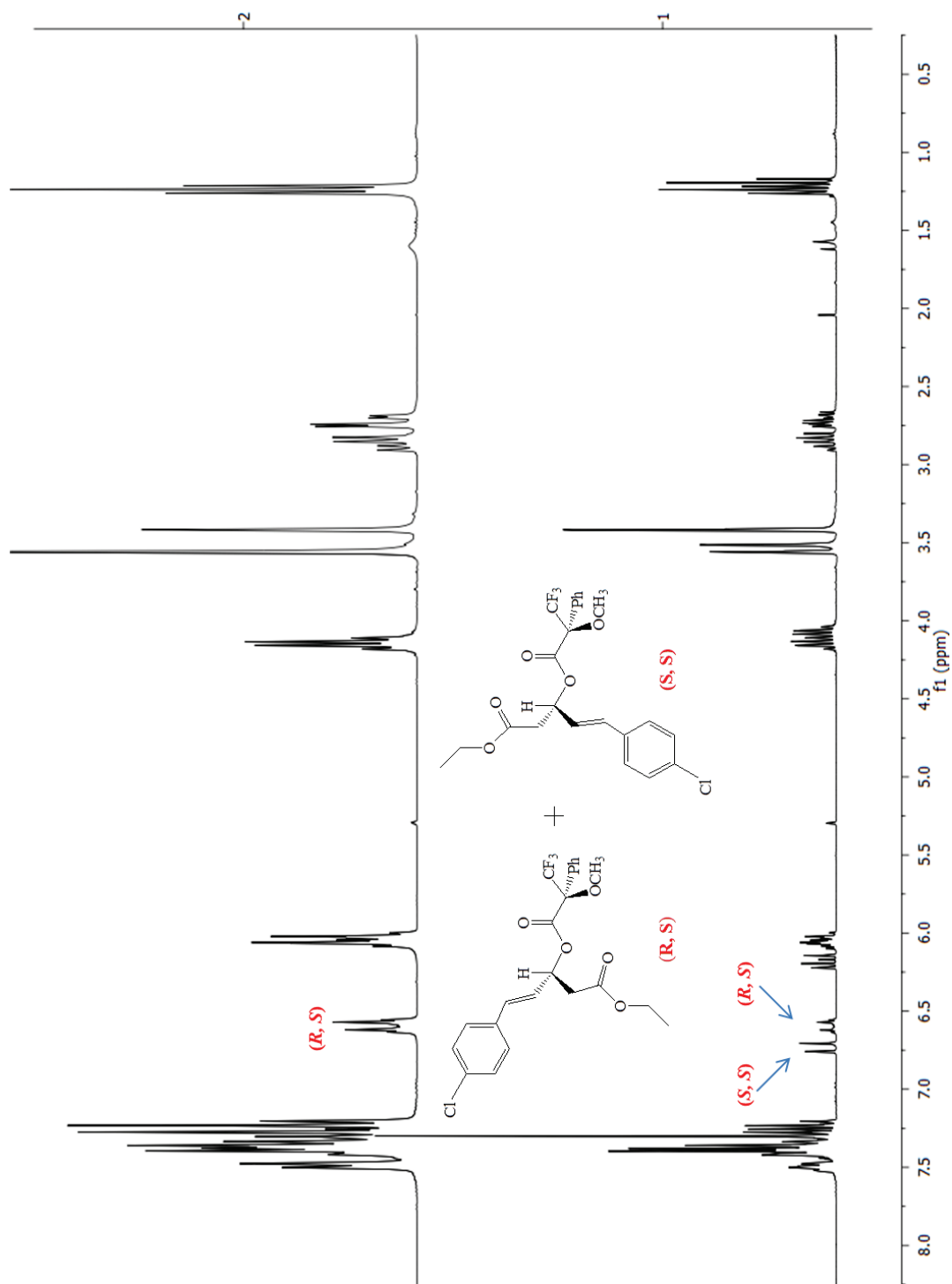


Figure A2.40. ^1H NMR spectra of (*S*)-MTPA ester of **3C** in CDCl_3 . Top: (*S*)-MTPA ester of **3C** made by enzyme 8 (KRED-P1-B05); Bottom: (*S*)-MTPA ester of Racemic-**3C**.

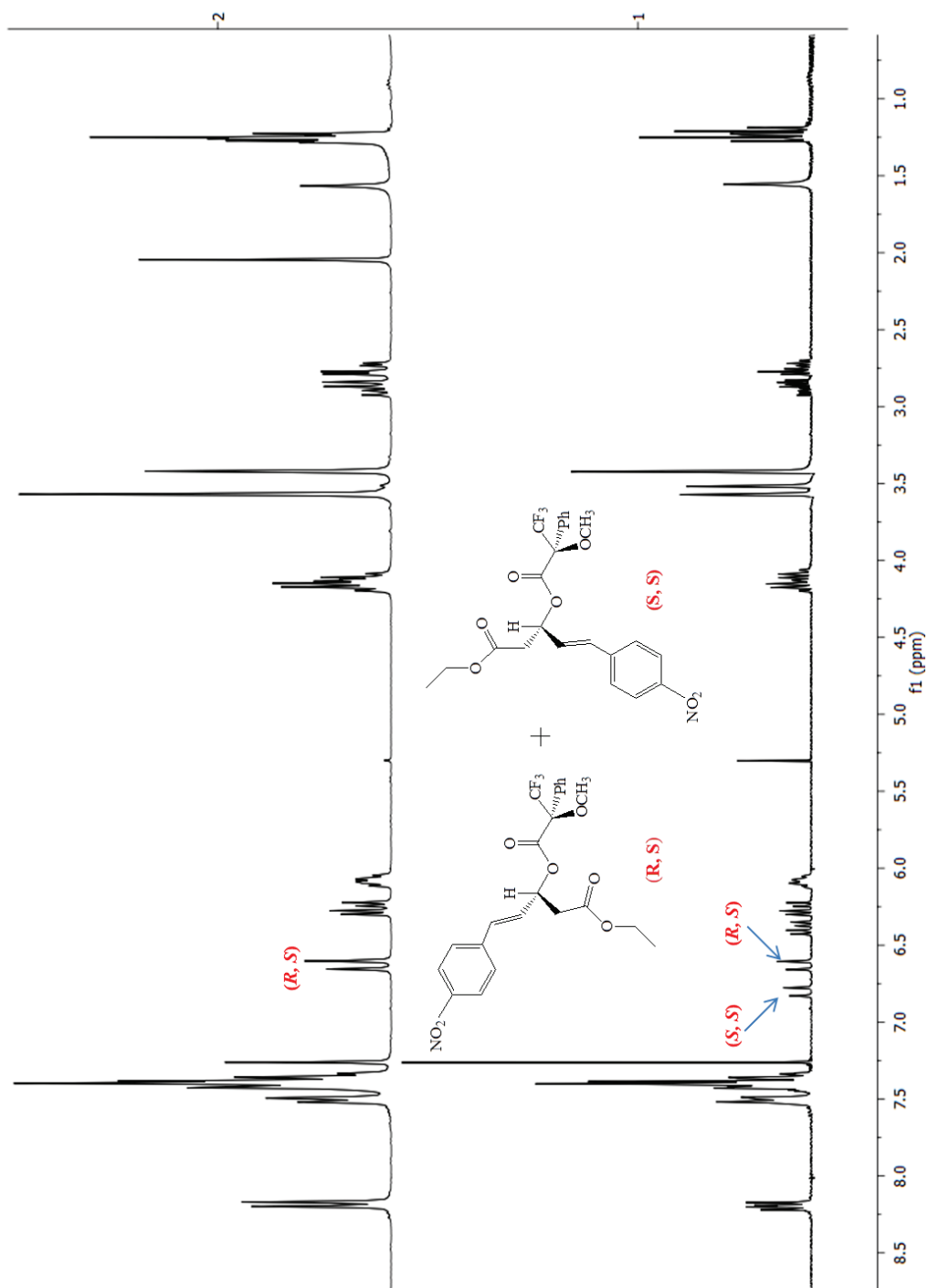


Figure A2.41. ^1H NMR spectra of (*S*)-MTPA ester of **3D** in CDCl_3 . Top: (*S*)-MTPA ester of **3D** made by enzyme 8 (KRED-P1-B05); Bottom: (*S*)-MTPA ester of Racemic-**3D**.

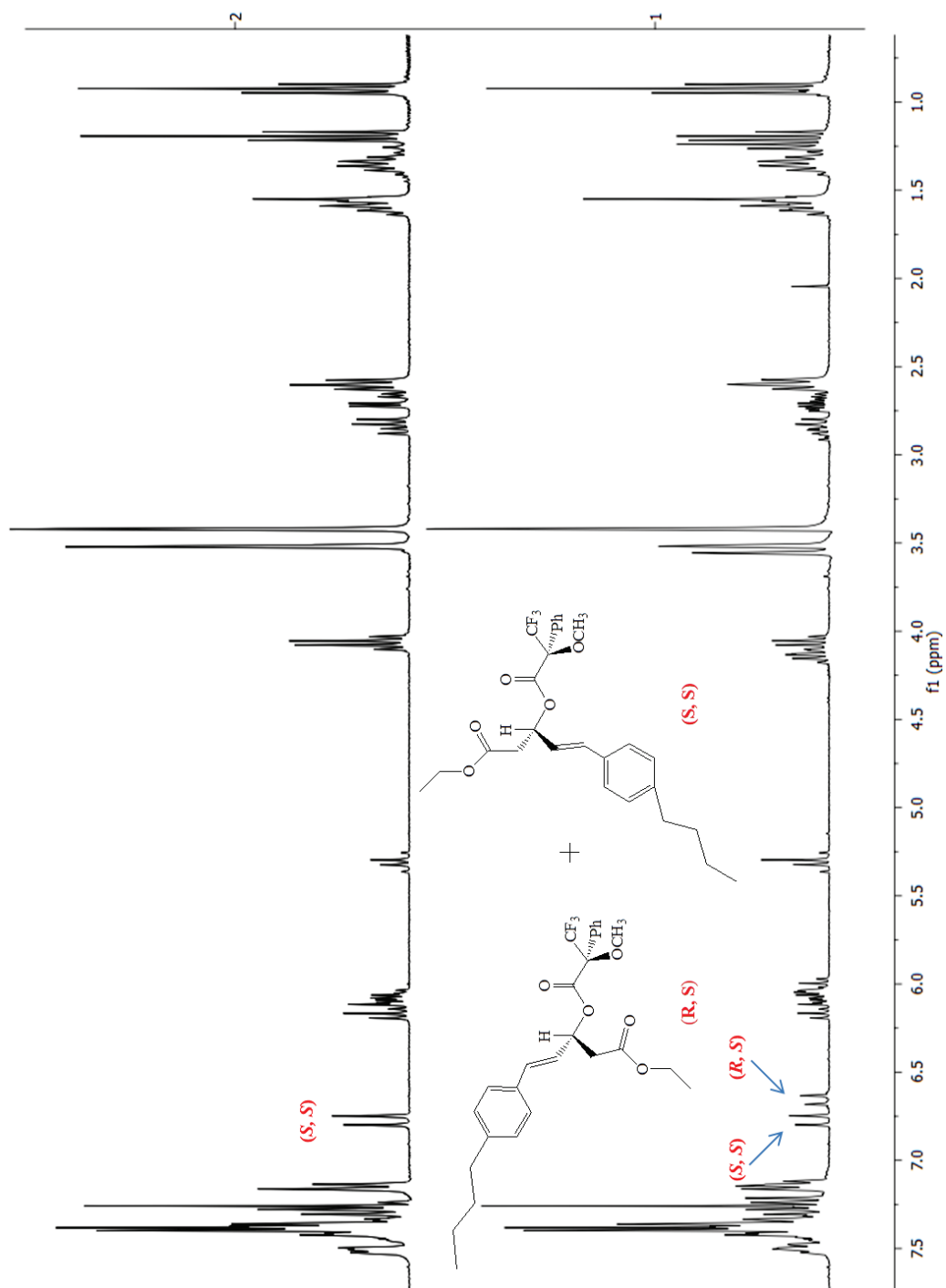


Figure A2.42. ^1H NMR spectra of (S)-MTPA ester of 3E in CDCl_3 . Top: (S)-MTPA ester of 3E made by enzyme 23 (KRED-P3-G09); Bottom: (S)-MTPA ester of Racemic 3E.

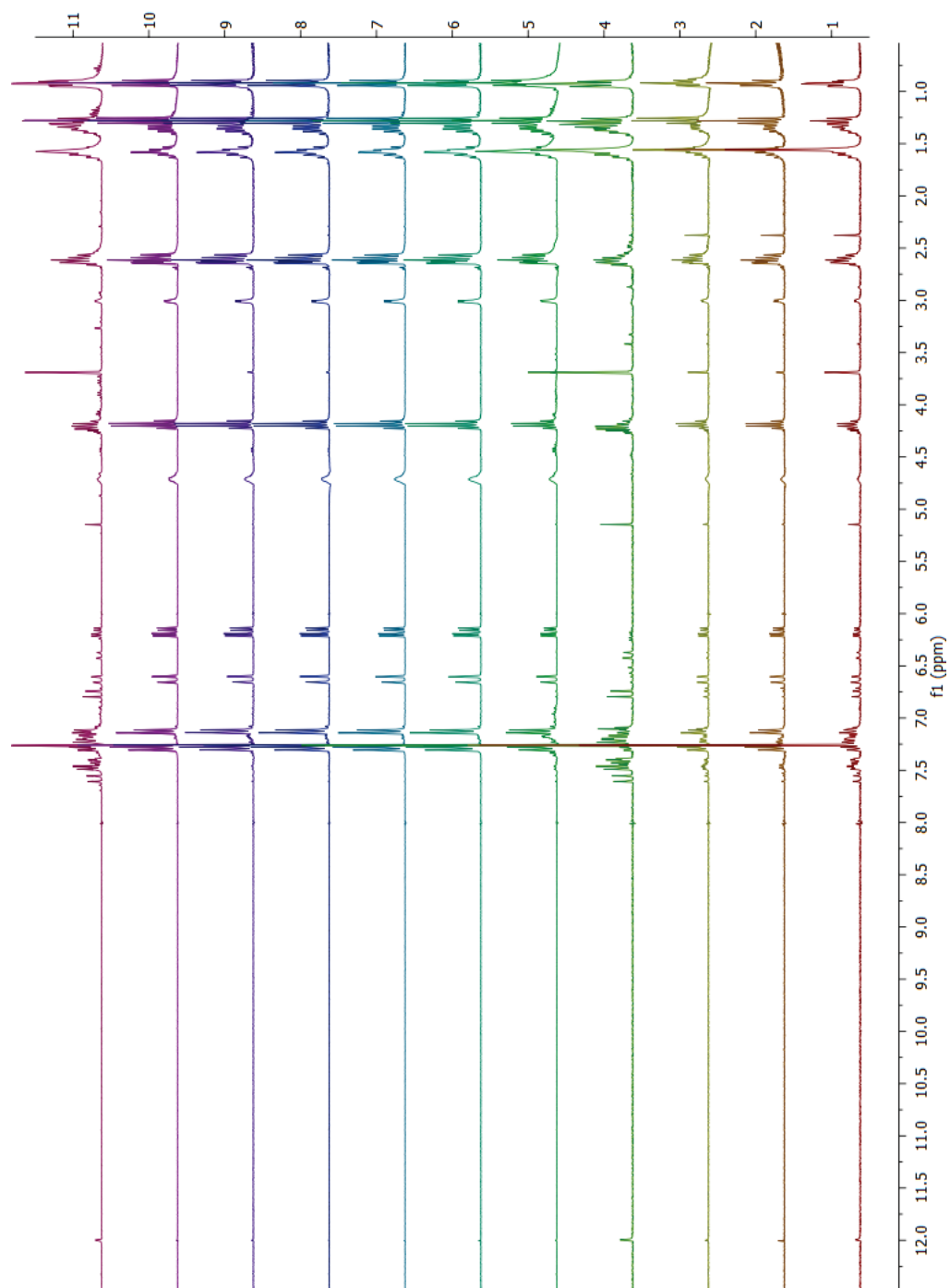


Figure A2.43. Stacked ¹H NMR spectra of crude enzymatic product **3E** in CDCl₃. 1): Enzyme #1; 2): Enzyme #2; 3): Enzyme #3; 4): Enzyme #5; 5): Enzyme #7; 6): Enzyme #8; 7): Enzyme #14; 8): Enzyme #15; 9): Enzyme #16; 10): Enzyme #20; 11): Enzyme #23

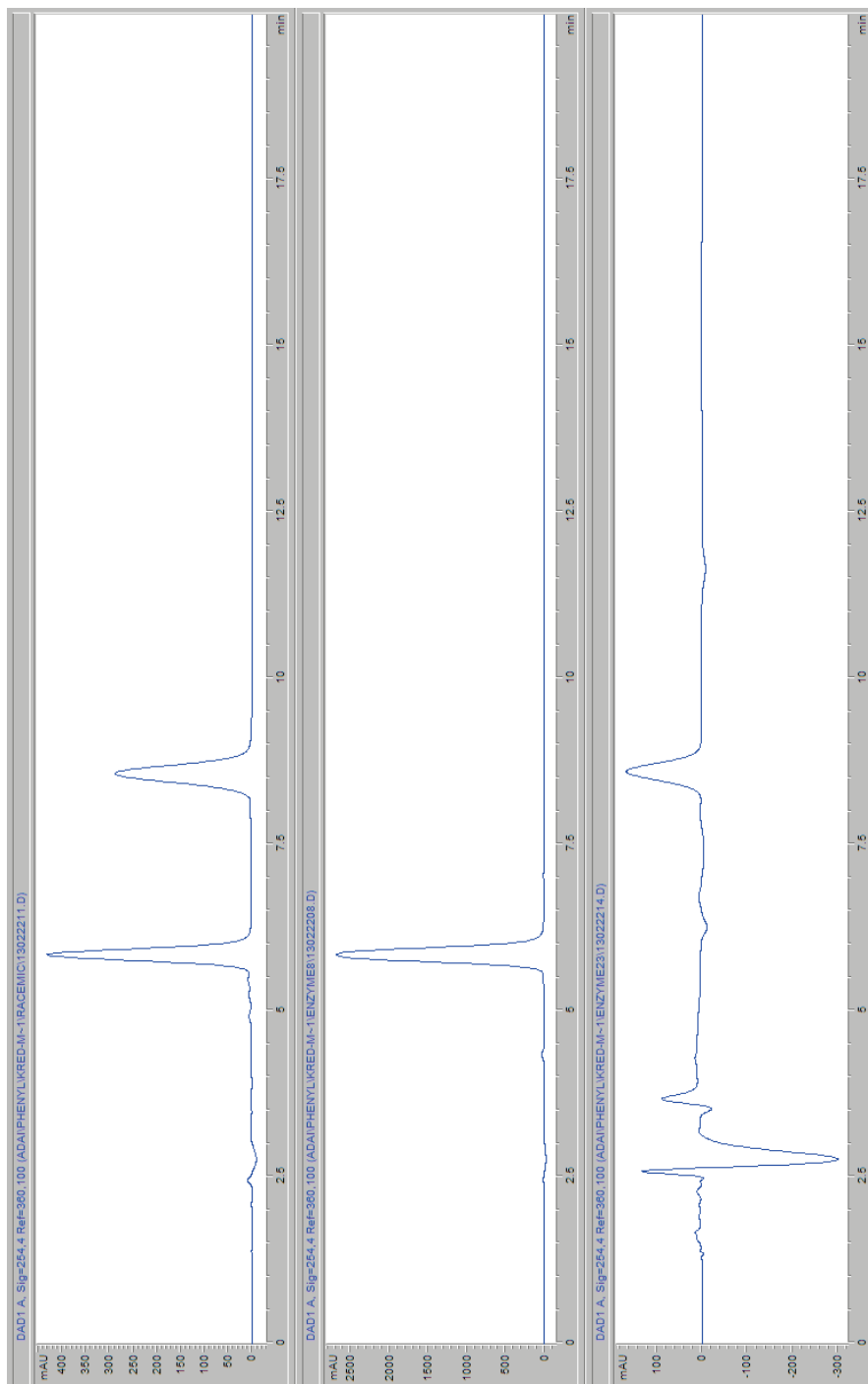


Figure A2.44. Chiral HPLC chromatograph of **3A**. Top spectrum: Racemic; Middle spectrum: crude product made from Enzyme # 8; Bottom Spectrum: crude product made from Enzyme # 23; HPLC column: Phenomenex[®] Lux 3 μ cellulose-1 column (50 x 4.60 mm); mobile phase: hexane: isopropanol = 9:1; Flow rate: 0.5 ml/min.

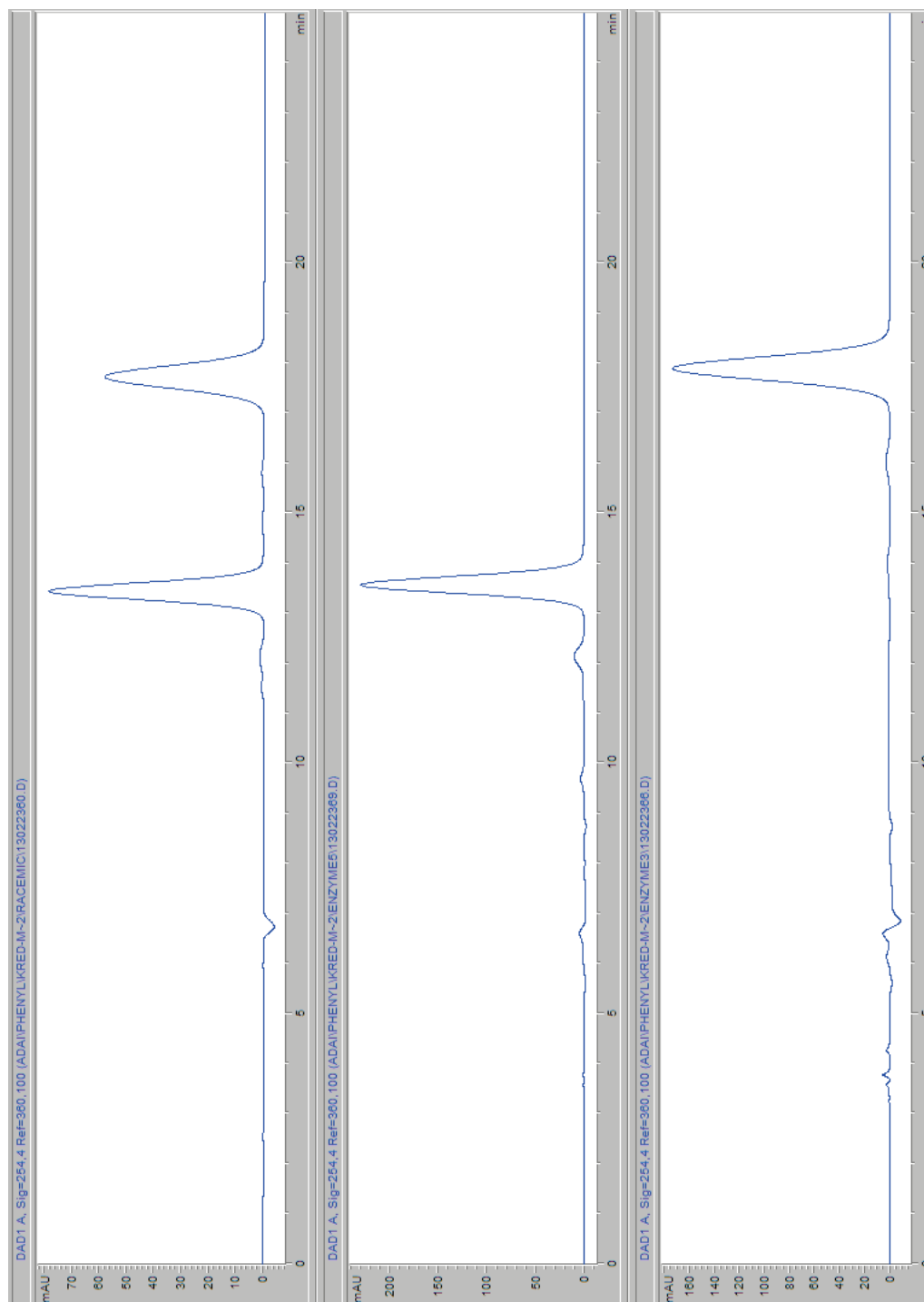


Figure A2.45. Chiral HPLC chromatograph of **3B**. Top spectrum: Racemic; Middle spectrum: crude product made from Enzyme #5; Bottom Spectrum: crude product made from Enzyme #3; HPLC column: Phenomenex[®] Lux 3 μ cellulose-1 column (50 x 4.60 mm); mobile phase: hexane: isopropanol = 9:1; Flow rate: 0.5 ml/min.

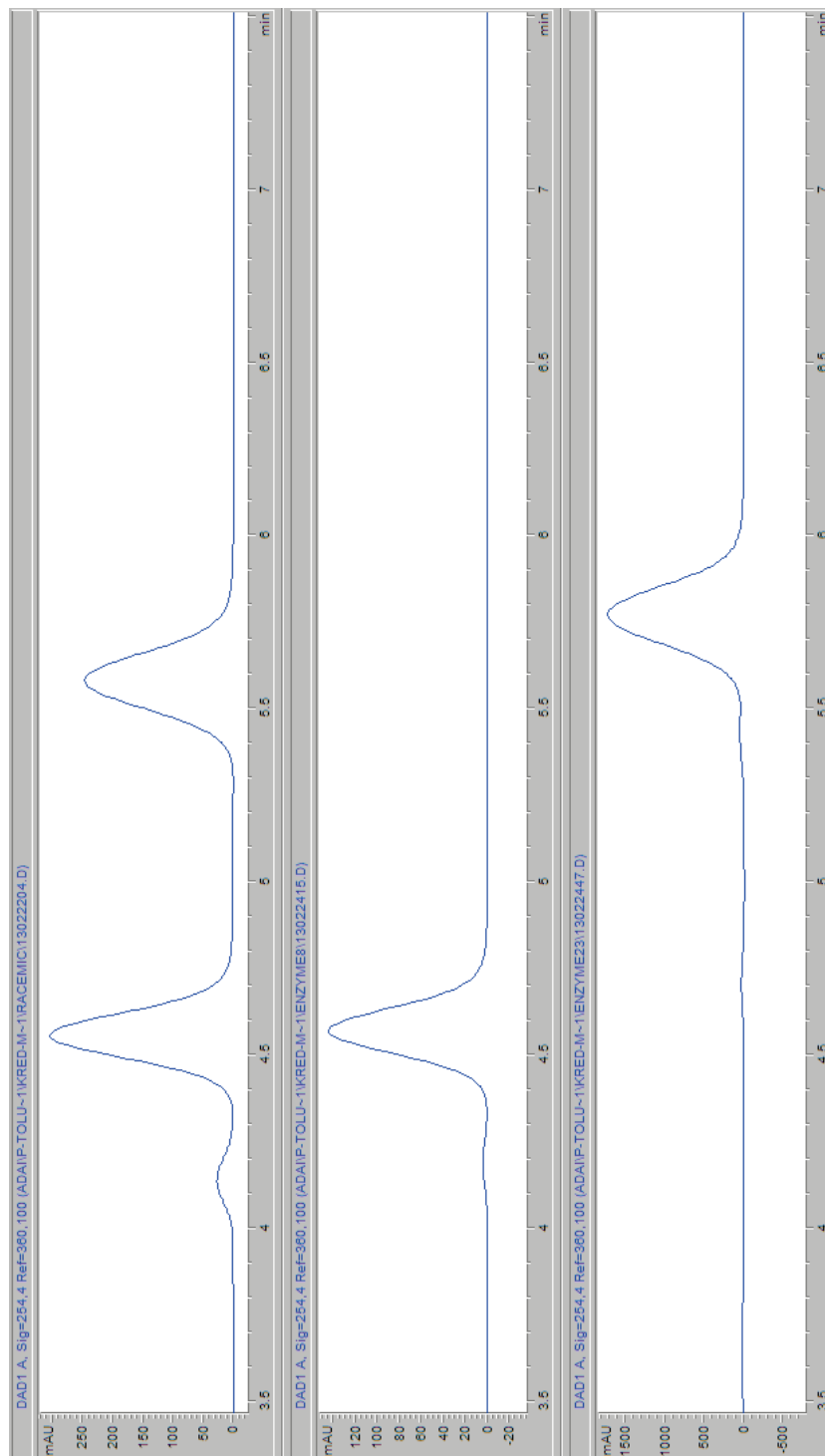


Figure A2.46. Chiral HPLC chromatograph of **3C**. Top spectrum: Racemic; Middle spectrum: crude product made from Enzyme # 8; Bottom Spectrum: crude product made from Enzyme # 23; HPLC column: Phenomenex[®] Lux 3 μ cellulose-1 column (50 x 4.60 mm); mobile phase: hexane: isopropanol = 9:1; Flow rate: 0.5 ml/min.

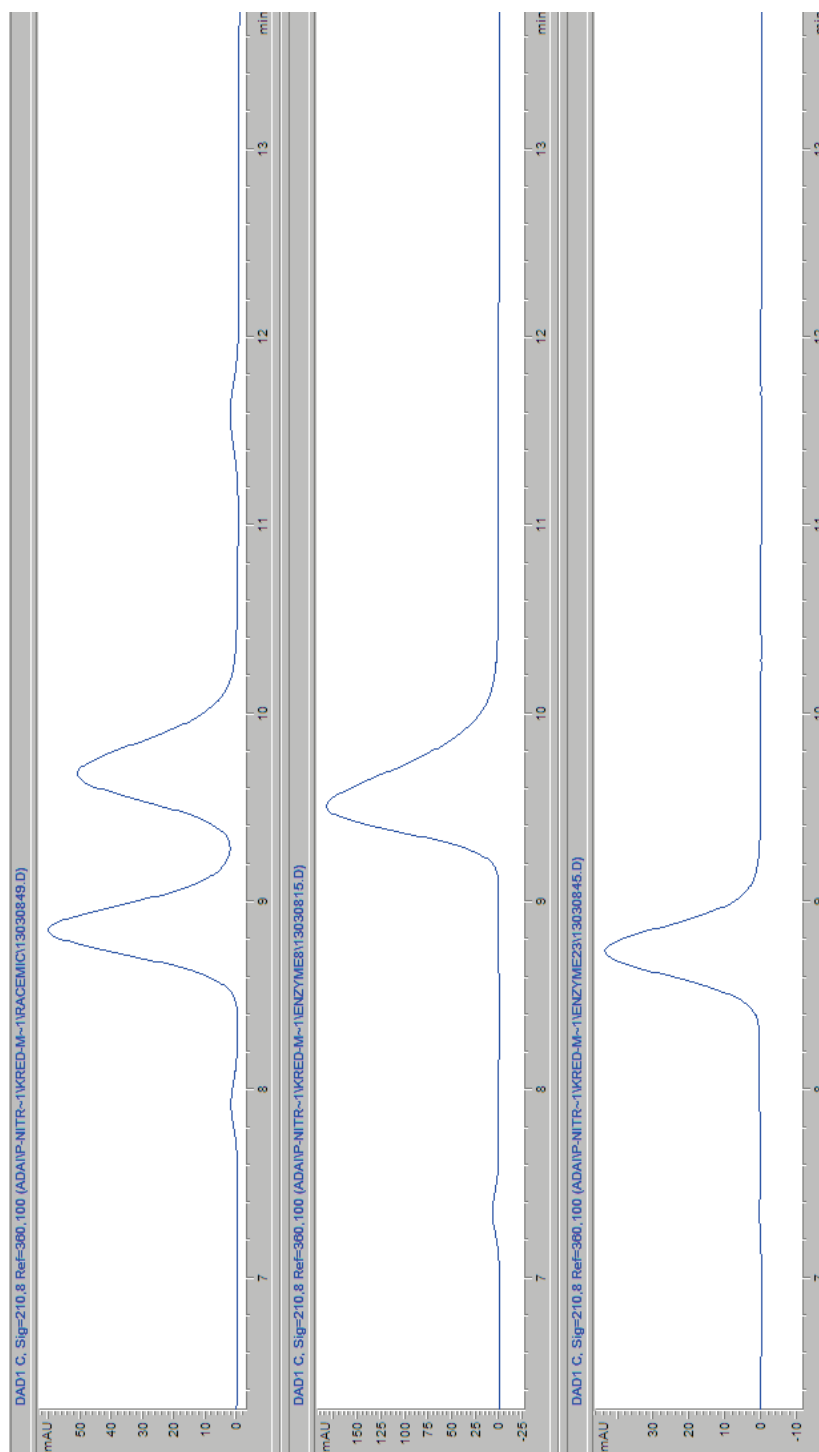


Figure A2.47. Chiral HPLC chromatograph of **3D**. Top spectrum: Racemic; Middle spectrum: crude product made from Enzyme # 8; Bottom Spectrum: crude product made from Enzyme # 23; HPLC column: Phenomenex[®] Lux 3 μ cellulose-1 column (50 x 4.60 mm); mobile phase: hexane: isopropanol = 9:1; Flow rate: 0.5 ml/min.

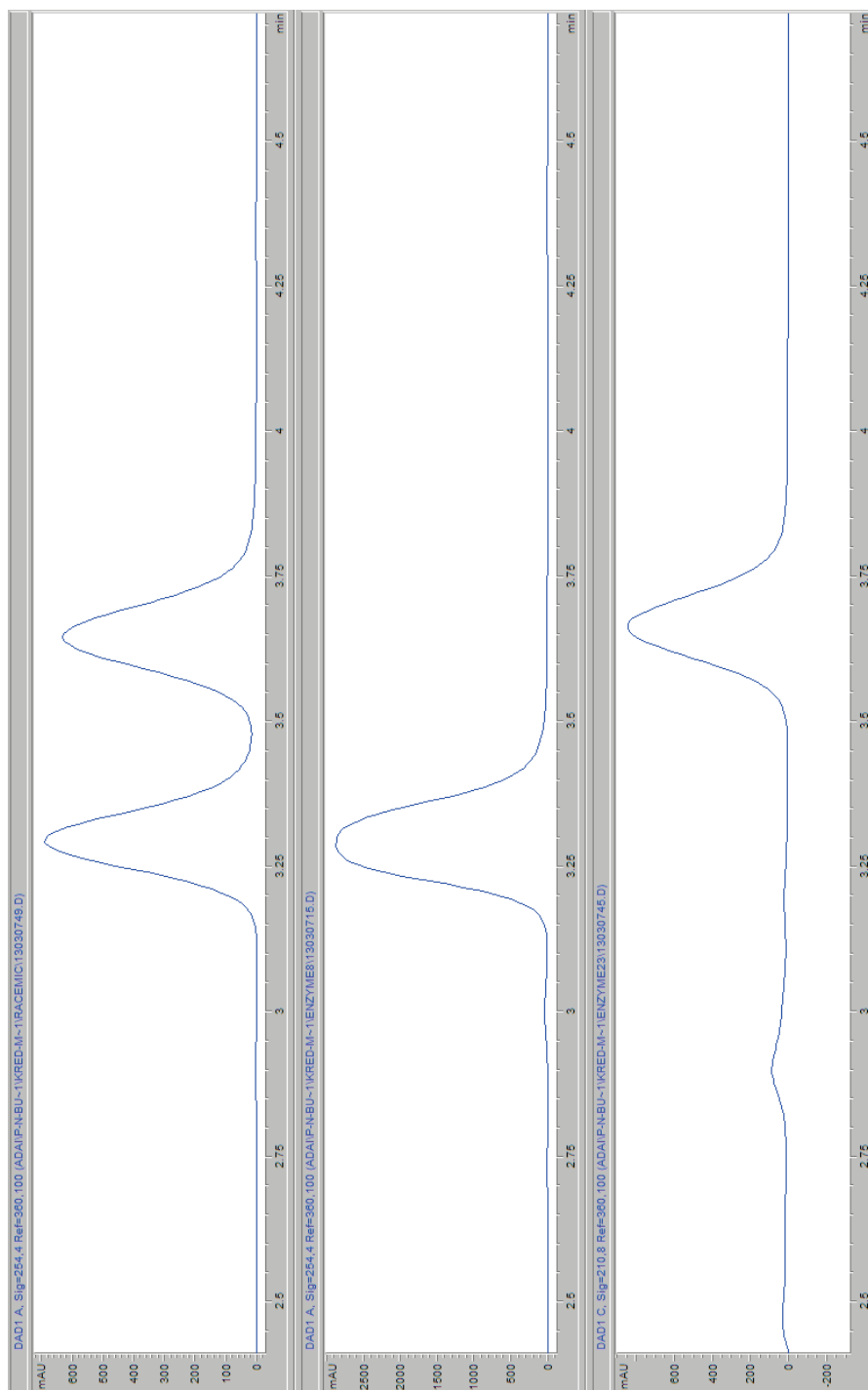


Figure A2.48. Chiral HPLC chromatograph of **3E**. Top spectrum: Racemic; Middle spectrum: crude product made from Enzyme # 8; Bottom Spectrum: crude product made from Enzyme # 23; HPLC column: Phenomenex[®] Lux 3 μ cellulose-1 column (50 x 4.60 mm); mobile phase: hexane: isopropanol = 9:1; Flow rate: 0.5 ml/min.

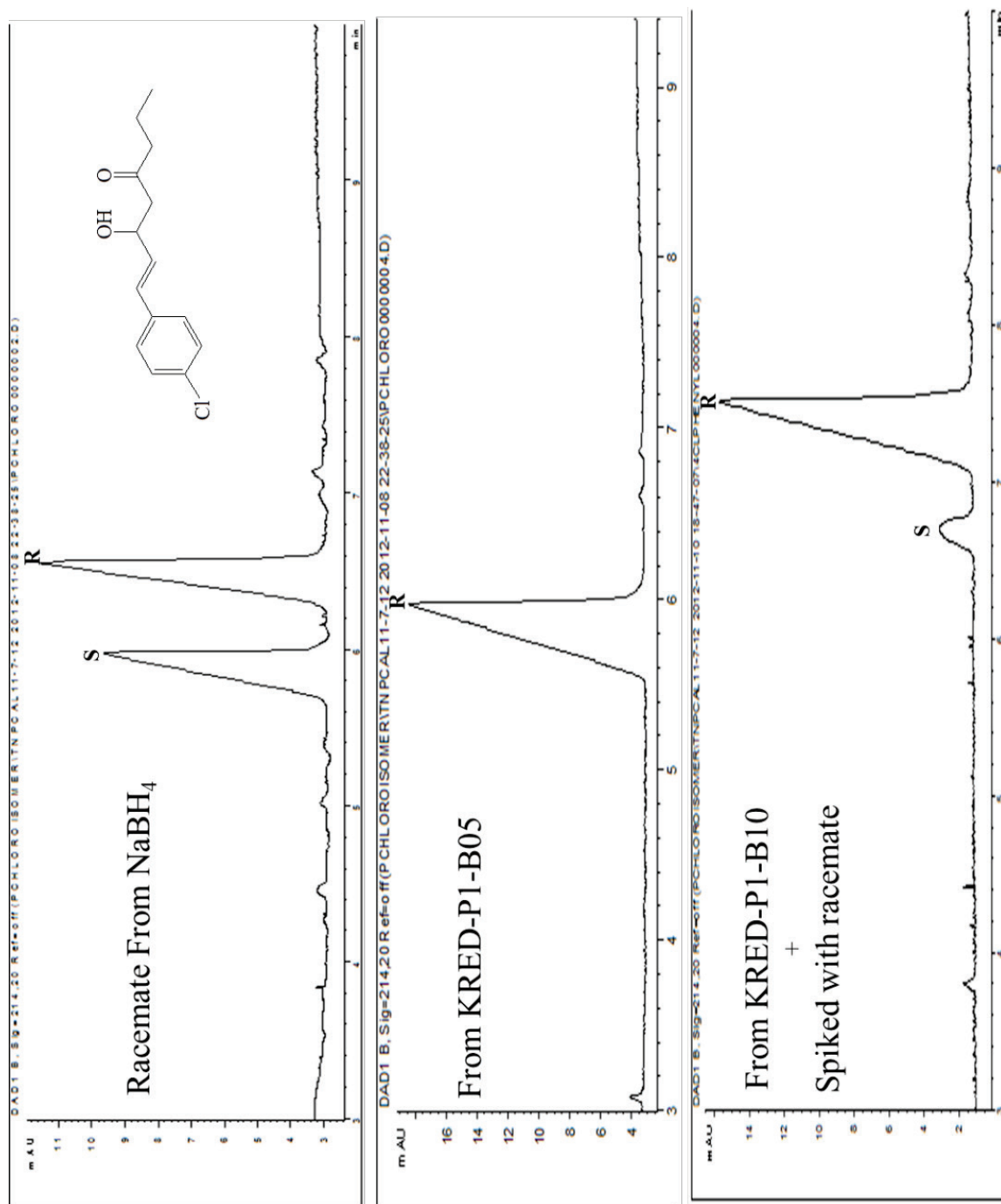


Figure A2.49. CE Electropherogram for 3C. Top: racemic-3C; Middle: product made from enzyme 8 (P1- B05); Bottom: product made from enzyme 8 spiked with racemic. CE condition: 50.0 μ m i.d., bare fused silica capillary, 32.5 cm total length, 24.0 cm to detector; detection 214 nm; Injection: 50.0 mBar/1s; BGE: 5.0 mM KSPDE in 25.0 mM phosphate, pH=2.5; reverse polarity, -15 kV. Crude product was injected directly.

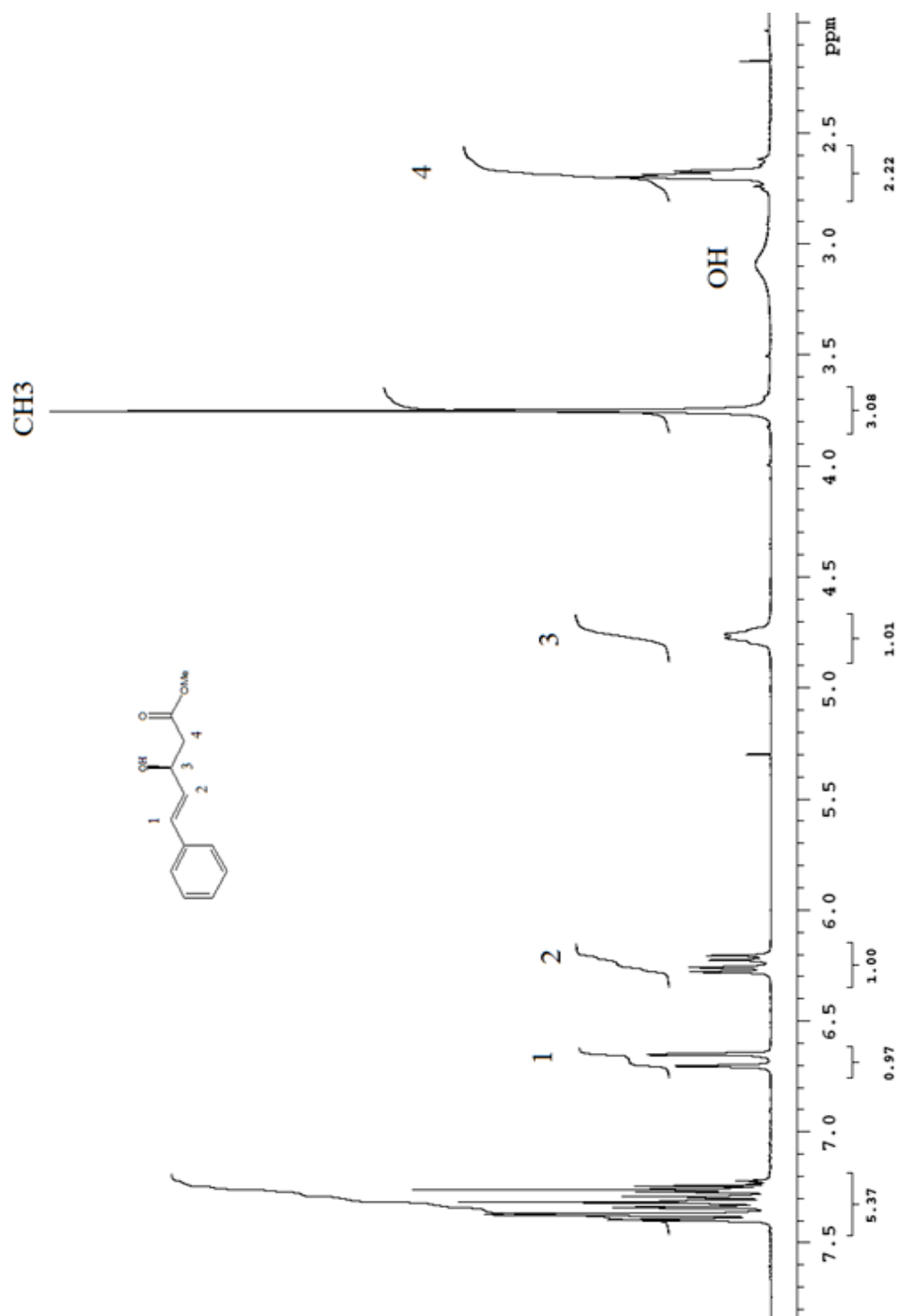


Figure A2.50. ^1H NMR spectra of methyl (3*S*, 4*E*)-3-hydroxy-5-phenylpent-4-enoate made from Mukaiyama aldol condensation.

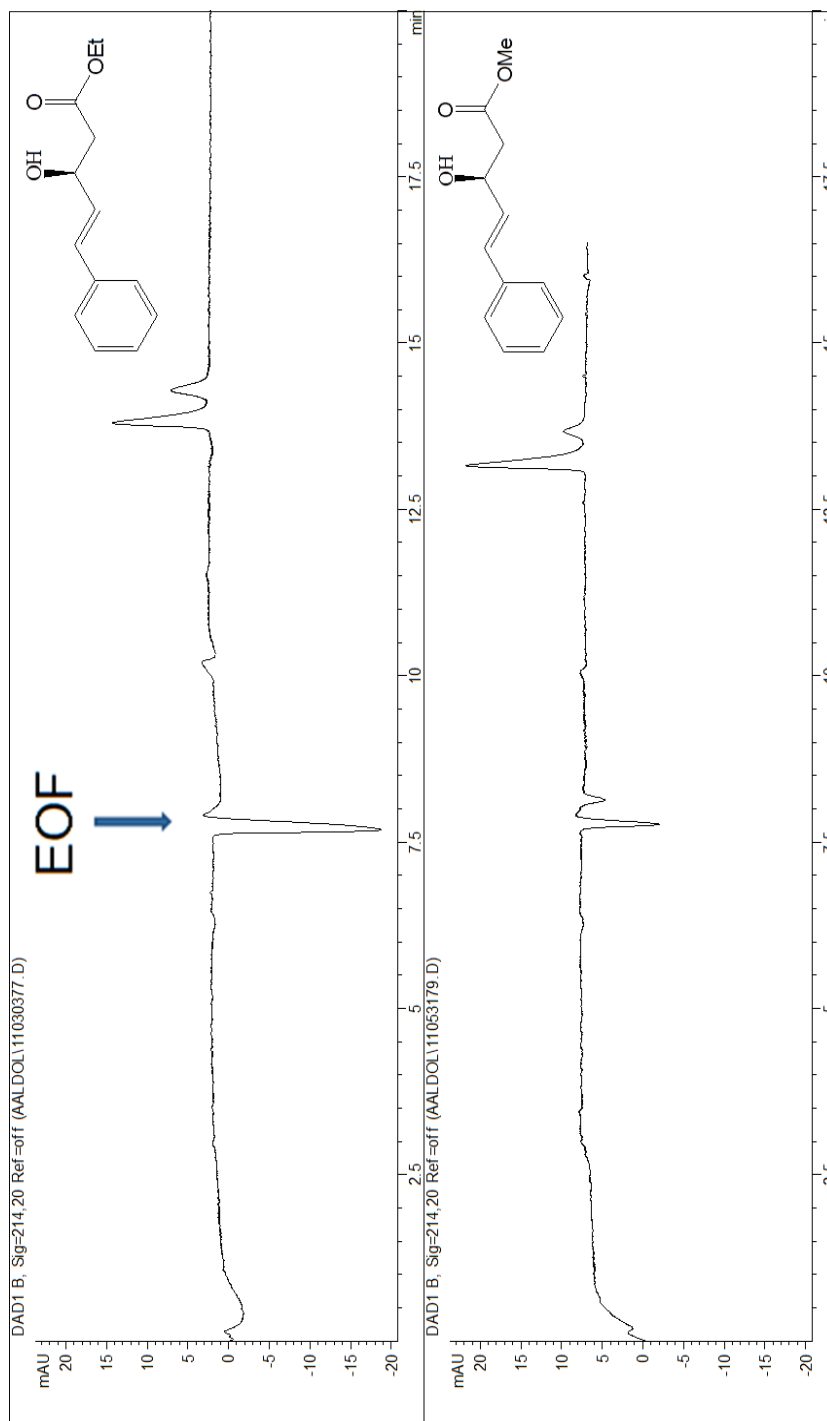


Figure A2.51. CE Electropherogram for *trans* γ , δ -unsaturated β -ketoester made from Mukaiyama Aldol condensation and Me-CBS-BH₃ catalyst. Capillary: 50 μ m *i.d.*, 32.5 cm total, 24.5 cm to detector; Voltage: 5.0 KV (normal polarity); Buffer: 20.0 mM Borate buffer, pH = 9.0; 15.0 mM KSPDM- β -CD; Injection: 50.0 mBar/1s.

Chapter 3

A Total New Synthesis of Ceramide and Sphingosine Analogues²

3.1. Introduction

Ceramide (Cer) is involved in regulation of anti-proliferative and apoptotic responses in various cancer cells (Hannun and Obeid 2002, Ogretmen and Hannun 2004). In sphingolipid metabolism cascade, Cer can be formed from the hydrolysis of sphingomyelin (SM) catalyzed by acid and neutral sphingomyelinase (SMase) or synthesized *de novo* from serine and palmitoyl-CoA (Ogretmen and Hannun 2004). Reciprocally, the level of Cer can be decreased by being converted to other interconnected bioactive sphingolipid species, which reduce the apoptotic effectiveness of Cer. Cer can be broken down by one of many ceramidases (CDase), leading to the formation of sphingosine (SP), which is either acylated back to Cer via ceramide synthase (CS) or phosphorylated to S1P by sphingosine kinase (SK), of which there are two isoforms, SK1 and SK2 (Hannun and Obeid 2008). According to the Cer-SP-S1P rheostat model, both Cer and sphingosine are apoptosis-induced lipids, whereas S1P lead to cell proliferation, inflammation and are referred as a tumour-promoting lipid (Spiegel and Milstien 2003, Milstien and Spiegel 2006, Wymann and Schneider 2008, Pyne and Pyne 2010). Cer can be phosphorylated into ceramide 1-phosphate (Cer1P) by ceramide kinase (CK), which antagonizes the pro-apoptotic action of ceramide and promotes

² Zhipeng Dai and Thomas K. Green. Submitted to *The Journal of Organic Chemistry*.

inflammation (Wymann and Schneider 2008). Cer can also be glycosylated to glucosylceramide (GluCer) mediated by glucosylceramide synthase (GCS) to result in the development of a multidrug resistance in many cancer cells (Ogretmen and Hannun 2004, Reynolds, Maurer et al. 2004). However, the intervention by stimulating or blocking only one or two of the pathways in Cer fails to control cancer cells proliferation, because cancer cells have developed strategies to escape apoptosis and accelerate proliferation by attenuating the pro-apoptotic effects of Cer (Kolesnick, Goñi et al. 2000, Radin 2003).

Different strategies have been developed to enhance the level of ceramide. For example, many anticancer drugs and stress-induced agonists are involved in the increase of endogenous Cer levels through *de novo* synthesis of Cer or the hydrolysis of SM. In addition, treating cancer cells *in vitro* with more easily dispersed short-chain Cer derivatives (C2 to C8-Cer) almost always produces apoptosis and cell-cycle arrest, and those exogenous Cers compete metabolically with natural ones and their metabolites (Radin 2003). Currently, a number of anticancer agents in clinical trials act to increase Cer levels by inhibiting the conversion of GluCer and Cer1P from Cer, or blocking the hydrolysis of Cer to S1P (Radin 2003). Sphingosine analogues such as DMS (*N, N*-dimethylsphingosine) (Yatomi, Ruan et al. 1996, Edsall, Van Brocklyn et al. 1998) and sphingamine (*D, L*-threo-dihydrosphingosine) (Ahn, Chang et al. 2006, Ahn and Schroeder 2010) have been developed and serve as pharmacological inhibitors of SK. FTY720 (fingolimod) has also been found to directly inhibit SK1 activity, reduce tumor metastasis and increase apoptosis (Lim, Tonelli et al. 2011). Aromatic sphingosine analogues have received considerable attention because they are stronger sphingosine

kinase inhibitors than natural sphingosine (Lim, Park et al. 2004, Murakami, Furusawa et al. 2005, Moreno, Murruzzu et al. 2011). For instance, a water soluble sphingosine analogue *BML-258*, in **Figure 3.1**, is an SK1 selective inhibitor and efficacious both *in vitro* and *in vivo* (Paugh, Paugh et al. 2008, Pyne, Bittman et al. 2011).

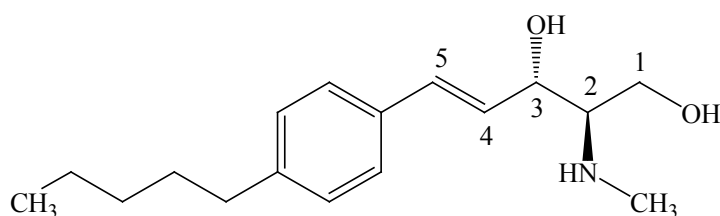


Figure 3.1. Structure of BLM-258, (2*R*, 3*S*, 4*E*)-*N*-methyl-5-(4'-pentylphenyl)-2-aminopent-4-ene-1, 3-diol).

Owing to this important bioactivity, many synthetic approaches have been developed to synthesize sphingosine and its analogues (Kobayashi, Hayashi et al. 1994, van den Berg, Korevaar et al. 2002, Cai, Ling et al. 2006, Yang and Liebeskind 2007, Llaveria, Díaz et al. 2008, Kumar, Dubey et al. 2010, van den Berg, van den Elst et al. 2011). Most syntheses begin with protected serine aldehyde (Dondoni, Fantin et al. 1988, Garner, Park et al. 1988, Herold 1988, Nimkar, Menaldino et al. 1988, Radunz, Devant et al. 1988, Van Overmeire, Boldin et al. 1999, Lim, Park et al. 2004, Murakami, Furusawa et al. 2005, Chandrasekhar, Saritha et al. 2006, Wong, Tan et al. 2009, Zipkin, Spiegel et al. 2010) and its derivatives (Moreno, Murruzzu et al. 2011). The synthesis of *BLM-258*, reported by Zipkin et al. (Zipkin, Spiegel et al. 2010), is a protected serine aldehyde-

based synthesis, which however is not highly stereospecific with respect to the C-2 and C-3 stereocenters. In fact, their first step in the synthesis results in a mixture of *threo* and *erythro* products (7.6:1) which required separation by preparative HPLC (Zipkin, Spiegel et al. 2010).

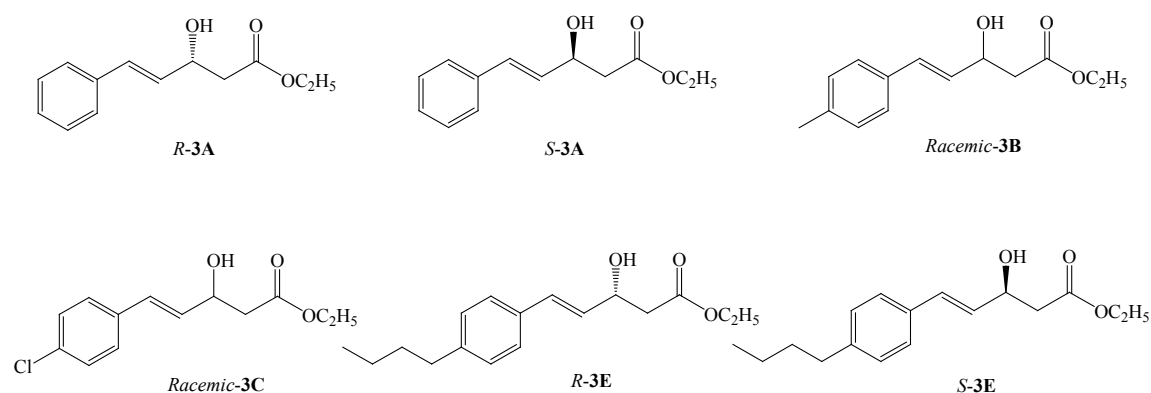


Figure 3.2. Structure of *trans*- γ , δ -unsaturated β -hydroxyesters. Enantiopure (>99%) *R*-**3A**, *R*-**3E** and *S*-**3E** are prepared from reduction of corresponding *trans*- γ , δ -unsaturated β -ketoesters by KREDs (Dai, Guillemette et al. 2013). *S*-**3A** (e.e. 75%) was prepared according to the literature (Carreira, Singer et al. 1994). Racemic-**3B** and **3C** were prepared from reduction of corresponding *trans*- γ , δ -unsaturated β -ketoesters by NaBH₄.

This chapter describes a totally new synthetic route to obtain a family of aromatic sphingosine derivatives starting with racemic and chiral *trans*- γ , δ -unsaturated β -hydroxyesters (**Figure 3.2**). The common structural feature of the targeted aromatic ceramide and sphingosine based analogues is represented by the general structure below (**Figure 3.3**). The focus of this chapter is to describe the stereoselective synthesis of this fundamental stereochemical framework.

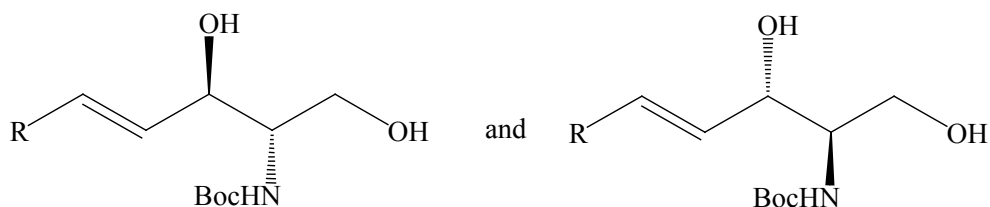
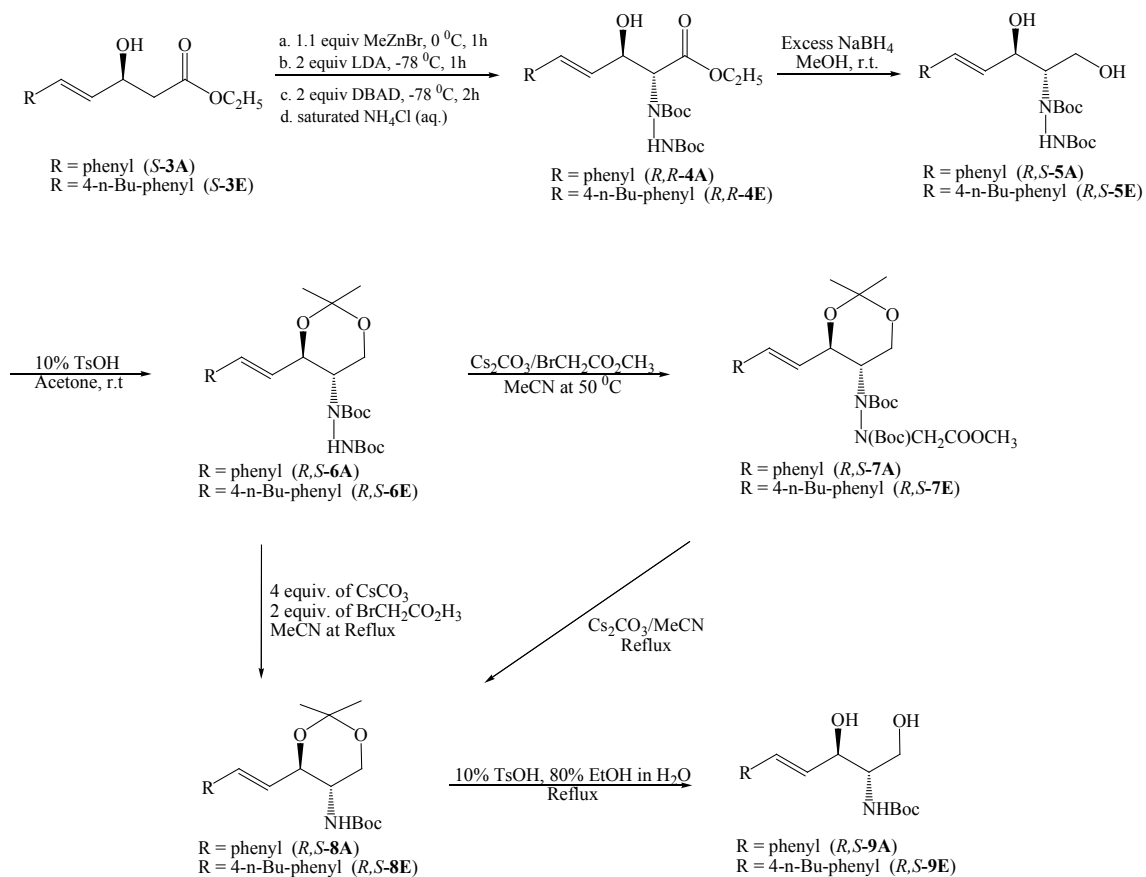


Figure 3.3. Basic Structural Feature of Sphingosine derivatives.

3.2. Results and discussion

Enantiopure *trans*- γ , δ -unsaturated β -hydroxyesters **3**, shown in **Scheme 3.1**, were used as the building blocks to introduce the first chiral center. Strategies for the diastereoselective formation of hydrazino and nonreductive eliminative cleavage of the hydrazino N-N bonds were required for the stereoselective attachment of the amino group. Diastereospecific electrophilic amination of the *trans*- γ , δ -unsaturated β -hydroxyesters **3** by di-*tert*-butyl azodicarboxylate (DBAD) produced anti *N*-Boc- α -hydrazino- β -hydroxyesters **4**, which introduced the second chiral center in the form of a hydrazino functionality. In the presence of excess NaBH₄, ethyl esters in anti *N*-Boc- α -hydrazino- β -hydroxyesters **4** were reduced into alcohols to afford *N*-Boc-2-hydrazino 1, 3-diols **5**. After the protection of 1,3-diols **5** in the form of 1,3-dioxanes **6**, nonreductive eliminative cleavage of the hydrazino N-N bond in 1,3- dioxanes **6** gave 1,3-dioxanes-2-carbamate **8** through intermediate **7**. Ceramide and sphingosine derivatives **9** were then synthesized economically and stereospecificly after the deprotection of 1,3- dioxanes 2-carbamate **8**.

Scheme 3.1 describes the generalized stereoselective synthesis of sphingosine analogues starting from *trans*- γ , δ -unsaturated β -(*S*)-hydroxyesters **S-3A** (75% e.e.) and **S-3E** (>99% e.e.).

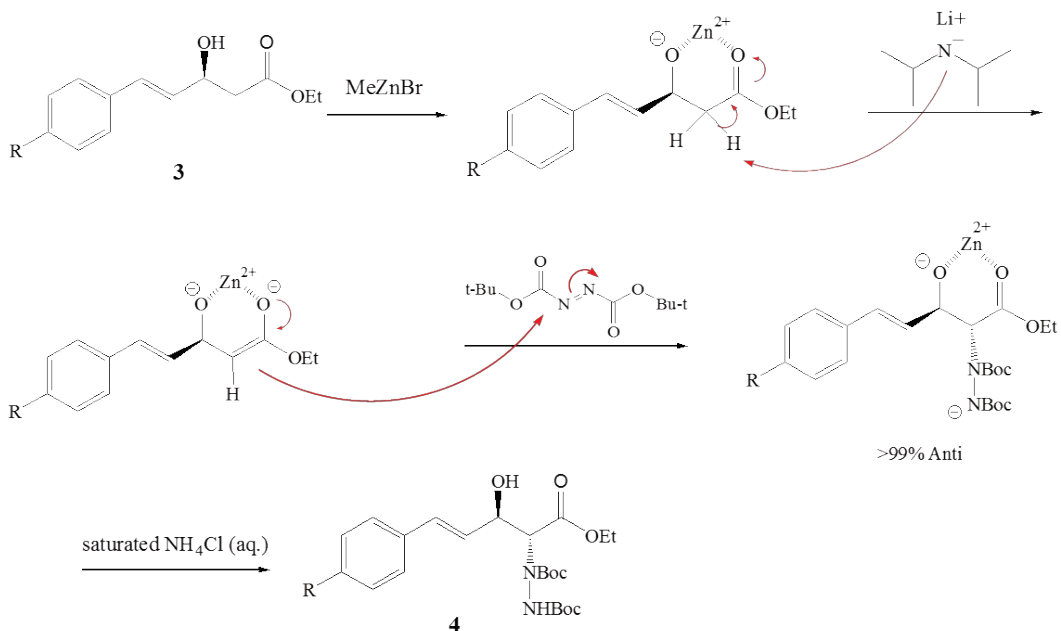


Scheme 3.1. General reaction scheme for the stereospecific synthesis of ceramide and Sphingosine derivatives from *trans*- γ , δ -unsaturated β -(*S*)-hydroxyesters **S-3A** and **S-3E**.

3.2.1. Anti *N*-Boc- α -hydrazino- β -hydroxyesters (**4**)

The diastereospecific formation of anti *N*-Boc- α -hydrazino- β -hydroxyesters **4** was performed via electrophilic amination of the β -hydroxyesters **3** with di-*tert*-

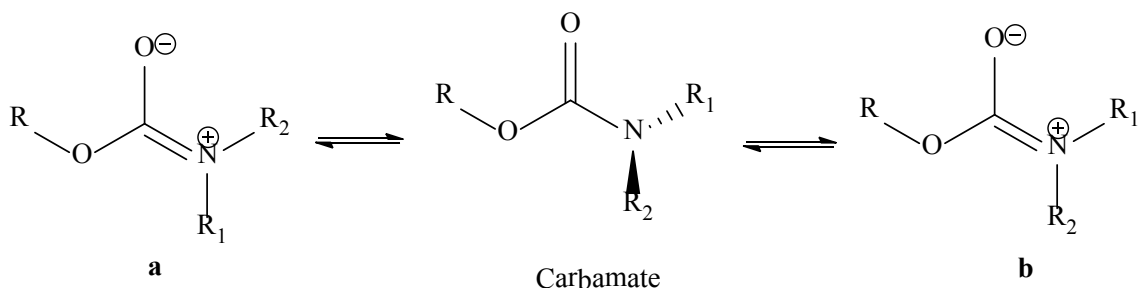
butylazodicarboxylate (DBAD) according to the procedure described by Greck and Phansavath and their colleagues (Greck, Bischoff et al. 1993, Girard, Greck et al. 1996, Greck and Genet 1997, Labeeuw, Phansavath et al. 2003). In order to obtain high diastereoisomeric excesses, the zinc enolate form of β -hydroxyesters **3** was required and obtained by adding one equivalent of methylzinc bromide at 0 °C for 1 h followed by two equivalents of lithiumdiisopropylamide at -78 °C for another 1 h (**Scheme 3.2**). Then, electrophilic amination was achieved through Michael addition to DBAD at -78 °C for another 2 h. The product was isolated by normal phase chromatography using a mobile phase consisting of CH₂Cl₂/EtOAc (10:1). The isolated percent yield is typically 50-60%. Unreacted β -hydroxyesters **3** could be recovered without racemization. Due to the rigid zinc enolate form of β -hydroxyesters **3**, the hydroxyl and hydrazino functionalities were preferentially formed as the *anti*-configurational isomer in excellent diastereoisomeric excesses (>99%). No *syn*-diastereoisomer was detected as indicated by ¹H NMR by the absence of additional signals in the δ 4 - 7 ppm range and the existence of only one set of signals in the ¹³C NMR spectrum.



Scheme 3.2. Chelated zinc enolates of β -hydroxyesters **3**.

Intermediates **4-6**, which all possess the *N*-Boc- α -hydrazino function, in many cases exhibit extremely broadened ^1H and ^{13}C resonances in their NMR spectra, in spite of being pure compounds as indicated by TLC and mass spectrometry (See **Figures 3.09-3.32, Appendix B**). The broad resonances are characteristic of molecules that undergo restricted bond rotation due to steric hindrance. The *N*-Boc- α -hydrazino function possesses two carbamate functions, which are known to undergo restricted intramolecular rotation about the carbamate C-N bond (Cox and Lectka 1998, Anand, Roy et al. 2007). As shown in **Scheme 3.3**, the delocalization of the N-lone electron pair in carbamate provides two conformers (**a** and **b**). Examples from the literature show the energy barrier to rotation to be around 16 kcal/mol (Anand, Roy et al. 2007). The interconversion

between two conformers is slow at ambient temperatures, owing to the restricted rotation in the amide portion of the carbamate. As the result, dynamic ^1H NMR spectroscopy on carbamates shows extreme broadening of ^1H NMR signals of the hydrogens (Pirkle, Simmons et al. 1979, Modarresi-Alam, Najafi et al. 2007). In anti *N*-Boc- α -hydrazino- β -hydroxyesters **4**, there are two carbamate groups. Theoretically, four conformers exist in anti *N*-Boc- α -hydrazino- β -hydroxyesters **4** due to the restricted rotation barrier of both carbamates C-N.



Scheme 3.3. Restricted rotation in carbamate. N-lone electron pair delocalization (**a** and **b**). $R_1 \neq R_2$

Consistent with previous findings, the ^1H NMR spectra at 25 °C of anti *N*-Boc- α -hydrazino- β -hydroxyesters **4**, such as methyl (4*E*)-2-[1,2-bis(*tert*-butoxycarbonyl)hydrazino]-2,4,5-trideoxy-5-phenyl-*D*-*erythro*-pent-4-enonate **4A** (**Figure 3.4**), reveals broad OH, H-2 and H-3 signals. (**Figure 3.5A**). In fact, the OH and H-2 hydrogens both show major and minor resonances, which is probably attributed to major and minor conformations which interconvert very slowly on the NMR timescale at 25 °C. The major and minor resonances of both the OH and H-2 resonances, respectively, coalesce into one broad peak when the ^1H NMR spectrum was collected at 55 °C, and the H-3 resonance

sharpens into a pentet. (**Figure 3.5B**). This coalescence behavior is consistent with a molecule that undergoes highly restricted rotation. As the temperature is increased, the rate of the interconversion of the conformers increases, and the resonances are observed as an average of the separate resonances. For **4A**, this restricted rotation could involve a combination of C-N carbamate and/or C-C bond bonds. Further investigation is required to fully characterize the dynamic behavior of these intermediates.

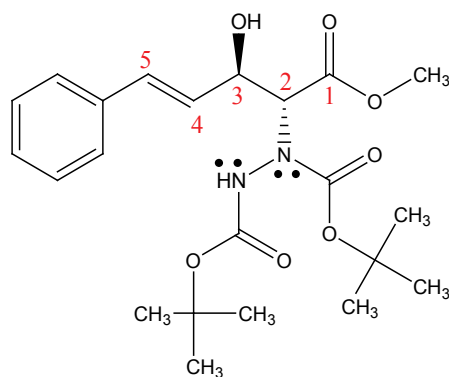


Figure 3.4. Methyl (4*E*)-2-[1,2-bis(*tert*-butoxycarbonyl)hydrazino]-2,4,5-trideoxy-5-phenyl-*D*-erythro-pent-4-enonate (**4A**).

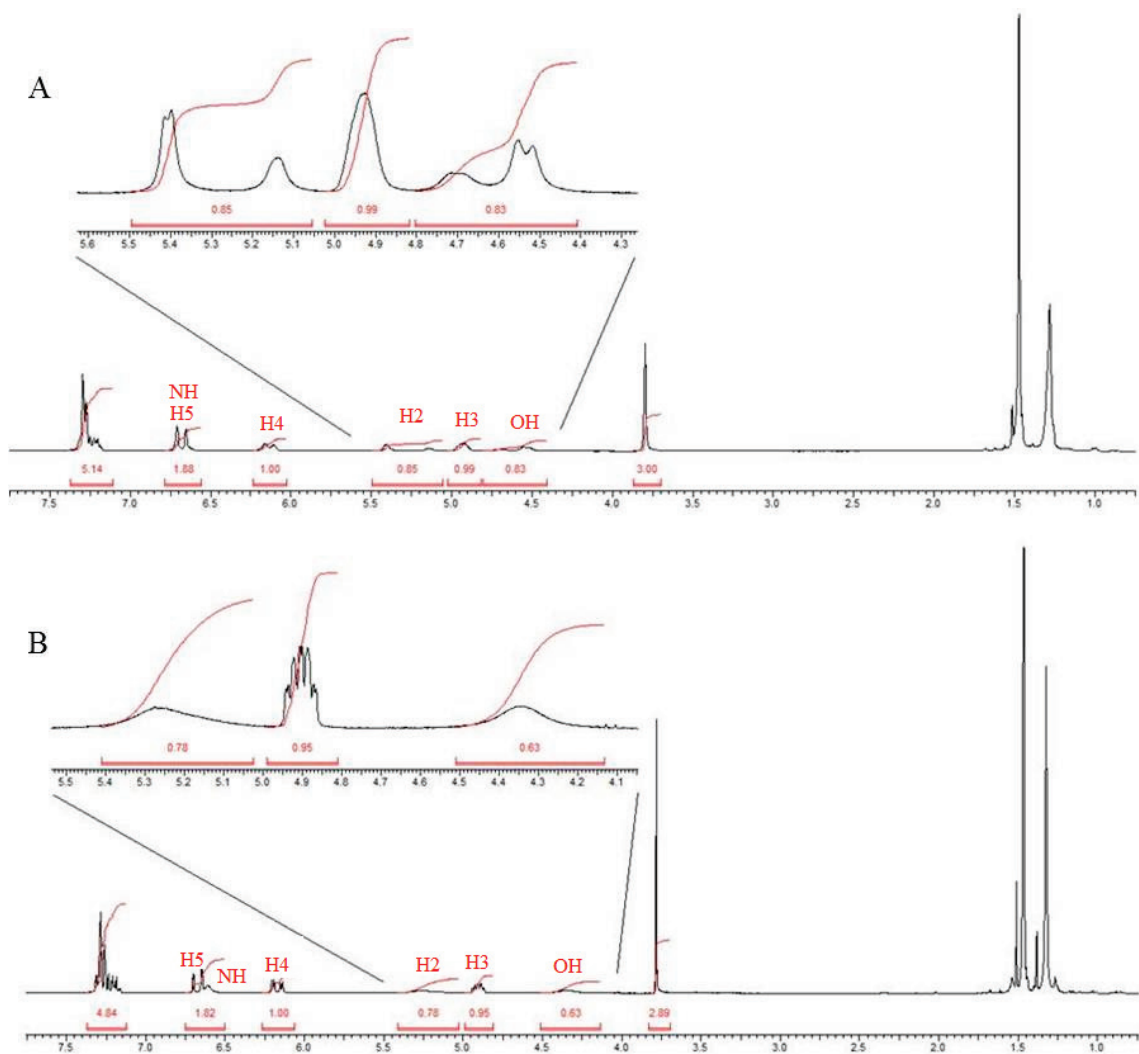


Figure 3.5. ^1H NMR spectrum of methyl (4*E*)-2-[1,2-bis(*tert*-butoxycarbonyl)hydrazino]-2,4,5-trideoxy-5-phenyl-*D*-*erythro*-pent-4-enonate (**4A**) in CDCl_3 . (A) at 25 °C; (B) at 55 °C.

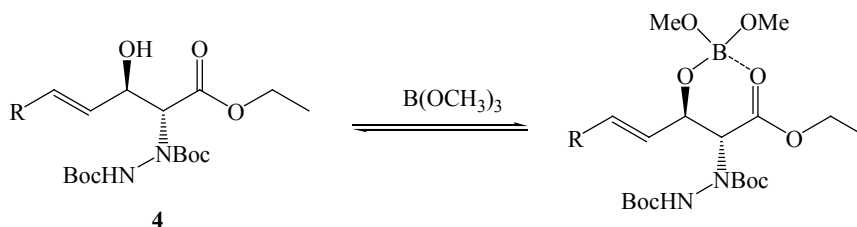
Thus, we have successfully introduced protected amino moieties as *N*-Boc- α -hydrazino- β -hydroxyesters **4**. Full assignments of **4** were made based on NMR spectra, and only *anti* *N*-Boc- α -hydrazino- β -hydroxyesters **4** were provided as detectable diastereomers according to ^1H NMR spectroscopy.

3.2.2. Anti 2-hydrazino 1, 3-diol (5)

As a highly chemoselective reducing agent, NaBH₄ is widely used in the reduction of aldehydes and ketones, but the reduction of esters by NaBH₄ directly shows no or less reactivity under ambient conditions. Many effects have been reported on adding additives to enhance the reactivity of NaBH₄ towards esters. For example, Lewis acids such as aluminum chloride (Brown and Rao 1956, Yamakawa, Masaki et al. 1991), zinc bromohydride (Narasimhan, Madhavan et al. 1995), iodine (Kanth and Periasamy 1991), and zinc chloride (Yamakawa, Masaki et al. 1991) could serve as additives to increase the reactivity of NaBH₄ towards esters. In the presence of a large excess of NaBH₄, the reduction of aliphatic and aromatic esters has also been accomplished. In 1963, Brown and his colleagues reported the reduction of saturated esters using a 20 fold excess of NaBH₄ in methanol (Brown and Rapoport 1963). However, they also found that unsaturated esters, in the presence of 10 fold excess of NaBH₄, yielded mostly saturated alcohol with small amounts of the saturated ester and unsaturated alcohol (Brown and Rapoport 1963). Kim *et al.* investigated reduction of saturated aromatic keto esters to diols by 3 equivalents of methanolic NaBH₄, and the reactions were completed with 0.5 to 3 hours (Kim, De Castro et al. 2010). Chaudhuri and his colleagues reacted 4 equivalents of methanolic NaBH₄ with γ -aryl- α , β -unsaturated- γ -ketoesters and obtained completely saturated diols (Chaudhuri, Saha et al. 2010).

The reduction of ethyl esters in *anti* *N*-Boc- α -hydrazino- β -hydroxyesters **4** to *anti* 2-hydrazino 1,3-diol **5** was accomplished using a modification of the method of Chaudhuri and Kim (Chaudhuri, Saha et al. 2010, Kim, De Castro et al. 2010). In this method

developed, ketoesters were reduced effectively to diols using three equivalents of NaBH_4 in MeOH solvent over a short reaction time at room temperature in the absence of any additives. A possible mechanism was proposed in which NaBH_4 was slowly decomposed in methanol to generate trimethoxy borane, which further served as a Lewis acid to form a ring intermediate with β -hydroxyesters **4** to activate and promote the reduction of ester by sodium alkoxyborohydride species. **Scheme 3.4** below shows a possible cyclic intermediate formed between *anti* N-Boc- α -hydrazino- β -hydroxyesters **4** and trimethoxy borane in our substrate molecules.

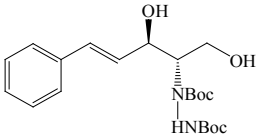
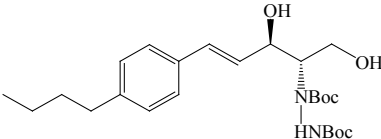
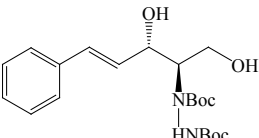
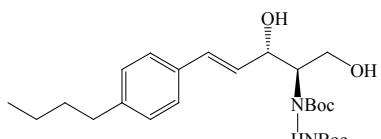
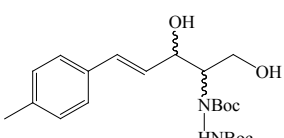
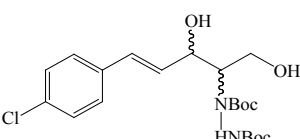


Scheme 3.4. A possible ring intermediate between *anti* N-Boc- α -hydrazino- β -hydroxyesters **4** and trimethoxy borane.

Under Kim's reaction conditions, only a few percent of compound **4** was reduced to 1,3-diol **5** by using three equivalents of NaBH_4 over three hours as indicated by TLC analysis. To increase the conversion of compound **4** to 1,3-diol **5** and avoid the hydrogenation of C=C bonds induced by a large excess of NaBH_4 , we modified the reaction conditions. In a typical procedure, three equivalents of NaBH_4 was added into compound **4** in methanol every 15 min until compound **4** was completely consumed as indicated by TLC plate (eluent: $\text{CH}_2\text{Cl}_2/\text{EtOAc} = 5:3$). The reaction was usually

completed within 3 - 4 h at ambient temperature and the total amount of NaBH₄ consumed was 36-51 equivalents. Excess NaBH₄ was destroyed with saturated NH₄Cl solution. After a simple chromatography on silica gel, a good yield with a range of 80-85% was obtained (**Table 3.1**). A very large excess of NaBH₄ was used to reduce *N*-Boc- α -hydrazino- β -hydroxyesters compared to Kim's reaction condition where only 3 equivalents of NaBH₄ was used to reduce saturated aromatic ketoesters. We believe that this arises from the cyclic intermediate in **Scheme 3.3**, which has steric hindrance due to the bulky α -hydrazino and aromatic ring functionalities. This steric effect decreases the reactivity of the intermediate and reduction rate by NaBH₄. The solvent methanol competes with the intermediate to consume most of NaBH₄. Therefore, the amount of NaBH₄ needs to be replenished every 15 min to ensure that the unreacted intermediate is completely reduced.

Table 3.1. Reduction of *anti* *N*-Boc- α -hydrazino- β -hydroxyesters **4** by excess NaBH₄.

Reactant	Product	NaBH ₄ (equiv.)	yield, %	d.e. %
<i>S</i> -3A		39	88	>99
<i>S</i> -3E		45	81	>99
<i>R</i> -3A		45	85	>99
<i>R</i> -3E		51	80	>99
<i>anti</i> -3B Racemic		36	83	>99
<i>anti</i> -3C Racemic		45	83	>99

The structures of the purified products 1,3-diols **5** were verified by NMR spectroscopy. The ¹H NMR spectra of these intermediates **5** were almost identical in the H-1 to H-5

region. The ^1H NMR of the purified **3A** is shown in **Figure 3.6**, and, consistent with highly restricted bond rotation, very broad, poorly resolved signals are observed. Broadened signals at 3.0-5.0 ppm belong to two hydroxyls and the hydrogens attached to C-1 to C-3 (integrates for 6H), and these proton signals are not assigned. A broadened peak centered at 6.35 ppm is characteristic of N-H which is overlapping with a doublet of doublet at 6.21 ppm assigned to H-4. A sharp hydrogen signal of one *tert*-butoxycarbonyl $[\text{C}(\text{CH}_3)_3]$ at 1.47 ppm is not identical with the hydrogen signal of the *tert*-butoxycarbonyl at 1.42 ppm which is broad, due to hindered rotation.

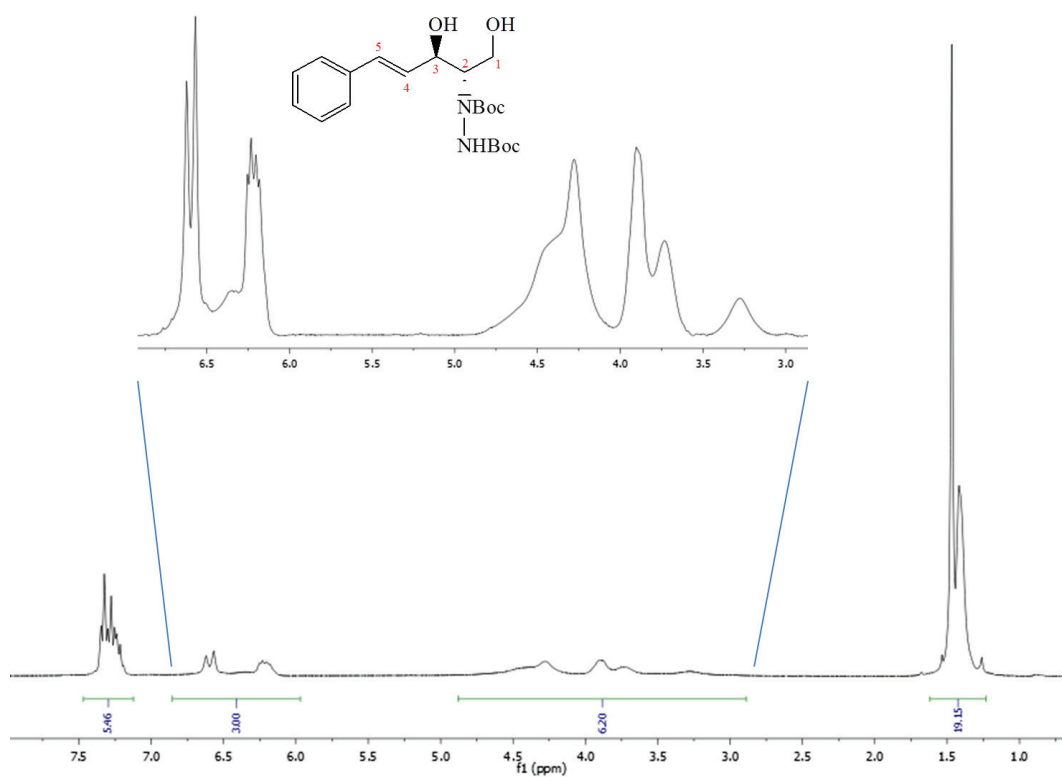


Figure 3.6. ^1H NMR spectrum of (4*E*)-2-[1,2-bis(*tert*-butoxycarbonyl)hydrazino]-2,4,5-trideoxy-5-phenyl-*D*-erythro-pent-4-enitol (**5A**) in CDCl_3 .

Chiral HPLC was employed to measure possible racemization of reduced 1,3-diol product **5**, and the result shows no racemization occurs during the reaction process using using a large excess of NaBH₄.

3.2.3. Non-reductive eliminative cleavage of the hydrazine N-N bonds

Many protocols have been recently developed to cleave N-N bonds. Although usually successful, these methods have inherent disadvantages and failure to cleave N-N bonds in anti *N*-Boc- α -hydrazino- β -hydroxyesters **4**. For example, H₂/Pd-C (Girard, Greck et al. 1996), H₂/Raney Ni (Hinman 1957, Denmark, Nicaise et al. 1990, Ghelfi and Parsons 2000, Raup, Cardinal-David et al. 2010) and BH₃·THF (Yamazaki and Kibayashi 1997) have been widely used to cleave N-N bonds, however, these conditions are incompatible with C=C bonds. Sapountzis *et al.* treated hydrazine derivatives with Zn/H⁺ to accomplish the reductive cleavage of N-N bonds (Sapountzis and Knochel 2004). However, for our substrate, acidic conditions will subsequently cause the deprotection of Boc protected group. What's more, Zhang and his colleague reported a reductive cleavage of N-N bonds in hydrazines using aqueous TiCl₃ under a broad pH range from acidic to basic conditions (Zhang, Tang et al. 2011). However, in our hands, a white precipitate formed during the basification of TiCl₃ by an aqueous solution NaOH to pH 10, and failed to cause N-N bond cleavage in anti *N*-Boc- α -hydrazino- β -hydroxyesters **4**. The reagent *t*-BuOK in DMSO and the presence of fluorenyl bromide has also been used

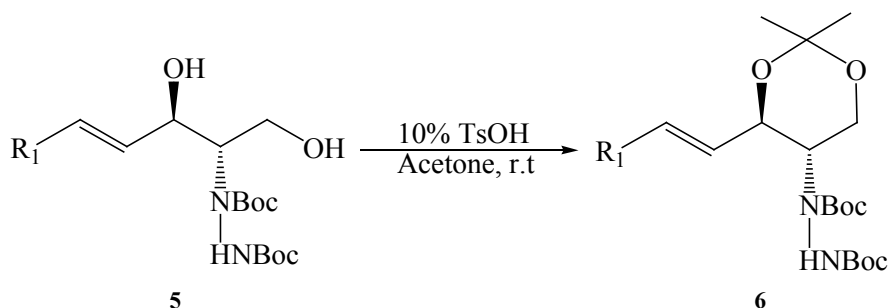
in the N-N bonds cleavage; however yields for this reaction are not practical (Gong, Bausch et al. 2001, Magnus, Garizi et al. 2009).

Other improvements in N-N bonds cleavage protocols have been developed. For example, SmI₂ has also been used in the reductive cleavage of the N-N bonds in hydrazine, where an activated acyl group on one of the nitrogen atoms is required to promote the N-N cleavage with SmI₂ (Friestad and Ding 2001, Ding and Friestad 2004, Errasti, Koundé et al. 2009). Recently, Magnus and his colleagues developed an *E1cB* eliminative cleavage of N-N bonds in diethoxycarbonyl hydrazino derivatives by treating the derivatives with methyl bromoacetate in the presence of Cs₂CO₃ in MeCN solvent at 50 °C, followed by refluxing to break N-N bonds and generate carbamates (Magnus, Garizi et al. 2009). These methods are compatible with alkene functionality. Both of these methods could potentially be used for the N-N bond cleavage of compound **5**.

Comparing the structure of anti 2-[1,2-bis(*tert*-butoxycarbonyl)]hydrazino 1,3-diol **5** with the structure of substrates used by Magnus, they have structural similarity except the bis(*tert*-butoxycarbonyl)hydrazino is used instead of diethoxycarbonyl hydrazino. Therefore, this dissertation research employed *E1cB* eliminative N-N bonds cleavage protocol to cleave the N-N bonds in compound **5**.

Before performing the *E1cB* eliminative N-N bonds cleavage on compound **5**, both OH groups in compound **5** need to be protected to prevent their alkylation by methyl bromoacetate in the presence of Cs₂CO₃ in MeCN. To prevent the OH alkylation, compound **5** was protected as 1, 3-diol ketal **6** with anhydrous acetone using 10 mol % *p*-

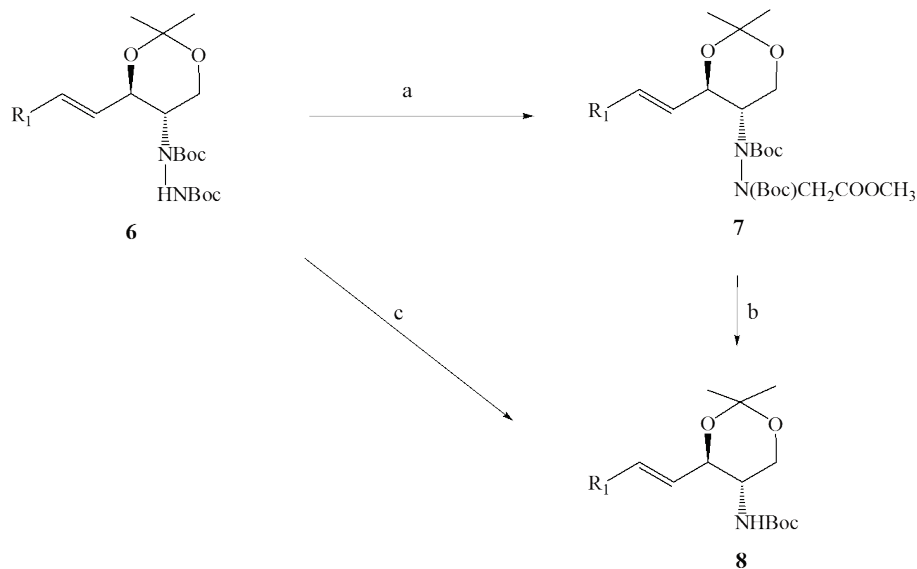
toluenesulfonic acid at RT (**Scheme 3.4**). TLC (eluent: CH₂Cl₂/EtOAc 10:1) was used to monitor the completion of protection.



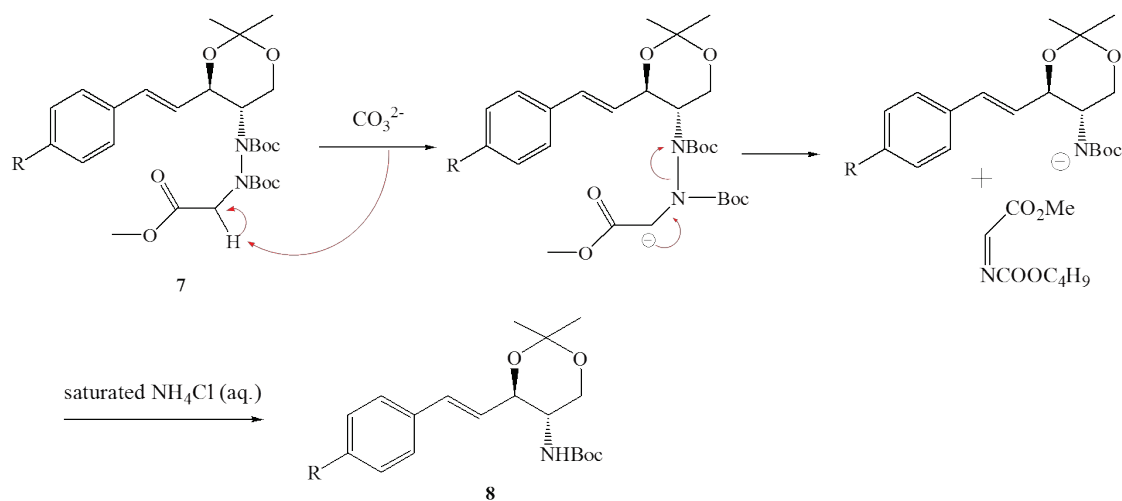
Scheme 3.5. Ketalization of anti 2-di-*tert*-butoxycarbonyl hydrazino 1,3-diol ketals (**6**).

As shown in **Scheme 3.6**, *anti* 2-*N*-alkylated-di-*tert*-butoxycarbonyl hydrazino 1,3-diol ketals **7** were obtained via alkylation on NH of *anti* 2-di-*tert*-butoxycarbonyl hydrazino 1,3-diol ketals **6** by methyl bromoacetate (2.0 equiv.) in anhydrous MeCN in the presence of 2.5 equiv. of Cs₂CO₃ at 50 °C. After purification by column chromatography on silica gel using 10:1 CH₂Cl₂/EtOAc, **7** were refluxed in anhydrous MeCN with 3 equiv. of suspended Cs₂CO₃ to give carbamates **8** as a white solid with a yield of 83-95%. The eliminative pathway is displayed in **Scheme 3.7**, where carbamates **8** is formed by *E1cB* (Elimination Unimolecular conjugate Base) in which the anion of **7** is formed in base, and then undergoes cleavage of N-N bond with a loss of a dehydroglycine derivative. Workup is by protonation using saturated aqueous NH₄Cl solution. Compound **6** could also be refluxed in a suspended solution of 4.0 equiv. of Cs₂CO₃ and 2.0 equiv. of methyl bromoacetate in anhydrous MeCN and give carbamates **8** directly with a high yield of 93%

after 24 h. As discussed by Magnus *et.al.*, the presence of water would slow the elimination process (Magnus, Garizi et al. 2009).



Scheme 3.6. *E1cB* non-reductive cleavage of N-N bonds into carbamates (**8**). (a) Cs₂CO₃ (2.5 equiv.), BrCH₂CO₂CH₃ (2 equiv.), MeCN, 50 °C; (b) Cs₂CO₃ (3.0 equiv.), MeCN, reflux; (c) Cs₂CO₃ (4.0 equiv.), BrCH₂CO₂CH₃ (2 equiv.), MeCN, reflux.



Scheme 3.7. *E1cB* elimination of N-N bonds in anti 2-N-alkylated-di-tert-butoxycarbonyl hydrazino 1,3-diol ketals (7) to obtain (8).

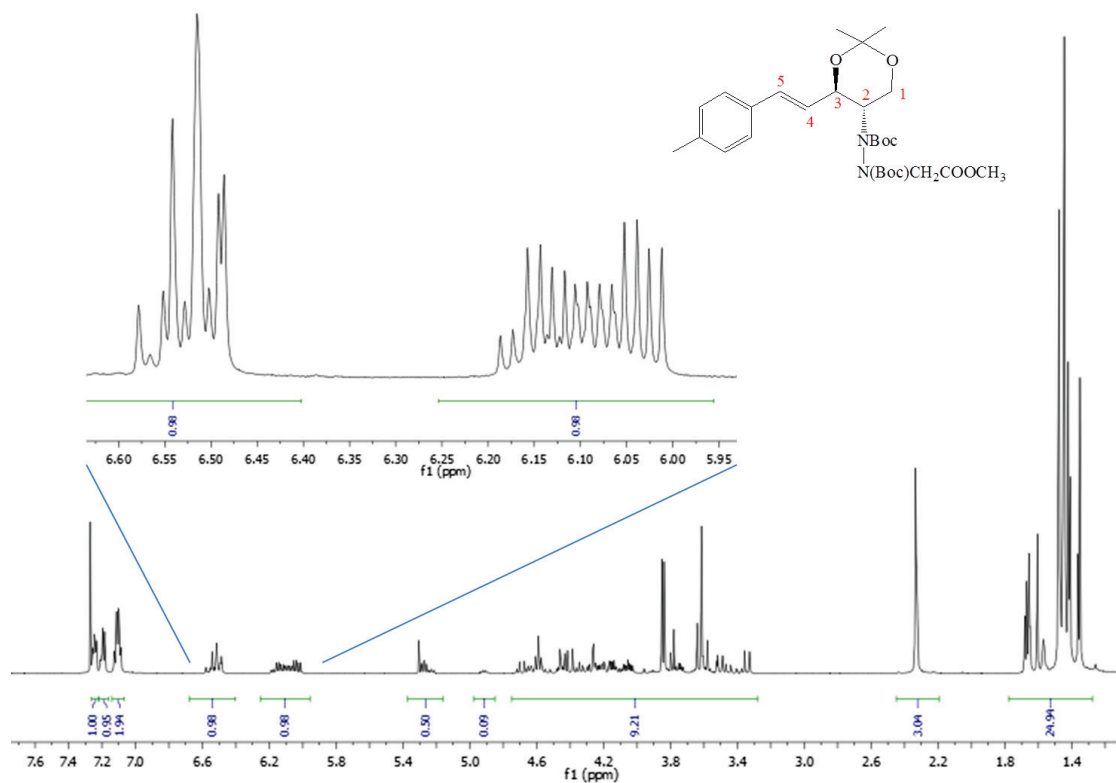


Figure 3.7. ^1H NMR spectrum of (7C) in CDCl_3 by a Bruker 600 MHz spectroscopy.

NMR spectra of *anti* 2-*N*-alkylated-di-*tert*-butoxycarbonyl hydrazino 1, 3-diol ketals **7** were obtained on a 300 MHz Varian Mercury FT-NMR spectrometer. Owing to very complicated ^1H and ^{13}C NMR spectra, no assignments are made. ^1H NMR spectrum of **7C** was collected on a Bruker 600 MHz NMR spectrometer, shown in **Figure 3.7**. The spectrum is enormously complicated in spite being a pure compound as indicated by TLC and mass spectrometry. The complexity, and the presence of the relatively high number of narrow resonances, indicates that the molecule exist in a number of conformations where the barrier to bond rotation is significantly above room temperature. In the ^1H NMR spectrum of **7C**, the signal of the alkene hydrogen attached to C-4 is split to at five sets of doublet of doublets in **7C**, which means at least six conformations of compound **7** exist at ambient temperature. The complexity can be attributed to the steric effect among two di-*tert*-butoxycarbonyl groups, methylacetate group, ketal and aromatic ring functionalities. **Figure 3.8** shows a temperature study of ^1H NMR spectra of **7C** in DMSO- d_6 . Olefin and aromatic hydrogen signals coalesce separately with increased temperature, which indicate interconversion of the conformations at higher temperatures. When heated at 100 °C for over an hour, compound **7** partially decomposed.

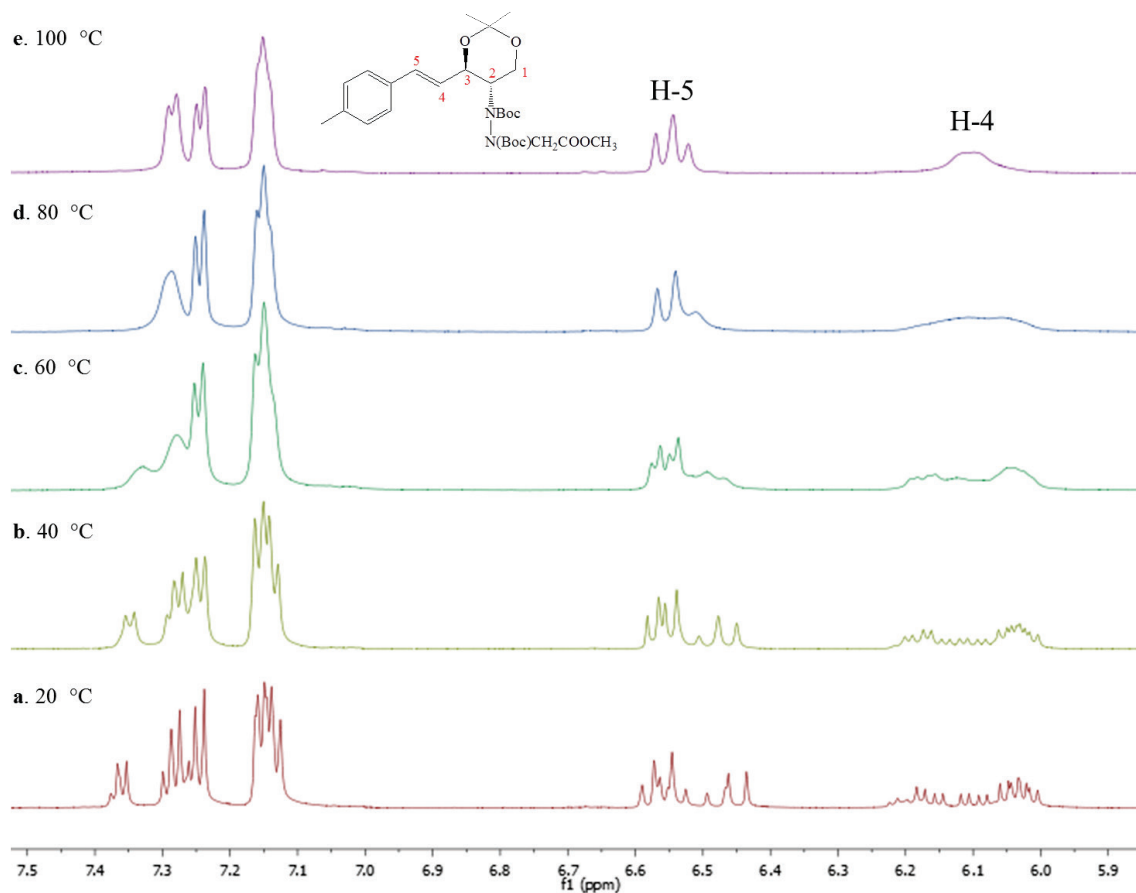


Figure 3.8. Stacked ^1H NMR spectra of olefin and aromatic hydrogen of **7C** in $\text{DMSO-}d_6$ at variant temperatures. a) 20 °C; b) 40 °C; c) 60 °C; d) 80 °C; e) 100 °C.

3.2.4. Deprotection of 2-Boc-amino-1,3-diol ketals (**8**) to provide target products.

2-Boc-amino-1,3-diol ketals **8** was then refluxed in the presence of 10 mol % of *p*-toluenesulfonic acid in 80% EtOH (in H_2O) to afford the final N-Boc-protected aromatic *erythro*-sphingosine analogues.

Chiral HPLC and capillary electrophoresis with anionic β -cyclodextrin as a chiral selector are applied on all intermediates and final products to measure the percent

enantiomeric excess, diastereomeric excess and racemization. No racemization is detected during the addition in each step. Thus, the enantiomers (*S, R*)-**9A**, (*S, R*)-**9E**, and (*R, S*)-**9E** (see **Table 3.2**) of N-Boc-*erthyro*-sphingosine analogues have been synthesized with over 99% optical purity.

Table 3.2. Configuration, diastereoisomeric excesses and isolated yields of all intermediates making from corresponding racemic, enantiomeric excess and enantiopure pure *trans*- γ , δ -unsaturated β -hydroxyesters.

Substance	Intermediates					SP analogues 9	Overall yield
	4	5	6	7	8		
ee (%)							
<i>R</i> -3A, >99	(S, S), >99, 58%	(S, R), >99, 85%	(S, R), >99, 94%	(S, R), >99, 99%	(S, R), >99, 85%	(S, R), >99, 96%	37%
<i>R</i> -3E, >99	(S, S), >99, 50%	(S, R), >99, 80%	(S, R), >99, 94%	(S, R), >99, 94%	(S, R), >99, 95%	(S, R), >99, 94%	32%
<i>S</i> -3A, 75							
<i>S</i> -3E, >99	(R,R), >99, 58%	(R,S), >99, 88%	(R,S), >99, 93%	(R,S), >99, 94%	(R,S), >99, 94%	(R,S), >99, 93%	41%
<i>S</i> -3E, >99	(R,R), >99, 60%	(R,S), >99, 81%	(R,S), >99, 94%	(R,S), >99, 95%	(R,S), >99, 86%	(R,S), >99, 95%	35%
3B racemic							
racemic	racemic, anti >99, 55%	racemic, anti >99, 83%	racemic, anti >99, 94%	racemic, anti >99, 98%	racemic, anti >99, 87%	racemic, anti >99, 94%	34%
3C racemic							
racemic	racemic, anti >99, 58%	racemic, anti >99, 83%	racemic, anti >99, 94%	racemic, anti >99, 99%	racemic, anti >99, 83%	racemic, anti >99, 92%	34%

a. Assignment of Configuration refers to (configuration of β position, configuration of α position) for *N*-Boc- α -hydrazino- β -hydroxyesters **2**; and (configuration of carbon-3, configuration of carbon-2) for compound **3** to **7**;
 b. The percent e.e. was measured by chiral HPLC; and the percent de was measured by both ^1H NMR and chiral HPLC;

3.3. Summary of the novel synthetic route.

Erthyro sphingosine analogues with aromatic groups in the side chain have been made using a novel and effective synthetic route. Configuration, diastereoisomeric excesses and

isolated yields of all intermediates and final analogues are summarized in **Table 3.2**. The synthetic route starts with *trans*- γ , δ -unsaturated β -hydroxyesters and includes five or six steps, which are (1) diastereospecific electrophilic amination of the *trans*- γ , δ -unsaturated β -hydroxyesters by DBAD to introduce chiral amino group in the form of anti *N*-Boc- α -hydrazino- β -hydroxyesters; (2) reduction of *N*-Boc- α -hydrazino- β -hydroxyesters to *N*-Boc-2-hydrazino-1,3-diols by excess amount of NaBH₄ in MeOH solution; (3) protection of *N*-Boc-2-hydrazino-1,3-diols catalyzed by 10 mol % of *p*-toluenesulfonic acid with anhydrous acetone to afford *N*-Boc-2-hydrazino-1,3-diols ketals; (4) *ElcB* non-reductively eliminative cleavage of the hydrazino N-N bond of *N*-Boc-2-hydrazino-1,3-diols ketals in the presence methyl bromoacetate and Cs₂CO₃ to form *N*-Boc-2-amino-1,3-diols ketals directly or via an intermediate *N*-Boc-2-alkylatedhydrazino-1,3-diols ketals; (5) deprotection of *N*-Boc-2-amino-1,3-diols ketals in the presence of 10 mol % of *p*-toluenesulfonic acid in 80% EtOH (in H₂O) to afford final *erthyro* aromatic sphingosine analogues. All final products and intermediates were successfully characterized by NMR spectroscopy and chiral HPLC. Excellent stereoselectivity with more than 99% d.e. was obtained and there was no racemization during the course of the synthesis. Either enantiomer of *erthyro* aromatic sphingosine analogues was achieved using the described method. The optical purity of the final aromatic sphingosine analogues depends on that of starting materials *trans*- γ , δ -unsaturated β -hydroxyesters.

3.4. General methods

3.4.1. Materials

All chemicals were purchased from VWR International, LLC and were of the highest purity unless otherwise noted. Lithium diisopropylamine, zinc bromide, Dess-Martin periodinane were purchased from Aldrich Chemical Co. (Milwaukee, WI). Ethyl acetate was purchased from Alfa Aesar (Ward Hill, MA). Zinc bromide was dried in an oven at 110 °C for a minimum of 24 h before using. Methylzinc bromide was prepared via the reaction of zinc bromide and methylmagnesium bromide according to the published procedure (Joly and Bucourt June 1962). THF was freshly distilled from sodium metal with benzophenone ketal indicator. Acetone was dried by simple distillation and stored over molecular sieves (4Å, 8-12 mesh). Acetonitrile was distilled from CaH₂ and stored over 4 Å molecular sieves. Aluminum coated silica gel WF_{254s} plates were used to monitor reactions products and flash chromatography eluents. Column chromatography were performed with silica gel SiliaFlash®P60 (40 - 60 µm, 230 - 400 mesh).

3.4.2. Instruments

NMR spectra were obtained on a Varian Mercury FT-NMR spectrometer, operating at 300 MHz for ¹H NMR and 75 MHz for ¹³C NMR unless other note. Assignments were made by ¹H, ¹³C and gCOSY techniques. Chemical shifts were reported in parts per million (ppm, δ) relative to tetramethylsilane (TMS, δ 0.00 ppm). ¹H NMR splitting patterns are designated as singlet (s), doublet (d), triplet (t), doublet of doublets (dd),

multiplet (m), broad (br). Coupling constants (J values) are reported in Hertz (Hz). HPLC was performed on Agilent 1100 series with isocratic pump and UV-visible detector. A Phenomenex® Lux 3 μ cellulose-1 column (50 x 4.60 mm) was used for the chiral separation at 23 °C. The mobile phase consisted of hexanes and isopropanol in the ratio of 90:10, and flow rate of 0.5 mL/min.

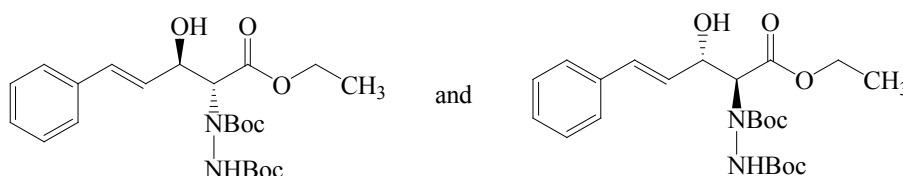
Abbreviations: THF, tetrahydrofuran; EtOAc, ethyl acetate; MeZnBr, methyl zinc bromide; LDA, Lithium diisopropylamide; DBAD, di-tert-butyl azodicarboxylate; MeOH, methanol; MeCN, acetonitrile; KREDs, ketoreductases

3.4.3. Diastereospecific formation of *anti* N-Boc- α -hydrazino- β -hydroxyesters (4)

Under N₂, to a solution of *trans*- γ , δ -unsaturated β -hydroxyesters (**3**) (1.0 mmol) in 2 mL anhydrous THF at 0 °C, was added 1.2 equivalent of zinc methyl bromide (1.2 mmol, 0.4 M in THF). The reaction mixture was stirred for 1 h. After the reaction mixture was cooled to -78 °C, 2.0 equivalents of LDA (2.0 mmol, 2M in heptane/THF/ethyl benzene) were added dropwise. After 1 h at -78 °C, 2 equivalents of DBAD (2.0 mmol) in 1 mL anhydrous THF was added slowly, the reaction mixture continued to stir for another 2 h. The reaction mixture was quenched at -78 °C with saturated NH₄Cl solution (aq.) (4 mL), warmed to room temperature, extracted with Et₂O (2 x 10 mL). The combined organic layer was dried over anhydrous Na₂SO₄ and concentrated under vacuum to afford crude product. Purification by column chromatography on silica gel using 100% CH₂Cl₂ to

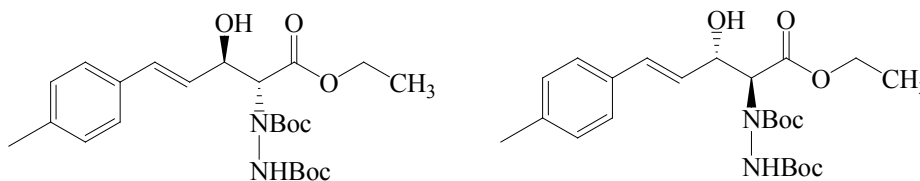
elute unreacted DBAD, then gradient elution using 10:1= CH₂Cl₂: EtOAc to afford anti N-Boc- α -hydrazino- β -hydroxyesters **4**.

3.4.3.1. Ethyl (4*E*)-2-[1,2-bis(*tert*-butoxycarbonyl)hydrazino]-2,4,5-trideoxy-5-phenyl-D-*erythro*-pent-4-enonate (**4A**)



White solid; isolated yield: 58%; Diastereomeric excess (*d.e.*) >99% (*anti*); (*S*, *S*)-**4A**: $[\alpha_{589}^{23}] +105^\circ$ (*c* = 1.71, CHCl₃); ¹H NMR (300 MHz, CDCl₃): δ 7.15 -7.28 (5H), 6.77 (s, 1H), 6.65 (dd, *J* = 3, 15.0 Hz, 1H), 6.15 (dd, *J* = 3.0 Hz, 15.0 Hz, 1H), 5.09-5.37 (br, 1H), 4.90 (m, 1H), 4.53-4.72 (br, 1H), 4.23 (m, *J* = 6 Hz, 2H), 1.45 (s, 9H), 1.28 (t, *J* = 6 Hz, 3H), 1.26 (s, 9H); ¹³C NMR (75 MHz, CDCl₃) 169.49, 169.31, 156.58, 155.01, 136.97, 129.76, 128.38, 127.88, 127.41, 126.49, 83.13, 82.36, 82.09, 69.78, 65.57, 63.36, 61.58, 27.99, 14.26

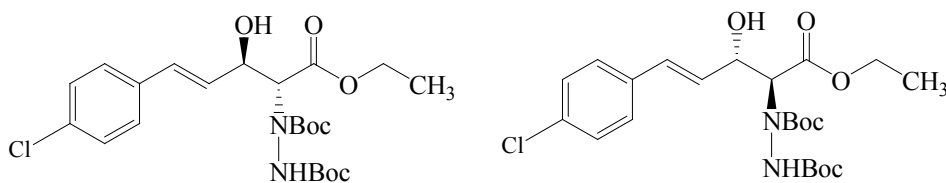
3.4.3.2. Ethyl (4*E*)-2-[1,2-bis(*tert*-butoxycarbonyl)hydrazino]-2,4,5-trideoxy-5-phenyl-D-*erythro*-pent-4-enonate (**4B**)



Racemic mixture

White solid; Isolated yield: 55%; Diastereomeric excess (*d.e.*) >99% (*anti*); ^1H NMR (300 MHz, CDCl_3): δ 7.19 (d, $J = 9.0$ Hz, 2H), 7.08 (d, $J = 9.0$ Hz, 2H), 6.75 (s, 1H), 6.63 (d, $J = 15.0$ Hz, 1H), 6.10 (dd, $J = 3.0$ Hz, 15.0 Hz, 1H), 5.11-5.38 (br, 1H), 4.90 (m, 1H), 4.53-4.73 (br, 1H), 4.23 (m, $J = 6.0$ Hz, 2H), 2.32 (s, 3H), 1.47 (s, 9H), 1.31 (s, 9H), 1.30 (t, $J = 6.0$ Hz, 3H); ^{13}C NMR (75 MHz, CDCl_3) 169.53, 169.34, 157.23, 156.55, 155.03, 137.17, 134.18, 129.85, 129.08, 126.81, 126.40, 83.13, 82.36, 82.10, 69.96, 65.57, 63.35, 61.55, 28.03, 21.18, 14.26. HRMS (ESI) calcd for $\text{C}_{24}\text{H}_{36}\text{N}_2\text{O}_7\text{Na}$ ($\text{M}+\text{Na}$) $^+$ 487.2415, found 487.2419.

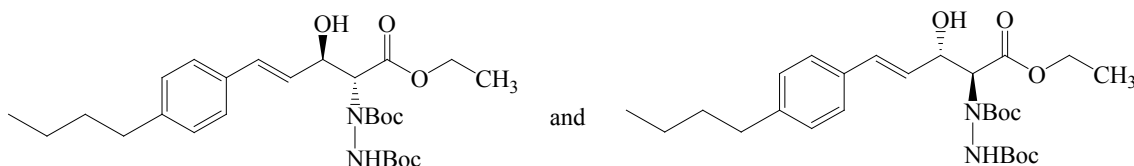
3.4.3.3. Ethyl (*4E*)-2-[1,2-bis(*tert*-butoxycarbonyl)hydrazino]-5-(4-chlorophenyl)-2,4,5-trideoxy-*D*-erythro-pent-4-enonate (**4C**).



Racemic mixture

White solid; Isolated yield: 58%; Diastereomeric excess (*d.e.*) >99% (*anti*); ^1H NMR (300 MHz, CDCl_3): δ 7.20-7.28 (m, 5H), 6.72 (s, 1H), 6.85 (d, $J = 15.0$ Hz, 1H), 6.15 (dd, $J = 3.0, 15.0$ Hz, 1H), 5.10-5.38 (br, 1H), 4.91 (m, 1H), 4.54-4.70 (br, 1H), 4.21-4.29 (m, 2H), 1.47 (s, 9H), 1.31 (t, $J = 6.0$ Hz, 3H) 1.29 (s, 9H); ^{13}C NMR (75 MHz, CDCl_3) 169.46, 169.28, 157.26, 156.59, 155.14, 154.96, 135.54, 132.98, 128.67, 128.57, 128.42, 127.68, 83.26, 82.51, 82.20, 69.62, 65.51, 63.33, 61.66, 28.02, 14.28. HRMS (ESI) calcd for $\text{C}_{23}\text{H}_{33}\text{N}_2\text{O}_7\text{ClNa}$ ($\text{M}+\text{Na}$) $^+$ 507.1869, found 507.1877.

3.4.3.4. Ethyl (4E)-2-[1,2-bis(*tert*-butoxycarbonyl)hydrazino]-5-(4-butylphenyl)-2,4,5-trideoxypent-4-enonate (4E**)**

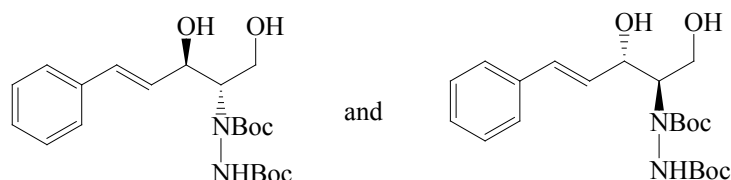


Slightly yellow solid; Isolated yield: 50% and 60%; Diastereomeric excess (*d.e.*) >99% (*anti*); (*R, R*)-**4E**: $[\alpha_{589}^{23}]_{-89^\circ}$ (*c* = 0.56, CHCl₃); (*S, S*)-**4E**: $[\alpha_{589}^{23}]_{+130^\circ}$ (*c* = 0.23, CHCl₃); ¹H NMR (300 MHz, CDCl₃): δ 7.21 (d, *J* = 9.0 Hz, 2H), 7.08 (d, *J* = 9.0 Hz, 2H), 6.85 (dd, *J* = 3.0, 15.0 Hz, 1H), 6.11 (dd, *J* = 3.0, 15.0 Hz, 1H), 5.11-5.38 (br, 1H), 4.91 (m, 1H), 4.50-4.70 (br, 1H), 4.21 (m, *J* = 6.0 Hz, 2H), 2.58 (t, *J* = 6.0 Hz, 2H), 1.57 (m, 2H), 1.47 (s, 9H), 1.36 (m, 2H), 1.33 (t, *J* = 6.0 Hz, 3H), 1.30 (s, 9H), 0.91 (t, *J* = 6.0 Hz, 3H); ¹³C NMR (75 MHz, CDCl₃) 169.55, 169.33, 157.17, 156.51, 155.19, 155.05, 142.27, 134.38, 129.85, 128.45, 126.78, 126.42, 83.14, 82.36, 82.09, 69.95, 65.60, 63.40, 61.56, 35.31, 33.38, 28.00, 22.23, 14.26, 13.94. HRMS (ESI) calcd for C₂₇H₄₂N₂O₇Na (M+Na)⁺ 529.2884, found 529.2886.

3.4.4. Synthesis of *anti* 2-di-*tert*-butoxycarbonyl hydrazino 1, 3-diol (**5**)

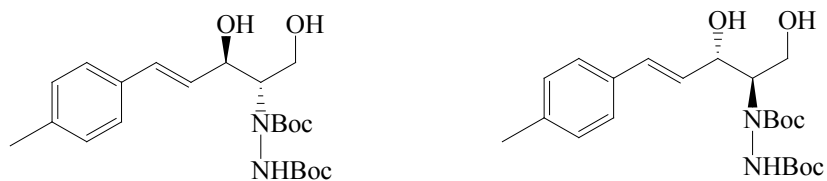
Into a solution of anti N-Boc- α -hydrazino- β -hydroxyesters (**4**) (1 mmol) in 25 mL methanol, 3 equivalents of NaBH₄ was added every 15 min till the starting material was consumed as indicated by TLC. A total 36 - 51 equiv. of NaBH₄ was added. Afterwards, the reaction was quenched with saturated NH₄Cl (aq.) (10 mL); and the reaction mixture was concentrated under vacuum, extracted with EtOAc, and the combined extracts were washed with brine, dried over anhydrous Na₂SO₄, and the organic solvent was removed by rotovaporization at 60 - 70 °C. Purification by chromatography on silica gel using 5:3 CH₂Cl₂/EtOAc as eluent afforded the product.

3.4.4.1. (*E*)-2-[1,2-bis(*tert*-butoxycarbonyl)hydrazino]-2,4,5-trideoxy-5-phenyl-D-erythro-pent-4-enitol (**5A**).



White solid; Isolated yield: 88% and 85%; Diastereomeric excess (*d.e.*) >99% (*anti*); (3*R*, 2*S*)-**5A**: [α_{589}^{23}]+10° (*c* = 0.49, CHCl₃); (3*S*, 2*R*)-**5A**: [α_{589}^{23}]-18° (*c* = 1.13, CHCl₃); ¹H NMR (300 MHz, CDCl₃): δ 7.24 (m, 5H), 6.60 (d, *J* = 15.0 Hz, 1H), 6.35 (br, 1H), 6.21 (br, *J* = 6.0, 15.0 Hz, 1H), 2.85-4.98 (br, 6H), 1.47 (s, 9H), 1.42 (s, 9H); ¹³C NMR (75 MHz, CDCl₃) 158.54, 157.83, 155.36, 136.31, 132.26, 129.12, 128.52, 127.86, 126.55, 82.61, 82.40, 81.88, 71.99, 64.68, 62.35, 59.18, 28.10. HRMS (ESI) calcd for C₂₁H₃₂N₂O₆Na (M+Na)⁺ 431.2153, found 431.2147.

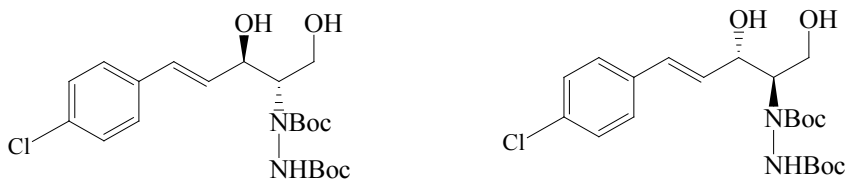
3.4.4.2. (4*E*)-2-[1,2-bis(*tert*-butoxycarbonyl)hydrazino]-2,4,5-trideoxy-5-(4-methylphenyl)-*D*-erythro-pent-4-enitol (**5B**).



Racemic mixture

White solid; Isolated yield: 83%; Diastereomeric excess (*d.e.*) >99% (*anti*); ^1H NMR (300 MHz, CDCl_3): δ 7.24 (d, $J = 6.0$ Hz, 2H), 7.10 (d, $J = 6.0$ Hz, 2H), 6.58 (d, $J = 15.0$ Hz, 1H), 6.36 (br, 1H), 6.18 (dd, $J = 6.0, 15.0$ Hz, 1H), 3.50-4.70 (br, 5H), 2.50-3.10 (br, 1H), 2.32 (s, 3H), 1.48 (s, 9H), 1.42 (s, 9H); ^{13}C NMR (75 MHz, CDCl_3) 158.51, 157.74, 155.35, 137.84, 133.38, 132.18, 129.26, 127.86, 126.48, 82.69, 82.46, 81.90, 72.30, 64.62, 62.52, 59.29, 28.10, 21.20. HRMS (ESI) calcd for $\text{C}_{22}\text{H}_{34}\text{N}_2\text{O}_6\text{Na}$ ($\text{M}+\text{Na}$) $^+$ 445.2309, found 445.2305.

3.4.4.3. (4*E*)-2-[1,2-bis(*tert*-butoxycarbonyl)hydrazino]-5-(4-chlorophenyl)-2,4,5-trideoxy-*D*-erythro-pent-4-enitol (**5C**).

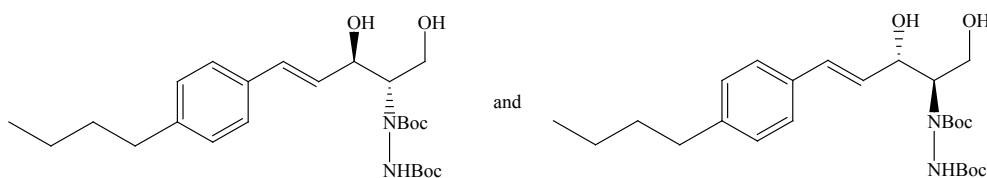


Racemic mixture

White solid; Isolated yield: 83%; Diastereomeric excess (*d.e.*) >99% (*anti*); ^1H NMR (300 MHz, CDCl_3): δ 7.25 (s, 4H), 6.55 (d, $J = 15.0$ Hz, 1H), 6.35 (br, 1H), 6.20 (dd, $J =$

6.0, 15.0 Hz, 1H), 2.85-4.90 (br, 6H), 1.47 (s, 9H), 1.41 (s, 9H); ^{13}C NMR (75 MHz, CDCl_3) 158.41, 157.83, 155.40, 135.08, 133.33, 130.59, 129.94, 128.88, 127.74, 82.54, 82.01, 71.81, 64.53, 62.50, 59.31, 28.09. HRMS (ESI) calcd for $\text{C}_{21}\text{H}_{31}\text{N}_2\text{O}_6\text{ClNa}$ ($\text{M}+\text{Na}$) $^+$ 465.1763, found 465.1764.

3.4.4.5. (1*E*)-4-[1,2-bis(*tert*-butoxycarbonyl)hydrazino]-1-(4-butylphenyl)-1,2,4-trideoxypent-1-enitol (**5E**).

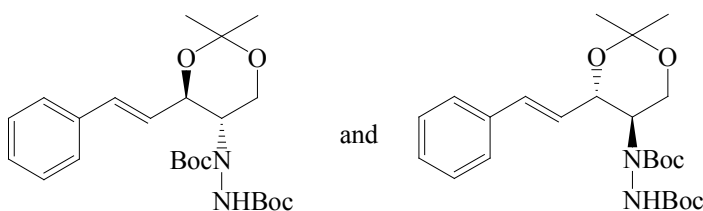


White solid; Isolated yield: 81% and 80%; Diastereomeric excess (*d.e.*) >99% (*anti*); (3*R*, 2*S*)-**5E**: $[\alpha]_{589}^{23} +83^\circ$ ($c = 0.24$, CHCl_3); (3*S*, 2*R*)-**5E**: $[\alpha]_{589}^{23} -35^\circ$ ($c = 0.29$, CHCl_3); ^1H NMR (300 MHz, CDCl_3): δ 7.26 (d, $J = 9$ Hz, 2H), 7.12 (d, $J = 9$ Hz, 2H), 6.58 (d, $J = 15.0$ Hz, 1H), 6.34 (br, 1H), 6.17 (dd, $J = 6.0, 15.0$ Hz, 1H), 3.35-5.00 (br, 5H), 2.59 (t, $J = 6.0$ Hz, 2H), 2.0 (s, 1H), 1.58 (m, 2H), 1.48 (s, 9H), 1.45 (s, 9H), 1.34 (m, 2H), 0.92 (t, $J = 6.0$ Hz, 3H); ^{13}C NMR (75 MHz, CDCl_3) 158.46, 157.74, 155.36, 142.99, 133.60, 132.31, 128.65, 127.90, 126.50, 82.71, 82.49, 81.93, 72.39, 64.55, 62.55, 59.28, 35.36, 33.55, 28.11, 22.31, 13.94. HRMS (ESI) calcd for $\text{C}_{25}\text{H}_{40}\text{N}_2\text{O}_6\text{Na}$ ($\text{M}+\text{Na}$) $^+$ 487.2779, found 487.2792.

3.4.5. Synthesis of anti 2-di-*tert*-butoxycarbonyl hydrazino 1, 3-diol ketal (**6**)

Under N₂, the mixture of *anti* 2-di-*tert*-butoxycarbonyl hydrazino 1,3-diol (**5**) (0.15 mmol) and 10% molar equivalent of *p*-toluene sulfonic acid monohydrate (0.015 mmol) in 5.0 mL of anhydrous acetone was stirred at room temperature till the reaction was completed as monitored by TLC plate (eluent: CH₂Cl₂: EtOAc = 5:3) (24h). The reaction mixture was quenched with 5% NaHCO₃ and extracted by CH₂Cl₂. The combined organic layers were dried over anhydrous Na₂SO₄, and removed under vacuum. The product was purified by flash chromatography on silica gel using 10:1 CH₂Cl₂/EtOAc as eluent.

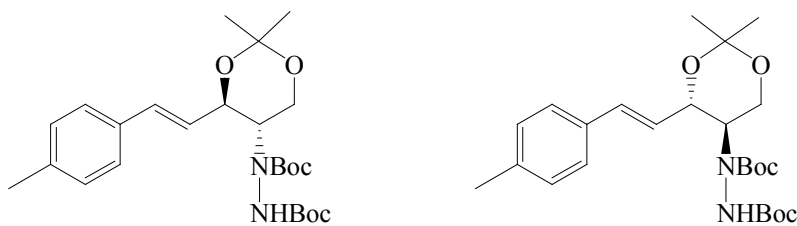
3.4.5.1. (1*E*)-4-[1,2-bis(*tert*-butoxycarbonyl)hydrazino]-1,2,4-trideoxy-3,5-O-(1-methylethylidene)-1-phenylpent-1-enitol (**6A**).



Slightly yellow solid; isolated yield: 93% and 94%; (3*R*, 2*S*)-**6A**: [α_{589}^{23}]_D+44° (c = 0.45, CHCl₃); (3*S*, 2*R*)-**6A**: [α_{589}^{23}]_D-40° (c = 0.75, CHCl₃); ¹H NMR (300 MHz, CDCl₃): δ 7.37 (d, *J* = 6 Hz, 2H), 7.20 – 7.32 (m, 3H), 6.66 (d, *J* = 15.0 Hz, 1H), 6.00-6.35 (br, 2H), 4.56 (m, 1H), 3.70-4.28 (br, 1H), 4.02 (br, 2H), 1.55 (s, 3H), 1.48 (s, 9H), 1.45 (s, 3H), 1.37 (s, 9H); ¹³C NMR (75 MHz, CDCl₃) 156.59, 155.79, 154.64, 154.28, 136.38, 136.22, 133.32, 128.45, 127.93, 127.27, 126.74, 126.61, 98.61, 82.25, 81.84, 81.65, 72.02, 71.40, 60.90,

60.47, 56.25, 53.36, 29.00, 28.12, 28.02, 19.60, 19.44. HRMS (ESI) calcd for $C_{24}H_{36}N_2O_6Na$ ($M+Na$)⁺ 471.2466, found 471.2470.

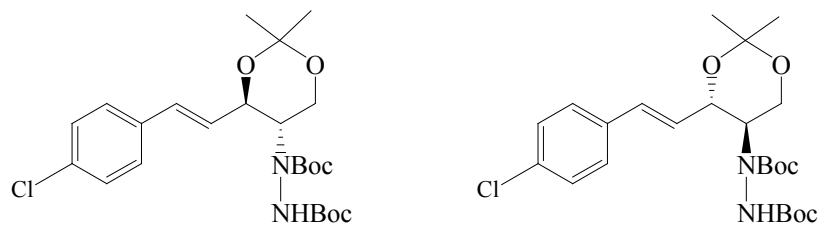
3.4.5.2. (*E*)-4-[1,2-bis(*tert*-butoxycarbonyl)hydrazino]-1,2,4-trideoxy-3,5-O-(1-methylethylidene)-1-(4-methylphenyl)pent-1-enitol (**6B**).



Racemic mixture

White solid; isolated yield: 94%. ¹H NMR (300 MHz, CDCl₃): δ 7.25 (d, 2H), 7.08 (d, *J* = 6 Hz, 3H), 6.62 (d, *J* = 15.0 Hz, 1H), 5.86-6.30 (br, 2H), 4.53 (br, 1H), 3.75-4.26 (br, 1H), 4.00 (br, 2H), 2.31 (s, 3H), 1.54 (s, 3H), 1.47 (s, 9H), 1.43 (s, 3H), 1.37 (s, 9H); ¹³C NMR (75 MHz, CDCl₃) 156.60, 155.77, 154.63, 154.28, 137.81, 133.57, 133.35, 129.16, 126.67, 126.53, 126.14, 125.53, 98.58, 82.22, 81.84, 81.62, 72.19, 71.57, 60.92, 60.50, 56.34, 53.44, 29.03, 28.12, 28.02, 21.22, 19.58, 19.43. HRMS (ESI) calcd for $C_{25}H_{38}N_2O_6Na$ ($M+Na$)⁺ 485.2622, found 485.2632.

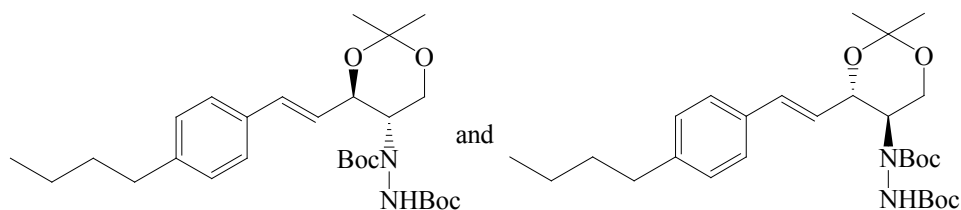
3.4.5.3. (*E*)-2-[1,2-bis(*tert*-butoxycarbonyl)hydrazino]-5-(4-chlorophenyl)-2,4,5-trideoxy-1,3-*O*-(1-methylethylidene)-*D*-erythro-pent-4-enitol (**6C**).



Racemic mixture

White solid; isolated yield: 94%; $^1\text{H NMR}$ (300 MHz, CDCl_3): δ 7.30 (d, $J = 9.0$ Hz, 2H), 7.26 (d, $J = 9.0$ Hz, 2H), 6.63 (d, $J = 15.0$ Hz, 1H), 6.00-6.55 (br, 2H), 4.56 (br, 1H), 4.00-4.39 (br, 1H), 4.01 (br, 2H), 1.54 (s, 3H), 1.48 (s, 9H), 1.44 (s, 3H), 1.36 (s, 9H); $^{13}\text{CNMR}$ (75 MHz, CDCl_3) 156.65, 155.80, 154.63, 154.28, 134.90, 133.45, 132.33, 131.71, 128.64, 128.60, 127.93, 127.76, 98.61, 82.19, 81.81, 81.65, 71.84, 71.12, 80.78, 60.39, 56.35, 53.31, 28.93, 28.11, 28.01, 19.43. HRMS (ESI) calcd for $\text{C}_{24}\text{H}_{35}\text{N}_2\text{O}_6\text{ClNa}$ ($\text{M}+\text{Na}$) $^+$ 505.2076, found 505.2068.

3.4.5.4. (*E*)-4-[1,2-bis(*tert*-butoxycarbonyl)hydrazino]-1-(4-butylphenyl)-1,2,4-trideoxy-3,5-*O*-(1-methylethylidene)pent-1-enitol (**6E**).



Slightly yellow oil; isolated yield: 94%; (*3R*, *2S*)-**6E**: $[\alpha]_{589}^{23} +67^\circ$ ($c = 0.30$, CHCl_3); (*3S*, *2R*)-**6E**: $[\alpha]_{589}^{23} -56^\circ$ ($c = 0.61$, CHCl_3); $^1\text{H NMR}$ (300 MHz, CDCl_3): δ 7.28 (d, $J = 6$ Hz,

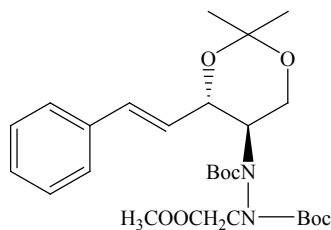
2H), 7.10 (d, $J = 6.0$ Hz, 2H), 6.63 (d, $J = 15.0$ Hz, 3H), 5.85-6.11 (br, 2H), 4.55 (m, 1H), 3.75-4.26 (br, 1H), 4.01 (br, 2H), 2.58 (t, $J = 6.0$ Hz, 2H), 1.58 (m, 2H), 1.55 (s, 3H), 1.48 (s, 9H), 1.46 (s, 3H), 1.39 (s, 9H), 1.32 (m, 2H), 0.92 (t, $J = 6.0$ Hz, 3H); ^{13}C NMR (75 MHz, CDCl_3) 156.58, 155.82, 154.64, 154.27, 142.92, 134.14, 133.57, 128.22, 126.66, 126.54, 126.17, 125.62, 98.60, 82.27, 81.86, 81.65, 71.62, 60.95, 60.54, 56.28, 53.55, 35.55, 33.49, 29.03, 28.11, 28.01, 22.29, 19.44, 13.94. HRMS (ESI) calcd for $\text{C}_{28}\text{H}_{44}\text{N}_2\text{O}_6\text{Na}$ ($\text{M}+\text{Na}$) $^+$ 527.3092, found 527.3088.

Synthesis of *anti* 2-BocAmino 1, 3-diol ketal (**8**) via *anti* 2-alkylhydrazino 1, 3-diol ketal (**7**)

3.4.6. Synthesis *anti* 2-alkylhydrazino 1, 3-diol ketal (**7**)

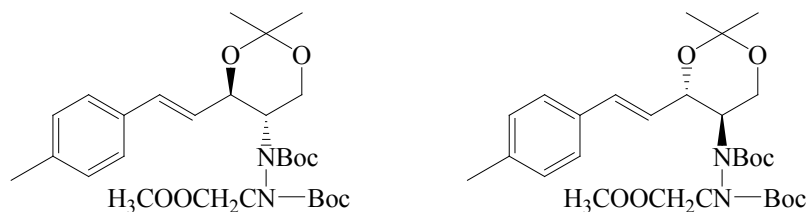
Into a suspension solution of *Anti* 2-di-*tert*-butoxycarbonyl hydrazino 1, 3-diol ketal (**6**) (0.242 mmol) and Cs_2CO_3 (0.61 mmol) in 2.5 mL CH_3CN under N_2 , was added methyl bromoacetate (0.484 mmol) in 0.5 mL CH_3CN . The reaction mixture was heated at 50 °C for 3-8 h as indicated by TLC plate (eluent: 10:1 $\text{CH}_2\text{Cl}_2/\text{EtOAc}$). The reaction was quenched with saturated NH_4Cl (aq.), extracted with EtOAc. The combined extracts were washed with brine, and dried over anhydrous Na_2SO_4 , and the solvent was removed under vacuum. The *Anti* 2-alkylhydrazino 1, 3-diol ketal (**7**) was purified by flash chromatography on silica gel using 10:1 $\text{CH}_2\text{Cl}_2/\text{EtOAc}$ eluent as white solid.

3.4.6.1. (1*E*)-4-[1,2-bis(*tert*-butoxycarbonyl)-2-(2-methoxy-2-oxoethyl)hydrazino]-1,2,4-trideoxy-3,5-*O*-(1-methylethylidene)-1-phenyl-*D*-*erythro*-pent—enitol (**7A**).



White solid; isolated yield: >99%; (3*S*, 2*R*)-**7A**: [α_{589}^{23}]-63° (c = 1.76, CHCl₃); ¹H NMR (300 MHz, CDCl₃): δ 7.23-7.26 (m, 5H), 6.50-6.62 (m, 1H), 6.05-6.26 (m, 1H), 3.31-5.36 (m, 9H), 1.34-1.68 (m, 24H); ¹³C NMR (75 MHz, CDCl₃) 170.18, 169.78, 169.71, 169.36, 169.29, 156.51, 155.87, 155.21, 154.58, 154.12, 153.86, 153.71, 153.54, 153.25, 153.07, 136.30, 136.28, 136.13, 136.03, 136.00, 135.97, 135.92, 134.97, 134.78, 134.64, 134.58, 133.68, 133.37, 133.32, 128.56, 128.52, 128.45, 128.24, 128.11, 128.05, 127.91, 127.88, 127.60, 127.45, 127.27, 126.91, 126.78, 126.75, 126.54, 126.43, 126.40, 126.37, 98.78, 98.73, 98.71, 98.62, 98.54, 82.74, 82.66, 82.56, 82.45, 82.41, 82.30, 82.20, 81.79, 81.70, 81.53, 81.46, 72.48, 72.23, 71.86, 71.35, 70.57, 70.48, 68.07, 62.80, 60.53, 60.32, 60.16, 59.59, 59.29, 56.77, 56.35, 56.18, 56.00, 55.55, 55.35, 54.83, 54.62, 54.07, 53.42, 53.35, 52.40, 52.32, 52.22, 52.19, 51.96, 51.86, 29.33, 29.30, 29.04, 29.00, 28.58, 28.54, 28.52, 28.19, 28.17, 28.14, 28.05, 28.00, 27.96, 27.90, 20.29, 20.21, 19.92, 19.89, 19.36, 19.28. HRMS (ESI) calcd for C₂₇H₄₀N₂O₈Na (M+Na)⁺ 543.2677, found 543.2689.

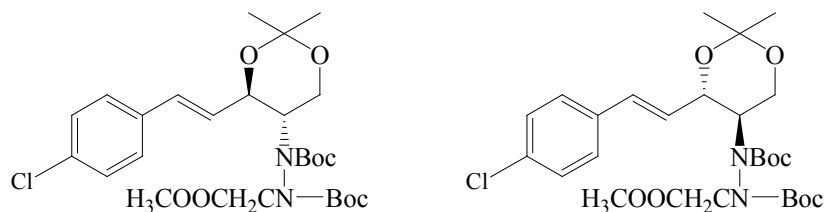
3.4.6.2. (1*E*)-4-[1,2-bis(*tert*-butoxycarbonyl)-2-(2-methoxy-2oxoethyl)hydrazino]-1,2,4-trideoxy-3,5-*O*-(1-methylethylidene)-1-(4-methylphenyl)pent-1-enitol (**7B**).



Racemic mixture

White solid; isolated yield: 98%; ^1H NMR (600 MHz, CDCl_3): δ 7.23-7.26 (m, $J = 3.0$, 6.0 Hz, 1H), 7.18-7.21 (m, $J = 6.0$ Hz, 1H), 7.10 (dd, $J = 3.0$, 6.0 Hz, 2H), 6.49-6.58 (m, 1H), 6.01-6.19 (m, 1H), 3.33-5.31 (m, 9H), 2.33 (s, 3H), 1.35-1.68 (m, 24H); ^{13}C NMR (150 MHz, CDCl_3) 170.22, 169.74, 169.42, 156.53, 155.90, 154.59, 154.13, 153.87, 153.55, 153.07, 138.20, 138.05, 138.04, 135.19, 134.84, 133.82, 133.54, 133.31, 133.15, 129.27, 129.24, 129.21, 129.16, 126.77, 126.73, 126.69, 126.50, 126.38, 126.33, 126.31, 126.28, 126.01, 125.69, 98.78, 98.70, 98.63, 98.53, 82.74, 82.55, 82.43, 82.39, 82.19, 81.79, 81.89, 81.50, 81.42, 72.51, 72.37, 71.92, 70.75, 7.65, 62.84, 60.56, 06.37, 59.30, 56.15, 55.53, 55.52, 54.80, 54.59, 54.06, 53.36, 52.43, 52.33, 52.02, 29.34, 29.30, 29.07, 29.02, 28.65, 28.54, 28.17, 28.12, 28.07, 28.00, 27.96, 27.90, 21.25, 19.91, 19.88, 19.34, 19.25. HRMS (ESI) calcd for $\text{C}_{28}\text{H}_{42}\text{N}_2\text{O}_8\text{Na}$ ($\text{M}+\text{Na}$) $^+$ 557.2833, found 557.2852.

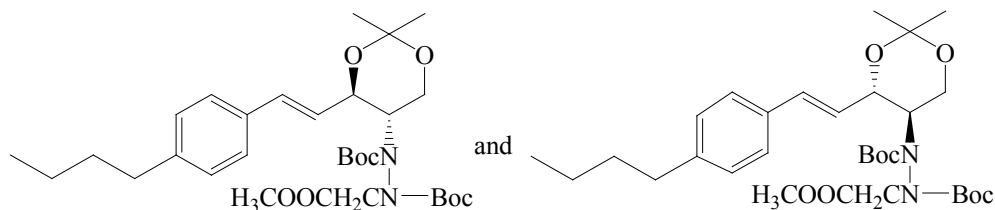
3.4.6.3. (1*E*)-4-[1,2-bis(*tert*-butoxycarbonyl)-2-(2-methoxy-2oxoethyl)hydrazino]-1-(4-chlorophenyl)-1,2,4-trideoxy-3,5-*O*-(1-methylethylidene)pent-1-enitol (**7C**).



Racemic mixture

White solid; isolated yield: >99%; ^1H NMR (300 MHz, CDCl_3): δ 7.26 (m, 4H), 6.46-6.59 (m, 1H), 6.05-6.25 (m, 1H), 3.28-5.32 (m, 9H), 1.35-1.67 (m, 24); ^{13}C NMR (75 MHz, CDCl_3) 170.13, 169.72, 169.67, 169.33, 169.25, 156.45, 155.80, 155.42, 155.17, 155.11, 154.54, 154.43, 154.18, 154.10, 154.02, 153.82, 153.72, 153.53, 153.23, 153.05, 134.94, 134.84, 134.68, 134.53, 133.88, 133.78, 133.68, 133.48, 133.30, 133.05, 133.00, 132.92, 132.23, 131.62, 131.66, 128.86, 128.81, 128.78, 128.70, 128.67, 128.60, 128.34, 128.23, 128.03, 127.96, 127.92, 127.69, 127.64, 127.60, 127.55, 98.80, 98.77, 98.72, 98.64, 98.60, 98.56, 82.83, 82.77, 82.71, 82.60, 82.52, 82.48, 82.43, 82.29, 81.84, 81.73, 81.61, 81.55, 72.44, 72.02, 71.78, 71.62, 71.05, 70.91, 70.32, 62.66, 62.31, 60.87, 60.50, 60.44, 60.20, 60.04, 59.61, 59.27, 56.82, 56.35, 56.16, 56.03, 55.55, 55.37, 54.87, 54.73, 54.00, 53.45, 53.34, 52.42, 52.33, 52.25, 52.21, 52.00, 51.97, 51.88, 29.27, 28.99, 28.96, 28.61, 28.52, 28.45, 28.17, 28.15, 28.11, 29.04, 27.97, 27.95, 27.89, 20.27, 20.11, 19.88, 19.83, 19.34, 19.27. HRMS (ESI) calcd for $\text{C}_{27}\text{H}_{39}\text{N}_2\text{O}_8\text{ClNa}$ ($\text{M}+\text{Na}$) $^+$ 577.2287, found 577.2299.

3.4.6.4. (1*E*)-4-[1,2-bis(*tert*-butoxycarbonyl)-2-(2-methoxy-2-oxoethyl)hydrazino]-1-(4-butylphenyl)-1,2,4-trideoxy-3,5-*O*-(1-methylethylidene)pent-1-enitol (**7E**).

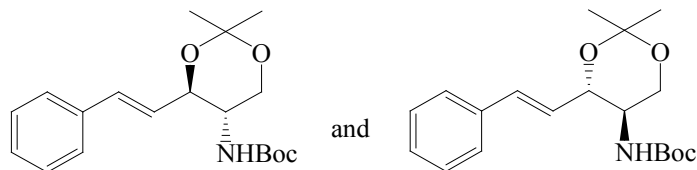


White solid, isolated yield: 95% and 94%; (3*R*, 2*S*)-**7E**: $[\alpha_{589}^{23}] + 83^\circ$ ($c = 0.24$, CHCl_3); (3*S*, 2*R*)-**7E**: $[\alpha_{589}^{23}] - 65^\circ$ ($c = 0.77$, CHCl_3); $^1\text{H NMR}$ (300 MHz, CDCl_3): δ 7.22 (m, 2H), 7.11 (m, 2H), 6.47-6.59 (m, 1H), 5.99-6.20 (m, 1H), 3.32-5.30 (m, 9H), 2.58 (t, $J = 6.0$ Hz, 2H), 1.26-1.68 (m, 28H), 0.92 (dt, $J = 3.0, 6.0$ Hz, 3H); $^{13}\text{C NMR}$ (75 MHz, CDCl_3) 170.19, 169.83, 169.80, 169.71, 169.37, 169.33, 156.52, 155.89, 155.24, 154.58, 154.13, 153.86, 153.54, 153.06, 143.23, 143.07, 143.04, 142.85, 135.15, 134.98, 134.86, 134.80, 133.75, 133.68, 133.54, 133.48, 133.41, 133.38, 128.61, 128.57, 128.55, 128.49, 126.93, 126.81, 126.72, 126.68, 126.49, 126.35, 126.31, 125.82, 98.76, 98.70, 98.68, 98.60, 98.51, 82.72, 82.54, 82.51, 82.42, 82.38, 82.17, 81.77, 81.69, 81.49, 81.41, 72.48, 72.34, 71.88, 71.55, 70.70, 70.58, 63.03, 62.87, 60.58, 60.38, 60.21, 59.57, 59.27, 56.76, 56.34, 56.18, 55.53, 55.32, 54.82, 54.60, 54.09, 53.37, 52.39, 52.31, 52.21, 52.15, 51.97, 51.87, 35.37, 33.50, 33.49, 33.46, 29.34, 29.30, 20.05, 29.01, 28.54, 28.19, 28.17, 28.13, 28.06, 28.00, 27.96, 29.90, 22.37, 22.34, 22.30, 22.29, 19.92, 19.89, 19.35, 19.26, 13.94. HRMS (ESI) calcd for $\text{C}_{31}\text{H}_{48}\text{N}_2\text{O}_8\text{Na}$ ($\text{M}+\text{Na}$) $^+$ 599.3303, found 599.3309.

3.4.7. Synthesis of *anti* 2-BocAmino 1, 3-diol ketal (**8**)

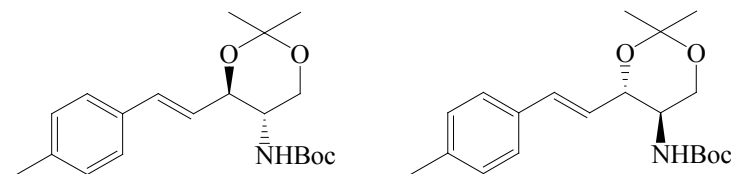
Into a suspension solution of (**7**) (0.22 mmol) in 5.0 mL CH₃CN under N₂, was added and 3 equivalents of Cs₂CO₃ (0.66 mmol), and the reaction mixture was refluxed for over 20 h till the starting material was consumed as indicated by TLC plate (Eluent: 10:1 CH₂Cl₂/EtOAc). The reaction was quenched with saturated NH₄Cl (aq.), extracted with EtOAc. The combined extracts were washed with brine, and dried over anhydrous Na₂SO₄, and the solvent was removed under vacuum. The product (**8**) was purified by flash chromatography on silica gel using 10:1 CH₂Cl₂/EtOAc eluent as white solid.

3.4.7.1. (1*E*)-4-[(*tert*-butoxycarbonyl)amino]-1,2,4-trideoxy-3,5-*O*-(1-methylethylidene)-1-phenylpent-1-enitol (**8A**).



White solid; isolated yield: 85%; (3*R*, 2*S*)-**8A**: [α_{589}^{23}]_D+21° (c = 0.24, CHCl₃); (3*S*, 2*R*)-**8A**: [α_{589}^{23}]_D-25° (c = 0.79, CHCl₃); ¹H NMR (300 MHz, CDCl₃): δ 7.38 (m, 2H), 7.20-7.32 (m, 3H), 6.65 (d, *J* = 15.0 Hz, 1H), 6.18 (dd, *J* = 6.0, 15.0 Hz, 1H), 4.43 (d, *J* = 9.0 Hz, 1H), 4.27 (br, 1H), 4.00 (dd, *J* = 6.0 Hz, 1H), 3.72 (m, 1H), 3.61 (m, 1H), 1.53 (s, 3H), 1.46 (s, 3H), 1.35 (s, 9H); ¹³C NMR (75 MHz, CDCl₃) 155.11, 136.34, 133.58, 128.44, 127.89, 126.71, 126.59, 98.81, 79.81, 74.65, 62.96, 49.11, 28.73, 28.21, 19.60. HRMS (ESI) calcd for C₁₉H₂₇NO₄Na (M+Na)⁺ 356.1832, found 356.1841.

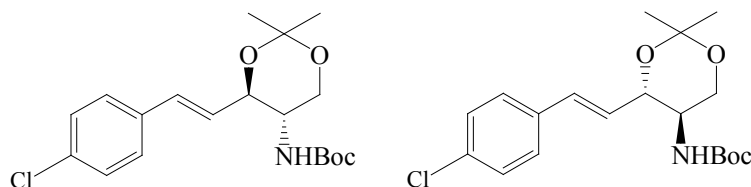
3.4.7.2. (1*E*)-4-[(*tert*-butoxycarbonyl)amino]-1,2,4-trideoxy-3,5-*O*-(1-methylethylidene)-1-(4-methylphenyl)pent-1-enitol (**8B**).



Racemic mixture

White solid; isolated yield: 87%; ^1H NMR (300 MHz, CDCl_3): δ 7.28 (d, $J = 6.0$ Hz, 2H), 7.10 (d, $J = 6.0$ Hz, 2H), 6.62 (d, $J = 15.0$ Hz, 1H), 6.11 (dd, $J = 6.0, 15.0$ Hz, 1H), 4.41 (d, $J = 9.0$ Hz, 1H), 4.25 (br, 1H), 4.00 (dd, $J = 6.0$ Hz, 1H), 3.71 (m, 1H), 3.63 (m, 1H), 2.32 (s, 3H), 1.53 (s, 3H), 1.46 (s, 3H), 1.35 (s, 9H); ^{13}C NMR (75 MHz, CDCl_3) 155.12, 137.76, 133.70, 133.53, 129.18, 126.63, 125.47, 98.79, 97.76, 74.71, 63.01, 49.11, 28.76, 28.23, 21.23, 19.60. HRMS (ESI) calcd for $\text{C}_{20}\text{H}_{29}\text{NO}_4\text{Na}$ ($\text{M}+\text{Na}$) $^+$ 370.1989, found 370.1993.

3.4.7.3. (1*E*)-4-[(*tert*-butoxycarbonyl)amino]-1-(4-chlorophenyl)-1,2,4-trideoxy-3,5-*O*-(1-methylethylidene)pent-1-enitol (**8C**).

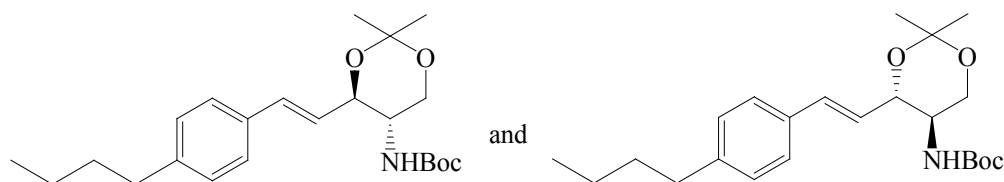


Racemic mixture

White solid; isolated yield: 83%; ^1H NMR (300 MHz, CDCl_3): δ 7.28 (ddd, $J = 3.0, 6.0$ Hz, 4H), 6.66 (d, $J = 15.0$ Hz, 1H), 6.16 (dd, $J = 6.0, 15.0$ Hz, 1H), 4.51 (br, 1H), 4.24 (br,

1H), 3.97 (dd, $J = 6.0$ Hz, 1H), 3.66 (m, 2H), 1.52 (s, 3H), 1.46 (s, 3H), 1.35 (s, 9H); ^{13}C NMR (75 MHz, CDCl_3) 155.13, 134.93, 133.48, 131.99, 128.63, 127.87, 127.38, 98.82, 79.79, 74.58, 62.88, 48.92, 28.73, 28.22, 19.53. HRMS (ESI) calcd for $\text{C}_{19}\text{H}_{26}\text{NO}_4\text{ClNa}$ ($\text{M}+\text{Na}$) $^+$ 390.1443, found 390.1448.

3.4.7.4. (1*E*)-4-[(*tert*-butoxycarbonyl)amino]-1-(4-butylphenyl)-1,2,4-trideoxy-3,5-*O*-(1-methylethylidene)pent-1-enitol (**8E**).



White solid, isolated yield: 86% and 95%; (3*R*, 2*S*)-**8E**: $[\alpha]_{589}^{23} +59^\circ$ ($c = 0.17$, CHCl_3); (3*S*, 2*R*)-**8E**: $[\alpha]_{589}^{23} -61^\circ$ ($c = 0.49$, CHCl_3); ^1H NMR (300 MHz, CDCl_3): δ 7.30 (d, $J = 6.0$ Hz, 2H), 7.11 (d, $J = 6.0$ Hz, 2H), 6.63 (d, $J = 15.0$ Hz, 1H), 6.12 (dd, $J = 6.0, 15.0$ Hz, 1H), 4.37 (br, 1H), 4.25 (br, 1H), 4.02 (dd, $J = 6.0$ Hz, 1H), 3.71 (m, 1H), 3.59 (m, 1H), 2.58 (t, $J = 6.0$ Hz, 2H), 1.58 (m, 2H), 1.53 (s, 3H), 1.46 (s, 3H), 1.35 (s, 9H), 1.32 (m, 2H), 0.92 (t, $J = 6.0$ Hz, 3H); ^{13}C NMR (75 MHz, CDCl_3) 155.09, 142.86, 133.74, 128.52, 126.64, 125.52, 98.81, 79.87, 74.68, 63.04, 49.23, 35.37, 33.50, 28.74, 28.23, 22.31, 19.64, 13.94. HRMS (ESI) calcd for $\text{C}_{23}\text{H}_{35}\text{NO}_4\text{Na}$ ($\text{M}+\text{Na}$) $^+$ 412.2458, found 412.2468.

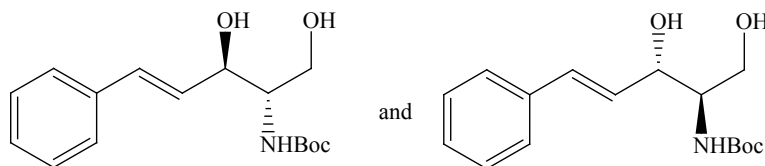
3.4.8. Direct synthesis of *anti* 2-BocAmino 1,3-diol ketal (**8**)

Under argon, 2 equivalents of methyl bromoacetate (0.085 mmol) was added into a suspension of *anti* 2-di-*tert*-butoxycarbonyl hydrazino 1, 3-diol ketal (**6**) (0.043 mmol) and 4 equivalents of Cs₂CO₃ (0.170 mmol) in 3 mL of anhydrous CH₃CN. The reaction mixture was stirred at reflux until the starting material was consumed as indicated by TLC plate (eluent: 10:1 CH₂Cl₂/EtOAc) (usually 15-24 h). After completion, the reaction was quenched with saturated NH₄Cl (aq.) and extracted with EtOAc. The combined extracts were washed with brine, and dried over anhydrous Na₂SO₄, and the solvent was removed under vacuum. The product **8** was purified by flash chromatography on silica gel using 10:1 CH₂Cl₂/EtOAc eluent as white solid.

3.4.9. *trans*-4,5-Unsaturated *anti* 2-BocAmino 1,3-diol (**9**)

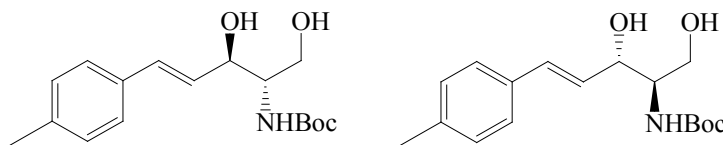
A mixture of *anti* 2-BocAmino 1, 3-diol ketal (**8**) (0.1 mmol) and 10 mol% of TsOH (0.05 mmol) in 10.0 mL 80% EtOH in H₂O was stirred at reflux till the starting material was consumed as indicated by TLC plate (Eluent: CH₂Cl₂: EtOAc = 5:3). After the reaction was completed (usually 1h), the reaction was quenched by 4 mL of 5% NaHCO₃. The mixture was concentrated under vacuum at 60-70 °C, extracted with EtOAc, dried over anhydrous Na₂SO₄. The product was isolated by column chromatography on silica gel using 5:3 CH₂Cl₂/EtOAc as eluent.

3.4.9.1. (1*E*)-4-[(*tert*-butoxycarbonyl)amino]-1,2,4-trideoxy-1-phenylpent-1-enitol (**9A**).



White solid; isolated yield: 96%; (3*R*, 2*S*)-**9A**: $[\alpha_{589}^{23}] -9^\circ$ ($c = 0.57$, CHCl_3), lit. - 19.4° ; (Moreno, Murruzzu et al. 2011) (3*S*, 2*R*)-**9A**: $[\alpha_{589}^{23}] +13^\circ$ ($c = 2.40$, CHCl_3); ^1H NMR (300 MHz, CDCl_3): δ 7.21-7.39 (m, 5H), 6.68 (d, $J = 15.0$ Hz, 1H), 6.26 (dd, $J = 6.0, 15.0$ Hz, 1H), 5.42 (d, $J = 6.0$ Hz, 1H), 4.53 (t, $J = 6.0$ Hz, 1H), 3.97 (dd, $J = 3.0, 12.0$ Hz, 1H), 3.76 (dd, $J = 3.0, 12.0$ Hz, 1H), 3.72 (br, 1H), 3.05 (br, 2H), 1.42 (s, 9H); ^{13}C NMR (75 MHz, CDCl_3) 156.26, 136.33, 131.78, 128.59, 128.54, 127.86, 126.55, 79.99, 74.60, 62.54, 55.44, 28.34. HRMS (ESI) calcd for $\text{C}_{16}\text{H}_{23}\text{NO}_4\text{Na}$ ($\text{M}+\text{Na}$) $^+$ 316.1519, found 316.1524.

3.4.9.2. (1*E*)-4-[(*tert*-butoxycarbonyl)amino]-1,2,4-trideoxy-1-(4-methylphenyl)pent-1-enitol (**9B**).

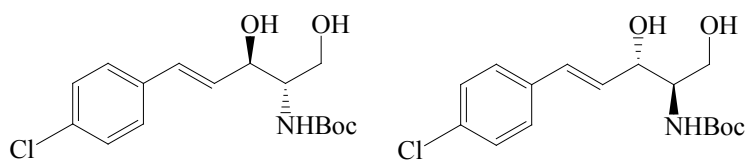


Racemic mixture

White solid; isolated yield: 94%; ^1H NMR (300 MHz, CDCl_3): δ 7.26 (d, $J = 6.0$ Hz, 2H), 7.11 (d, $J = 6.0$ Hz, 2H), 6.63 (d, $J = 15.0$ Hz, 1H), 6.20 (dd, $J = 6.0, 15.0$ Hz, 1H), 5.41 (d, $J = 6.0$ Hz, 1H), 4.51 (dd, $J = 3.0, 6.0$ Hz, 1H), 3.97 (dt, $J = 3.0, 12.0$ Hz, 1H), 3.75 (dt, $J = 3.0, 12.0$ Hz, 1H), 3.72 (m, 1H), 3.31 (d, $J = 3.0$ Hz, 1H), 3.00 (s, 1H), 2.33 (s,

3H), 1.43 (s, 9H); ^{13}C NMR (75 MHz, CDCl_3) 156.27, 137.75, 133.54, 131.76, 129.30, 127.44, 126.48, 79.95, 74.71, 62.57, 55.49, 28.36, 21.21. HRMS (ESI) calcd for $\text{C}_{17}\text{H}_{25}\text{NO}_4\text{Na}$ ($\text{M}+\text{Na}$) $^+$ 330.1676, found 330.1671.

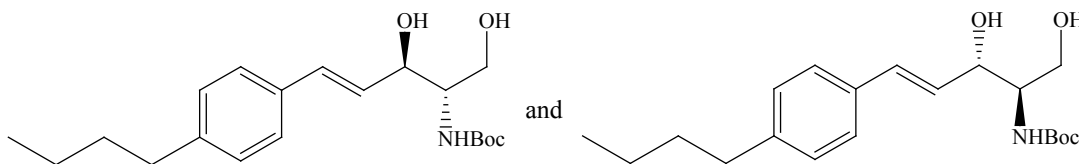
3.4.9.3. (1*E*)-4-[(*tert*-butoxycarbonyl)amino]-1-(4-chlorophenyl)-1,2,4-trideoxypent-1-enitol (**9C**).



Racemic mixture

White solid, isolated yield: 92%; ^1H NMR (300 MHz, CDCl_3): δ 7.27 (m, 4H), 6.65 (d, $J = 15.0$ Hz, 1H), 6.25 (dd, $J = 6.0, 15.0$ Hz, 1H), 5.38 (d, $J = 9.0$ Hz, 1H), 4.53 (dd, $J = 3.0, 6.0$ Hz, 1H), 3.98 (dt, $J = 3.0, 12.0$ Hz, 1H), 3.78 (dt, $J = 3.0, 12.0$ Hz, 1H), 3.72 (m, 1H), 3.24 (d, $J = 3.0$ Hz, 1H), 2.77 (s, 1H), 1.43 (s, 9H); ^{13}C NMR (75 MHz, CDCl_3) 156.21, 134.84, 133.53, 130.53, 129.27, 128.78, 127.76, 80.06, 74.58, 62.54, 55.36, 28.35. HRMS (ESI) calcd for $\text{C}_{16}\text{H}_{22}\text{NO}_4\text{ClNa}$ ($\text{M}+\text{Na}$) $^+$ 350.1130, found 350.1124.

3.4.9.4. (1*E*)-4-[(*tert*-butoxycarbonyl)amino]-1-(4-butylphenyl)-1,2,4-trideoxypent-1-enitol (**9E**).



White solid; isolated yield: 95% and 94%%; (3*R*, 2*S*)-**9E**: [α_{589}^{23}]-15° (c = 0.67, CHCl₃); (3*S*, 2*R*)-**9E**: [α_{589}^{23}]+10° (c = 0.97, CHCl₃); ¹H NMR (300 MHz, CDCl₃): δ 7.29 (d, *J* = 9.0 Hz, 2H), 7.13 (d, *J* = 9.0 Hz, 2H), 6.67 (d, *J* = 15.0 Hz, 1H), 6.21 (dd, *J* = 6.0, 15.0 Hz, 1H), 5.36 (d, *J* = 9.0 Hz, 1H), 4.54 (t, *J* = 3.0 Hz, 1H), 3.99 (dd, *J* = 3.0, 12.0 Hz, 1H), 3.76 (dt, *J* = 3.0, 12.0 Hz, 1H), 3.71 (m, 1H), 2.84 (br, 2H), 2.59 (t, *J* = 6.0 Hz, 2H), 1.54-1.65 (m, 2H), 1.44 (s, 9H), 1.29-1.41 (m, 2H), 0.92 (t, *J* = 6.0 Hz, 3H); ¹³C NMR (75 MHz, CDCl₃) 156.21, 142.91, 133.68, 131.80, 128.68, 127.40, 126.47, 79.93, 74.91, 62.65, 55.42, 35.36, 33.55, 28.34, 22.31, 13.93. HRMS (ESI) calcd for C₂₀H₃₁NO₄Na (M+Na)⁺ 372.2145, found 372.2156.

Reference

- Ahn, E.H., Chang, C.-C. and Schroeder, J.J. (2006). Evaluation of sphinganine and sphingosine as human breast cancer chemotherapeutic and chemopreventive agents. *Exp. Bio. Med.* 10: 1664-1672.
- Ahn, E.H. and Schroeder, J.J. (2010). Induction of apoptosis by sphingosine, sphinganine, and C2-ceramide in human colon cancer cells, but not by C2-dihydroceramide. *Anticancer Res.* 7: 2881-2884.
- Anand, A., Roy, A.D., Chakrabarty, R., Saxena, A.K. and Roy, R. (2007). Investigation of the barrier to the rotation of carbamate and amide C-N bonds in antidepressant (6a*R**,11b*S**)-7-[carbobenzyloxy-L-alanyl]-2-[(4-methylphenyl)sulfonyl]-1,2,3,4,6,6a,7,11b,2,12a(*S*)-decahydropyrazino[2',1':6,1]pyrido[3,4-*b*]indole by dynamic NMR and molecular mechanics. *Tetrahedron* 24: 5236-5243.
- Brown, H.C. and Rao, B.C.S. (1956). A new powerful reducing agent-sodium borohydride in the presence of aluminum chloride and other polyvalent metal halides. *J. Am. Chem. Soc.* 11: 2582-2588.
- Brown, M.S. and Rapoport, H. (1963). The reduction of esters with sodium borohydride. *J. Org. Chem.* 11: 3261-3263.
- Cai, Y., Ling, C.-C. and Bundle, D.R. (2006). A general, efficient and stereospecific route to sphingosine, sphinganines, phytosphingosines and their analogs. *Org. Biomol. Chem.* 6: 1140-1146.
- Carreira, E.M., Singer, R.A. and Lee, W.S. (1994). Catalytic, enantioselective aldol additions with methyl and ethyl-acetate O-silyl enolates - a chiral tridentate chelate as a Ligand for titanium(IV). *J. Am. Chem. Soc.* 19: 8837-8838.
- Chandrasekhar, S., Saritha, B., Jagadeshwar, V. and Prakash, S.J. (2006). Practical and highly stereoselective approaches to the total synthesis of (-)-codonopsinine. *Tetrahedron: Asymmetry* 9: 1380-1386.
- Chaudhuri, S.K., Saha, M., Saha, A. and Bhar, S. (2010). Systematic investigations on the reduction of 4-aryl-4-oxoesters to 1-aryl-1,4-butanediols with methanolic sodium borohydride. *Beilstein J. Org. Chem.* 6: 748-755.
- Cox, C. and Lectka, T. (1998). Solvent effects on the barrier to rotation in carbamates. *J. Org. Chem.* 8: 2426-2427.
- Dai, Z., Guillemette, K. and Green, T.K. (2013). Stereoselective synthesis of aryl γ,δ -unsaturated β -hydroxyesters by ketoreductases. *J. Mol. Catal. B: Enzym.* 264-269.
- Denmark, S.E., Nicaise, O. and Edwards, J.P. (1990). Lithium/ammonia cleavage of the nitrogen-nitrogen bond in N-(methoxycarbonyl)- and N-acetylhydrazines. *J. Org. Chem.* 25: 6219-6223.
- Ding, H. and Friestad, G.K. (2004). Trifluoroacetyl-activated nitrogen-nitrogen bond cleavage of hydrazines by samarium(II) iodide. *Org. Lett.* 4: 637-640.

Dondoni, A., Fantin, G., Fogagnolo, M. and Medici, A. (1988). Stereoselective mono- and bis-homologation of L-serinal via 2-trimethylsilylthiazole addition. The thiazole route to amino L-sugars and D-erythro-sphingosines. *J. Chem. Soc., Chem. Commun.* 1: 10-12.

Edsall, L.C., Van Brocklyn, J.R., Cuvillier, O., Kleuser, B. and Spiegel, S. (1998). N,N-Dimethylsphingosine is a potent competitive inhibitor of sphingosine kinase but not of protein kinase C: modulation of cellular levels of sphingosine 1-phosphate and ceramide. *Biochemistry* 37: 12892-12898.

Errasti, G., Koundé, C., Mirguet, O., Lecourt, T. and Micouin, L. (2009). Desymmetrization of Hydrazinocyclohexadienes: A new approach for the synthesis of polyhydroxylated aminocyclohexanes. *Org. Lett.* 13: 2912-2915.

Friestad, G.K. and Ding, H. (2001). Asymmetric allylsilane additions to enantiopure N-acylhydrazones with dual activation by fluoride and $\text{In}(\text{OTf})_3$. *Angew. Chem., Int. Ed.* 23: 4491-4493.

Garner, P., Park, J.M. and Malecki, E. (1988). A stereodivergent synthesis of D-erythro-sphingosine and D-threo-sphingosine from L-serine. *J. Org. Chem.* 18: 4395-4398.

Ghelfi, F. and Parsons, A.F. (2000). N,N-(dimethylamino)-2-pyrrolidinones from the rearrangement of N-allyl-N',N'-dimethyl-2,2-dichlorohydr-azides promoted by CuCl-N,N,N',N' -tetramethylethylenediamine. *J. Org. Chem.* 19: 6249-6253.

Girard, A., Greck, C., Ferroud, D. and Genêt, J.P. (1996). Syntheses of the syn and anti α -amino- β -hydroxy acids of vancomycin: (2S, 3R) and (2R, 3R) p-chloro-3-hydroxytyrosines. *Tetrahedron Lett.* 44: 7967-7970.

Gong, Y., Bausch, M.J. and Wang, L. (2001). Acylimine mediated N N bond cleavage of pyrazolidinediones and subsequent conversion to dihydropyrimidinediones and malonamides. *Tetrahedron Lett.* 1: 1-4.

Greck, C., Bischoff, L., Ferreira, F., Pinel, C., Piveteau, E. and Genet, J.P. (1993). Asymmetric-Synthesis of Anti N-Boc- α -Hydrazino- β -Hydroxyesters from β -Ketoesters by Sequential Catalytic-Hydrogenation and Electrophilic Amination. *Synlett* 7: 475-477.

Greck, C. and Genet, J.P. (1997). Electrophilic amination: New synthetic applications. *Synlett* 7: 741-748.

Hannun, Y.A. and Obeid, L.M. (2002). The ceramide-centric universe of lipid-mediated cell regulation: Stress encounters of the lipid kind. *J. Biol. Chem.* 29: 25847-25850.

Hannun, Y.A. and Obeid, L.M. (2008). Principles of bioactive lipid signalling: lessons from sphingolipids. *Nat. Rev. Mol. Cell Biol.* 2: 139-150.

Herold, P. (1988). Synthesis of D-erythro-sphingosine and D-threo-sphingosine derivatives from L-serine. *Helv. Chim. Acta* 2: 354-362.

Hinman, R.L. (1957). Hydrogenolysis of the Nitrogen-Nitrogen bond of acylhydrazines with raney Nickel. *J. Org. Chem.* 2: 148-150.

- Joly, R. and Bucourt, R. (June 1962). Organozinc solutions in N, N-dialkylamides and a process for their preparation. US Patent 3040079.
- Kanth, J.V.B. and Periasamy, M. (1991). Selective reduction of carboxylic acids into alcohols using sodium borohydride and iodine. *J. Org. Chem.* 20: 5964-5965.
- Kim, J., De Castro, K.A., Lim, M. and Rhee, H. (2010). Reduction of aromatic and aliphatic keto esters using sodium borohydride/MeOH at room temperature: a thorough investigation. *Tetrahedron* 23: 3995-4001.
- Kobayashi, S., Hayashi, T. and Kawasuji, T. (1994). Enantioselective syntheses of D-erythro-sphingosine and phytosphingosine from simple achiral aldehydes using catalytic asymmetric aldol reactions as key steps. *Tetrahedron Lett.* 51: 9573-9576.
- Kolesnick, R.N., Goñi, F.M. and Alonso, A. (2000). Compartmentalization of ceramide signaling: physical foundations and biological effects. *J. Cell. Physiol.* 3: 285-300.
- Kumar, P., Dubey, A. and Puranik, V.G. (2010). A general and concise asymmetric synthesis of sphingosine, safringol and phytosphingosines via tethered aminohydroxylation. *Org. Biomol. Chem.* 22: 5074-5086.
- Labeeuw, O., Phansavath, P. and Genêt, J.-P. (2003). A short total synthesis of sulfobacin A. *Tetrahedron Lett.* 34: 6383-6386.
- Lim, H.-S., Park, J.-J., Ko, K., Lee, M.-H. and Chung, S.-K. (2004). Syntheses of sphingosine-1-phosphate analogues and their interaction with EDG/S1P receptors. *Bioorg. Med. Chem. Lett.* 10: 2499-2503.
- Lim, K.G., Tonelli, F., Li, Z.G., Lu, X.Q., Bittman, R., Pyne, S. and Pyne, N.J. (2011). FTY720 Analogues as Sphingosine Kinase 1 Inhibitors enzyme inhibition kinetics, allostereism, proteasomal degradation, and actin rearrangement in MCF-7 breast cancer cells. *J. Biol. Chem.* 21: 18633-18640.
- Llaveria, J., Díaz, Y., Matheu, M.I. and Castellón, S. (2008). An efficient and general enantioselective synthesis of sphingosine, phytosphingosine, and 4-substituted derivatives. *Org. Lett.* 1: 205-208.
- Magnus, P., Garizi, N., Seibert, K.A. and Ornholt, A. (2009). Synthesis of carbamates from diethoxycarbonyl hydrazine derivatives by E1cB eliminative cleavage of the N-N'-bond rather than reduction. *Org. Lett.* 24: 5646-5648.
- Milstien, S. and Spiegel, S. (2006). Targeting sphingosine-1-phosphate: A novel avenue for cancer therapeutics. *Cancer Cell* 3: 148-150.
- Modarresi-Alam, A.R., Najafi, P., Rostamizadeh, M., Keykha, H., Bijanzadeh, H.-R. and Kleinpeter, E. (2007). Dynamic 1H NMR study of the barrier to rotation about the C-N Bond in primary carbamates and its solvent dependence. *J. Org. Chem.* 6: 2208-2211.
- Moreno, M., Murruzzu, C. and Riera, A. (2011). Enantioselective synthesis of sphingadienines and Aaromatic ceramide analogs. *Org. Lett.* 19: 5184-5187.

- Murakami, T., Furusawa, K., Tamai, T., Yoshikai, K. and Nishikawa, M. (2005). Synthesis and biological properties of novel sphingosine derivatives. *Bioorg. Med. Chem. Lett.* 4: 1115-1119.
- Narasimhan, S., Madhavan, S. and Prasad, K.G. (1995). Facile reduction of carboxylic acids to alcohols by zinc borohydride. *J. Org. Chem.* 16: 5314-5315.
- Nimkar, S., Menaldino, D., Merrill, A.H. and Liotta, D. (1988). A stereoselective synthesis of sphingosine, a protein kinase c inhibitor. *Tetrahedron Lett.* 25: 3037-3040.
- Ogretmen, B. and Hannun, Y.A. (2004). Biologically active sphingolipids in cancer pathogenesis and treatment. *Nat. Rev. Cancer* 8: 604-616.
- Paugh, S.W., Paugh, B.S., Rahmani, M., Kapitonov, D., Almenara, J.A., Kordula, T., Milstien, S., Adams, J.K., Zipkin, R.E., Grant, S. and Spiegel, S. (2008). A selective sphingosine kinase 1 inhibitor integrates multiple molecular therapeutic targets in human leukemia. *Blood* 4: 1382-1391.
- Pirkle, W.H., Simmons, K.A. and Boeder, C.W. (1979). Dynamic NMR studies of diastereomeric carbamates: implications toward the determination of relative configuration by NMR. *J. Org. Chem.* 26: 4891-4896.
- Pyne, N.J. and Pyne, S. (2010). Sphingosine 1-phosphate and cancer. *Nat. Rev. Cancer* 7: 489-503.
- Pyne, S., Bittman, R. and Pyne, N.J. (2011). Sphingosine kinase inhibitors and cancer: seeking the golden sword of hercules. *Cancer Res.* 21: 6576-6582.
- Radin, N.S. (2003). Killing tumours by ceramide-induced apoptosis: a critique of available drugs. *Biochem. J.* 243-256.
- Radunz, H.-E., Devant, R.M. and Eiermann, V. (1988). Eine effiziente und stereoselektive synthese von D-erythro-sphingosin. *Liebigs Ann. Chem.* 11: 1103-1105.
- Raup, D.E.A., Cardinal-David, B., Holte, D. and Scheidt, K.A. (2010). Cooperative catalysis by carbenes and Lewis acids in a highly stereoselective route to γ -lactams. *Nat. Chem.* 9: 766-771.
- Reynolds, C.P., Maurer, B.J. and Kolesnick, R.N. (2004). Ceramide synthesis and metabolism as a target for cancer therapy. *Cancer Lett.* 2: 169-180.
- Sapountzis, I. and Knochel, P. (2004). A general amination method based on the addition of polyfunctional arylmagnesium reagents to functionalized arylazo tosylates. *Angew. Chem., Int. Ed.* 7: 897-900.
- Spiegel, S. and Milstien, S. (2003). Sphingosine-1-phosphate: an enigmatic signalling lipid. *Nat. Rev. Mol. Cell Biol.* 5: 397-407.
- van den Berg, R.J.B.H.N., Korevaar, C.G.N., van der Marel, G.A., Overkleeft, H.S. and van Boom, J.H. (2002). A simple and low cost synthesis of D-erythro-sphingosine and D-erythro-azidosphingosine from D-ribo-phytosphingosine: glycosphingolipid precursors. *Tetrahedron Lett.* 46: 8409-8412.

van den Berg, R.J.B.H.N., van den Elst, H., Korevaar, C.G.N., Aerts, J.M.F.G., van der Marel, G.A. and Overkleeft, H.S. (2011). A rapid and efficient synthesis of D-erythro-sphingosine from D-ribo-phytosphingosine. *Eur. J. Org. Chem.* 33: 6685-6689.

Van Overmeire, I., Boldin, S.A., Dumont, F., Van Calenbergh, S., Slegers, G., De Keukeleire, D., Futerman, A.H. and Herdewijn, P. (1999). Effect of aromatic short-chain analogues of ceramide on axonal growth in hippocampal neurons. *J. Med. Chem.* 14: 2697-2705.

Wong, L., Tan, S.S.L., Lam, Y. and Melendez, A.J. (2009). Synthesis and evaluation of sphingosine analogues as inhibitors of sphingosine kinases. *J. Med. Chem.* 12: 3618-3626.

Wymann, M.P. and Schneider, R. (2008). Lipid signalling in disease. *Nat. Rev. Mol. Cell Biol.* 2: 162-176.

Yamakawa, T., Masaki, M. and Nohira, H. (1991). A new reduction of some carboxylic esters with sodium borohydride and zinc chloride in the presence of a tertiary amine. *Bull. Chem. Soc. Jpn.* 9: 2730-2734.

Yamazaki, N. and Kibayashi, C. (1997). Lewis acid-mediated S_N2 type displacement by grignard reagents on chiral perhydropyrindo[2,1-*b*]pyrrolo[1,2-*d*][1,3,4]oxadiazine. Chirality induction in asymmetric synthesis of 2-substituted piperidines. *Tetrahedron Lett.* 26: 4623-4626.

Yang, H. and Liebeskind, L.S. (2007). A concise and scalable synthesis of high enantiopurity (–)-D-erythro-sphingosine using peptidyl thiol ester–boronic acid cross-coupling. *Org. Lett.* 16: 2993-2995.

Yatomi, Y., Ruan, F., Megidish, T., Toyokuni, T., Hakomori, S.-i. and Igarashi, Y. (1996). N,N-dimethylsphingosine inhibition of sphingosine kinase and sphingosine 1-phosphate activity in human platelets. *Biochem.* 2: 626-633.

Zhang, Y., Tang, Q. and Luo, M. (2011). Reduction of hydrazines to amines with aqueous solution of titanium(iii) trichloride. *Org. Biomol. Chem.* 13: 4977-4982.

Zipkin, R.E., Spiegel, S. and Adams, J.K. (2010). Novel sphingosine kinase type 1 inhibitors, compositions and processes for using same. US. 12387228.

Appendix B, Supplementary for Chapter 3

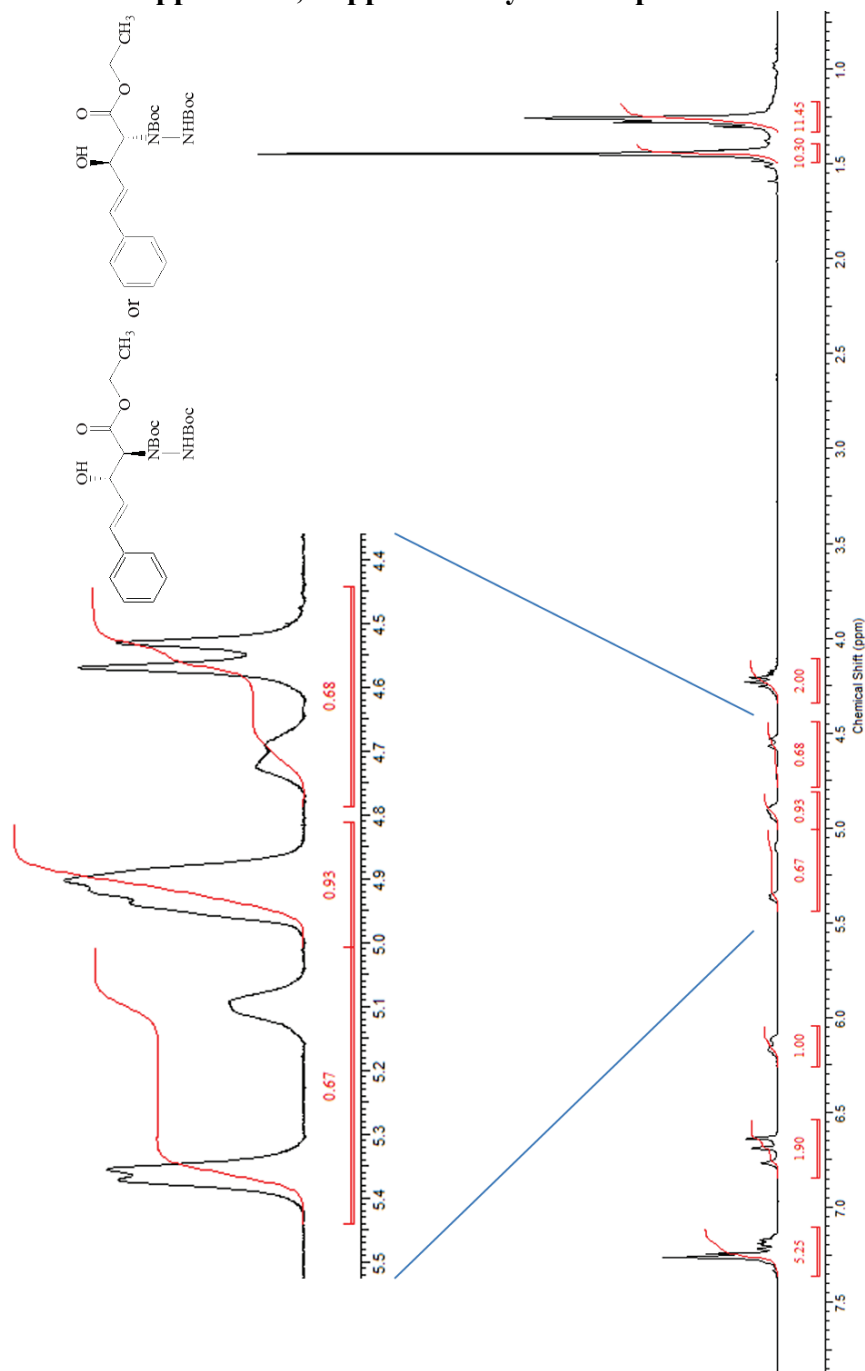


Figure B3.1. ^1H NMR spectrum of Ethyl (*4E*)-2-[1,2-bis(*tert*-butoxycarbonyl)hydrazino]-2,4,5-trideoxy-5-phenyl-D-*erythro*-pent-4-enonate (**4A**) at 25°C in CDCl_3 .

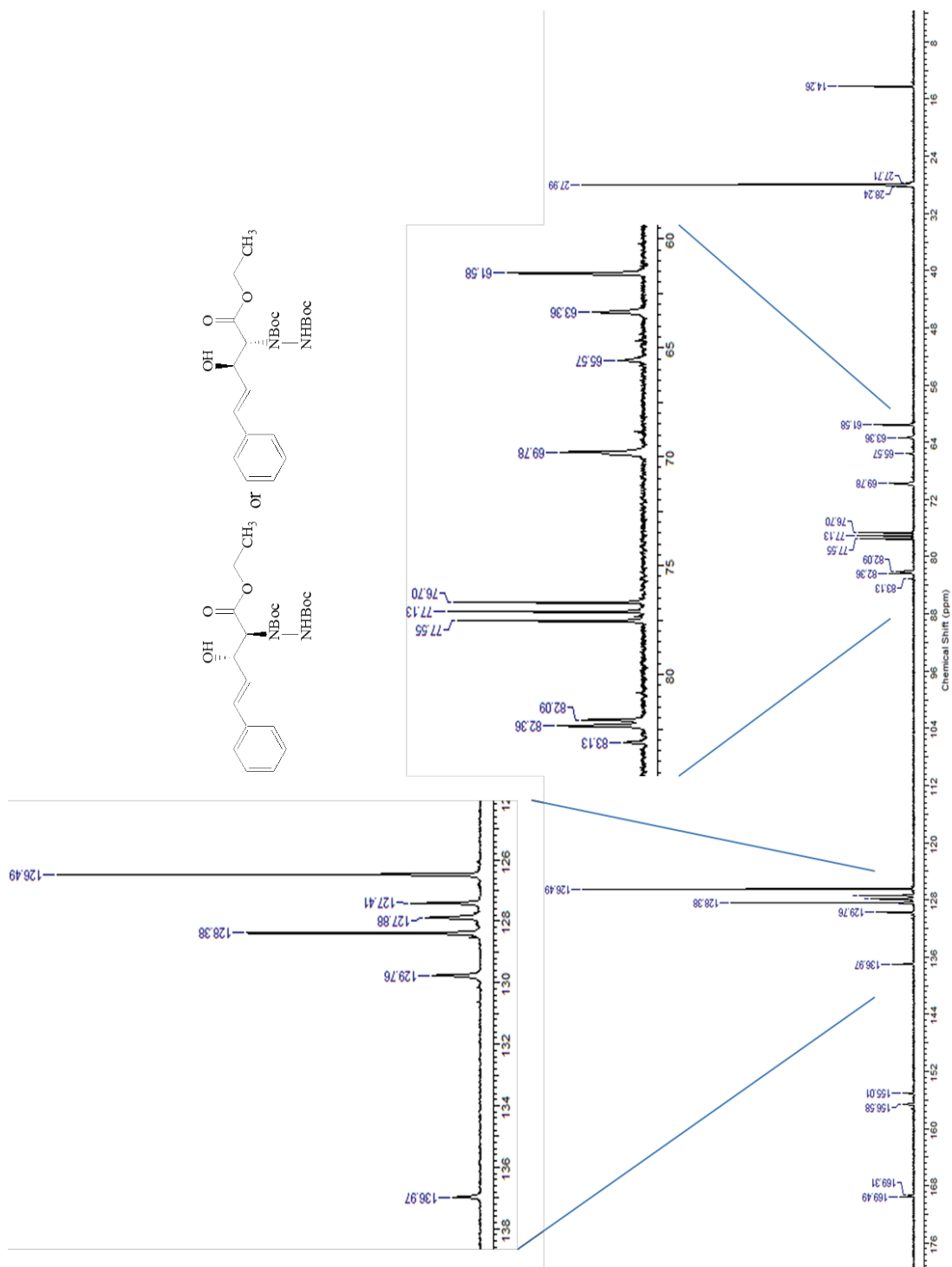


Figure B3.2. ^{13}C NMR spectrum of Ethyl (4E)-2-[1,2-bis(*tert*-butoxycarbonyl)hydrazino]-2,4,5-trideoxy-5-phenyl-D-*erythro*-pent-4-enonate (**4A**) at 25 °C in CDCl_3 .

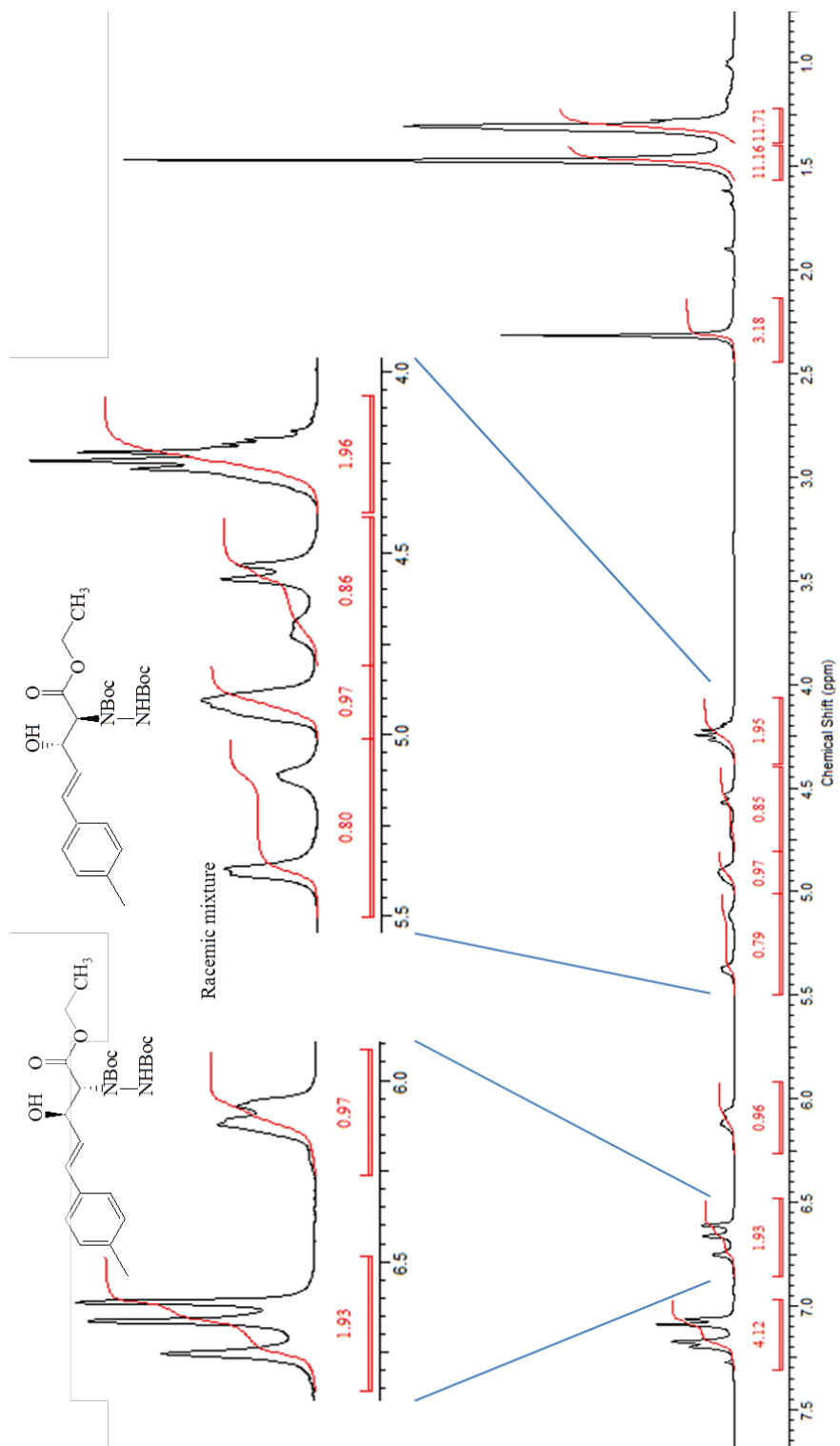


Figure B3.3. ^1H NMR spectrum of Ethyl (4E)-2-[1,2-bis(*tert*-butoxycarbonyl)hydrazino]-2,4,5-trideoxy-5-(4-methylphenyl)-D-erythro-pent-4-enonate (**4B**) at 25 °C in CDCl₃.

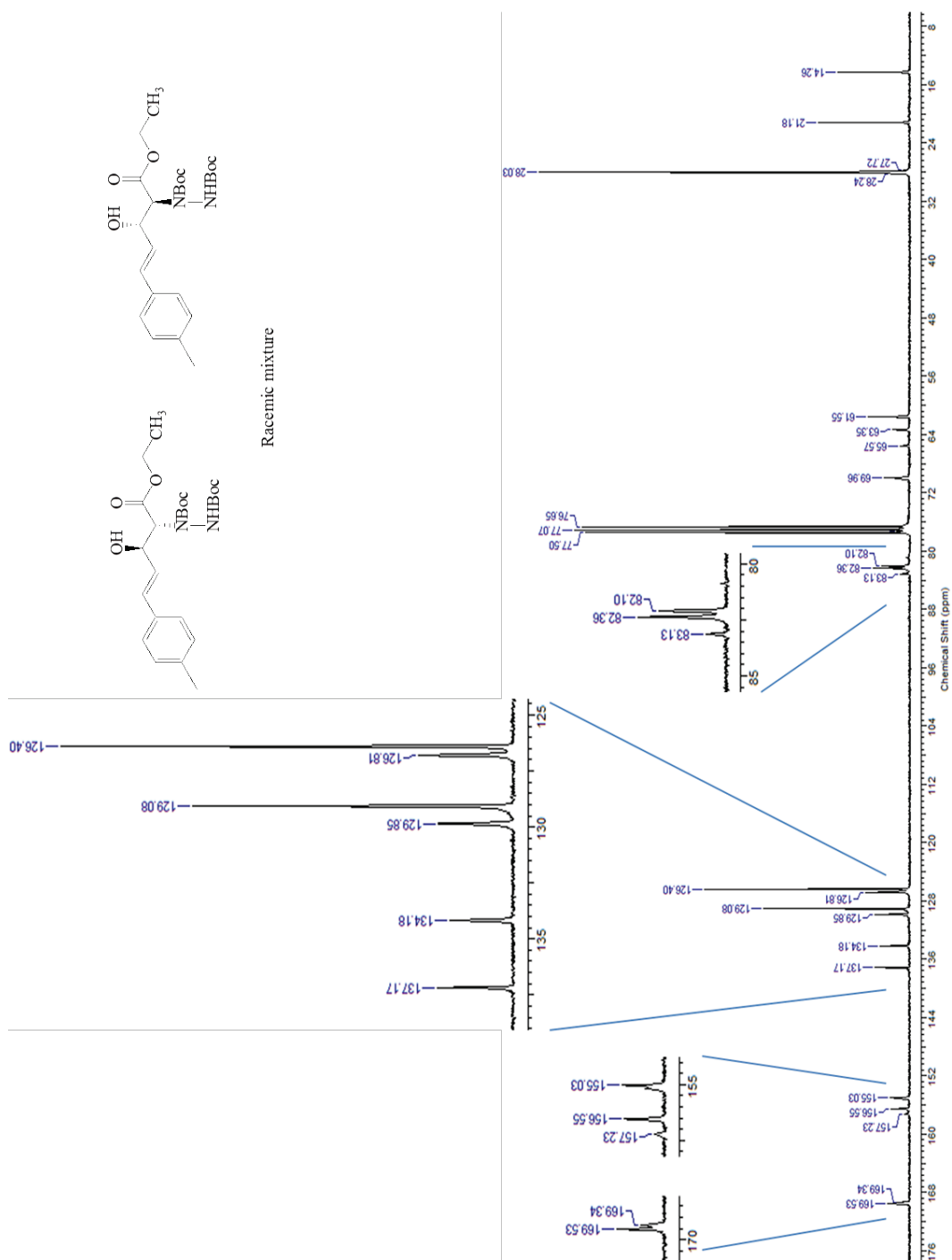


Figure B3.4. ^{13}C NMR spectrum of Ethyl (4*E*)-2-[1,2-bis(*tert*-butoxycarbonyl) hydrazino]-2,4,5-trideoxy-5-(4-methylphenyl)-*D*-erythro-pent-4-enonate (**4B**) at 25 °C in CDCl_3 .

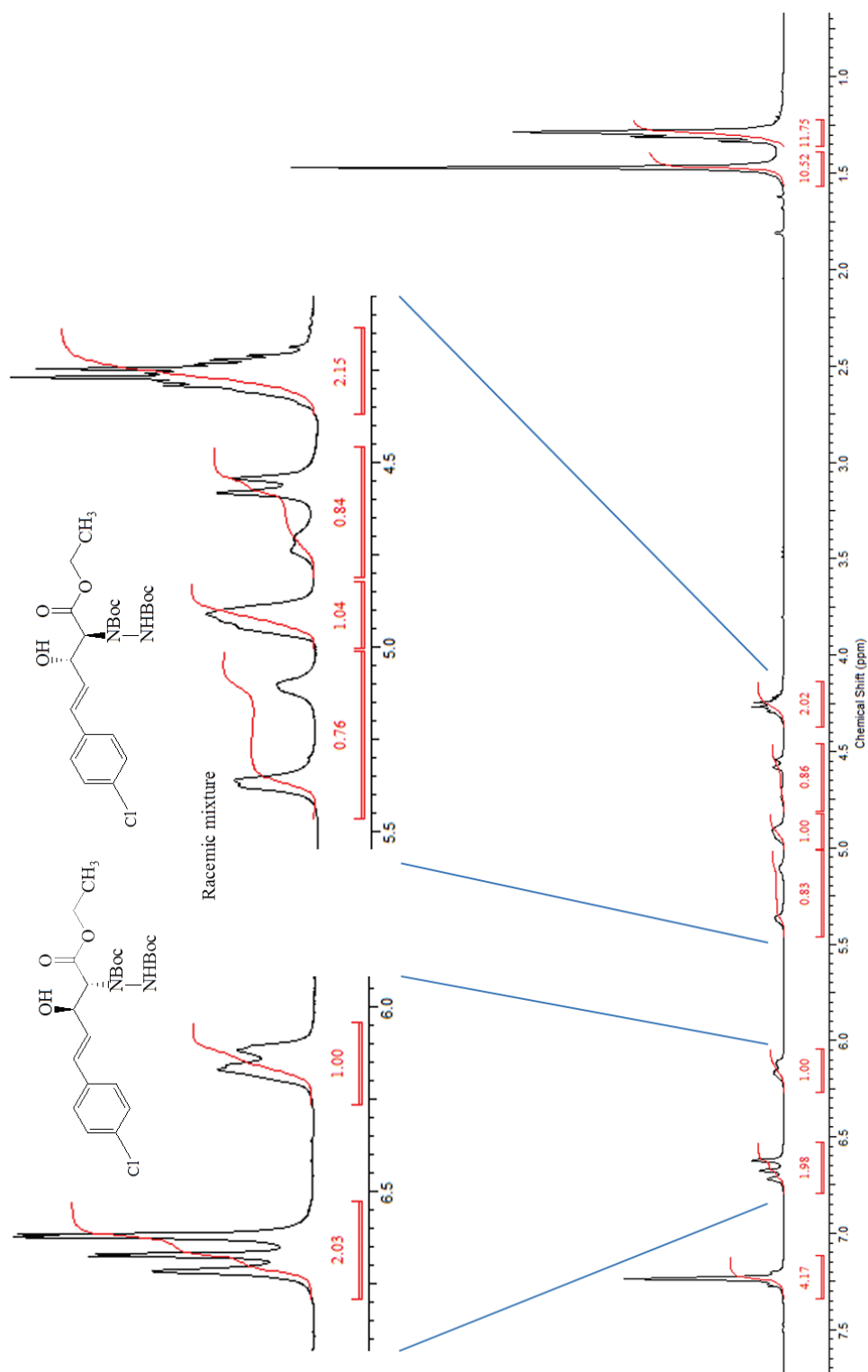


Figure B3.5. ¹H NMR spectrum of ethyl (4E)-2-[1,2-bis(*tert*-butoxycarbonyl)hydrazino]-5-(4-chlorophenyl)-2,4,5-trideoxy-D-*erythro*-pent-4-enonate (4C) at 25 °C in CDCl₃.

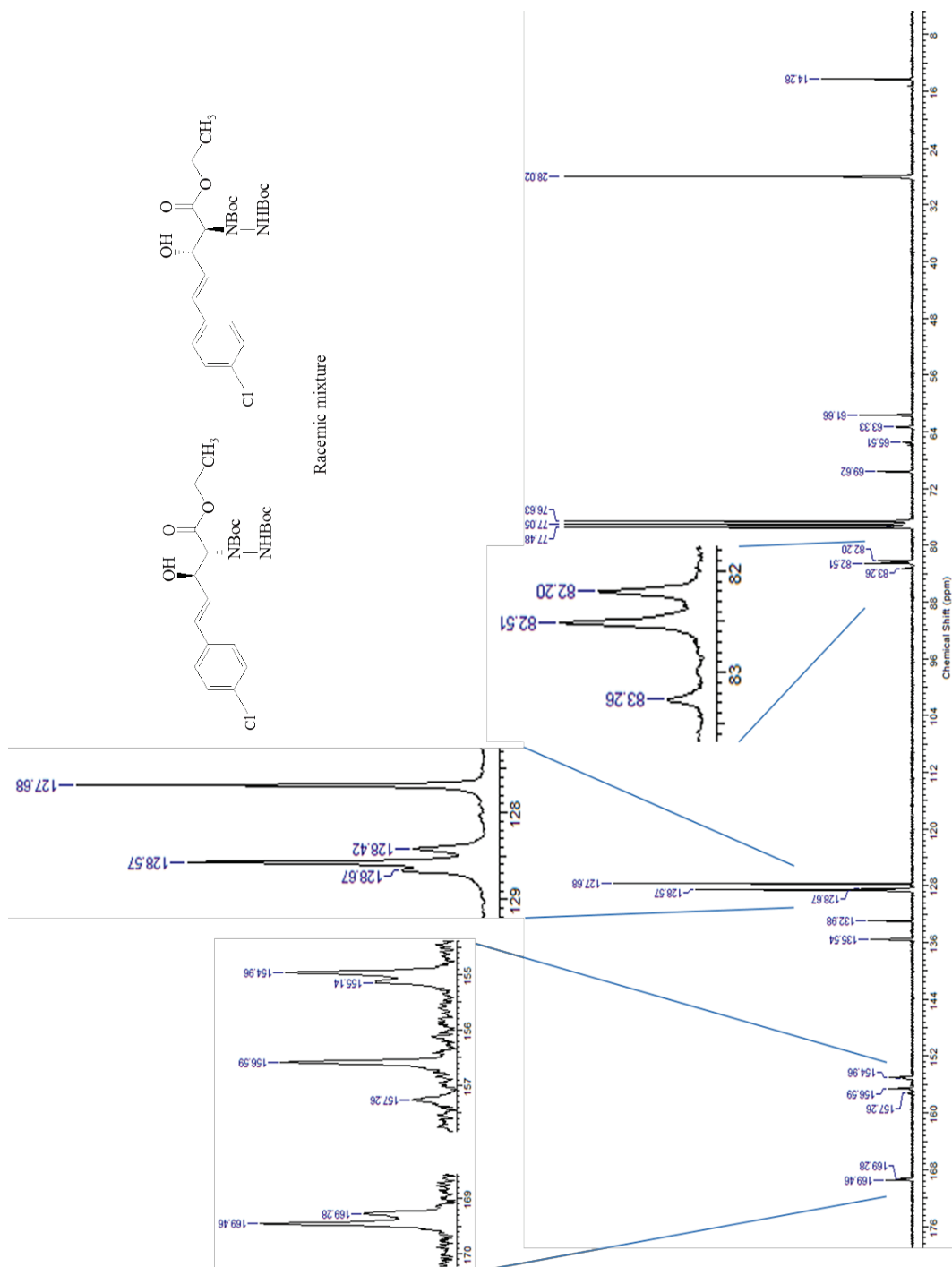


Figure B3.6. ^{13}C NMR spectrum of ethyl (4E)-2-[1,2-bis(*tert*-butoxycarbonyl) hydrazino]-5-(4-chlorophenyl)-2,4,5-trideoxy-D-erythro-pent-4-enonate (**4C**) at 25 °C in CDCl₃.

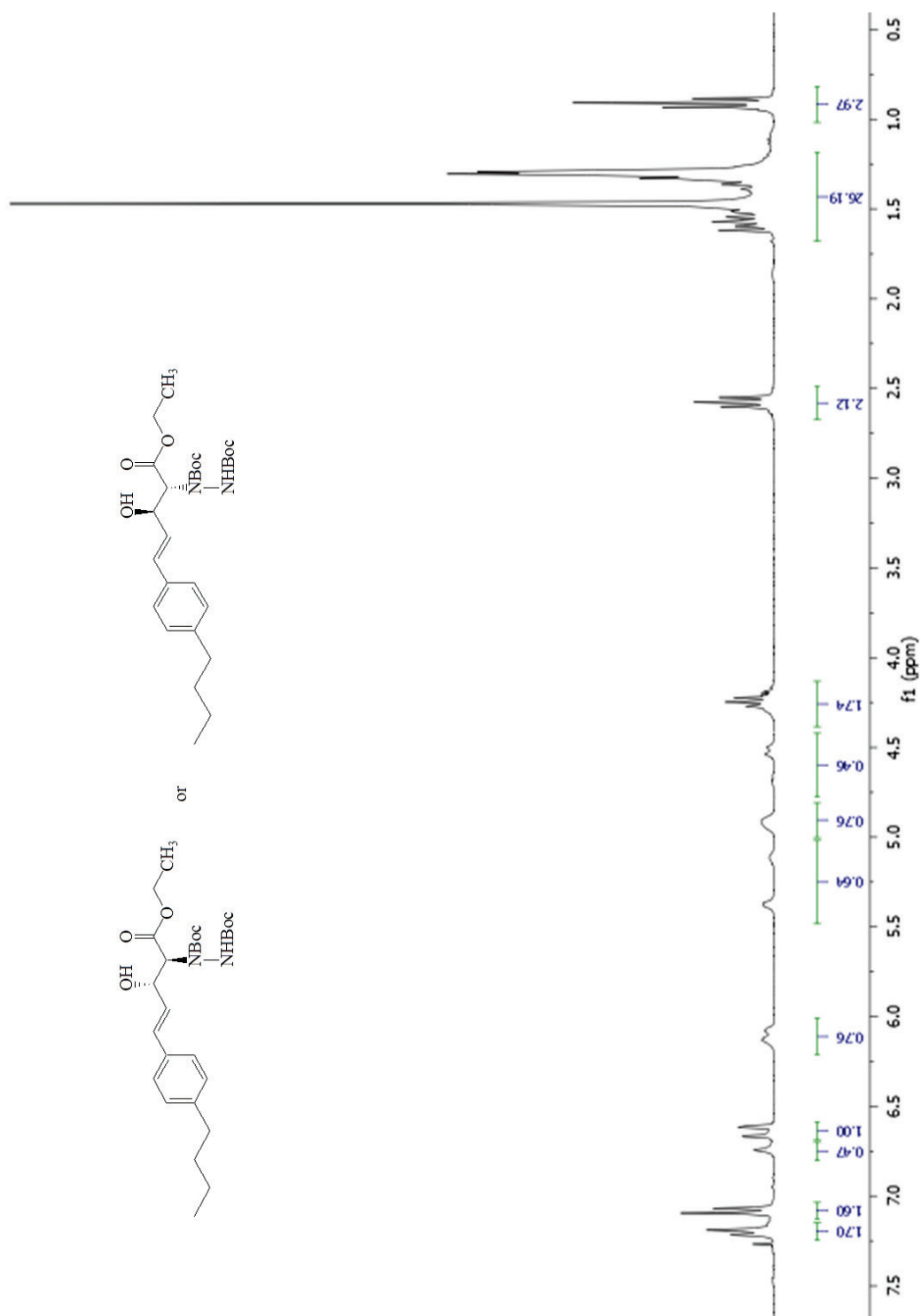


Figure B3.7. ¹H NMR spectrum of ethyl (4E)-2-[1,2-bis(*tert*-butoxycarbonyl) hydrazino]-5-(4-butylphenyl)-2,4,5-trideoxypent-4-enonate (**4E**) at 25 °C in CDCl₃.

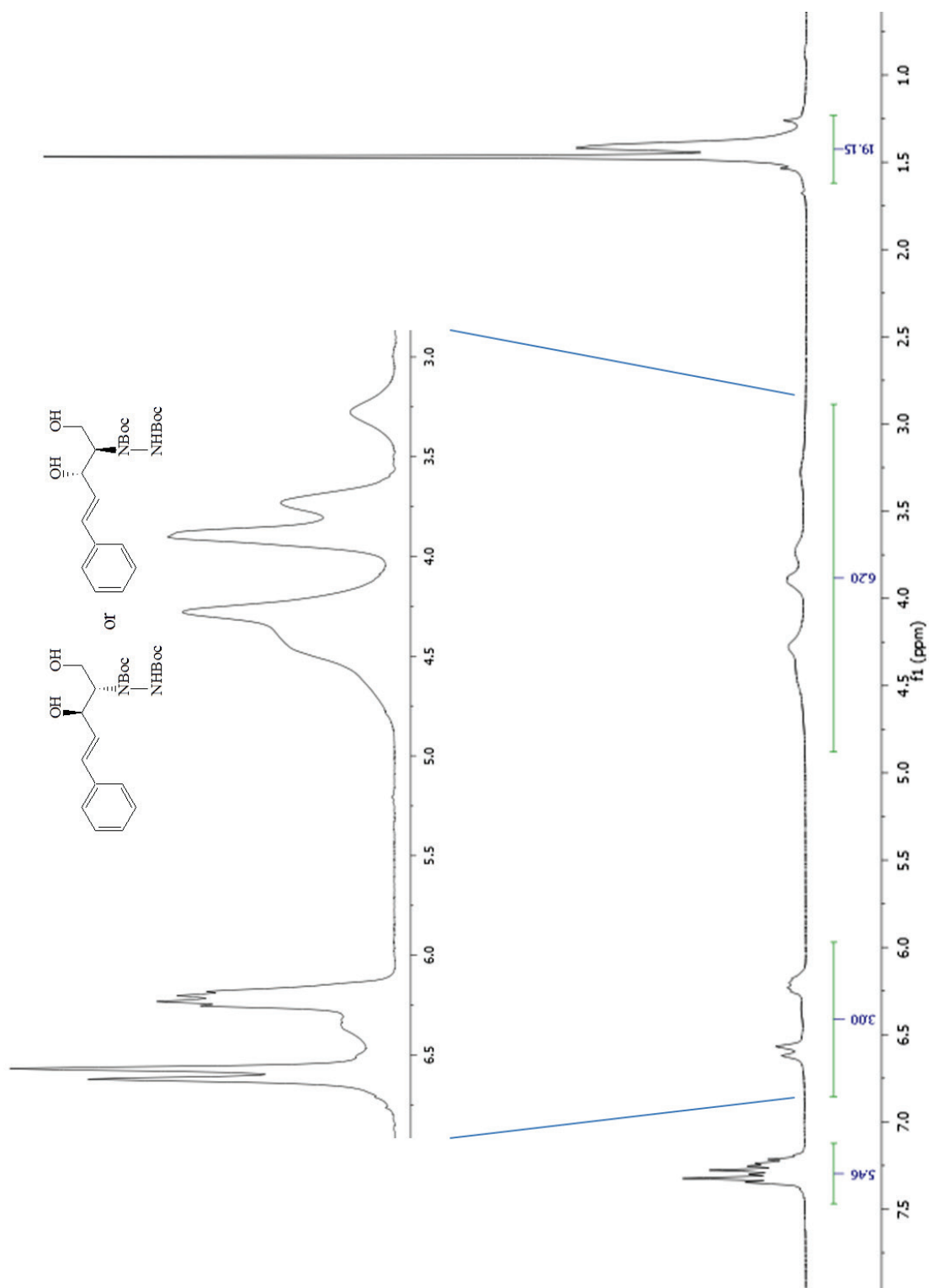


Figure B3.9. ^1H NMR spectrum of (4*E*)-2-[1,2-bis(*tert*-butoxycarbonyl)hydrazino]-2,4,5-trideoxy-5-phenyl-*D*-*erythro*-pent-4-enitol (**5A**) at 25 °C in CDCl_3 .

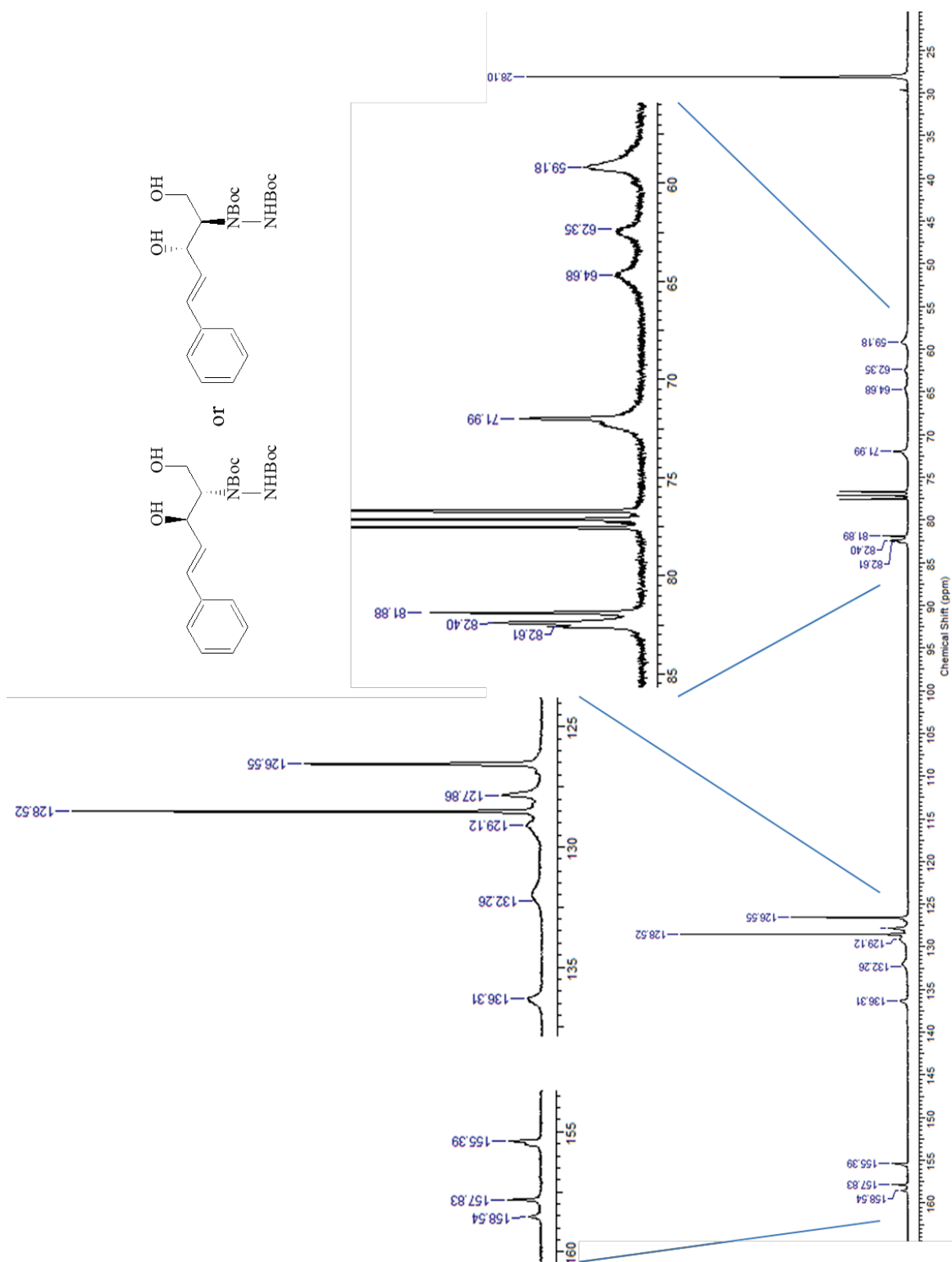


Figure B3.10. ^{13}C NMR spectrum of (4*E*)-2-[1,2-bis(*tert*-butoxycarbonyl)hydrazino]-2,4,5-trideoxy-5-phenyl-D-erythro-pent-4-enitol (**5A**) at 25 °C in CDCl_3 .

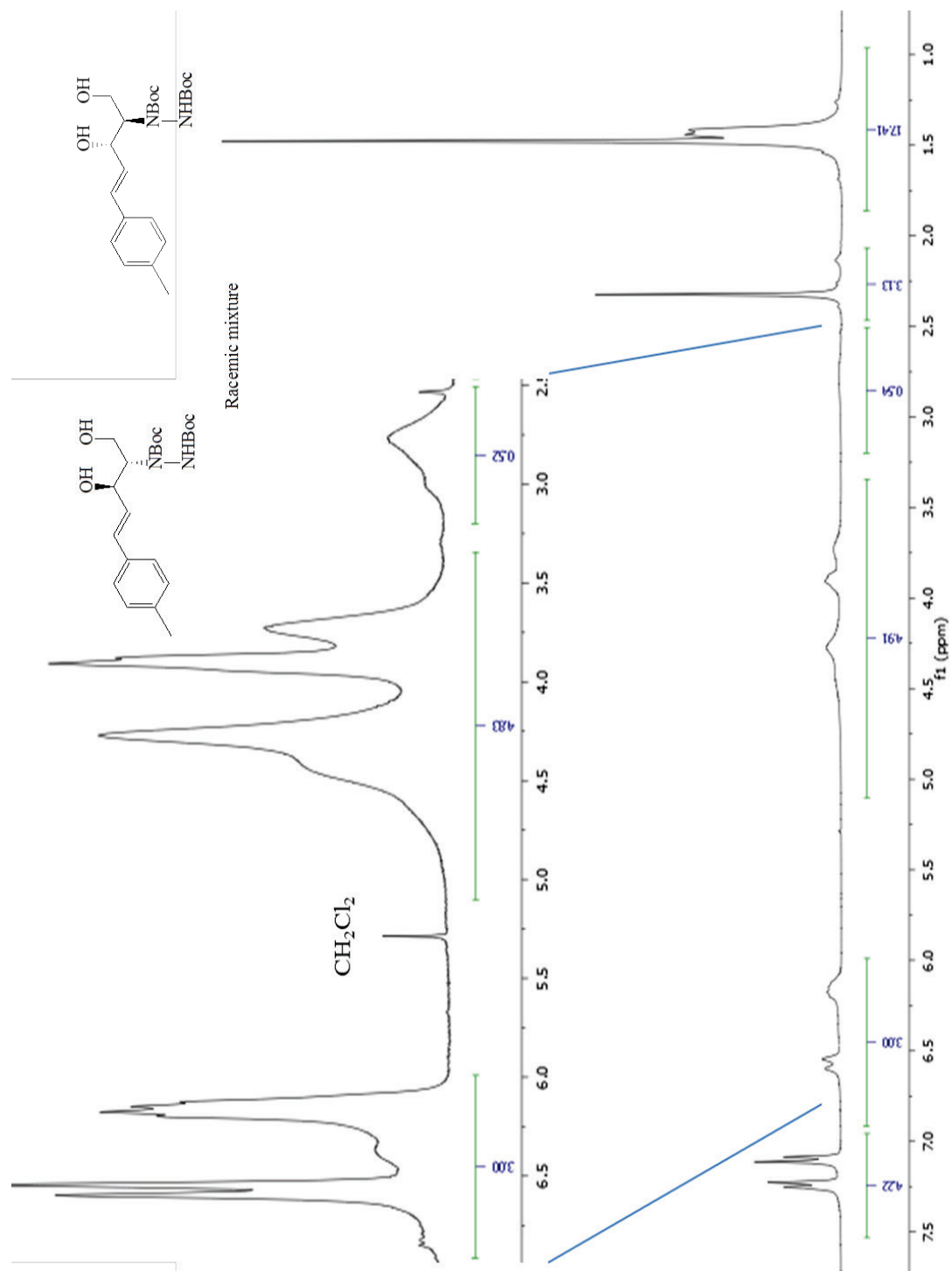


Figure B3.11. ^1H NMR spectrum of (4E)-2-[1,2-bis(*tert*-butoxycarbonyl)hydrazino]-2,4,5-trideoxy-5-(4-methylphenyl)-D-*erythro*-pent-4-enitol (**5B**) at 25 °C in CDCl_3 .

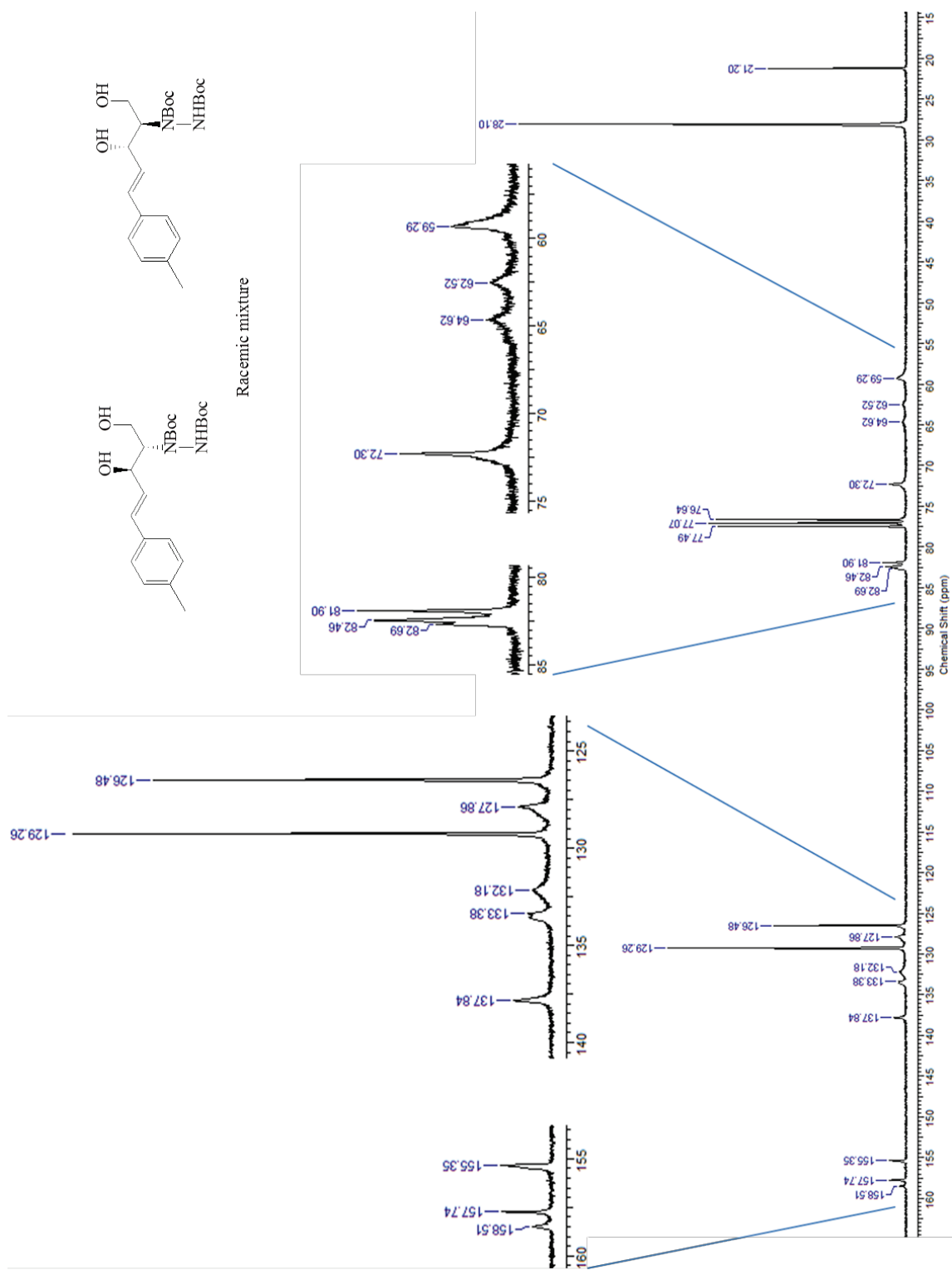


Figure B3.12. ¹³C NMR spectrum of (4*E*)-2-[1,2-bis(*tert*-butoxycarbonyl)hydrazino]-2,4,5-trideoxy-5-(4-methylphenyl)-*D*-erythro-pent-4-enitol (**5B**) at 25 °C in CDCl₃.

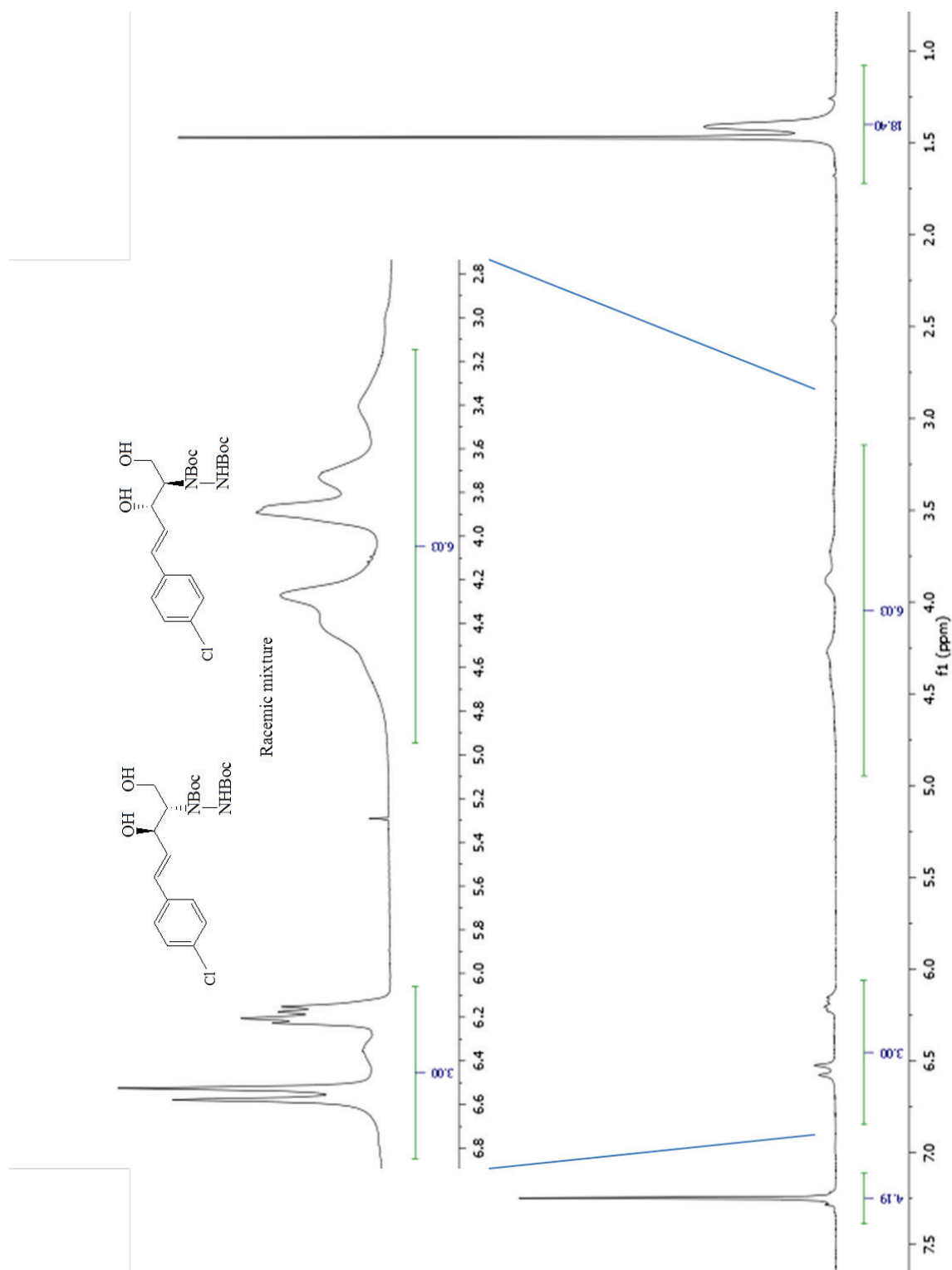


Figure B3.13. ^1H NMR spectrum of (4*E*)-2-[1,2-bis(*tert*-butoxycarbonyl)hydrazino]-5-(4-chlorophenyl)-2,4,5-trideoxy-*D*-erythro-pent-4-enitol (**5C**) in CDCl_3 .

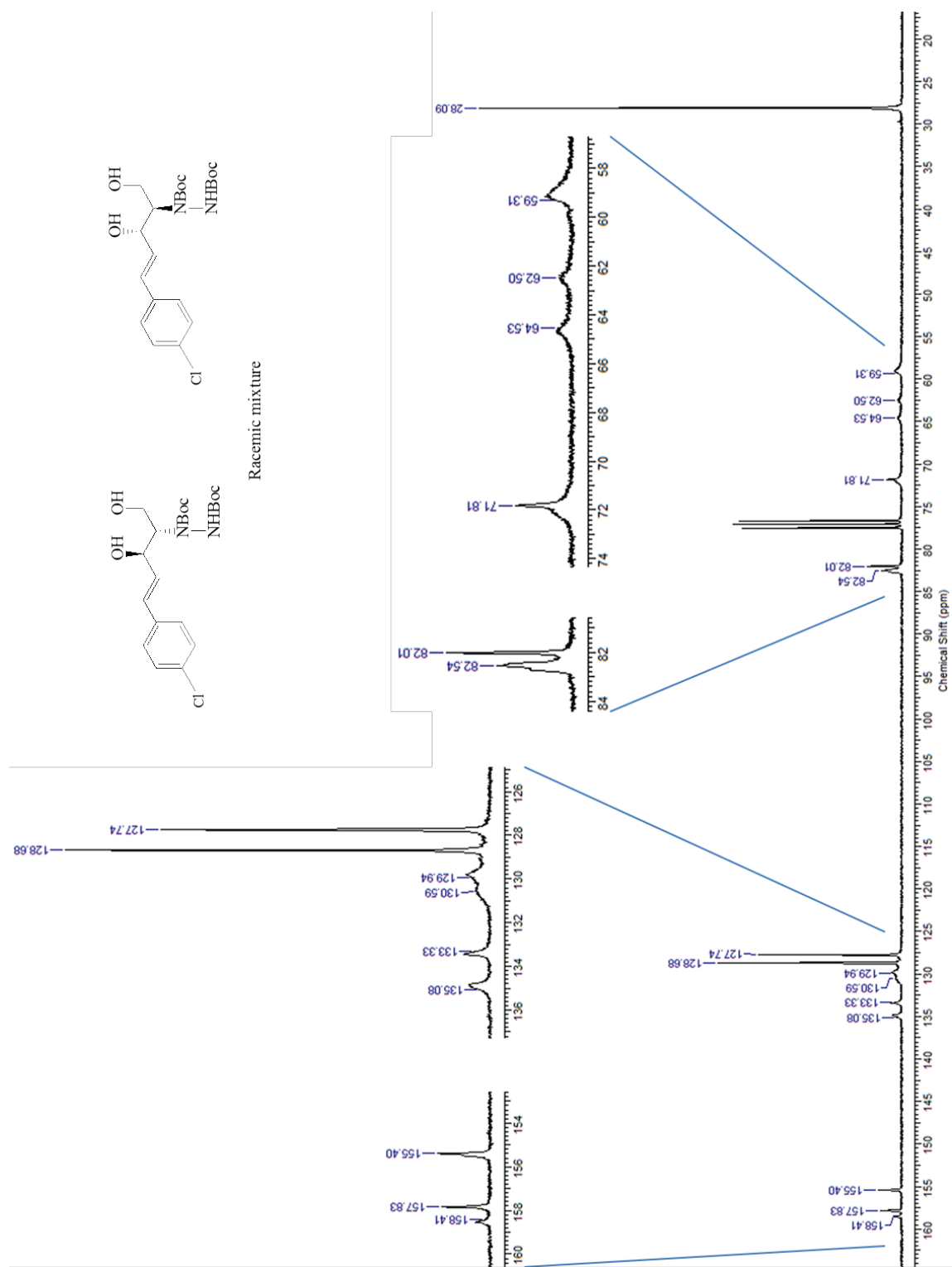


Figure B3.14. ¹³C NMR spectrum of (4E)-2-[1,2-bis(*tert*-butoxycarbonyl)hydrazino]-5-(4-chlorophenyl)-2,4,5-trideoxy-D-erythro-pent-4-enitol (**5C**) in CDCl₃.

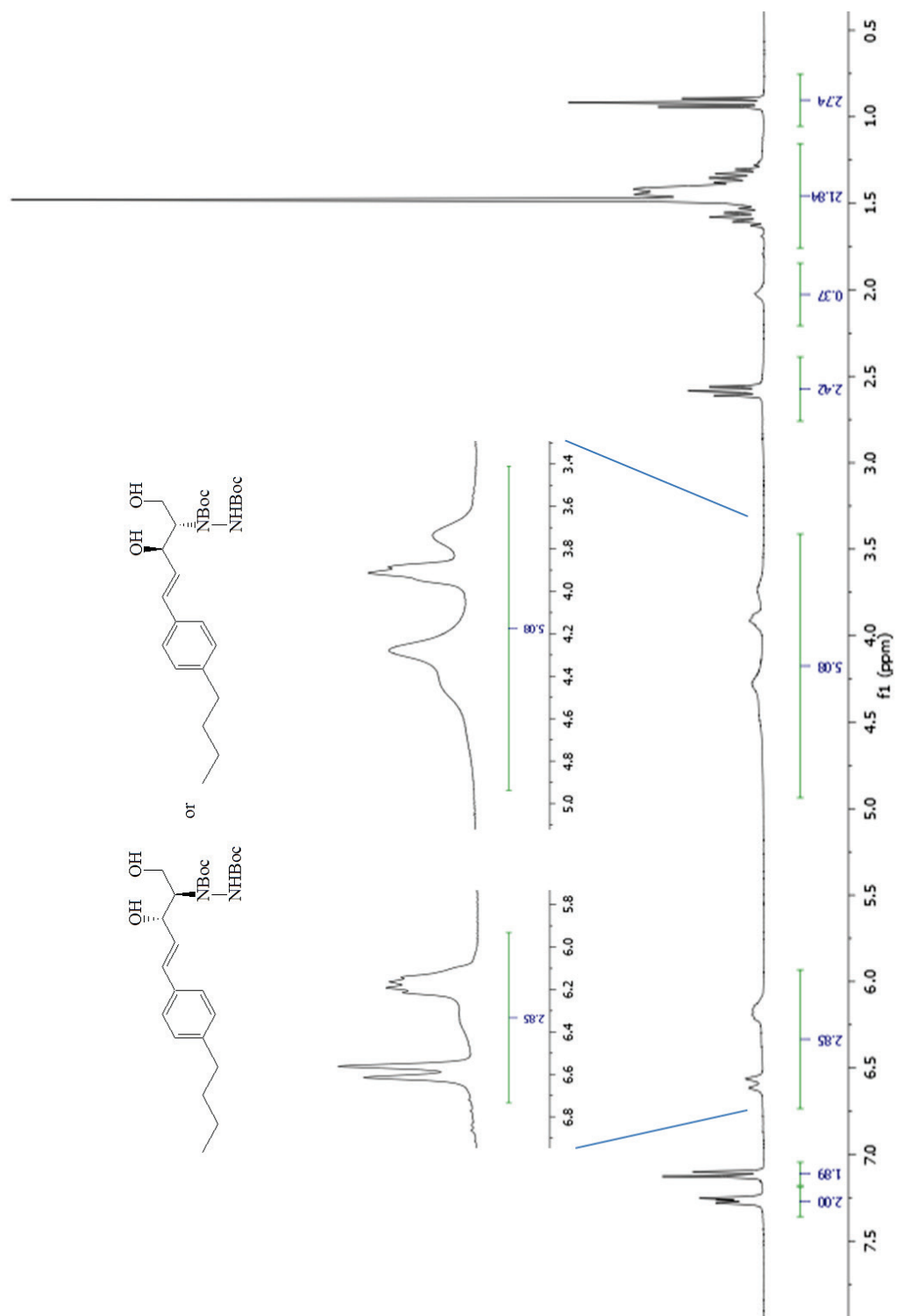


Figure B3.15. ¹H NMR spectrum of (*1E*)-4-[1,2-bis(tert-butoxycarbonyl)hydrazino]-1-(4-butylphenyl)-1,2,4-trideoxypent-1-enitol (**5E**) in CDCl₃.

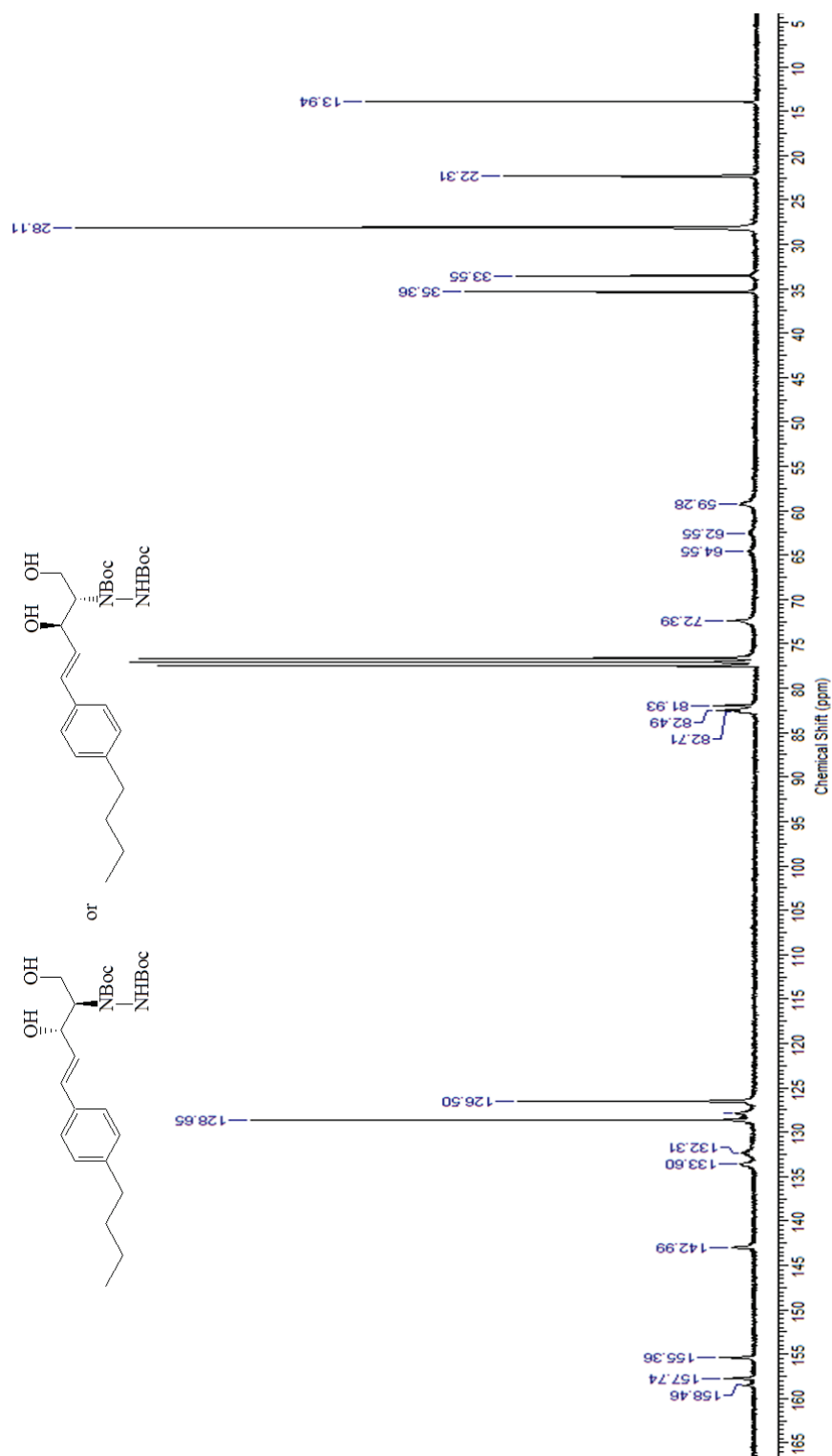


Figure B3.15. ^{13}C NMR spectrum of (*1E*)-4-[1,2-bis(tert-butoxycarbonyl)hydrazino]-1-(4-butylphenyl)-1,2,4-trideoxypent-1-enitol (**5E**) in CDCl_3 .

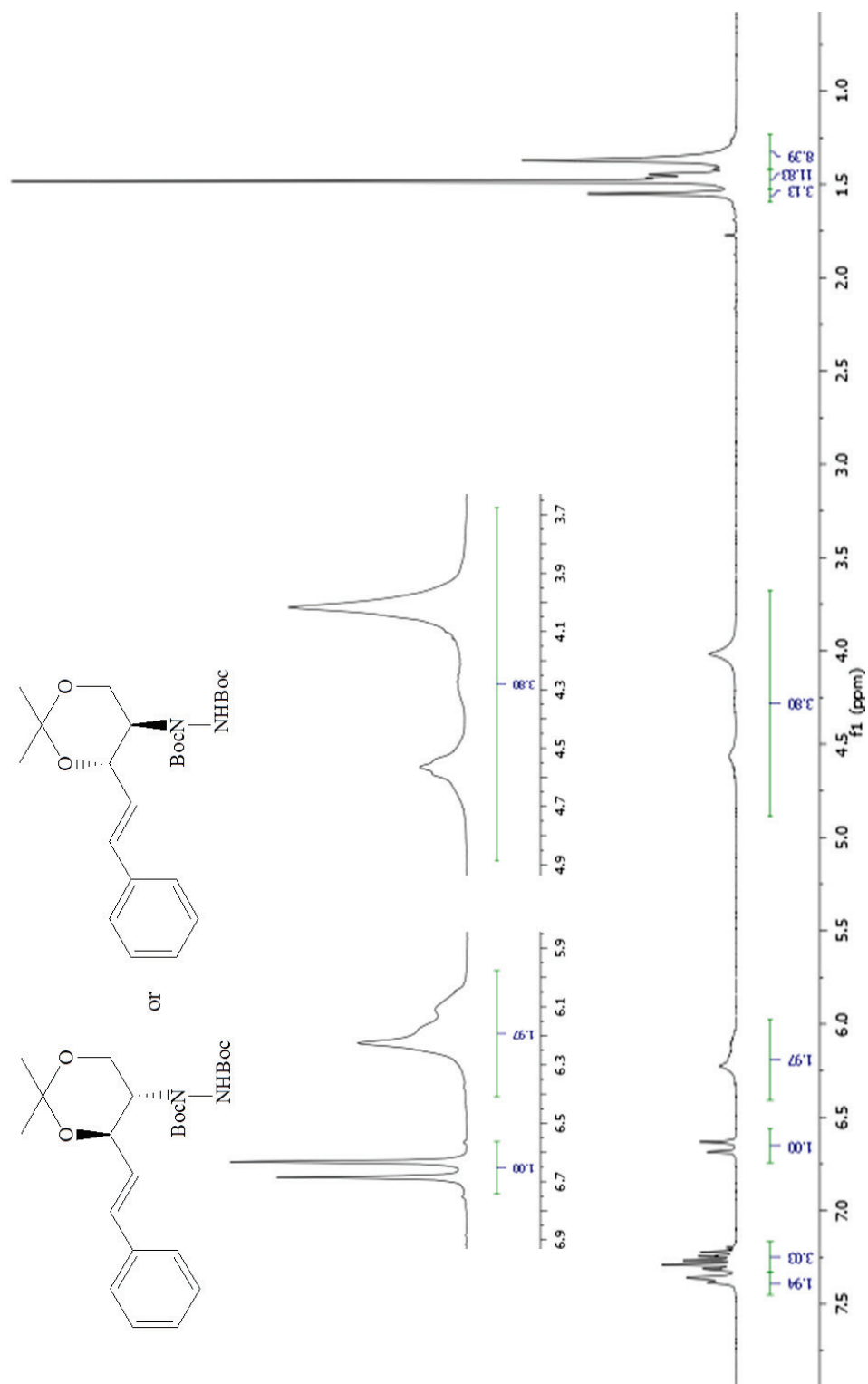


Figure B3.17. ¹H NMR spectrum of (*1E*)-4-[1,2-bis(*tert*-butoxycarbonyl)hydrazino]-1,2,4-trideoxy-3,5-*O*-(1-methylethylidene)-1-phenylpent-1-enitol (**6A**) in CDCl₃.

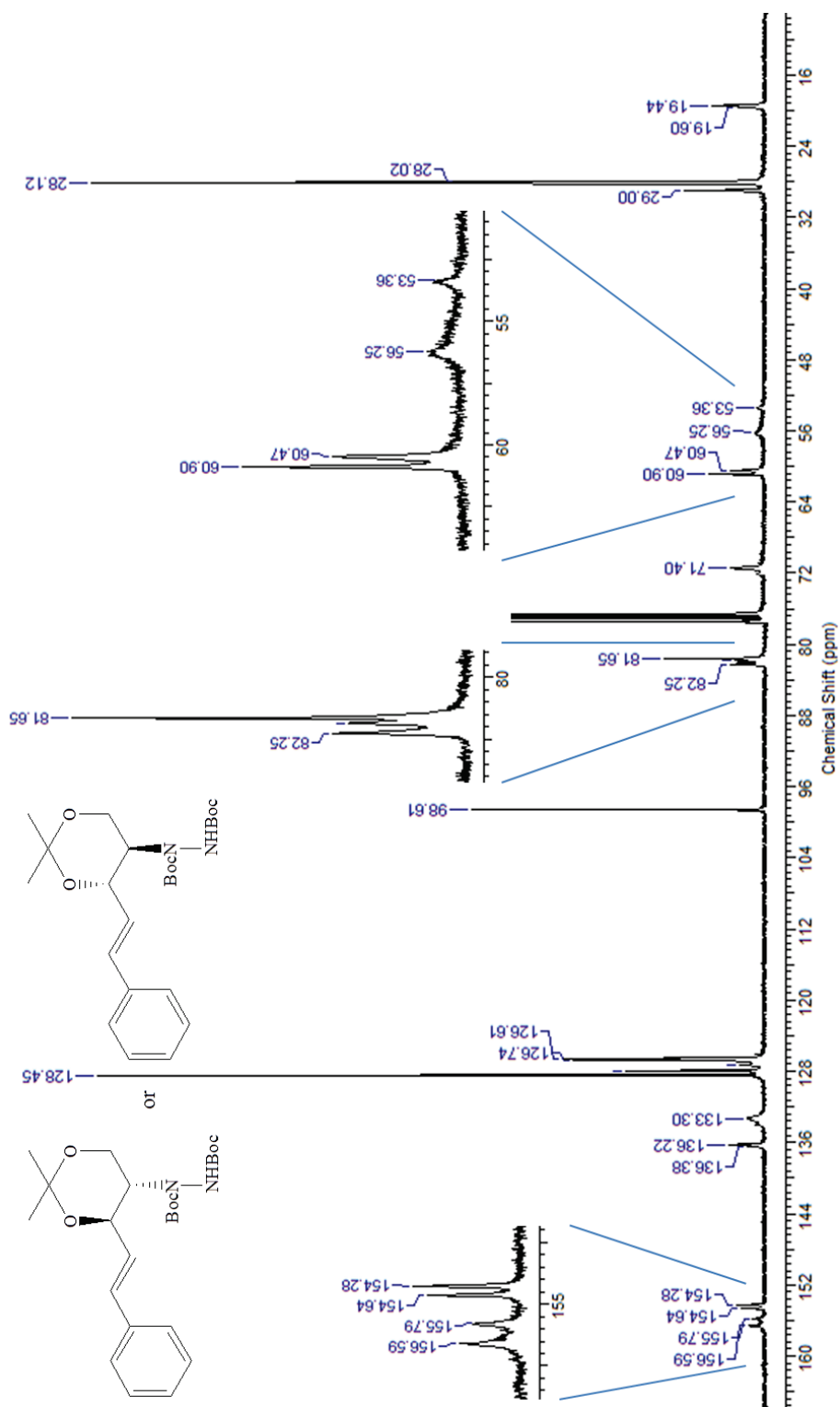


Figure B3.18. ^{13}C NMR spectrum of (*1E*)-4-[1,2-bis(*tert*-butoxycarbonyl)hydrazino]-1,2,4-trideoxy-3,5-*O*-(1-methylethylidene)-1-phenylpent-1-enitol (**6A**) in CDCl_3 .

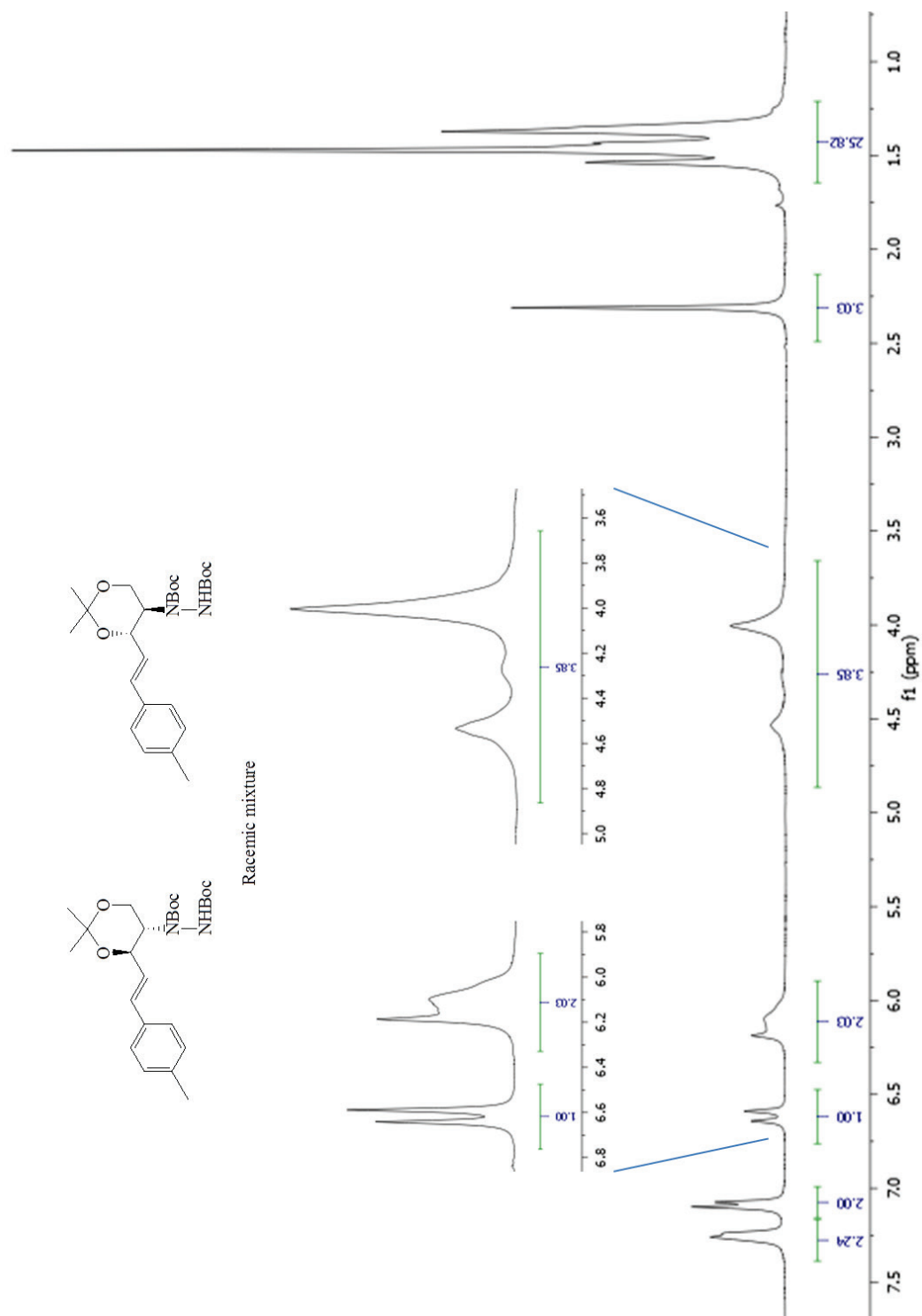


Figure B3.19. ^1H NMR spectrum of (*1E*)-4-[1,2-bis(*tert*-butoxycarbonyl)hydrazino]-1,2,4-trideoxy-3,5-*O*-(1-methylethylidene)-1-(4-methylphenyl)pent-1-enitol (**6B**) in CDCl_3 .

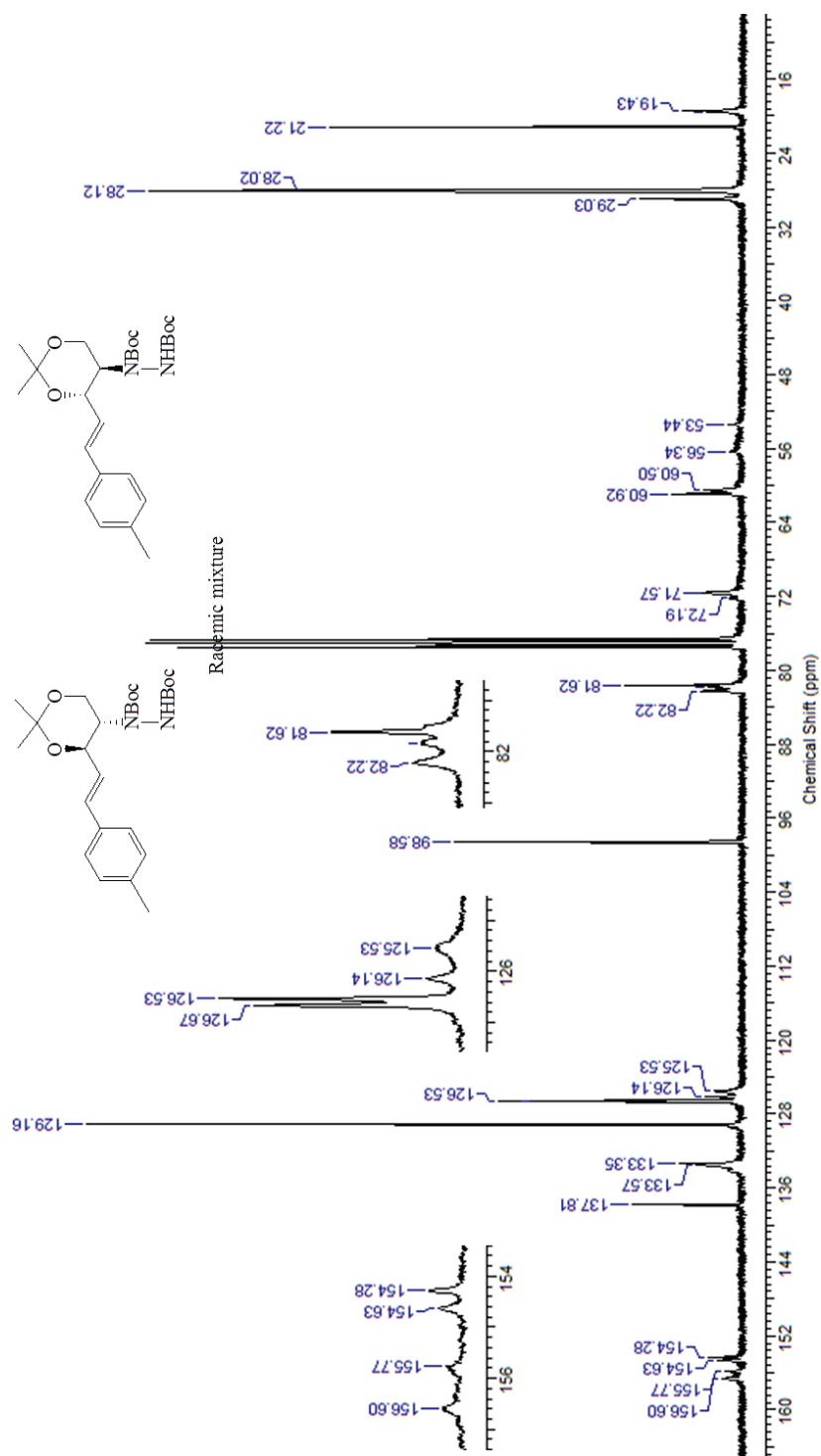


Figure B3.20. ^{13}C NMR spectrum of (*1E*)-4-[1,2-bis(*tert*-butoxycarbonyl)hydrazino]-1,2,4-trideoxy-3,5-*O*-(1-methylethylidene)-1-(4-methylphenyl)pent-1-enitol (**6B**) in CDCl_3 .

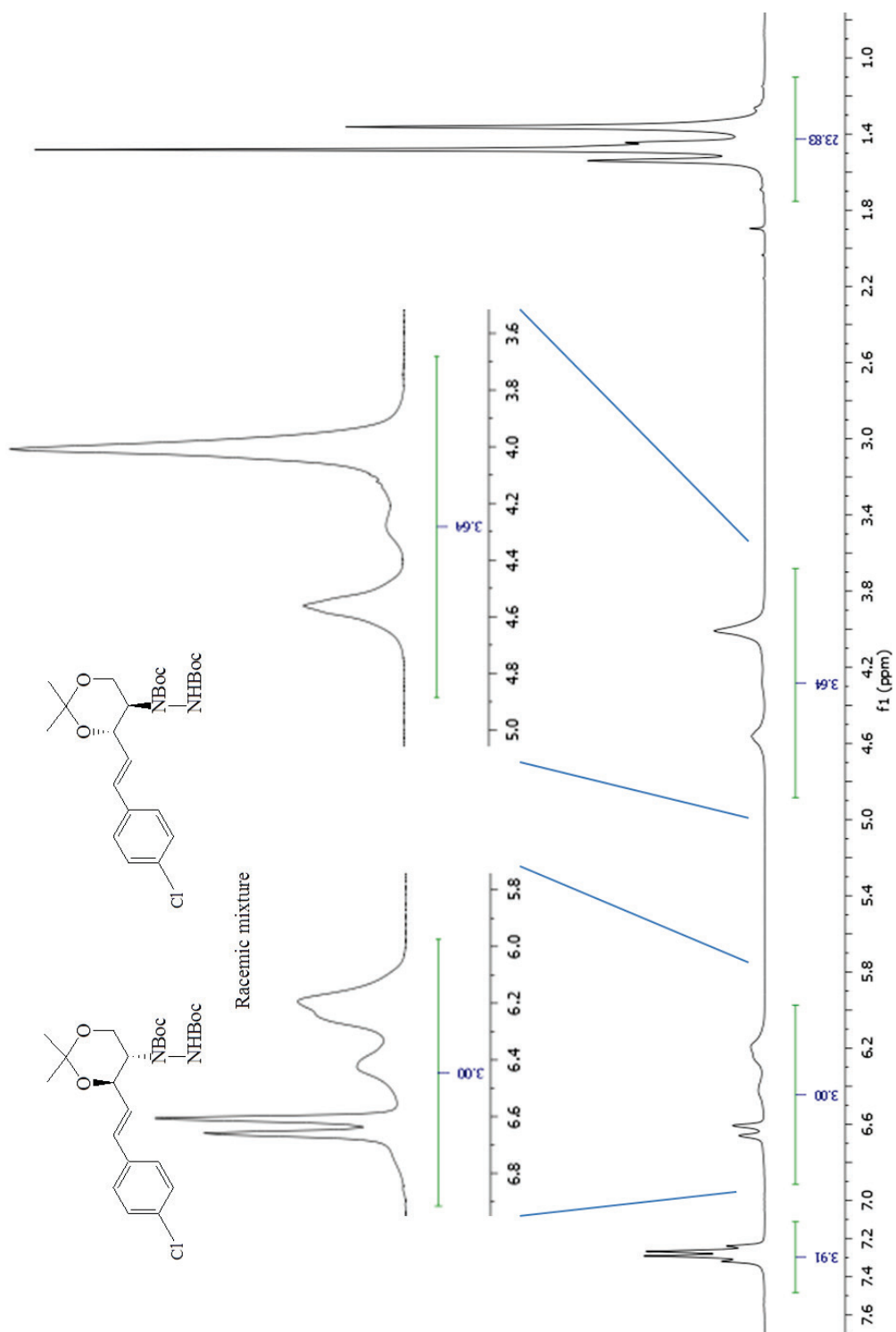


Figure B3.20. ^1H NMR spectrum of (*E*)-2-[1,2-bis(*tert*-butoxycarbonyl)hydrazino]-5-(4-chlorophenyl)-2,4,5-trideoxy-1,3-O-(1-methylethylidene)-*D*-*erythro*-pent-4-enitol (**6C**) in CDCl_3 .

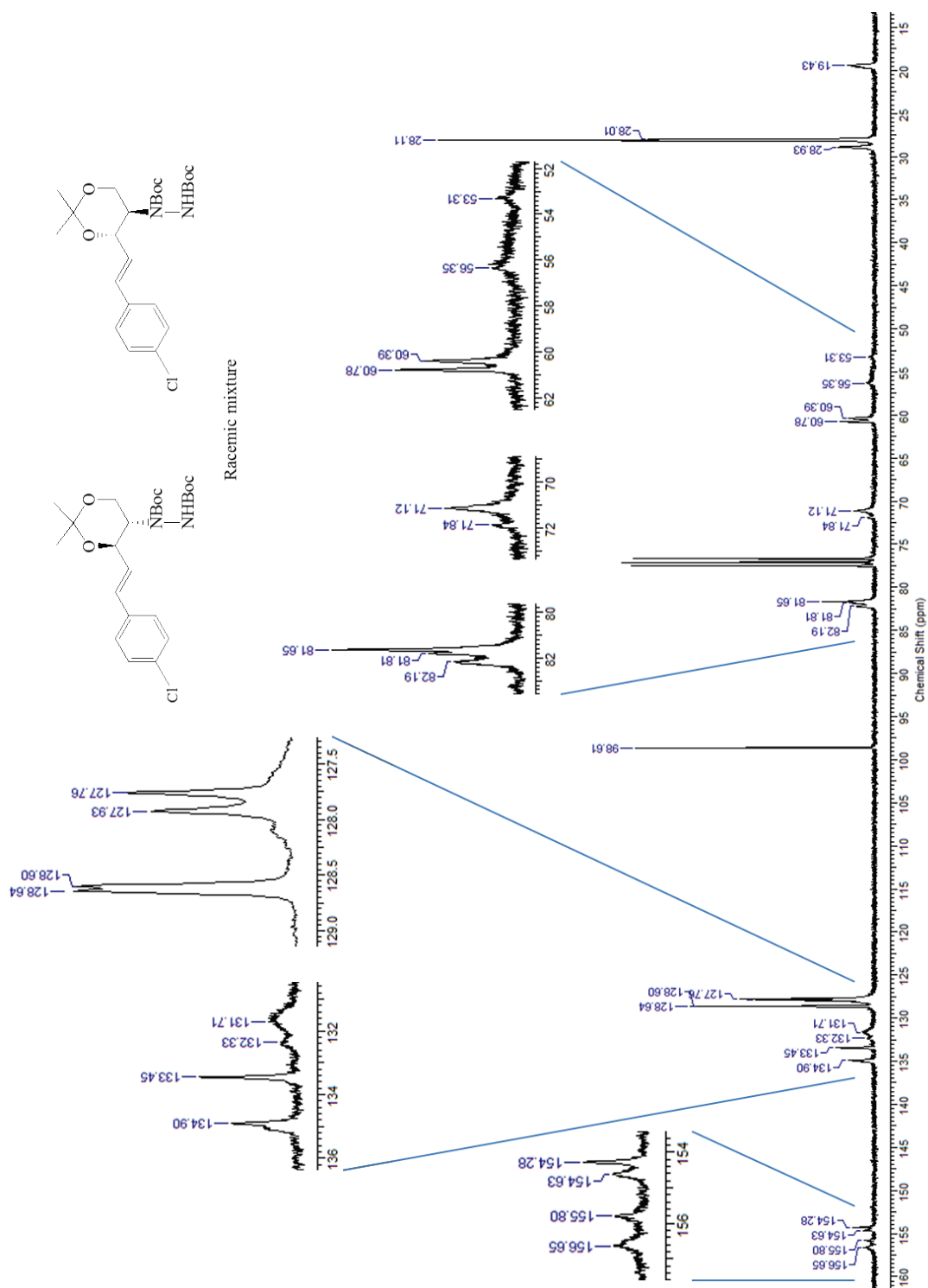


Figure B3.22. ^{13}C NMR spectrum of *(4E)*-2-[1,2-bis(*tert*-butoxycarbonyl)hydrazino]-5-(4-chlorophenyl)-2,4,5-trideoxy-1,3-O-(1-methylethylidene)-*D*-*erythro*-pent-4-enitol (**6C**) in CDCl_3 .

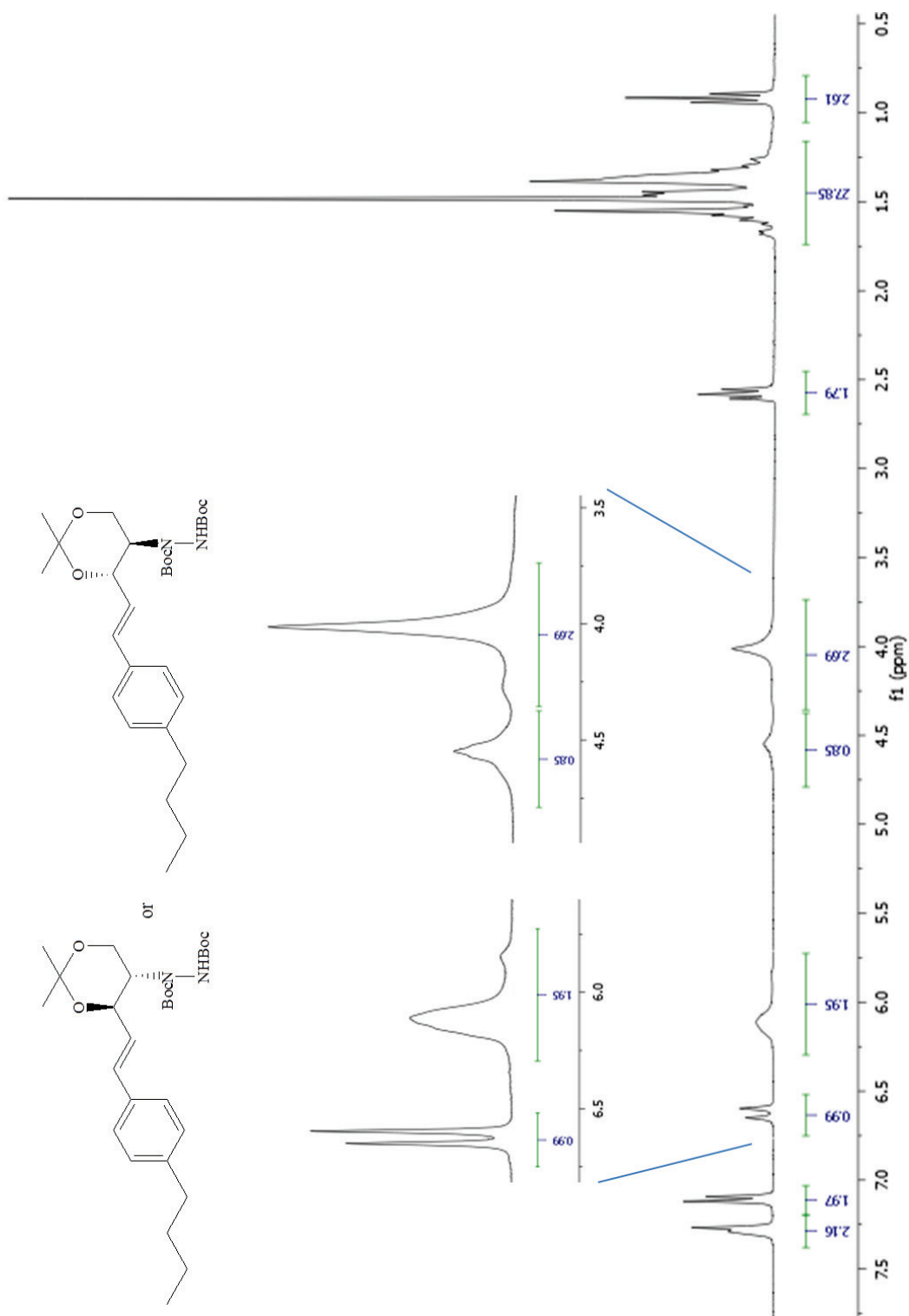


Figure B3.23. ^1H NMR spectrum of (*1E*)-4-[1,2-bis(*tert*-butoxycarbonyl)hydrazino]-1-(4-butylphenyl)-1,2,4-trideoxy-3,5-*O*-(1-methylethylidene)pent-1-enitol (**6E**) in CDCl_3 .

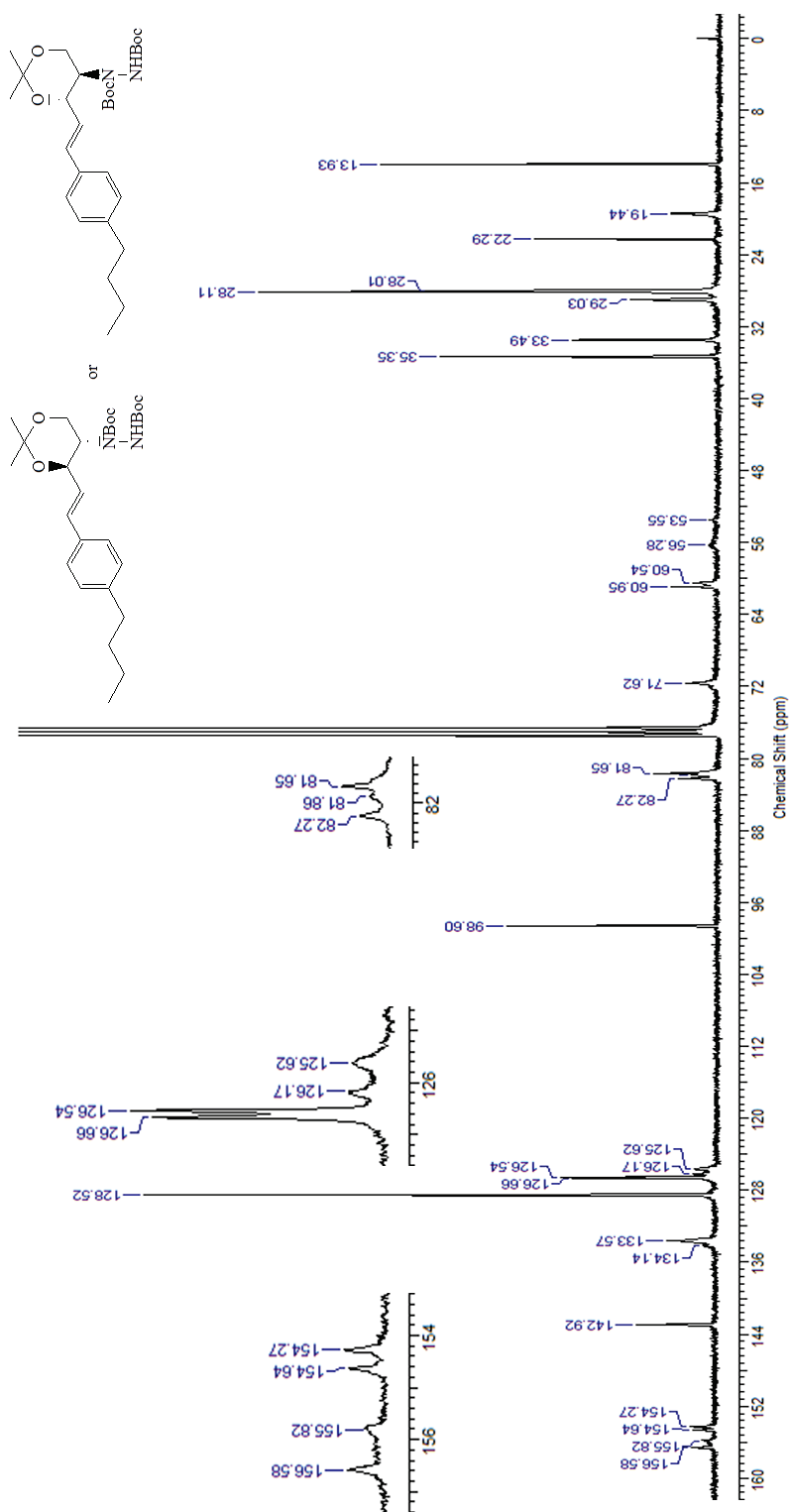


Figure B3.24. ^{13}C NMR spectrum of $(1E)$ -4-[1,2-bis(*tert*-butoxycarbonyl)hydrazino]-1-(4-butylphenyl)-1,2,4-trideoxy-3,5-*O*-(1-methylethylidene)pent-1-enitol (**6E**) in CDCl_3 .

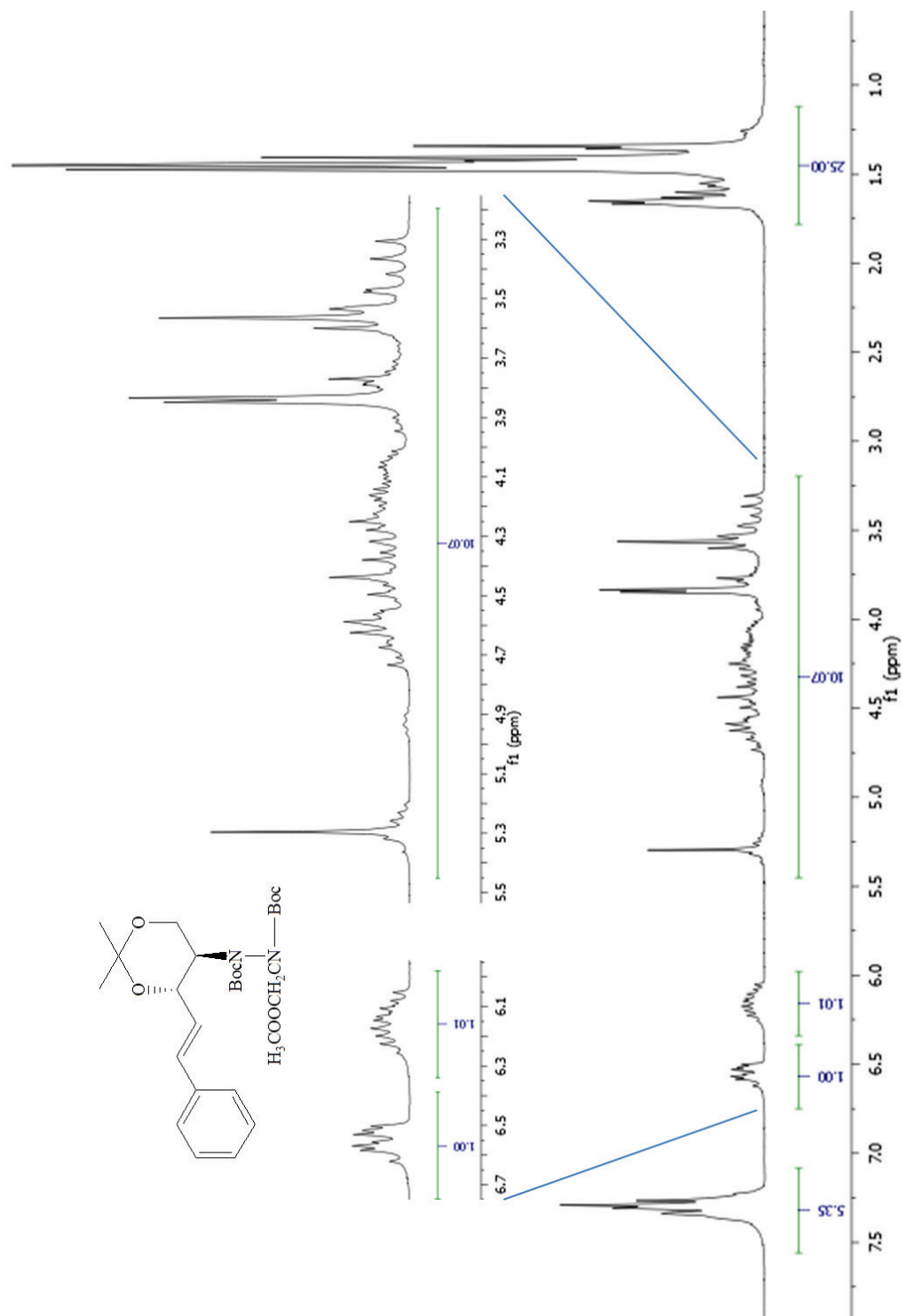


Figure B3.25. ¹H NMR spectrum of (*1E*)-4-[1,2-bis(*tert*-butoxycarbonyl)-2-(2-methoxy-2-oxoethyl)hydrazino]-1,2,4-trideoxy-3,5-*O*-(1-methylethylidene)-1-phenyl-*D*-erythro-pent-enitol (**7A**) in CDCl₃.

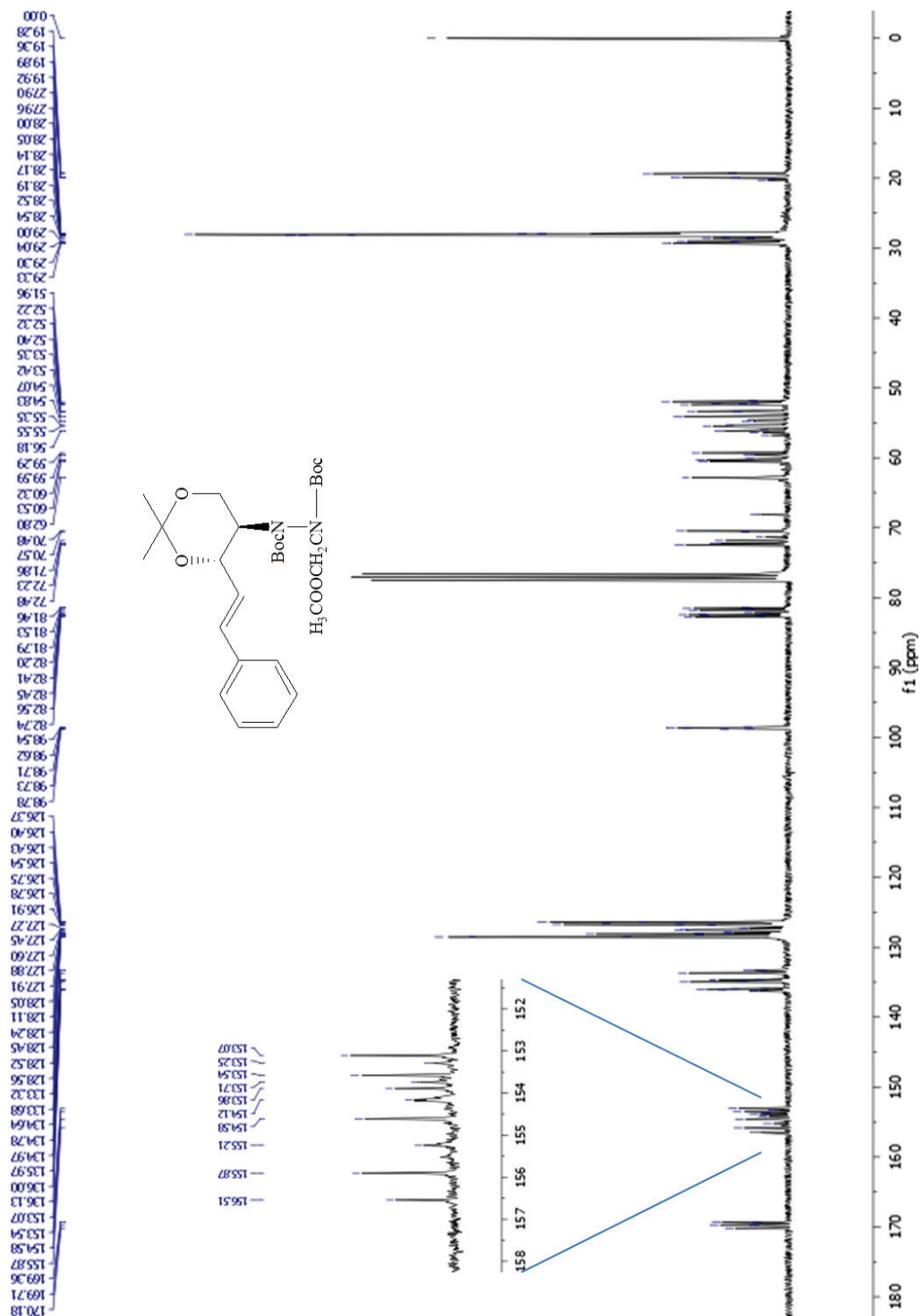


Figure B3.26. ^{13}C NMR spectrum of (*1E*)-4-[1,2-bis(*tert*-butoxycarbonyl)-2-(2-methoxy-2-oxoethyl)hydrazino]-1,2,4-trideoxy-3,5-*O*-(1-methylethylidene)-1-phenyl-*D*-erythro-pent-enitol (7A) in CDCl_3 .

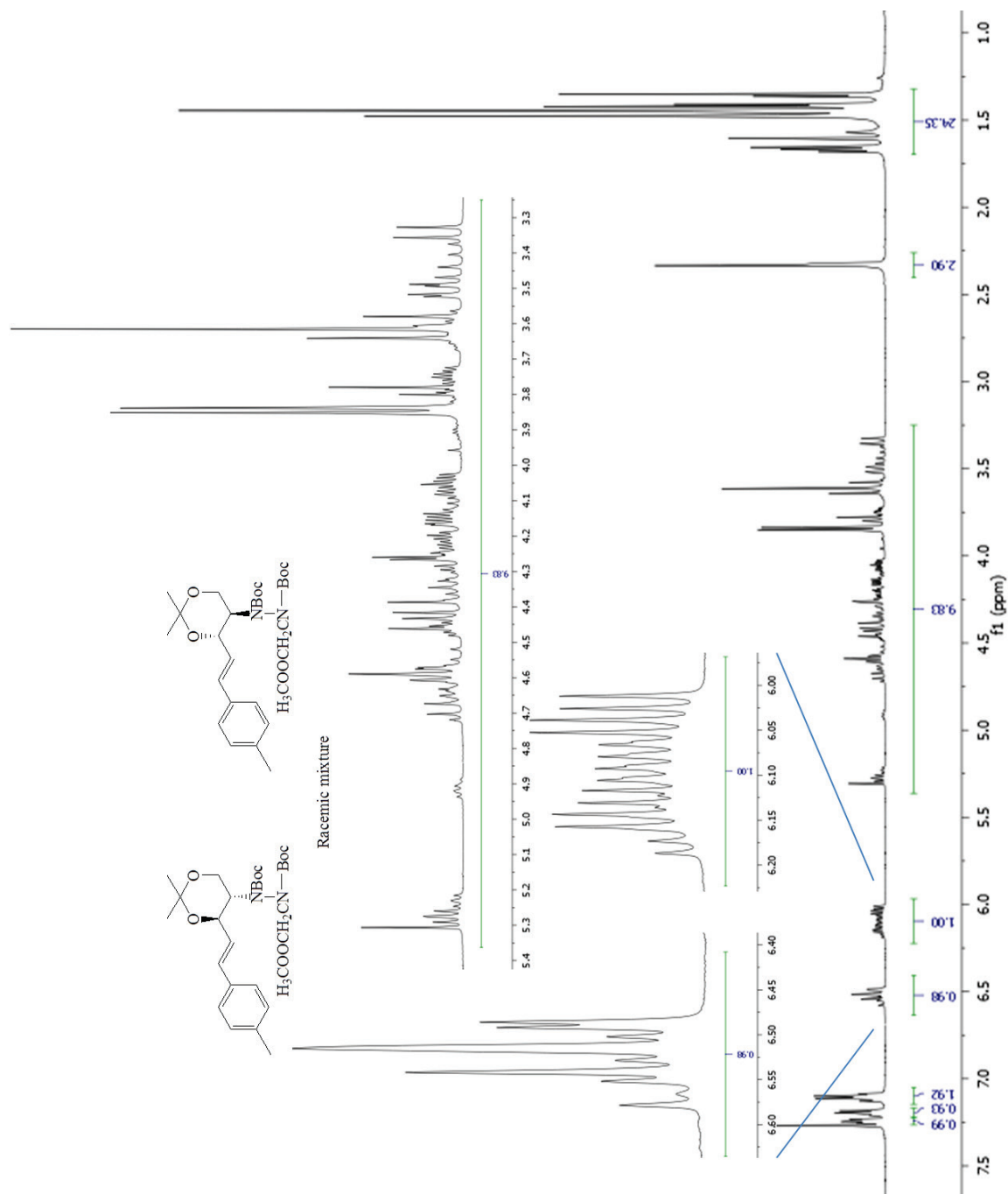


Figure B3.27. ¹H NMR spectrum of (*1E*)-4-[1,2-bis(*tert*-butoxycarbonyl)-2-(2-methoxy-2oxoethyl)hydrazino]-1,2,4-trideoxy-3,5-*O*-(1-methylethylidene)-1-(4-methylphenyl)pent-1-enitol (**7B**) in CDCl₃.

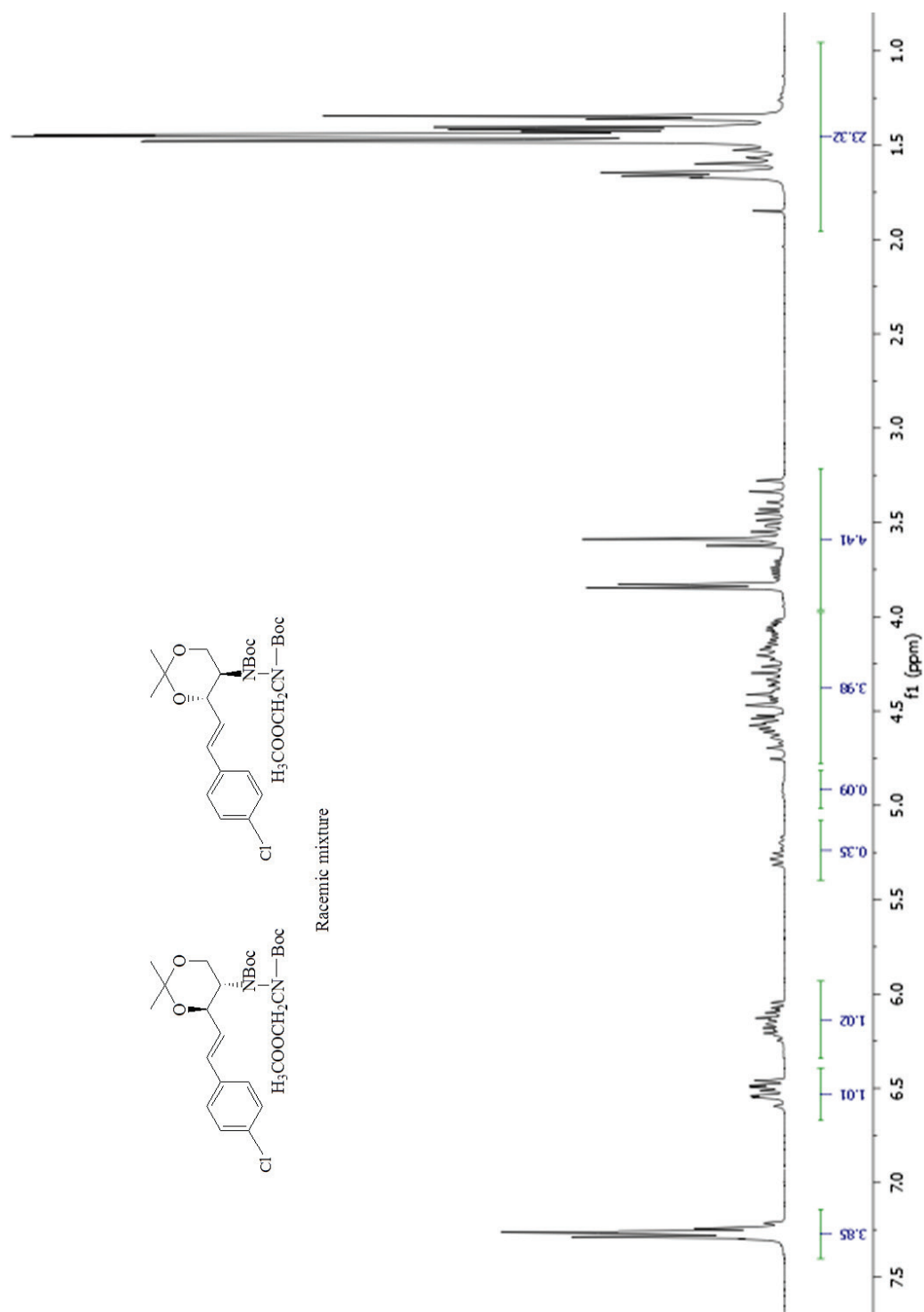


Figure B3.29. ¹H NMR spectrum of (*1E*)-4-[1,2-bis(*tert*-butoxycarbonyl)-2-(2-methoxy-2-oxoethyl)hydrazino]-1-(4-chlorophenyl)-1,2,4-trideoxy-3,5-*O*-(1-methylethylidene)pent-1-enitol (**7C**) in CDCl₃ on a 600 MHz Bruker spectroscopy in CDCl₃.

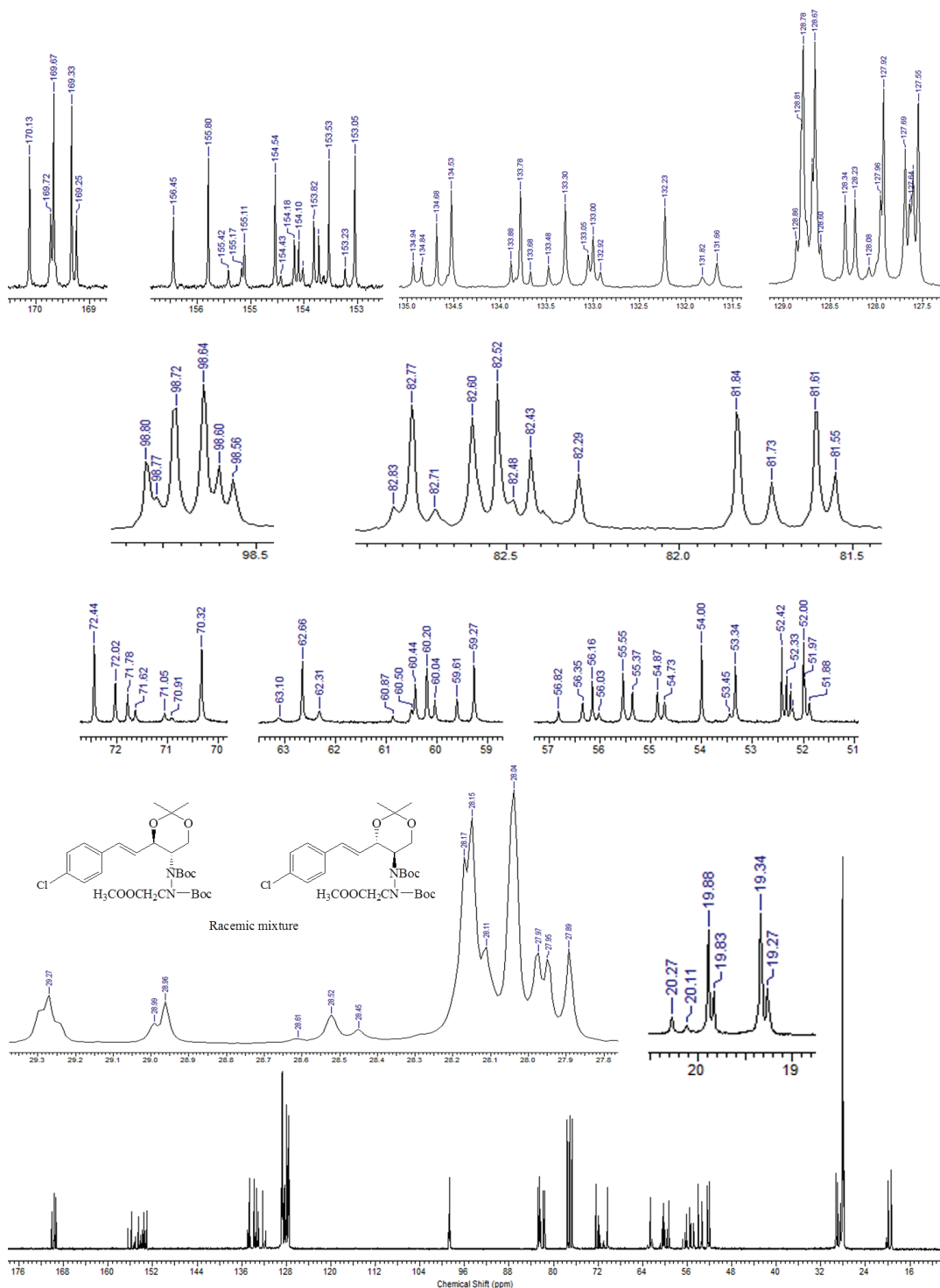


Figure B3.30. ^{13}C NMR spectrum of (*1E*)-4-[1,2-bis(*tert*-butoxycarbonyl)-2-(2-methoxy-2oxoethyl)hydrazino]-1-(4-chlorophenyl)-1,2,4-trideoxy-3,5-*O*-(1-methylethylidene)pent-1-enitol (**7c**) in CDCl_3 on a 600 MHz Bruker spectroscopy in CDCl_3 .

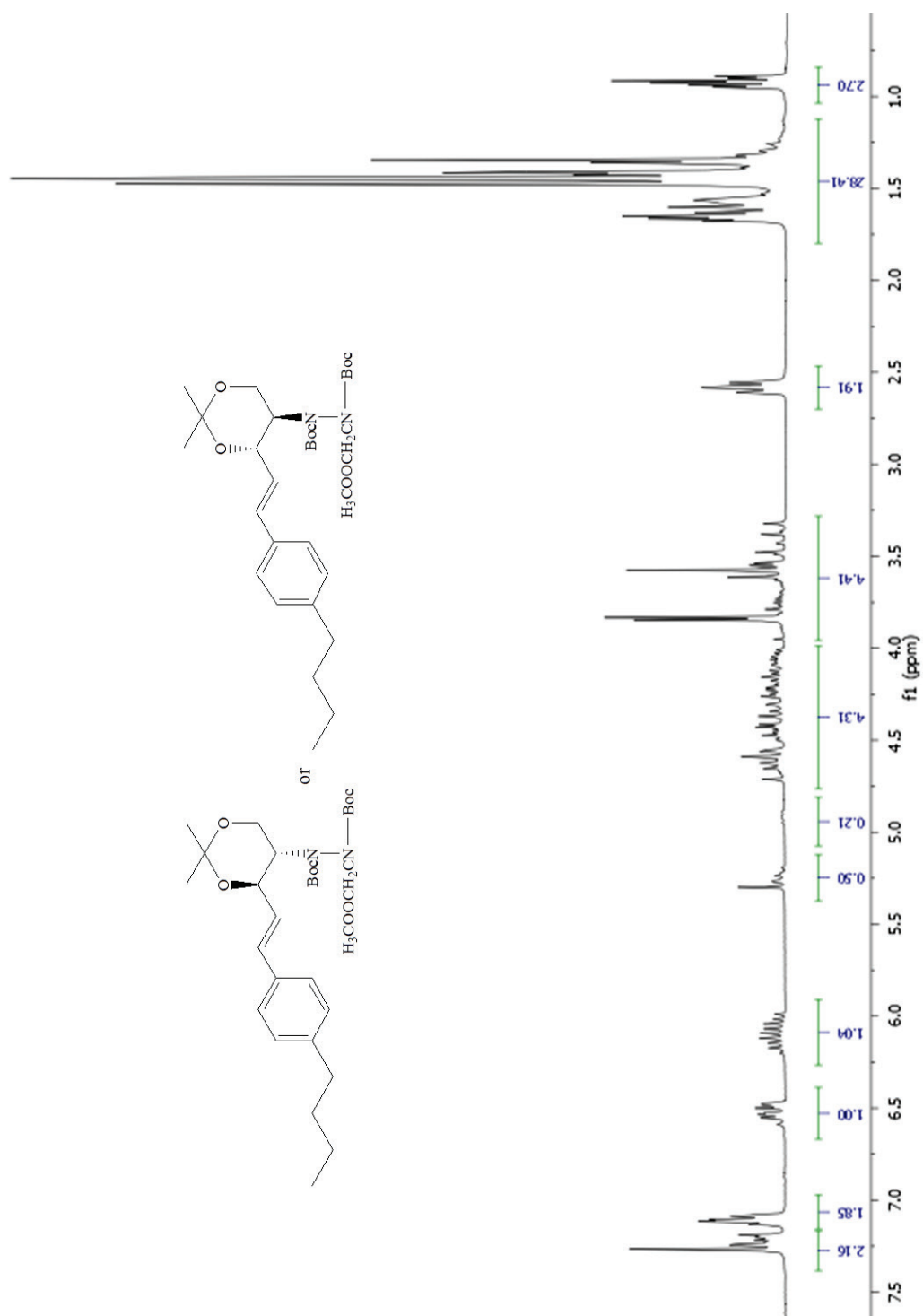


Figure B3.31. ^1H NMR spectrum of (*IE*)-4-[1,2-bis(*tert*-butoxycarbonyl)-2-(2-methoxy-2-oxoethyl)hydrazino]-1-(4-butylphenyl)-1,2,4-trideoxy-3,5-*O*-(1-methylethylidene)pent-1-enitol (**7E**) in CDCl_3 .

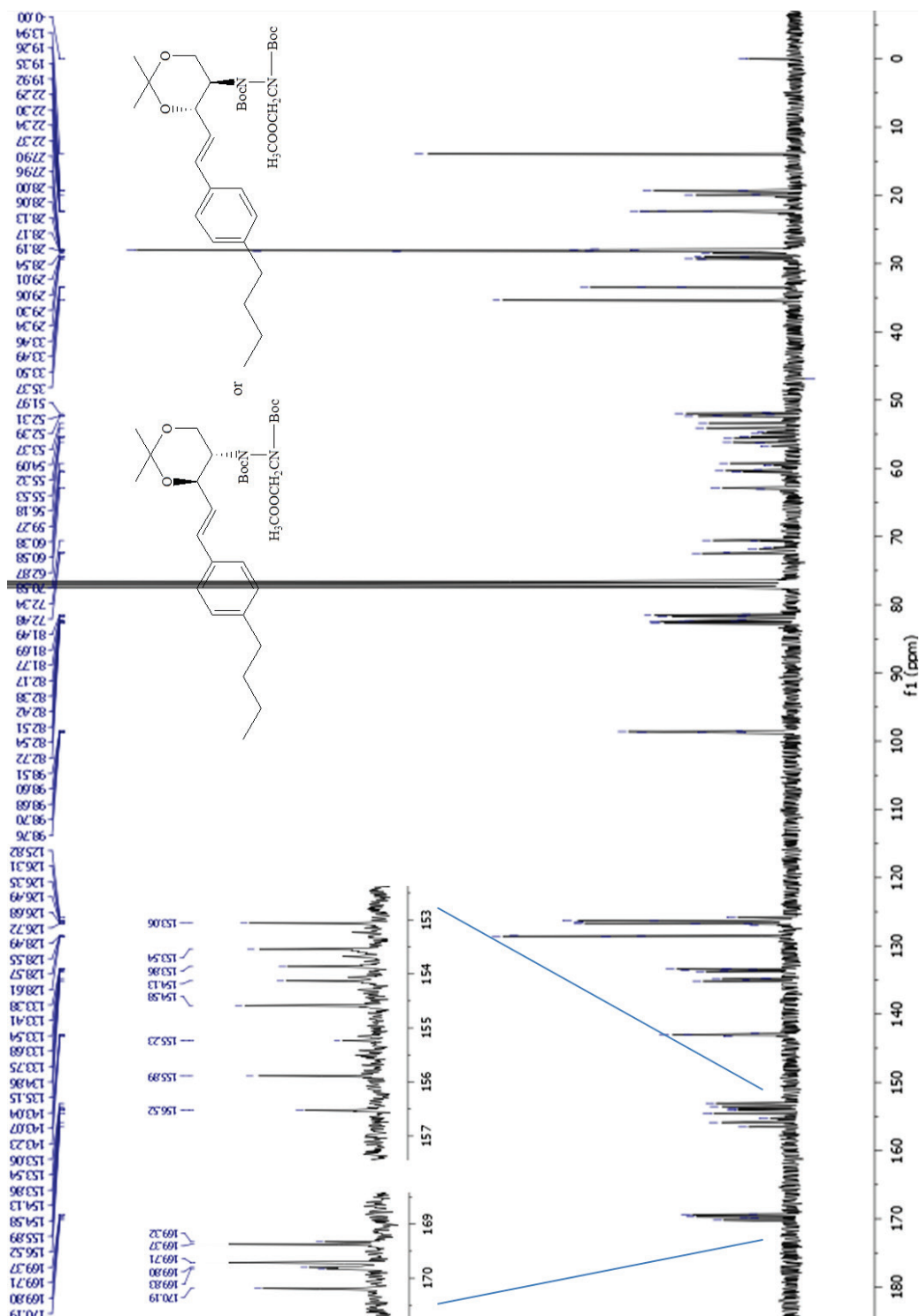


Figure B3.32. ^{13}C NMR spectrum of *(1E)*-4-[1,2-bis(*tert*-butoxycarbonyl)-2-(2-methoxy-2-oxoethyl)hydrazino]-1-(4-butylphenyl)-1,2,4-trideoxy-3,5-*O*-(1-methylethylidene)pent-1-enitol (**7E**) in CDCl_3 .

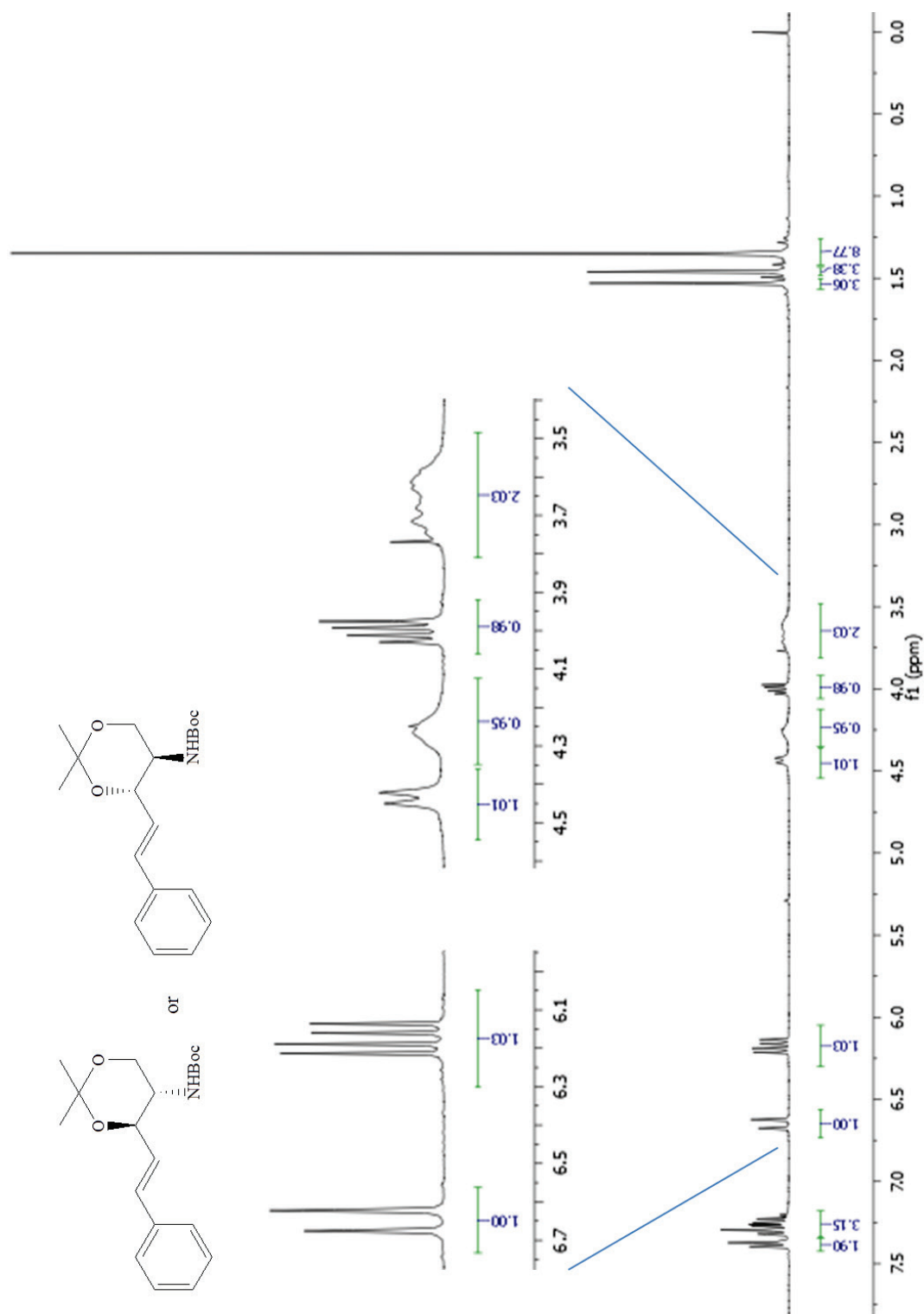


Figure B3.33. ¹H NMR spectrum of (1*E*)-4-[(*tert*-butoxycarbonyl)amino]-1,2,4-trideoxy-3,5-*O*-(1-methylethylidene)-1-phenylpent-1-enitol (**8A**) in CDCl₃.

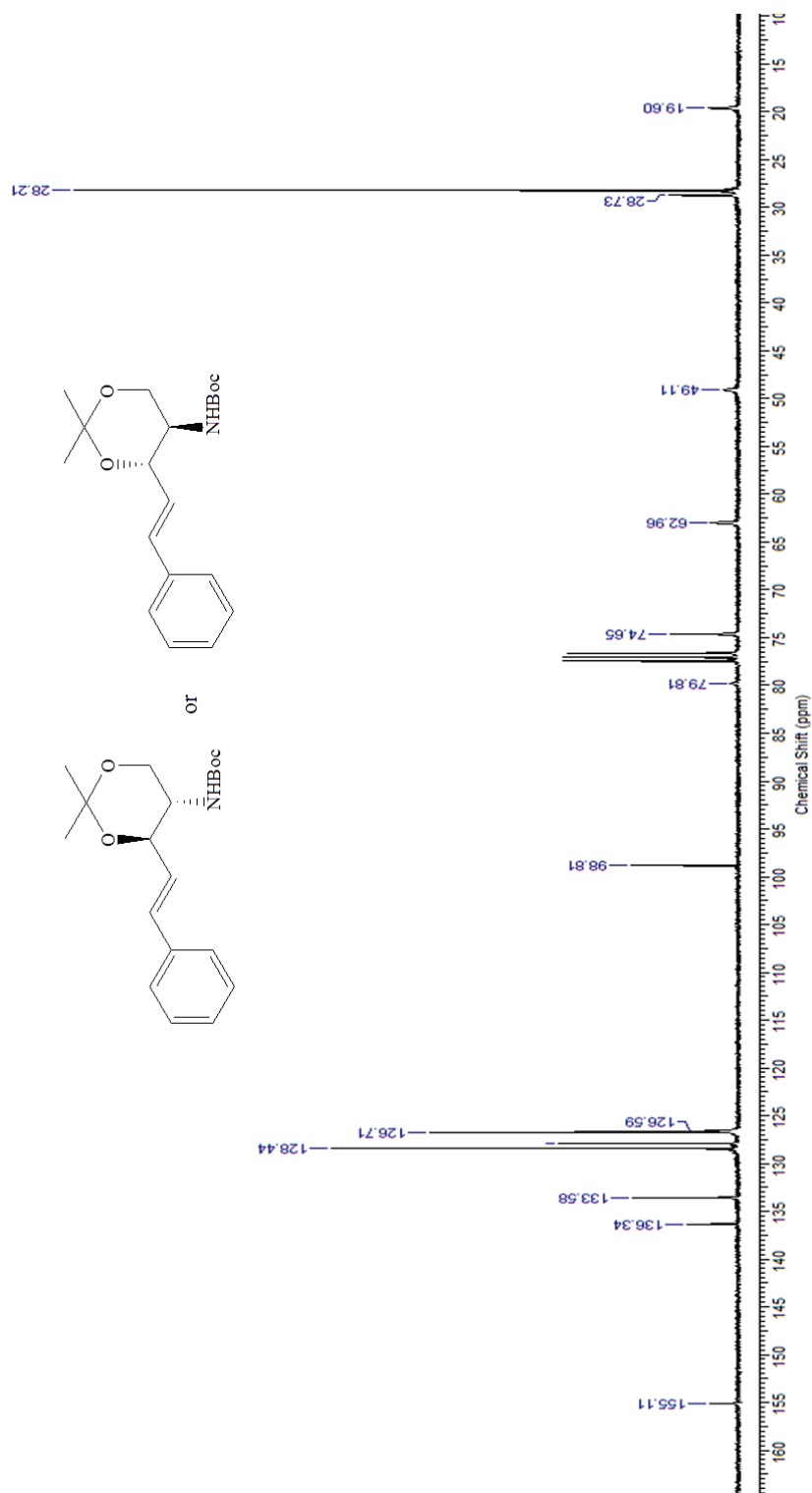


Figure B3.34. ^{13}C NMR spectrum of (1*E*)-4-[(*tert*-butoxycarbonyl)amino]-1,2,4-trideoxy-3,5-*O*-(1-methylethylidene)-1-phenylpent-1-enitol (**8A**) in CDCl_3 .

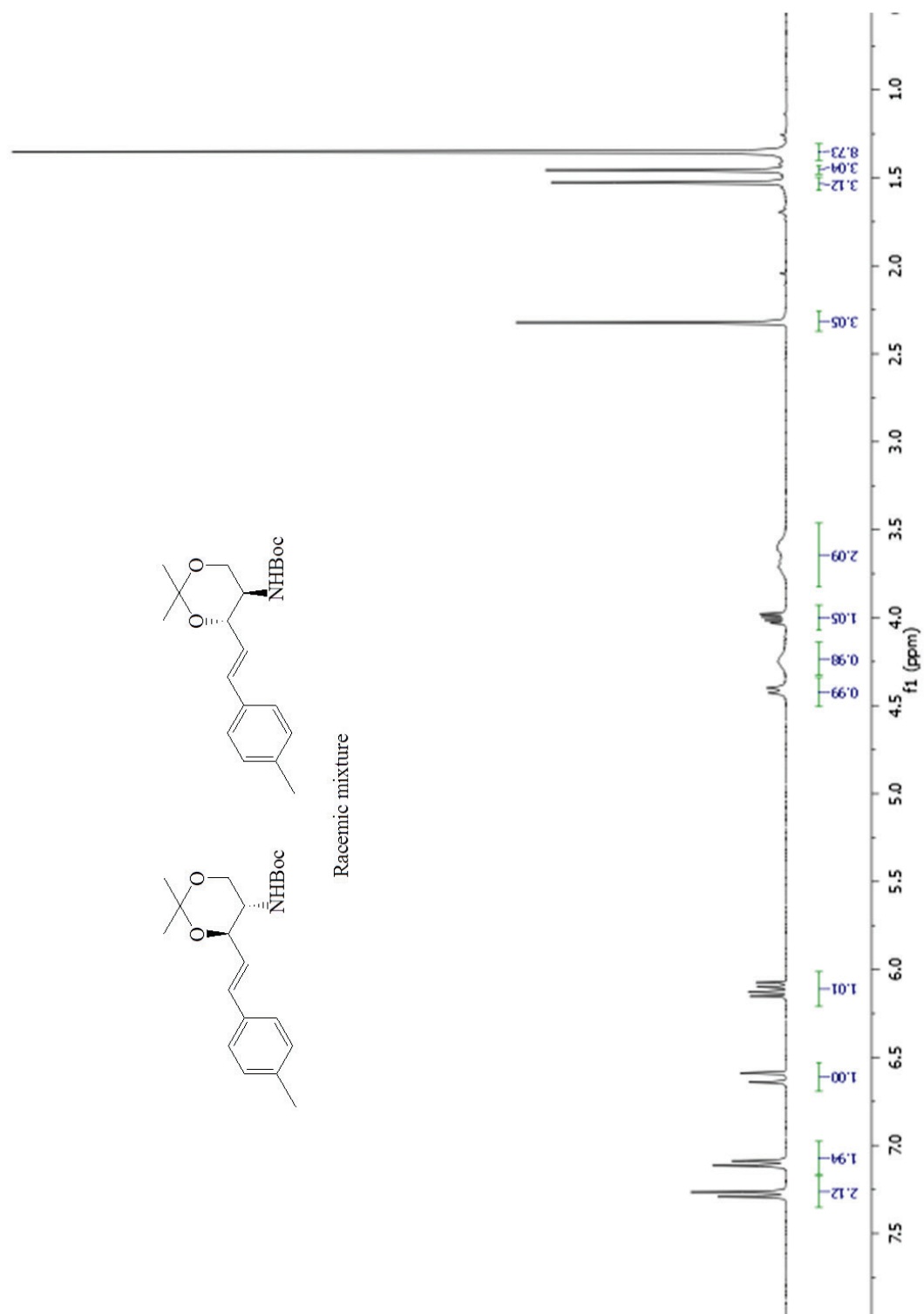


Figure B3.35. ¹H NMR spectrum of (1*E*)-4-[(*tert*-butoxycarbonyl)amino]-1,2,4-trideoxy-3,5-*O*-(1-methylethylidene)-1-(4-methylphenyl)pent-1-enitol (**8B**) in CDCl₃.

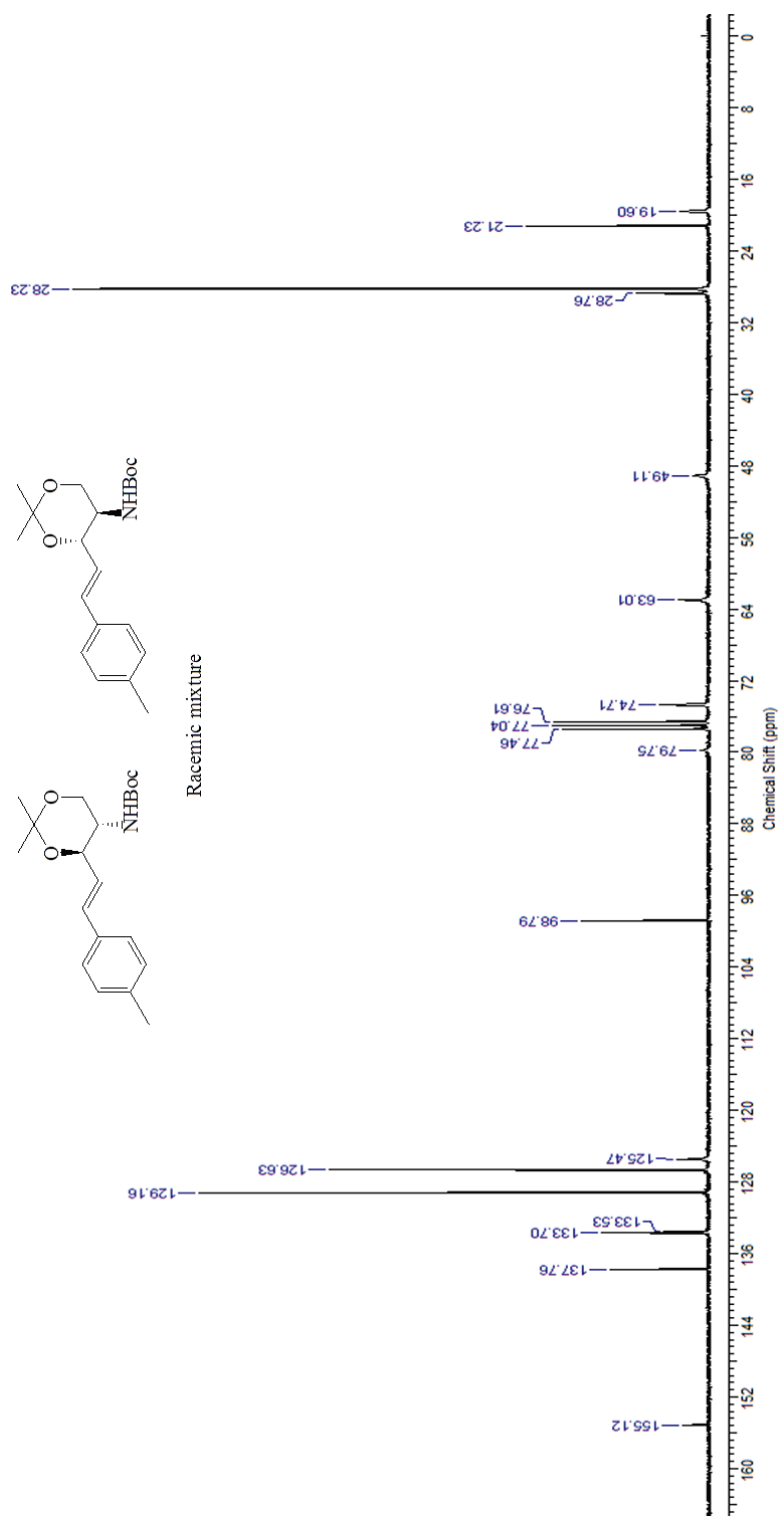


Figure B3.36. ^{13}C NMR spectrum of (1*E*)-4-[(*tert*-butoxycarbonyl)amino]-1,2,4-trideoxy-3,5-*O*-(1-methylethylidene)-1-(4-methylphenyl)pent-1-enitol (**8B**) in CDCl_3 .

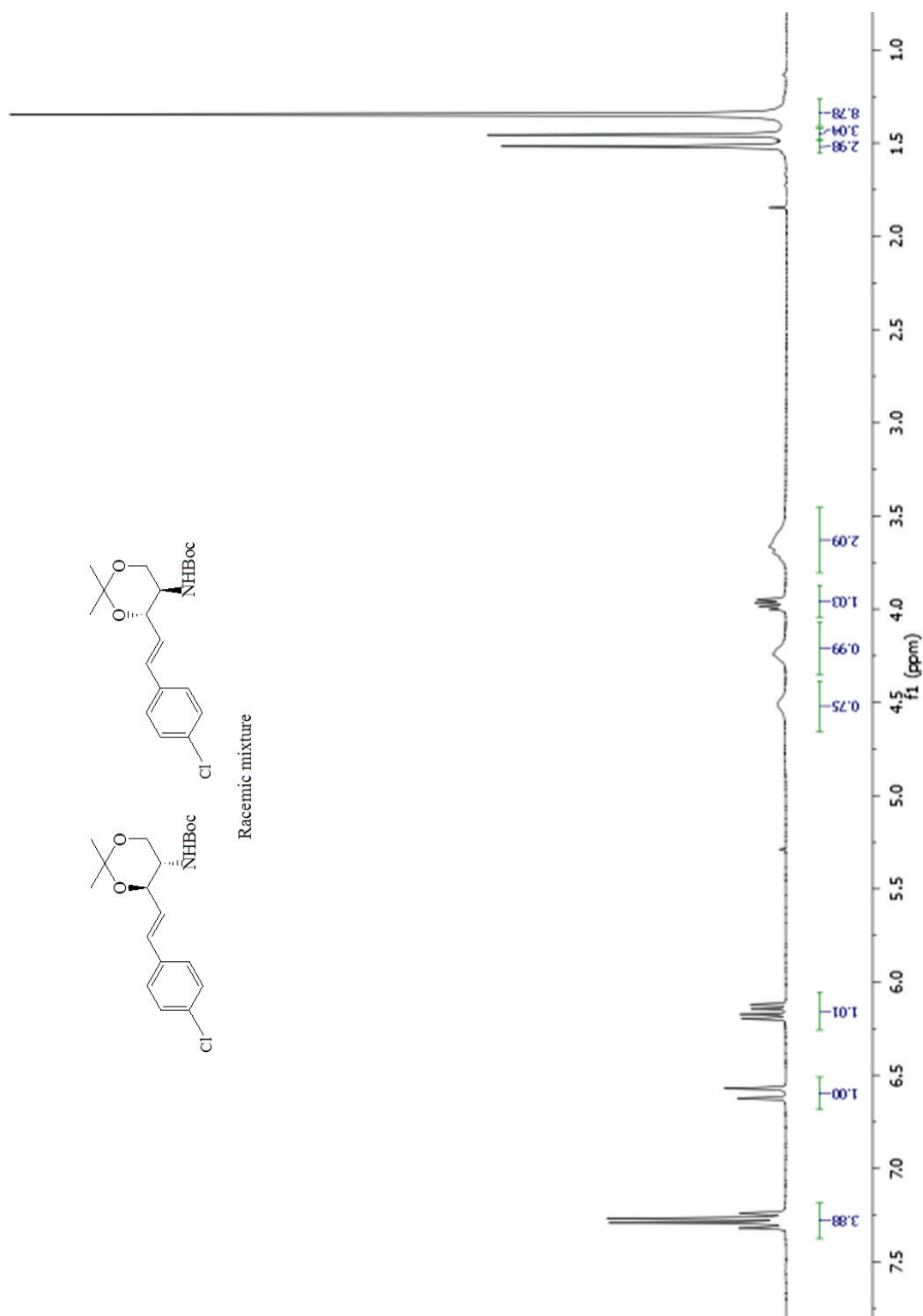


Figure B3.37. ¹H NMR spectrum of (1E)-4-[(*tert*-butoxycarbonyl)amino]-1-(4-methylphenyl)-1,2,4-trideoxy-3,5-*O*-(1-methylethylidene)pent-1-enitol (**8C**) in CDCl₃.

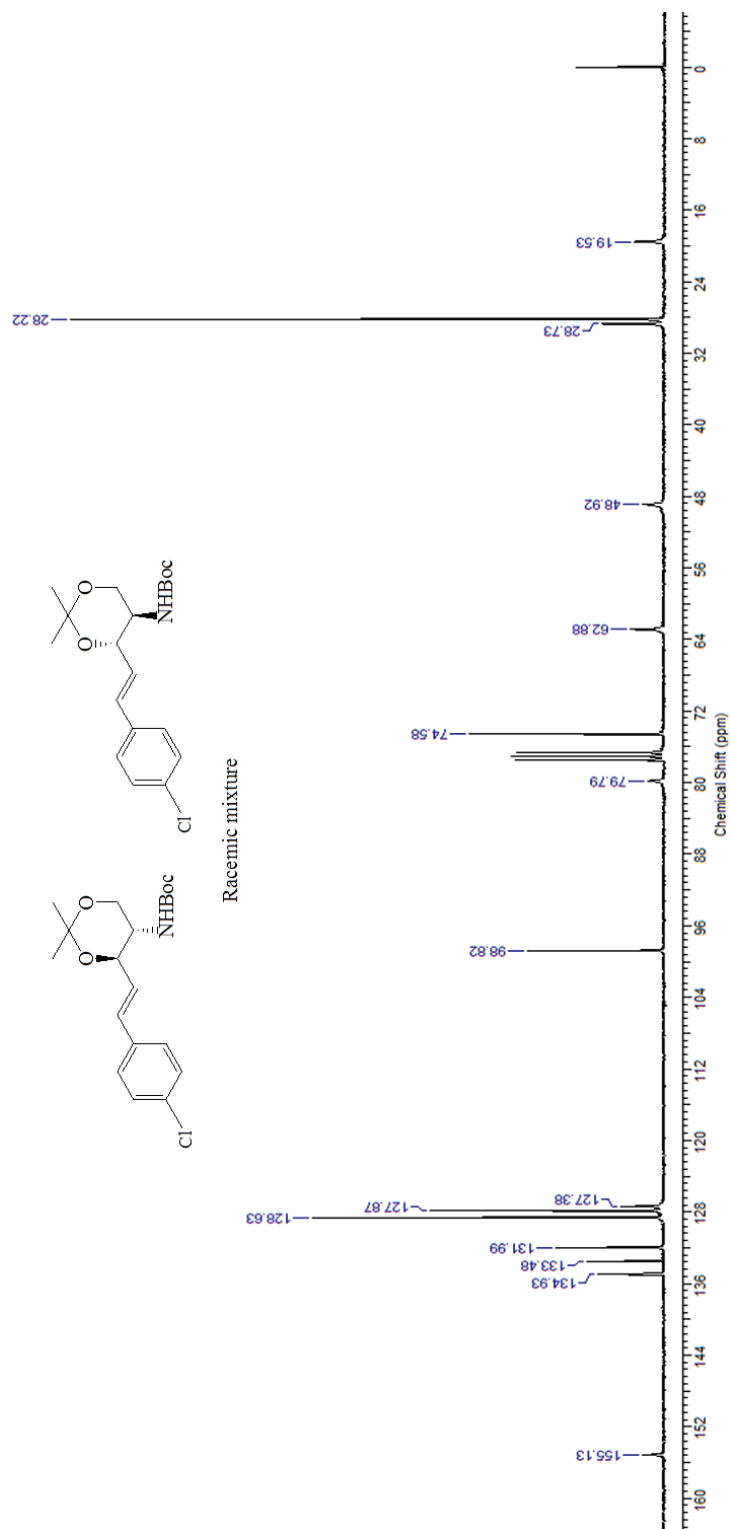


Figure B3.38. ^{13}C NMR spectrum of (1*E*)-4-[(*tert*-butoxycarbonyl)amino]-1-(4-methylphenyl)-1,2,4-trideoxy-3,5-*O*-(1-methylethylidene)pent-1-enitol (**8C**) in CDCl_3 .

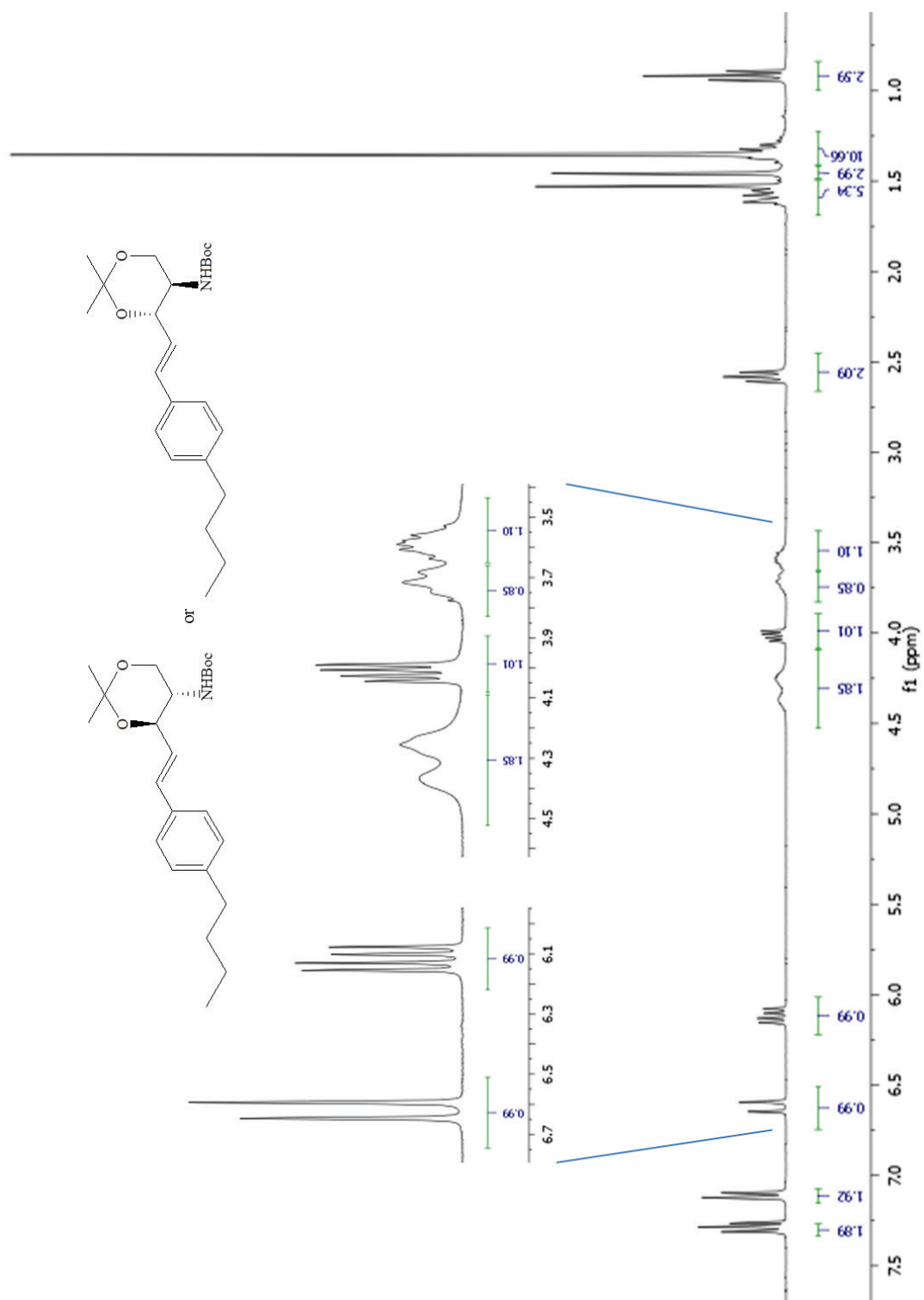


Figure B3.39. ^1H NMR spectrum of (1*E*)-4-[(*tert*-butoxycarbonyl)amino]-1-(4-butylphenyl)-1,2,4-trideoxy-3,5-*O*-(1-methylethylidene)pent-1-enitol (**8E**) in CDCl_3 .

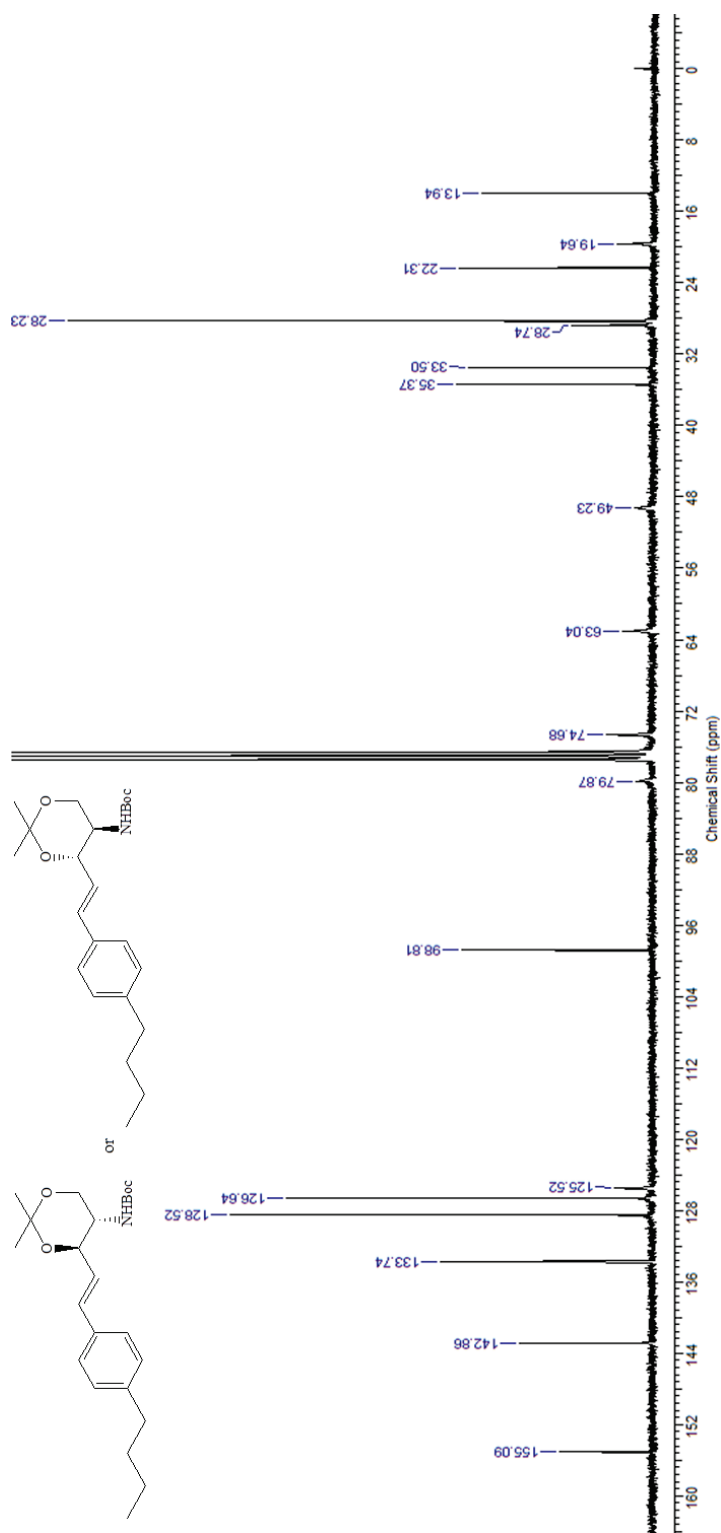


Figure B3.40. ^{13}C NMR spectrum of (1*E*)-4-[(*tert*-butoxycarbonyl)amino]-1-(4-butylphenyl)-1,2,4-trideoxy-3,5-*O*-(1-methylethylidene)pent-1-enitol (**8E**) in CDCl_3 .

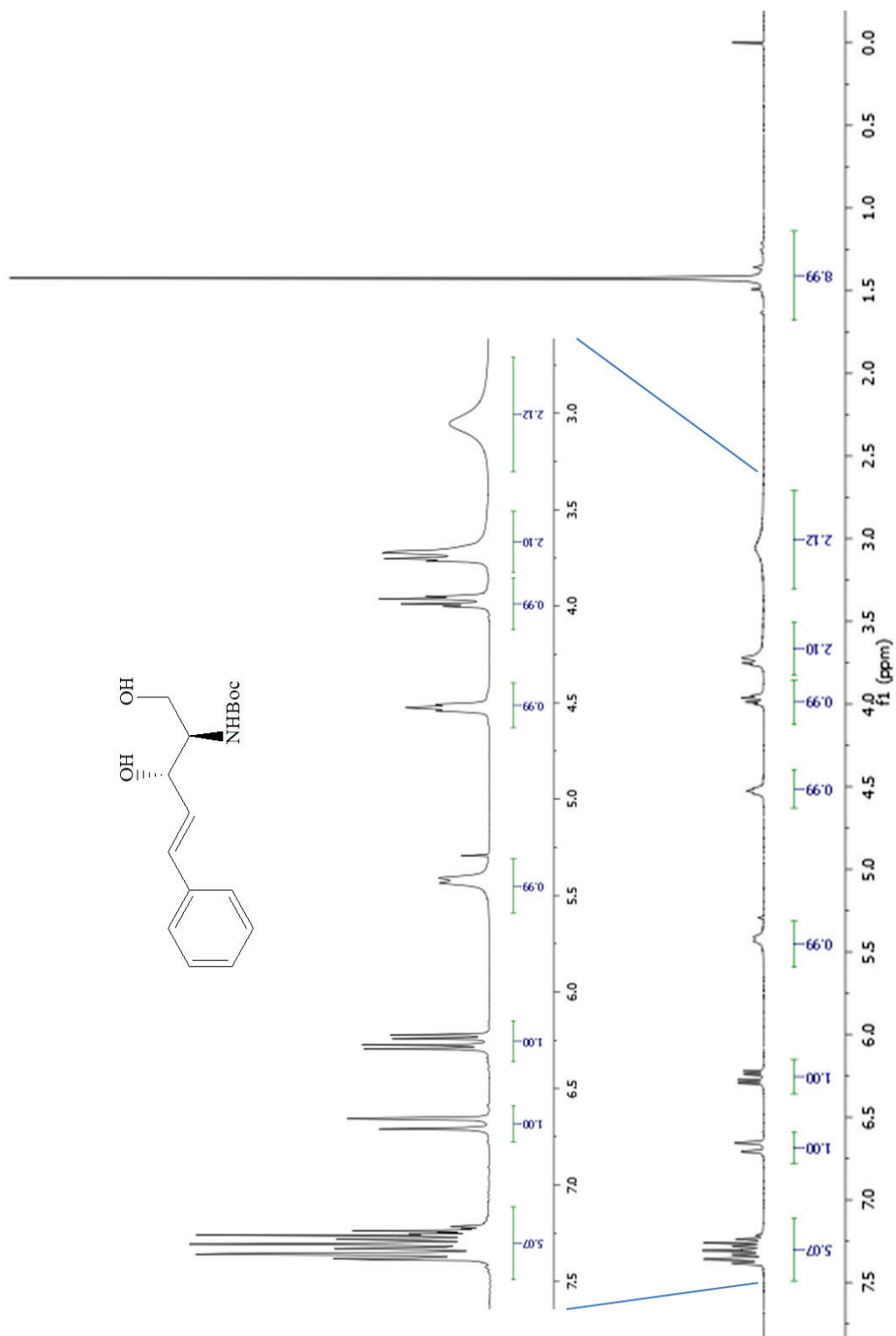


Figure B3.41. ^1H NMR spectrum of (1*E*)-4-[(*tert*-butoxycarbonyl)amino]-1,2,4-trideoxy-1-phenylpent-1-enitol (**9A**) in CDCl_3 .

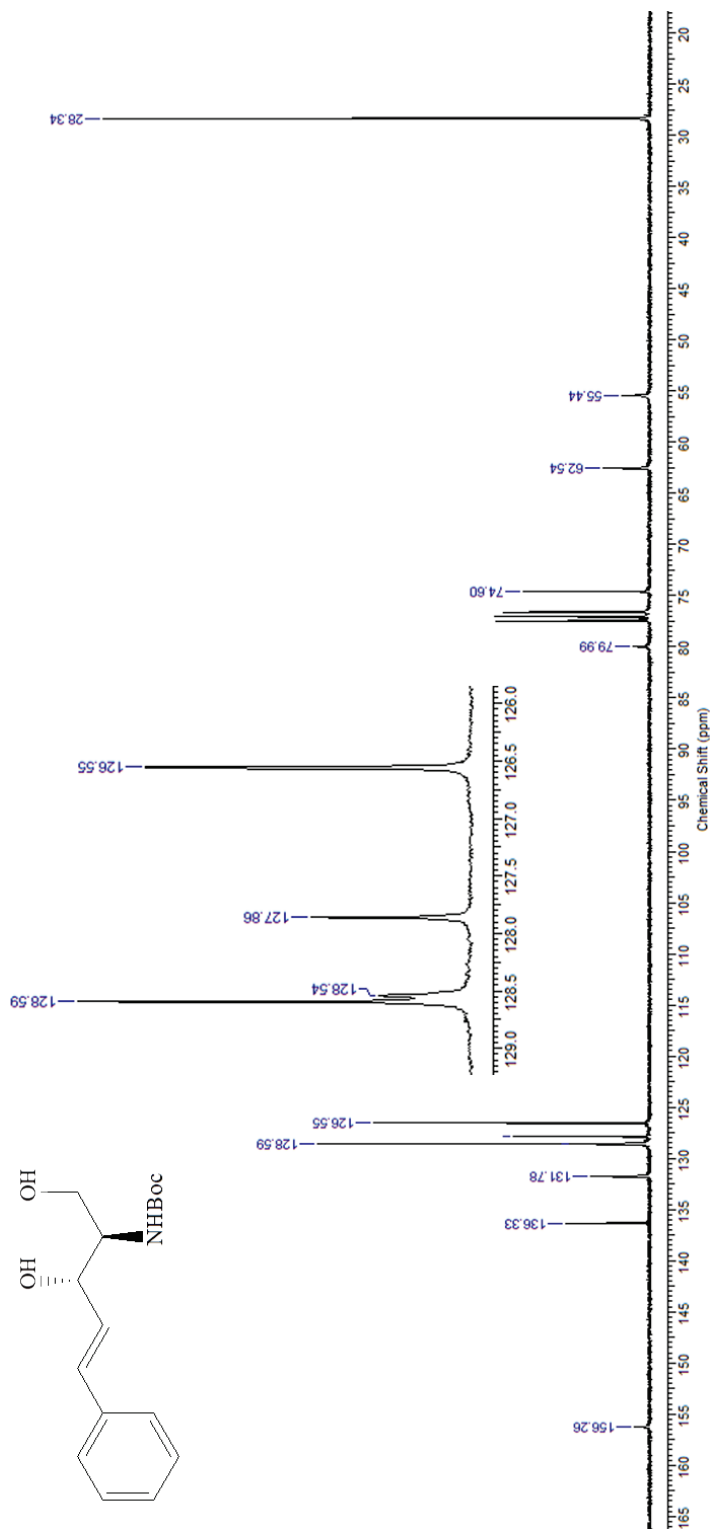


Figure B3.42. ^{13}C NMR spectrum of (1E)-4-[(*tert*-butoxycarbonyl)amino]-1,2,4-trideoxy-1-phenylpent-1-enitol (**9A**) in CDCl_3 .

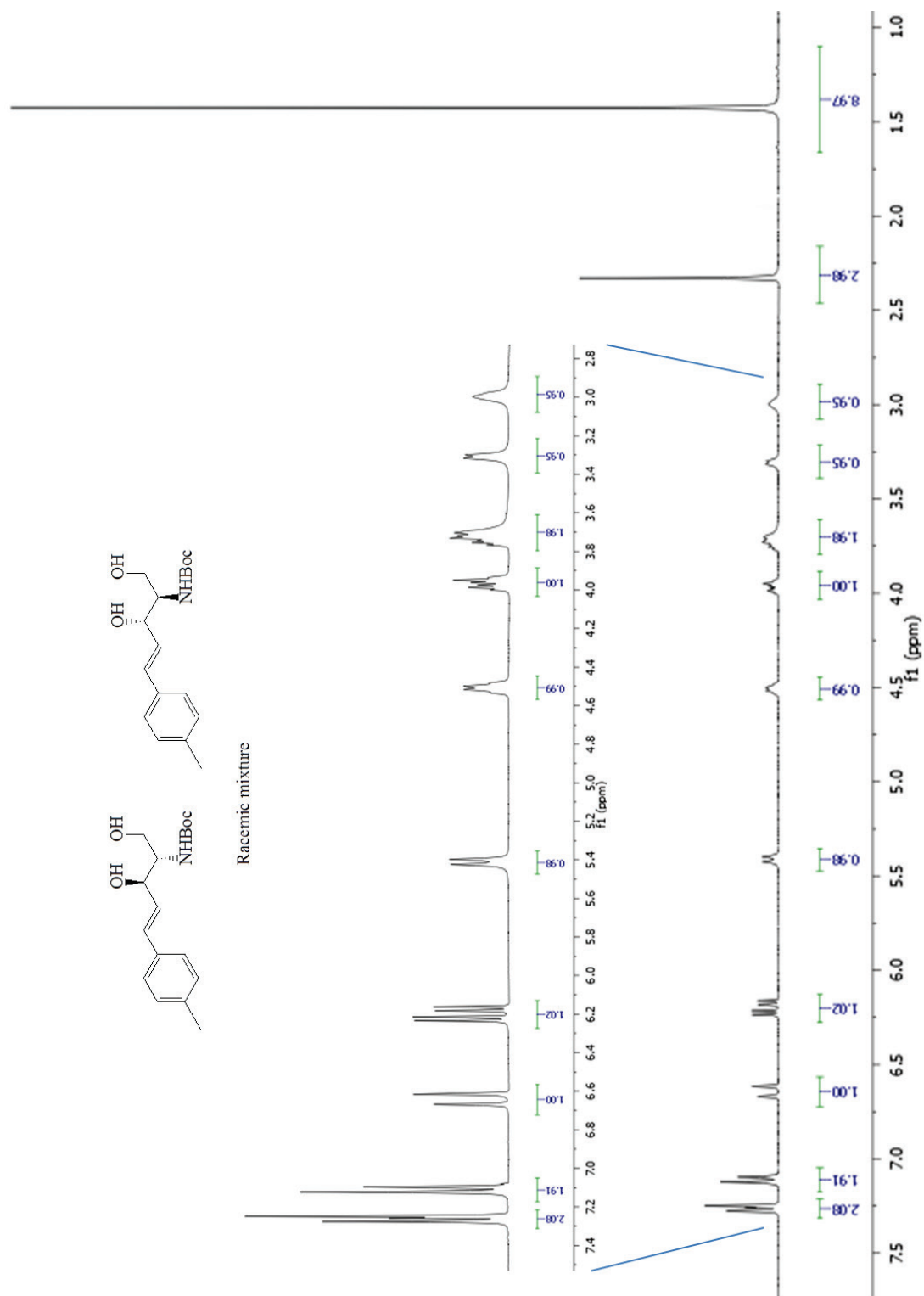


Figure B3.43. ¹H NMR spectrum of (1*E*)-4-[(*tert*-butoxycarbonyl)amino]-1,2,4-trideoxy-1-(4-methylphenyl)pent-1-enitol (**9B**) in CDCl₃.

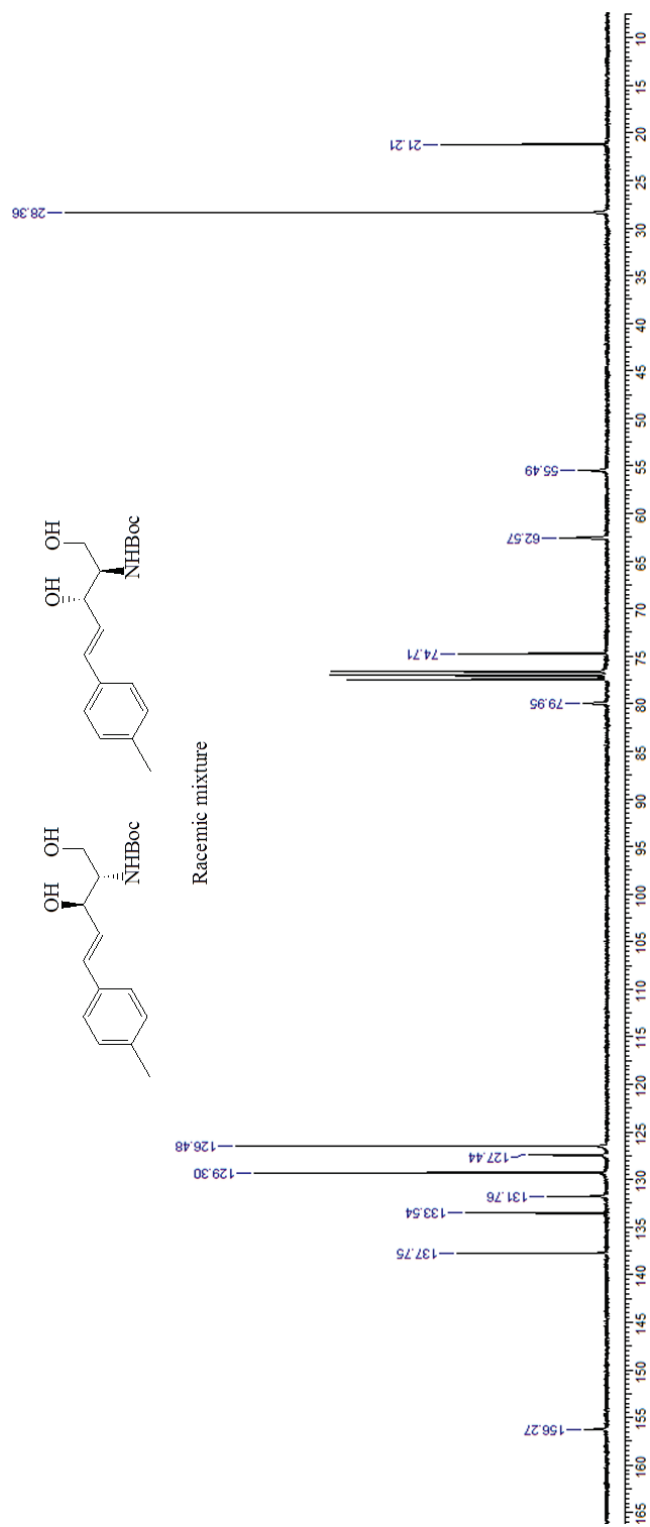


Figure B3.44. ^{13}C NMR spectrum of (1*E*)-4-[(*tert*-butoxycarbonyl)amino]-1,2,4-trideoxy-1-(4-methylphenyl)pent-1-enitol (**9B**) in CDCl_3 .

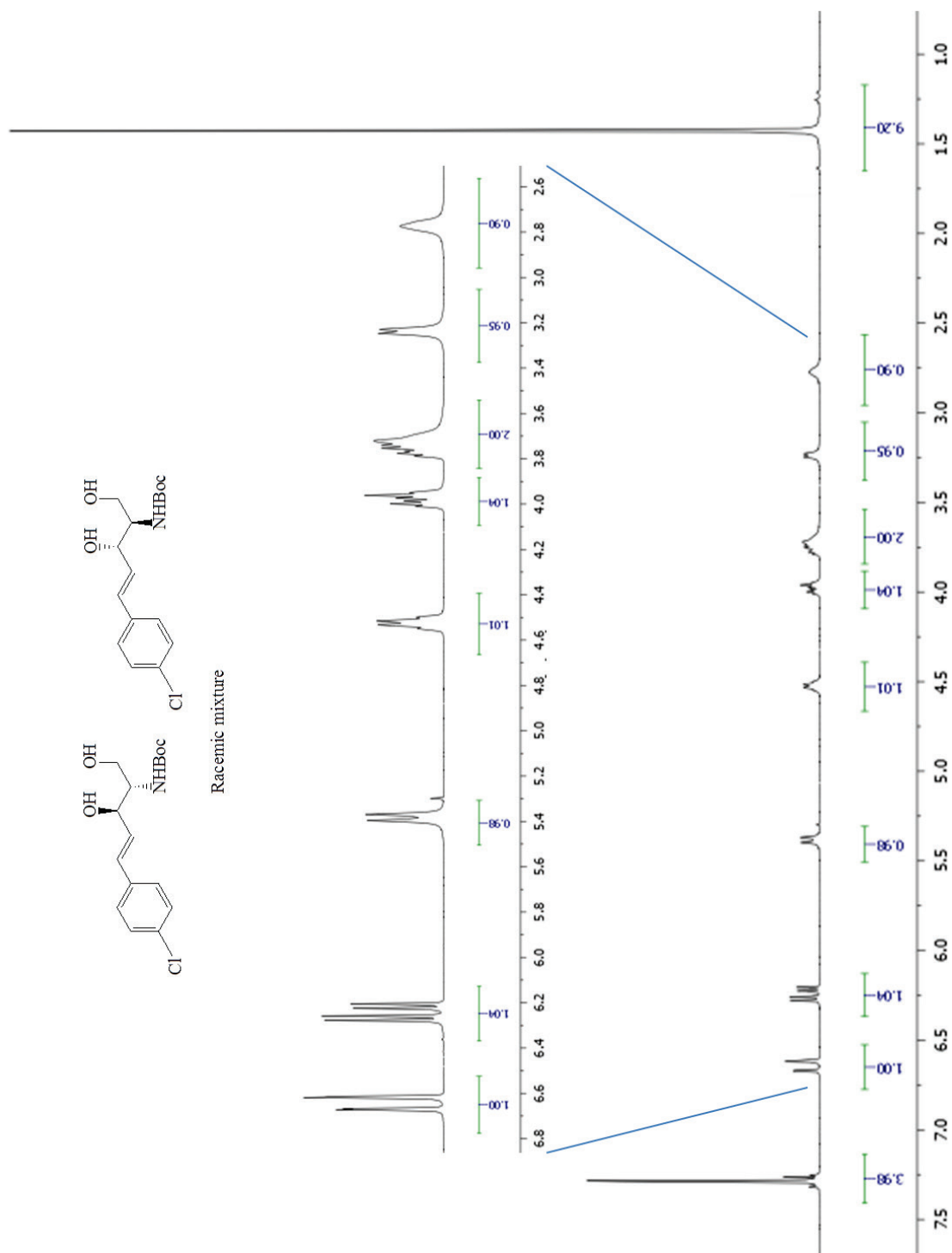


Figure B3.45. ^1H NMR spectrum of (1*E*)-4-[(*tert*-butoxycarbonyl)amino]-1-(4-chlorophenyl)-1,2,4-trideoxypent-1-enitol (**9C**) in CDCl_3 .

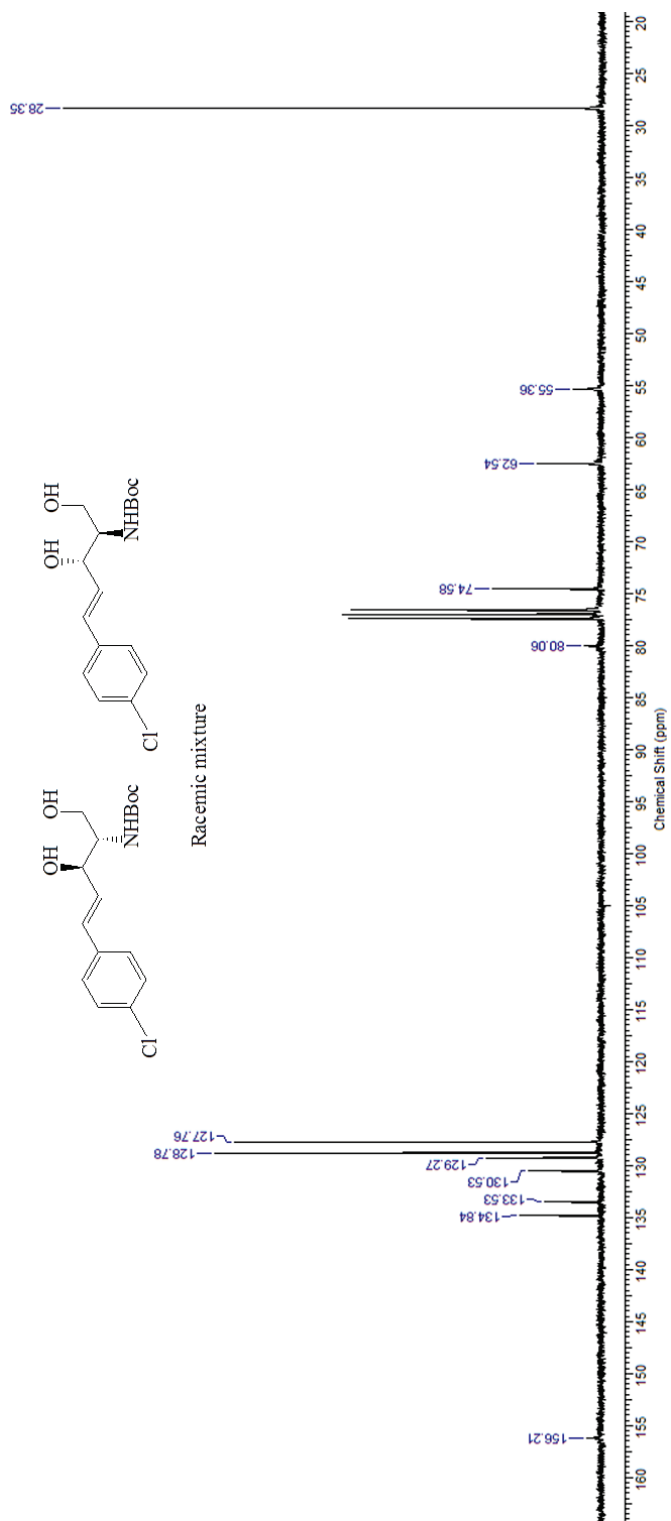


Figure B3.46. ^{13}C NMR spectrum of (1*E*)-4-[(*tert*-butoxycarbonyl)amino]-1-(4-chlorophenyl)-1,2,4-trideoxypent-1-enitol (**9C**) in CDCl_3 .

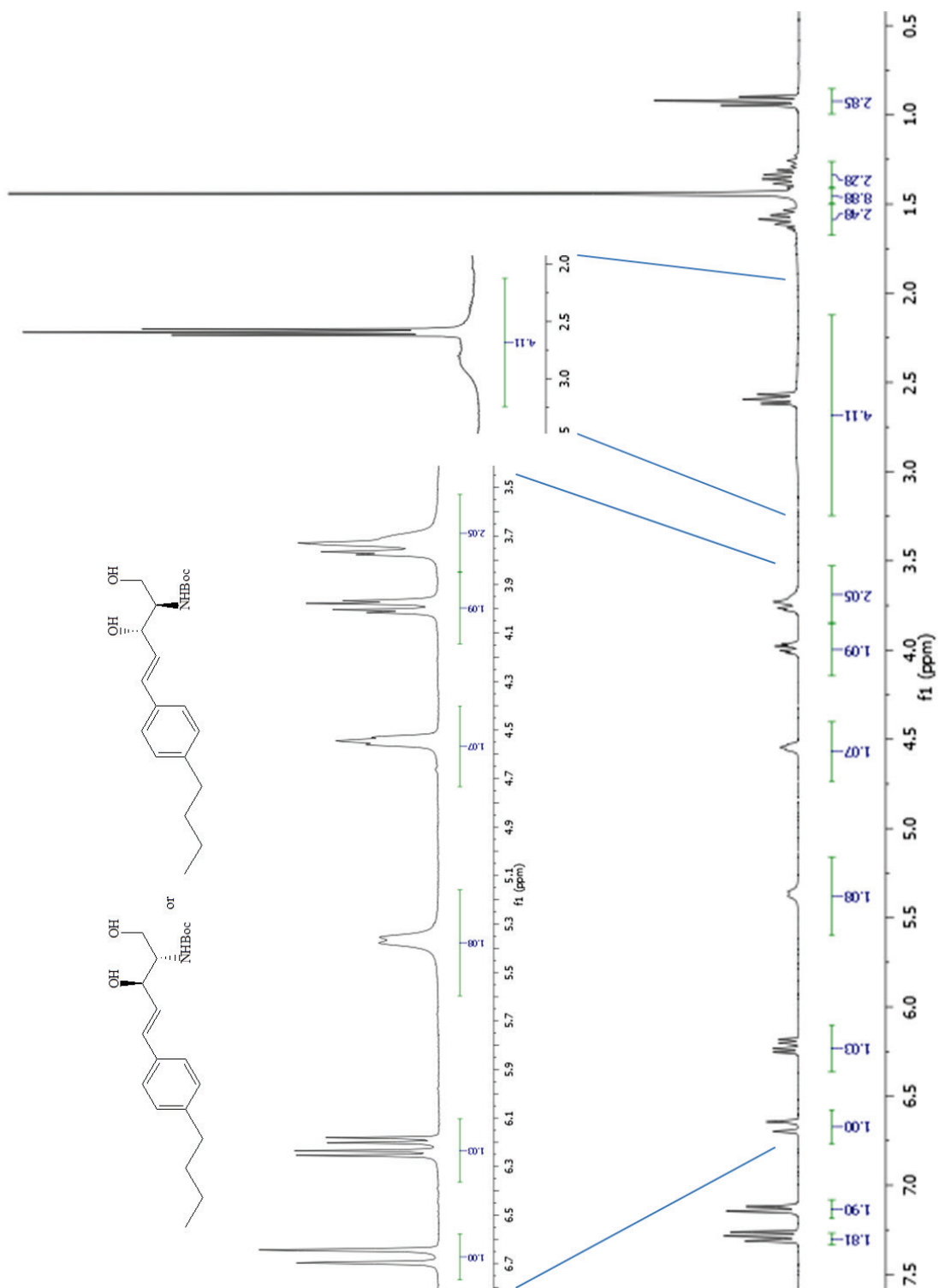


Figure B3.47. ^1H NMR spectrum (1*E*)-4-[(*tert*-butoxycarbonyl)amino]-1-(4-butylphenyl)-1,2,4-trideoxypent-1-enitol (**9E**) in CDCl_3 .

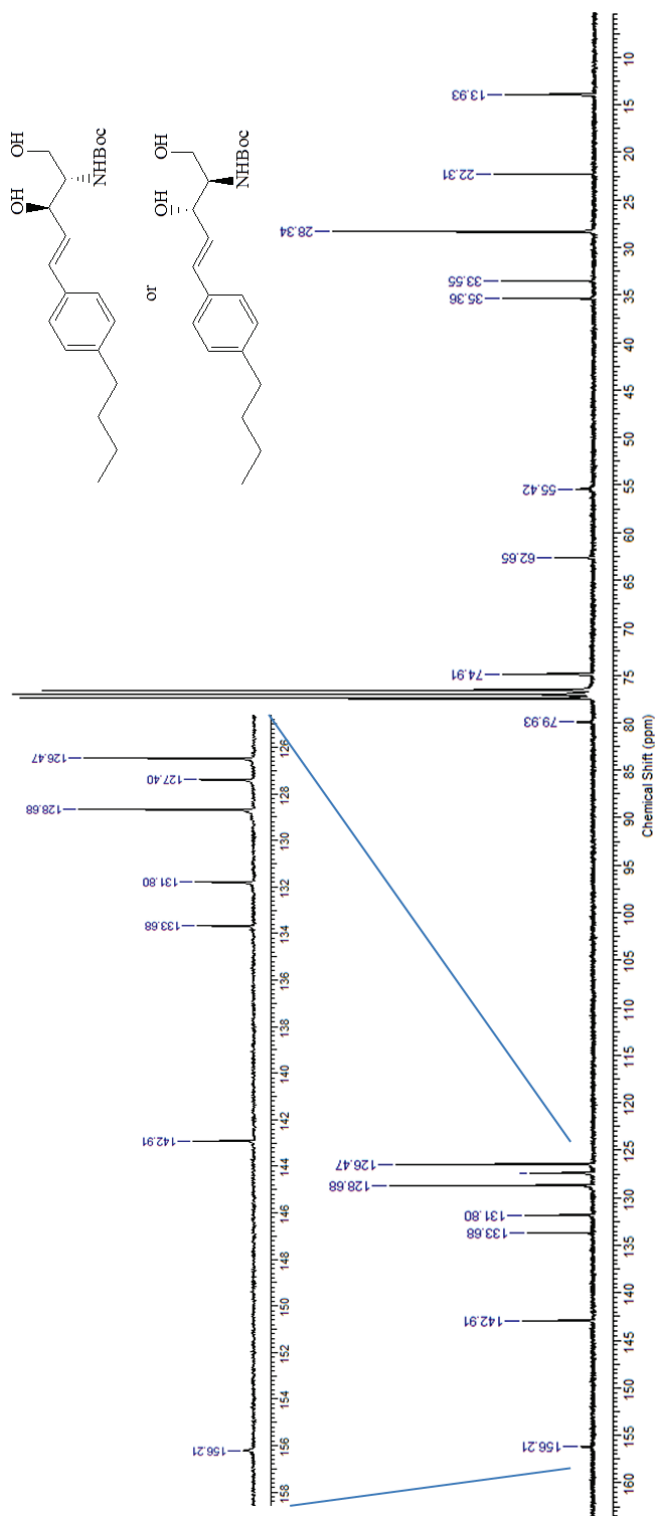


Figure B3.48. ¹³C NMR spectrum of (1E)-4-[(*tert*-butoxycarbonyl)amino]-1-(4-butylphenyl)-1,2,4-trideoxypent-1-enitol (**9E**) in CDCl₃.

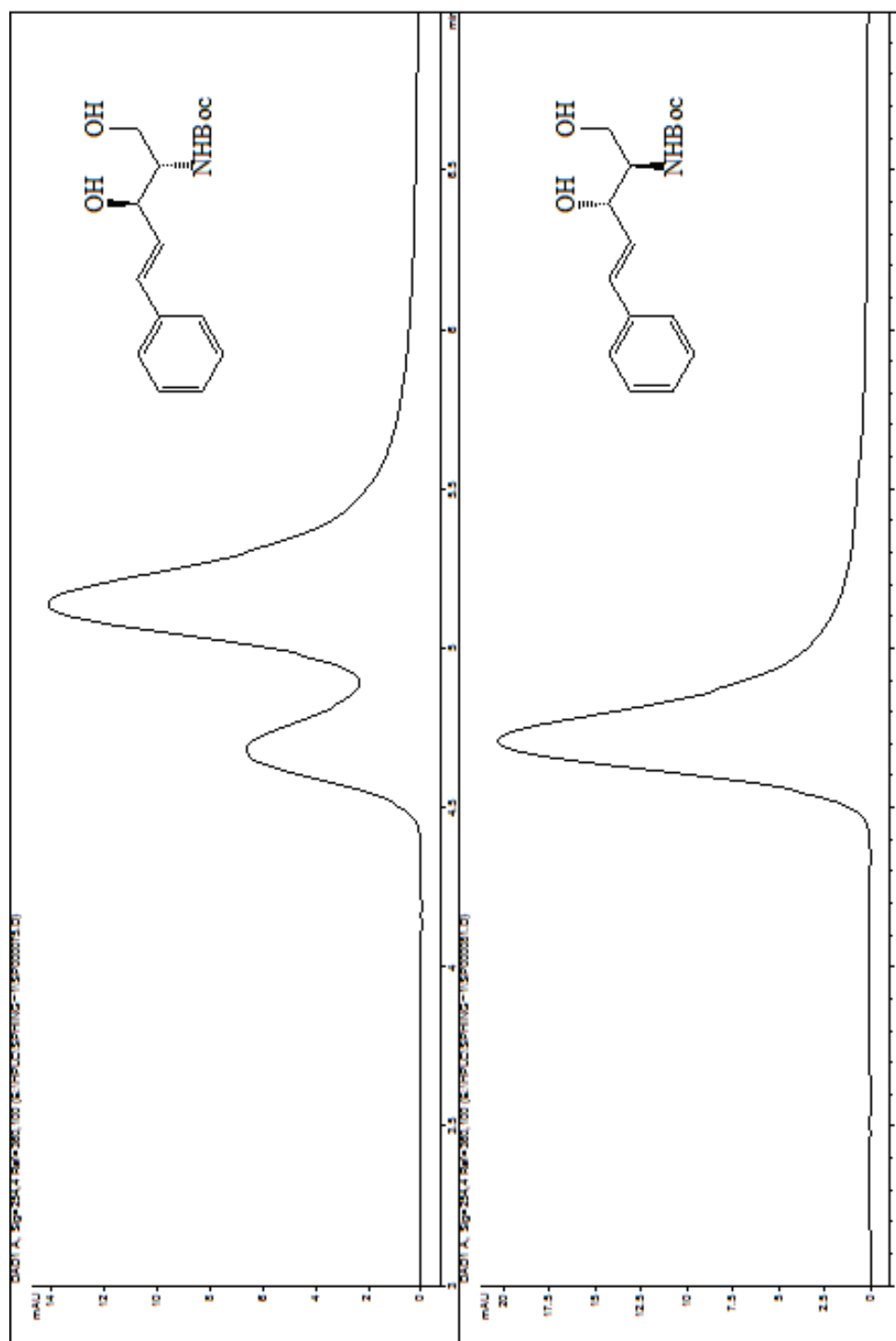


Figure B3.49. Chiral HPLC chromatograph of **9A**. Top: (3*R*, 2*S*)-**9A** made from *S*-**3A**; Bottom: (3*S*, 2*R*)-**9A** made from *R*-**3A**. HPLC column: Phenomenex[®] Lux 3 μ cellulose-1 column (50 x 4.60 mm); mobile phase: hexane: isopropanol = 9:1; Flow rate: 0.5 ml/min.

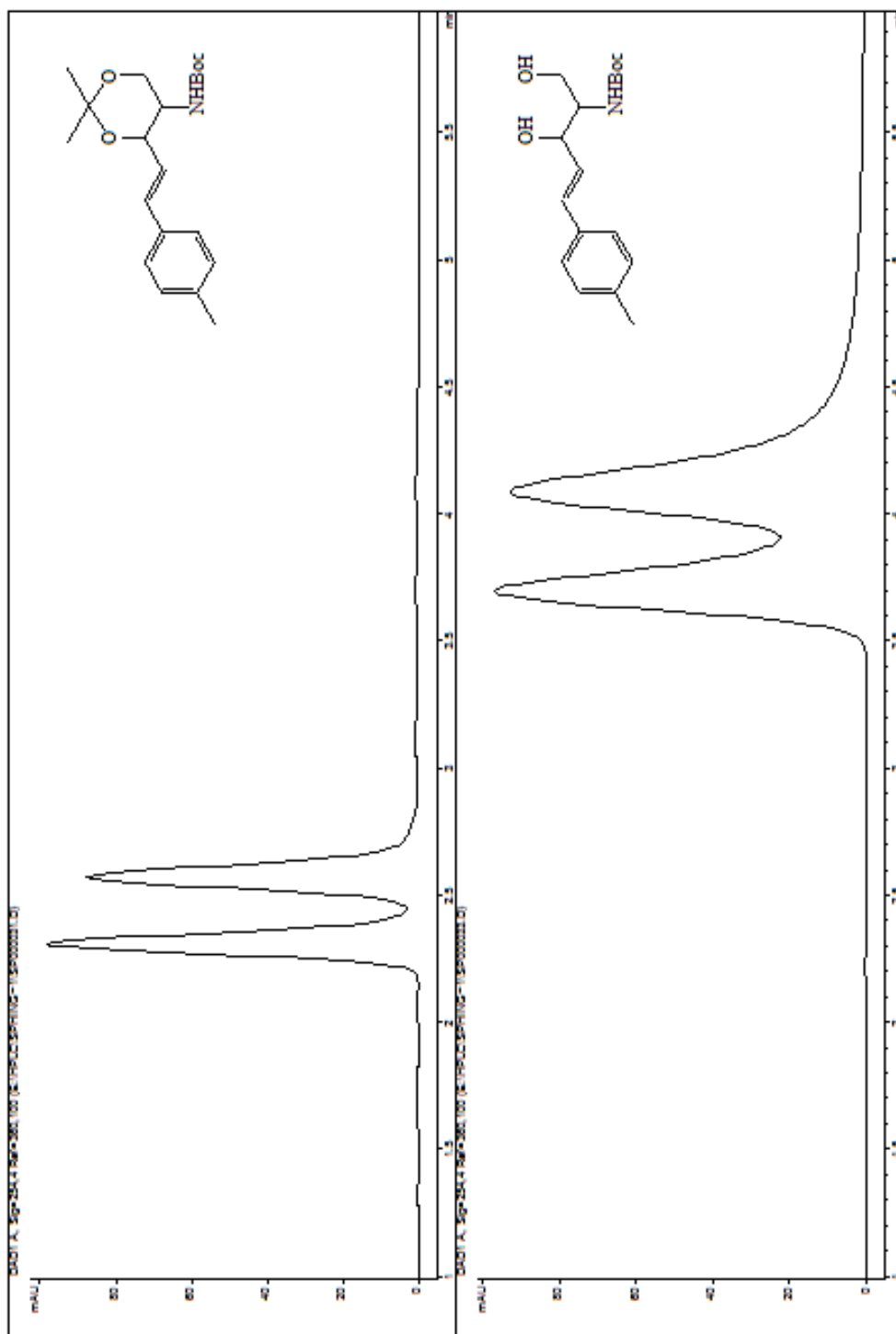


Figure B3.50. Chiral HPLC chromatograph of **8B** and **9B**; **Top: 8B** made from **3B**; **Bottom: 9B** made from **3B**. HPLC column: Phenomenex[®] Lux 3 μ cellulose-1 column (50 x 4.60 mm); mobile phase: hexane: isopropanol = 9:1; Flow rate: 0.5 ml/min.

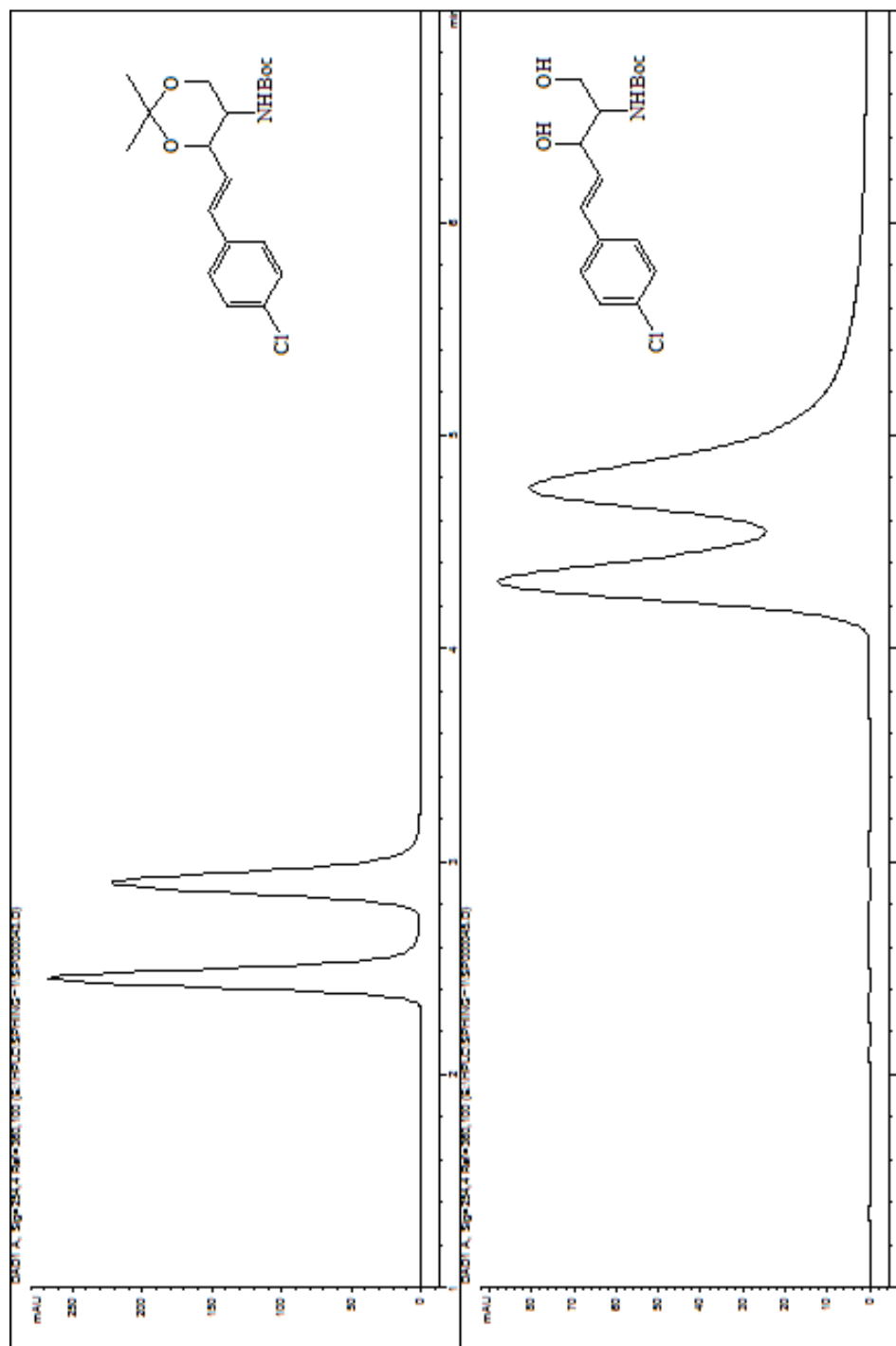


Figure B3.51. Chiral HPLC chromatograph of **8C** and **9C**; Top: **8C** made from **3C**; Bottom: **9C** made from **3C**. HPLC column: Phenomenex[®] Lux 3 μ cellulose-1 column (50 x 4.60 mm); mobile phase: hexane: isopropanol = 9:1; Flow rate: 0.5 ml/min.

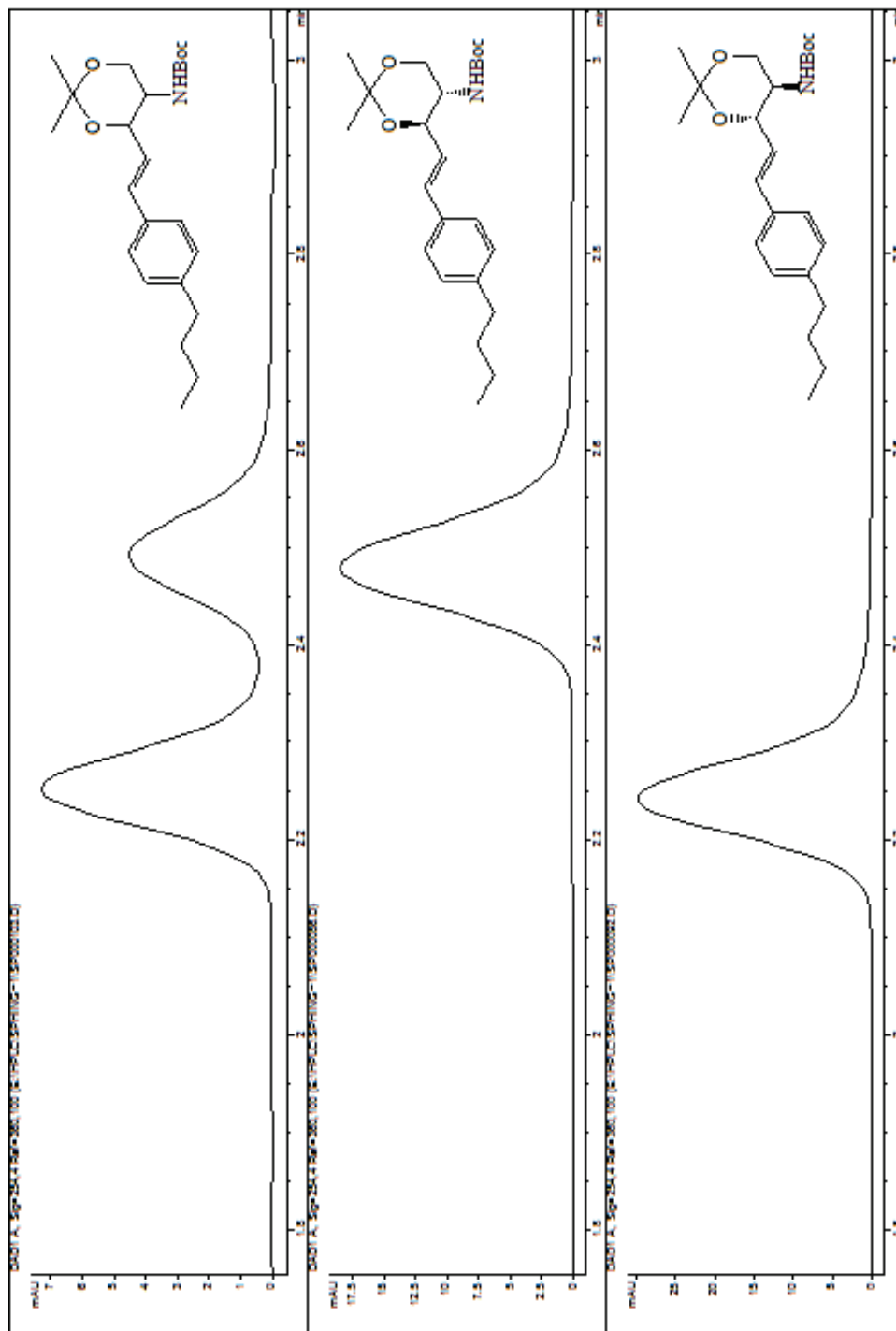


Figure B3.52. Chiral HPLC chromatograph of **8E**; **Top**: mixture of (3*R*, 2*S*)-**8E** and (3*S*, 2*R*)-**8E**; **Middle**: (3*R*, 2*S*)-**8E** made from *S*-**3E**; **Bottom**: (3*S*, 2*R*)-**6B** made from *R*-**3E**. HPLC column: Phenomenex[®] Lux 3 μ cellulose-1 column (50 x 4.60 mm); mobile phase: hexane: isopropanol = 9:1; Flow rate: 0.5 ml/min.

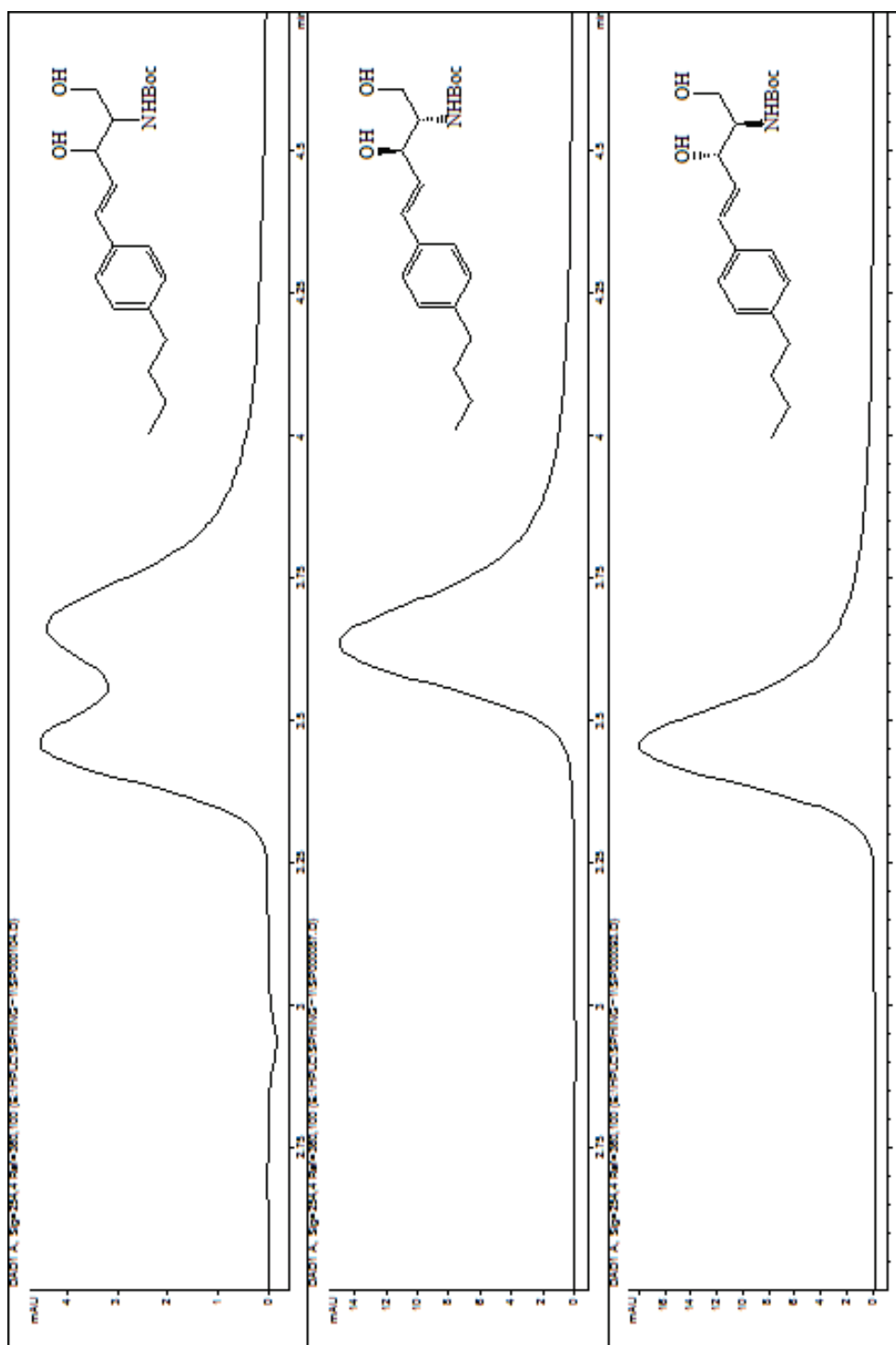


Figure B3.53. Chiral HPLC chromatograph of **9E**; **Top**: mixture of (3*R*, 2*S*)-**9E** and (3*S*, 2*R*)-**9E**; **Middle**: (3*R*, 2*S*)-**9E** made from *S*-**3E**; **Bottom**: (3*S*, 2*R*)-**9E** made from *R*-**3E**. HPLC column: Phenomenex[®] Lux 3 μ cellulose-1 column (50 x 4.60 mm); mobile phase: hexane: isopropanol = 9:1; Flow rate: 0.5 ml/min.

Chapter 4

Conclusion

4.1. Overview

The primary focus of this dissertation was to develop a new synthetic route to sphingosine analogues. A considerable effort was made to synthesize intermediate chiral *trans*- γ , δ -unsaturated β -hydroxy esters in high enantiopurity. We found that the reduction of the corresponding β -keto esters by commercially available ketoreductases was far superior to chemical methods for providing these critical enantiopure intermediates. The chiral *trans*- γ , δ -unsaturated β -hydroxy esters could then be conveniently α -aminated diastereospecifically using zinc chelation and Michael reaction with azodicarboxylate to produce α -hydrazino intermediates. The N-N bond was then effectively cleaved using known nonreductive *ElcB* elimination to preserve the double bond stereochemistry. Thus, a family of aromatic sphingosine analogues can be synthesized in high purity by the new synthetic route.

4.2. Conclusions on KREDs induced reduction of aryl γ , δ -unsaturated- β -ketoesters.

Saturated β -hydroxy esters have been asymmetrically prepared by many traditional methods and some biological methods. However, no literature was found to describe the asymmetrical formation of aryl *trans*- γ , δ -unsaturated β -hydroxyesters with high

enantioselectivity. In this research, an efficient enzymatic method was developed systematically utilizing isolated NAD(P)H dependent ketoreductases for the direct and stereoselective reduction of γ , δ -unsaturated β -keto esters.

For each γ , δ -unsaturated β -ketoesters, at least one enzyme could catalyze the formation of the corresponding (*S*)-enantiomer of γ , δ -unsaturated β -hydroxyesters and several enzymes could afford the corresponding (*R*)-enantiomer, both in excellent optical purity (>99%) and with good to excellent conversion for at least one ketoreductase. For several γ , δ -unsaturated β -ketoesters, the reactions were scaled (100-200 mg) with a chosen enzyme under the same reaction condition. The isolated yields are very close to the conversion of micro reactions monitored by ^1H NMR spectroscopy and with same optical purity (>99%).

Traditional chemical methods including Mukaiyama aldol condensation and Me-CBS-Borane catalyst reduction were also performed for formation of aryl γ , δ -unsaturated β -hydroxyester. Mukaiyama aldol condensation between *trans*-cinnamaldehyde and silyl ketene acetal afforded methyl (3*S*, 4*E*)-3-hydroxy-5-phenylpent-4-enoate with 80% yield and only 75% e.e.. Me-CBS-Borane catalyzed reduction of ethyl (4*E*)-3-oxo-5-phenylpent-4-enoate to ethyl (3*S*, 4*E*)-3-hydroxy-5-phenylpent-4-enoate gave 50% yield and only 44% e.e.. Thus, the enzymatic route to *trans*- γ , δ -unsaturated β -hydroxyesters is deemed far superior to the chemical methods explored here.

4.3. Conclusion of a novel and effective synthesis of erythro aromatic sphingosine analogues.

This research dissertation described a new and effective synthetic route to synthesize a family of sphingosine analogues. The synthetic route started with *trans*- γ , δ -unsaturated β -hydroxyesters. The synthetic route includes five or six steps. The key steps of this synthesis are (1) diastereospecific electrophilic amination of the *trans*- γ , δ -unsaturated β -hydroxyesters by DBAD to introduce chiral amino group and generate anti *N*-Boc- α -hydrazino- β -hydroxyesters and (2) *E1cB* non-reductively eliminative cleavage of the hydrazino N-N bond of *N*-Boc-2-hydrazino-1,3-diols ketals in the presence methyl bromoacetate and Cs₂CO₃.

In the diastereospecific electrophilic amination of the *trans*- γ , δ -unsaturated β -hydroxyesters, highly diastereospecificity is obtained for the *anti*-product and no *syn* product is detected. Zinc chelation appears to be necessary for the high diastereoselectivity, owing to the rigid zinc enolate form of *trans*- γ , δ -unsaturated β -hydroxyesters which facilitate the Michael addition of DBAD from the less sterically hindered side. The yields are 50% and the unreacted *trans*- γ , δ -unsaturated β -hydroxyesters can be recovered. Optimization needs to be carried out to increase the yield of this step.

E1cB non-reductively eliminative cleavage can be accomplished in two steps by separating intermediates *N*-Boc-2-alkylatedhydrazino-1,3-diols ketals and further cleaving N-N bonds under reflux. These two steps for N-N cleavage provide a combined

yield of 82-89%. Alternatively, *ElcB* non-reductively eliminative cleavage could also be performed without isolating intermediates with a higher overall yield. This one-step pathway is preferred because it is faster and provides higher overall yield.

In summary, excellent stereochemistry with more than 99% d.e. was obtained using the above described methodology, and no loss of stereochemistry is detected over the entire synthetic pathway. In this way, this methodology provides an improvement over more traditional approaches of sphingosine synthesis using serine-based strategies. The optical purity of final aromatic sphingosine analogues is dependent on that of the starting *trans*- γ , δ -unsaturated β -hydroxyesters. When starting with enantiopure γ , δ -unsaturated β -hydroxyesters, excellent e.e. and d.e. (>99 e.e. and >99 d.e.) were obtained in the final analogues. Using the described synthetic approach, either enantiomer of *erthyro* aromatic sphingosine analogues could be obtained, with 32-41% overall yield.

4.4. Final remarks

Analogues of this nature may prove useful as novel and specific inhibitors, which can be used potential drug candidates.

The novel synthetic approach described in this dissertation offers an opportunity to introduce variable substituents into sphingosine backbone, which to some extent will affect the ability of sphingosine analogues to act as agonists or antagonists. Further studies could focus on the convenient incorporation of a substituent, for example a methyl group, onto the C-2 position, which is in close proximity to the phosphorylation

site in the SP to S1P transformation. Incorporation of a substituent at the C-2 position is desirable because it may block phosphorylation and render the molecule as a competitive inhibitor. What is more, incorporation of structural variations into Carbon 1, 2, 4 and 5 positions of sphingosine backbone can also be explored in the future.

In the future, saturation transfer difference (STD) NMR can also be applied to study the interaction between aromatic sphingosine analogues and enzymes in sphingolipid metabolism pathway. This ligand based NMR method is applicable for screening aromatic sphingosine analogues and identifying the moieties for binding, which as a result will help us to improve the modification of sphingosine analogues based drug discovery process.

Appendix C

Atropisomers of Serotonin Dimer³

C.1 Abstract

This dissertation also describes a preparative scale synthesis of a dimer of serotonin (5-HT). DHBT or 5,5'-dihydroxy-4,4'-bitryptamine is prepared in good yield using methanol in the presence of copper (II) chloride and air at room temperature. Exclusion of air resulted in no DHBT. Neither 5-HT hydrochloride nor N-BOC-protected 5-HT yielded DHBT under identical reaction conditions, evidence that the primary amino group of 5-HT plays a critical role in the dimerization reaction. Computational studies using the HF/6-31G** method reveal that DHBT exhibits highly restricted rotation about the 4, 4'-biaryl carbon-carbon bond, consistent with the existence of enantiomeric atropisomers of DHBT. The atropisomers can be resolved by chiral capillary electrophoresis. Atropisomerism needs to be considered as a source of chirality when evaluating possible neurodegenerative roles of DHBT in biological systems.

Contributions: Sitara Chauhan contributed to the preliminary analysis of DHBT using capillary electrophoresis. Christopher Iceman contributed to Computational simulations of DHBT.

³ Zhipeng Dai, Sitara Chauhan, Christopher Iceman and Thomas K. Green. (Manuscript in preparation)

C.2. Introduction

5-Hydroxytryptamine (5-HT, serotonin, **Figure C1a**) occurs naturally in central and peripheral nervous system, where it plays a key role in regulation of body temperature, appetite, alcoholism, drug abuse, sleep and emotional states, as well as in cognition including memory and learning (Heath and Hen 1995, Lesch, Bengel et al. 1996, Walther, Peter et al. 2003, Sambeth, Riedel et al. 2009). Previous studies have indicated that 5-HT forms higher order structures in a faulty oxidative environment that could deplete serotonin levels and cause certain types of mental disorders including depression (Wrona and Dryhurst 1990), schizophrenia (Woolley and Shaw 1954) and Alzheimer's disease (Wrona and Dryhurst 1998, Brownrigg, Theisen et al. 2011). Studies on 5-HT oxidation products have suggested that 5-HT dimer, 5,5'-dihydroxy-4,4'-bitryptamine (DHBT, **Figure C1b**) is potentially neurotoxic and contributes to neurodegenerative diseases (Eriksen, Martin et al. 1960, Wrona, Goyal et al. 1992, Huether, Fettkotter et al. 1997, Jones, Underwood et al. 2007). Following an early report by Eriksen's group on a non-enzymatic oxidation of 5-HT by using inorganic CuSO_4 oxidant (Eriksen, Martin et al. 1960), Wrona and Dryhurst proposed an electrochemical oxidative pathway of 5-HT to DHBT by coupling of phenoxy radicals (Wrona and Dryhurst 1987). They further reported that DHBT is the major nitrogen-centered radicals to induce the generation of C(4)-C(4') and N(1)-C(4') dimers in the course of this initial autoxidation product of 5-HT at physiological pH and temperature (Wrona and Dryhurst 1990, Wrona, Goyal et al. 1992). Jones and his colleagues studied the formation of DHBT induced by low concentration of Cu^{2+} ion (1 mmol/L). They showed that DHBT had only a minor toxic

effect on the neuronal cell model PC12, suggesting that reactive oxygen species are primarily responsible for the observed toxic effect (Jones, Underwood et al. 2007). Heuether et al. showed that 5-HT is oxidized to DHBT in the presence of peroxidase and hydrogen peroxide (Huether, Reimer et al. 1990). The major product was analytically isolated and analyzed by mass spectrometry.

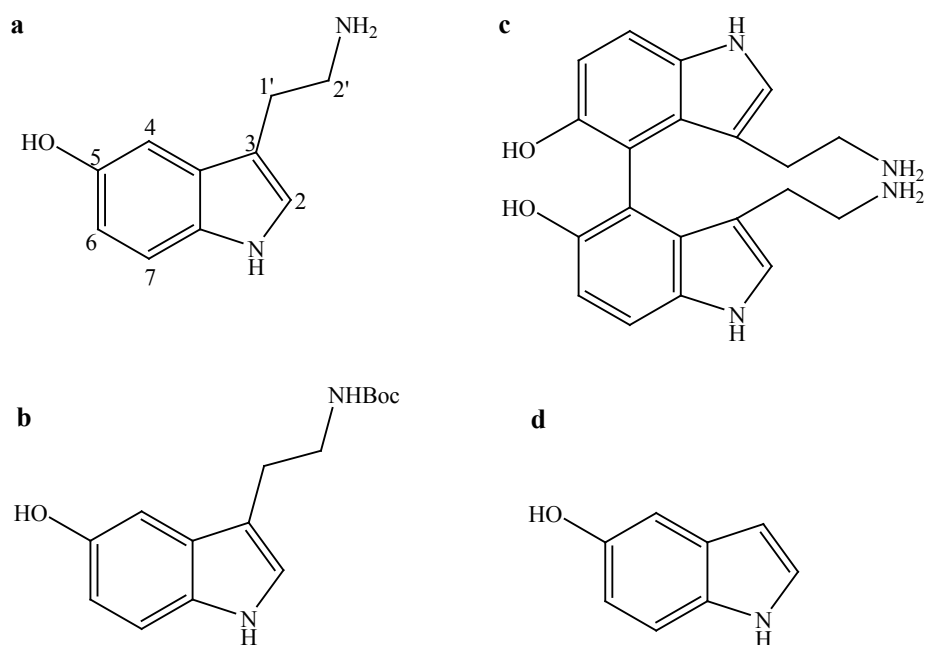


Figure C1. **a.** Schematic of 5-hydroxytryptamine (Serotonin) showing numbering scheme used in this work; **b.** DHBT; **c.** Boc-protected 5-HT; **d.** 5-Hydroxyindole

Apart from the foregoing studies on the formation and neurotoxicity of DHBT, no further work has appeared on preparative scale synthesis of DHBT. We report here the convenient synthesis of DHBT using copper (II) chloride in methanol in the presence of air. We find that both air (molecular oxygen) and the primary amino function of 5-HT are essential for good yield. Consistent with computational results, DHBT is found to exhibit atropisomerism, a type of axial stereoisomerism which results from sterically hindered

rotation about a bond axis. The atropisomers can be separated by chiral capillary electrophoresis.

C.3. Results and Discussion

C.3.1. Synthesis and NMR studies of DHBT

DHBT was obtained by the approach shown in **Scheme C1**. *In situ* ^1H NMR spectroscopy studies were used to establish the optimum amount of copper (II) chloride and added base. A typical result is shown in **Figure C2**, where the ^1H NMR spectra of 5-HT prior to reaction without added Cu^{2+} (bottom), after reaction for 1 h (middle), and purified DHBT (top) in methanol- d_4 are presented. The H-7 resonance intensity of 5-HT (d, 7.2 ppm) decreases as the H-7/H-7' resonance (d, 7.4 ppm) of DHBT appears, the H-6 resonance of 5-HT (dd, 6.7 ppm) decreases as the H-6/H-6' resonance of DHBT appears (d, 6.9 ppm), and the upfield resonances H-1' and H-2' of 5-HT (t, 3.0 and t, 3.2 ppm) decrease with the appearance of a complex, broad multiplet in the region of 2.2 - 2.5 ppm. These results are similar to those reported by Jones et al. (Jones, Underwood et al. 2007)

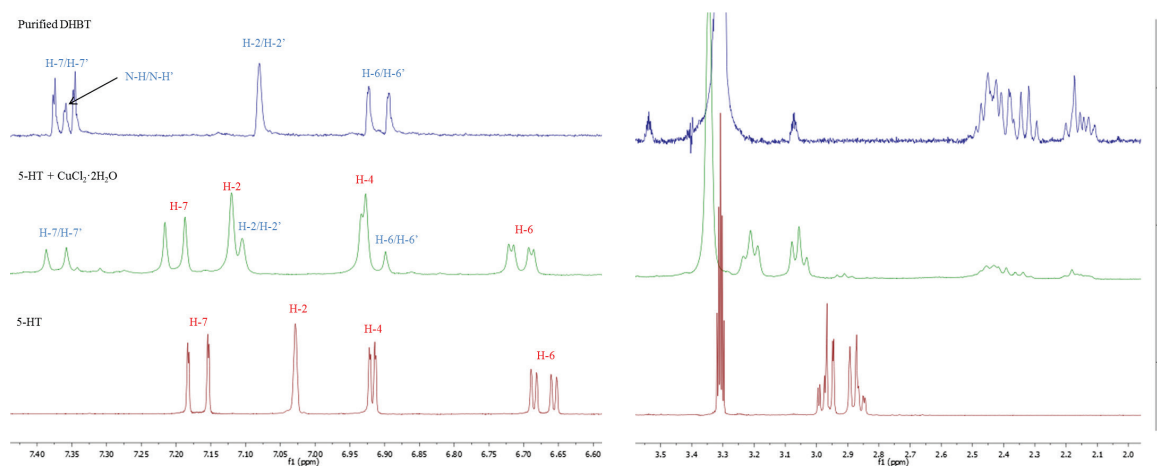
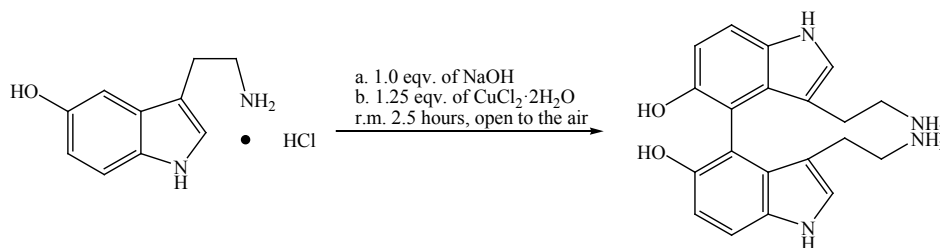


Figure C2. ^1H NMR spectra of 5-HT neutralized by 1.0 equivalent of NaOH then reacted with 1.25 equivalents of $\text{CuCl}_2 \cdot 2\text{H}_2\text{O}$ in methanol- d_4 on a Varian 300 MHz NMR spectroscopy. **Bottom** spectrum: 5-HT; **Middle** spectrum: Reaction of 5-HT after 1 h. **Top** spectrum: purified DHBT.

No significant difference between 0.625 and 1.25 equivalents of Cu^{2+} on yield of DHBT was observed, but 1.8 and 2.5 equivalents resulted in significantly lower NMR yields. Thus preparative scale synthesis of DHBT was accomplished in the presence of 1.25 molar equivalents of copper (II) chloride dihydrate in methanol, which provided the highest isolated yield. The respective DHBT dihydrochloride salt was readily purified by Sephadex LH-20 column chromatography (pH 2) in 45% yield.



Scheme C1. Cu (II) induced oxidative coupling reaction of 5-HT.

When addition of base was omitted, no DHBT was isolated. Indeed, addition of one equivalent of base caused an immediate reaction to occur with formation of a black suspension, and led eventually to the color change of the reaction mixture to reddish. This finding led us to consider that the primary amino group was indispensable for the Cu^{2+} -induced oxidative formation of DHBT. To study this finding systematically, we varied the amount of base to neutralize 5-HT·HCl before adding copper (II) chloride dihydrate (**Figure C3**), and then measured the NMR yield after one hour. Addition of 1.0 and 1.5 equivalent base gave similar NMR yields, but the highest isolated DHBT yield was obtained when 5-HT·HCl was neutralized with 1.0 equivalent of base.

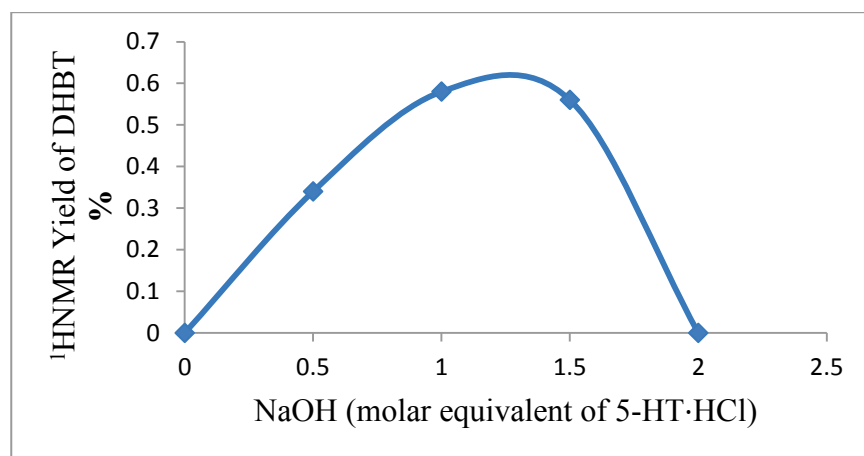


Figure C3. Effect of various amounts of base added on the conversion of 5-HT to DHBT after 1 hour of reaction time as monitored by ^1H NMR spectroscopy.

To further investigate the influence of the primary amino function, BOC-protected 5-HT (**Figure C1c**) and 5-hydroxyindole (**Figure C1d**), which lack the primary amino function, were evaluated under the same reaction conditions shown in **Scheme C1**. *In situ*

^1H NMR spectroscopy in methanol- d_4 did not reveal formation of dimer for either substrate, but rather the disappearance of some resonances was observed from an otherwise unchanging spectrum. The results are interpreted as hydrogen/deuterium exchange of H-4 of Boc-protected 5-HT (complete in 1.5 h) and both H-3 and H-4 of 5-hydroxyindole (complete in <5 min and 1 h, respectively) in the presence of Cu^{2+} ion (**Figure C4 and C5**). Exchange did not take place in the absence of Cu^{2+} ion. These results indicate that, while aryl H-D exchange is promoted by Cu^{2+} , the aminoethyl group ($-\text{CH}_2\text{CH}_2\text{NH}_2$) is essential to the Cu^{2+} -induced oxidative coupling of 5-HT under the conditions studied.

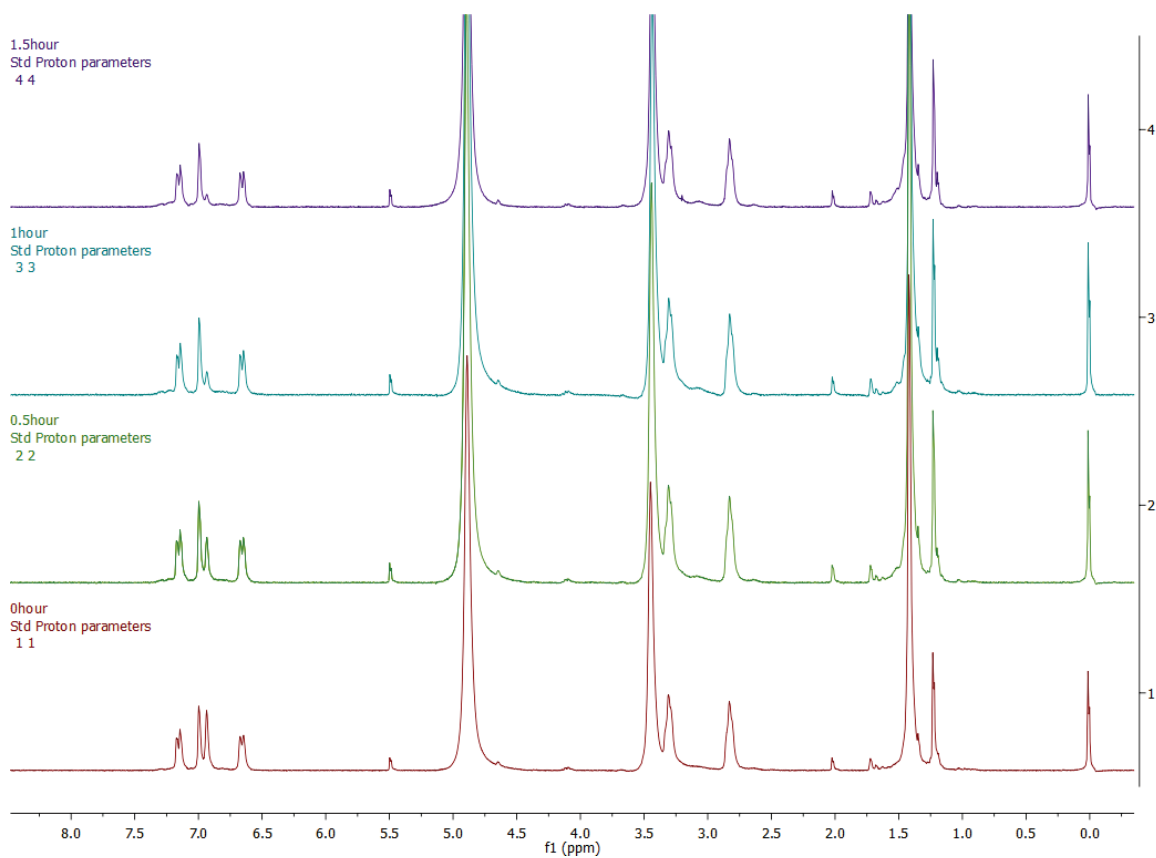


Figure C4. ^1H NMR spectra of Boc-protected 5-HT in the presence of 1.25 equivalents of $\text{CuCl}_2 \cdot 2\text{H}_2\text{O}$ in methanol- d_4 on a Varian 300 MHz NMR spectroscopy.

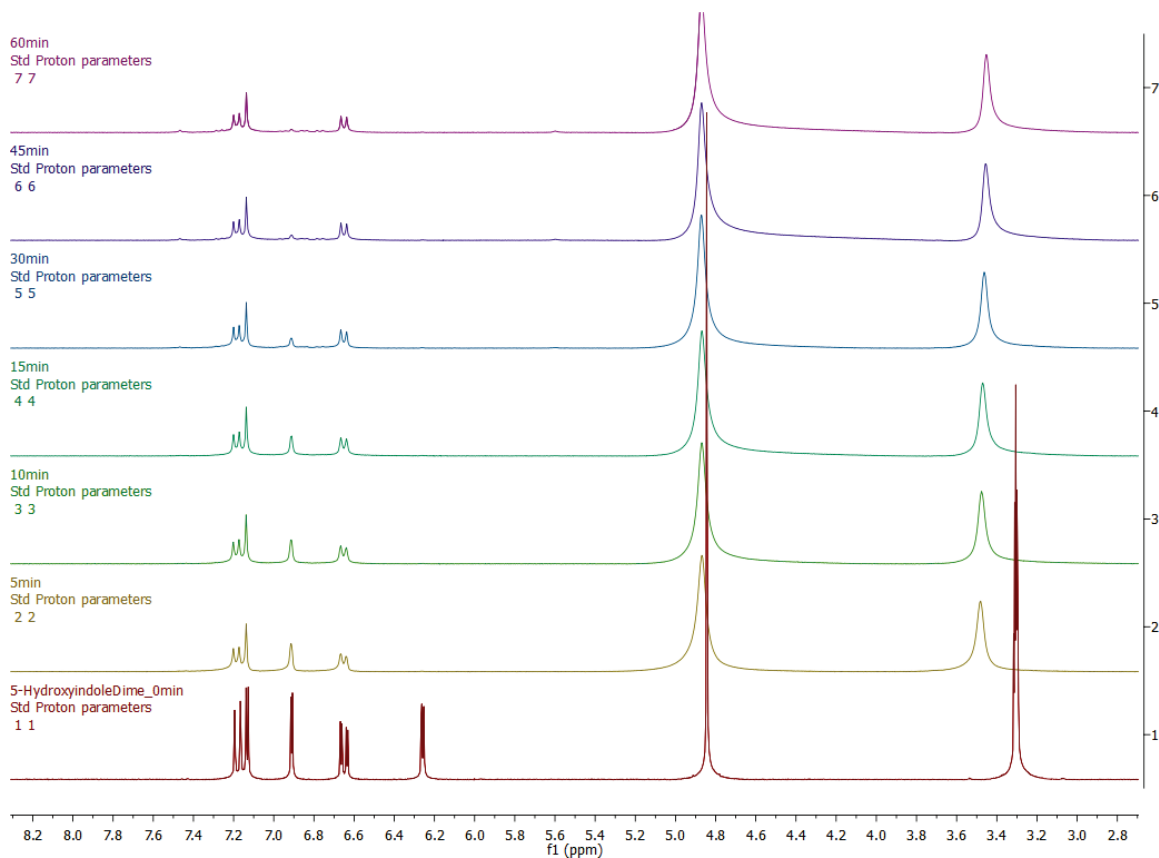


Figure C5. ^1H NMR spectra of 5-Hydroxyindole in the presence of 1.25 equivalents of $\text{CuCl}_2 \cdot 2\text{H}_2\text{O}$ in methanol- d_4 on a Varian 300 MHz NMR spectroscopy.

Copper-mediated or -catalyzed oxidative couplings have been extensively studied for the synthesis of biaryl compounds. Cupric-amine complexes in particular have been studied as attractive oxidants for the coupling reaction, for instance the oxidative coupling of phenols (Feringa and Wynberg 1977) and naphthols (Feringa and Wynberg 1978, Smrčina, Lorenc et al. 1991). In the oxidative coupling of 5-HT, the primary amino function is critical for achieving high yield of DHBT. The amino group may coordinate to Cu^{2+} to form Cu^{2+} -5-HT complexes, which contributes to the black colored suspension

mentioned above, and facilitates the oxidative coupling of two 5-HT molecules within the coordination sphere of Cu^{2+} .

In the presence of air, DHBT could be observed with *in situ* ^1H NMR spectroscopy using either methanol- d_4 or D_2O as solvent. When the reaction was performed under anaerobic conditions, no DHBT formed. Oxygen may serve to reoxidize Cu(I) to Cu(II), thus allowing for a catalytic cycle (Noji, Nakajima et al. 1994, Hassan, Sévignon et al. 2002).

C.3.2. Atropisomers of DHBT

Many biaryl compounds similar in structure to DHBT (**Figure C1b**) are known to exhibit atropisomerism. Atropisomerism is a type of stereoisomerism, which results from steric hindrance rotation along a bond axis (Christie and Kenner 1922, Oki 1983, Bringmann, Mortimer et al. 2005, Clayden, Moran et al. 2009). Often atropisomers can be thermally interconverted via an intramolecular dynamic process without bond breaking (LaPlante, Fader et al. 2011), depending on the activation energy for bond rotation. The rotational barrier is directly related to the half-time of the interconversion between atropisomers (Roussel, Vanthuyne et al. 2008). Atropisomers can be analytically isolated when the half-time of inter-conversion is at least 1000 s (Oki 1983). The computational rotational energy barrier serves as a guideline to determine whether atropisomers should be isolated as a racemic mixture or as a single compound. There is good agreement shown between computed and experimental determined rotational

barriers (Tobler, Lammerhofer et al. 2001, Clayden, Moran et al. 2009, LaPlante, Edwards et al. 2011).

Computational simulations of the DHBT transformation from one stereoisomer to the other are depicted in **Figure C6**. We find that the rotation of the molecule through the dihedral angle C4-C5-C5'-C4' shown in **Figure C7** is highly hindered with the smallest barrier to rotation of 350 kJ/mol occurring through interactions of the hydroxyl and ethyl amine groups of the 5-HT dimer, while an even larger barrier to rotation of >600 kJ/mol evolves through interactions of the two ethyl amine groups. The two enantiomers are clearly thermally inaccessible to each other.

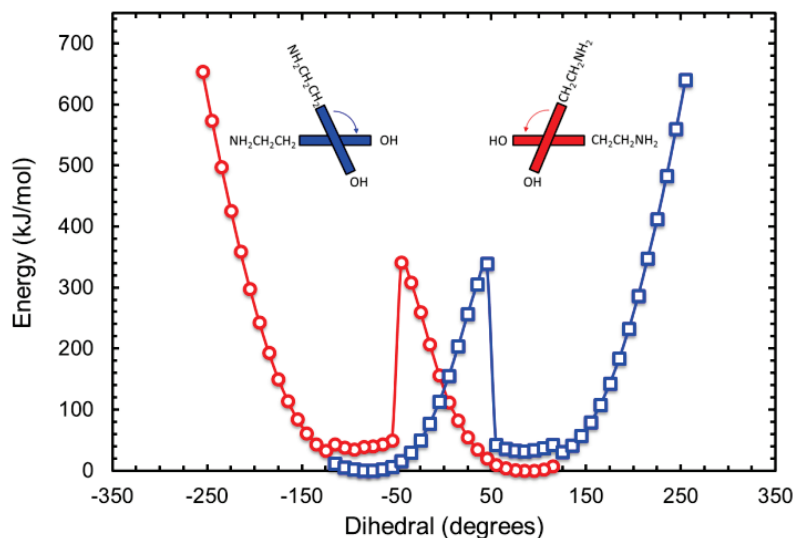


Figure C6. Computational simulations of DHBT where the dihedral C4-C5-C5'-C4' was restrained. Two separate calculations of DHBT were initiated in each isomeric form and a progression of dihedral angles (48 steps of 10 degrees) was explored using a relaxed potential energy surface (RPES) scan rotating between the two stereoisomers.

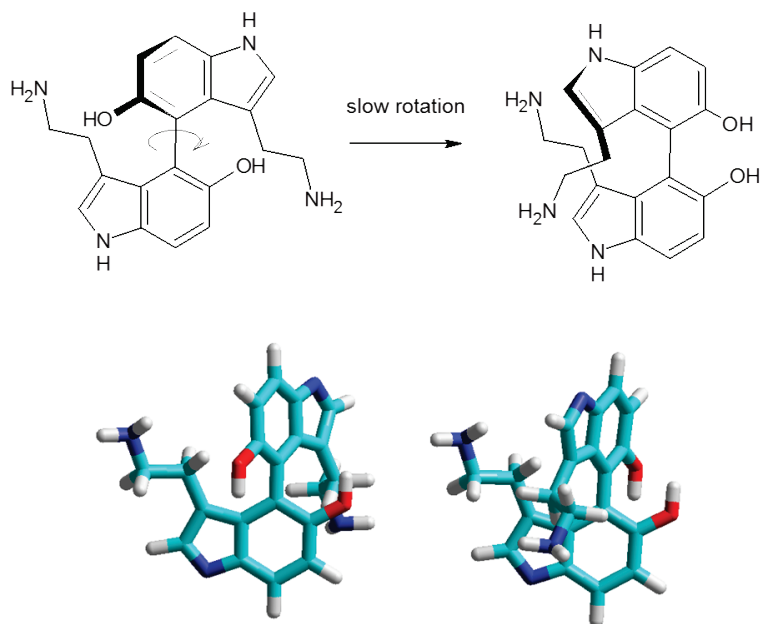


Figure C7. Atropisomers of DHBT attributed to slow rotation about 4-4' carbon-carbon bond.

Thus, DHBT is predicted as a pair of enantiomeric atropisomers with chirality arising from hindered rotation about the biaryl C4-C4' bond (**Figure C7**). Consistent with this prediction, the chiral separation of DHBT enantiomeric atropisomers was successfully achieved by capillary electrophoresis with sodium taurodeoxycholate (STDC) as chiral selector (**Figure C8**). After a systematic study, a buffer system composing of 80 mM STDC in 20.0 mM Tris at pH=8.0 was adopted to generate nearly baseline resolution for DHBT enantiomeric atropisomers. This technique could be used for monitoring conversion of 5-HT to DHBT during the course of the reaction.

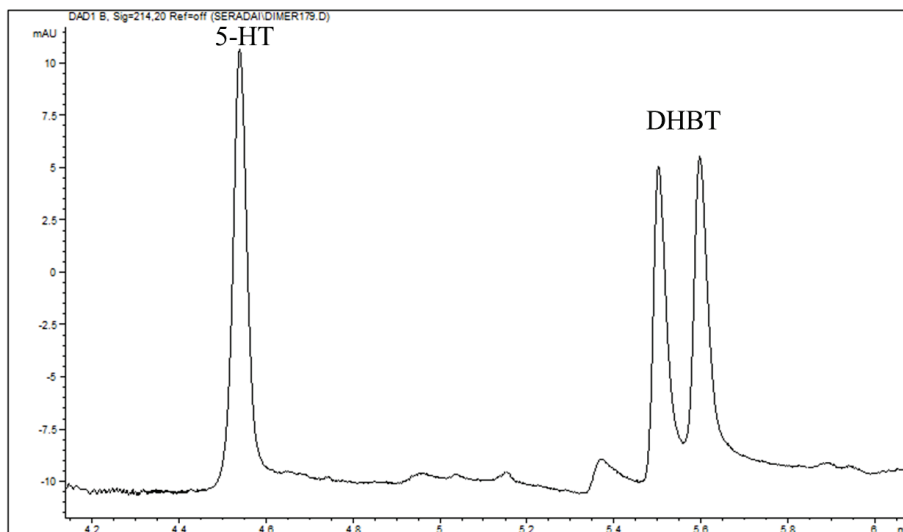


Figure C8. Electropherogram for 5-HT and DHBT atropisomers. 50.0 μm i.d., bare fused silica capillary, 32.5 cm total length, 24.0 cm to detector; detection 214 nm; Injection: 50.0 mBar/1s; BGE: 80 mM taurodeoxycholate in 20.0 mM Tris, pH=8.0; normal polarity, 10 kV. Sample was injected during the course of the reaction.

The NMR spectrum also supports the existence of atropisomers of DHBT. The four hydrogens of the ethylamino group are diastereotopic by virtue of the chiral axis and reveal distinct, baseline-resolved resonances in the 600 MHz ^1H NMR spectrum as shown in **Figure C9**. Spin simulation of the spectrum yields the chemical shifts and couplings constants, J , for each resonance, as described in the **Figure C9**. The chemical shifts of the DHBT methylene resonances are significantly upfield shifted (2.15-2.60 ppm) compared to 5-HT methylene resonances (2.85 -3.00 ppm). The upfield shift is probably attributed to the positioning of the DHBT methylene hydrogens in the shielding cone of the adjacent aromatic ring system (see **Figure C7**).

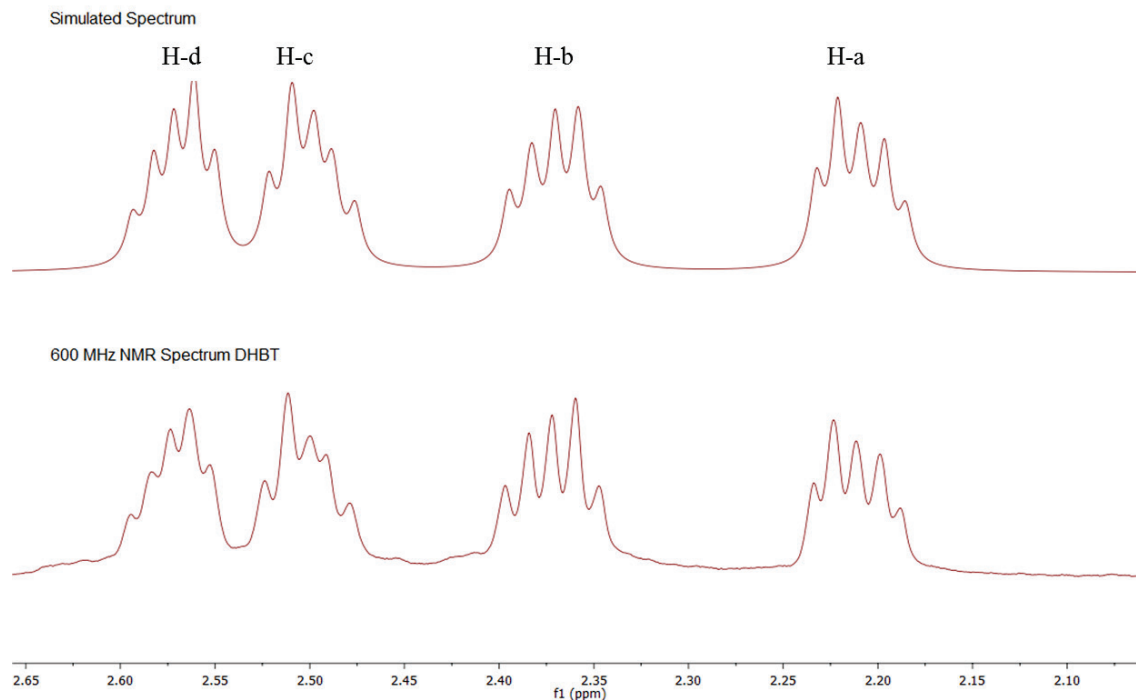


Figure C6. 600 MHz ^1H NMR spectrum of upfield region of 5, 5'-dihydroxy-4, 4'-bitryptamine (DHBT) in D_2O (lower spectrum) and simulated spectrum using chemical shifts (δ) and coupling constants (J). The hydrogens are assigned to the $-\text{CH}_2\text{CH}_2\text{NH}_2$ group and are diastereotopic due to the chiral axis. Chemical shifts are 2.21 (H-a), 2.37 (H-b), 2.50 (H-c) and 2.57 (H-d). Coupling constants, J , in Hz are $^2J_{ab}=14.8$, $^3J_{ac}=6.8$, $^3J_{ad}=6.8$, $^3J_{bc}=7.8$, $^3J_{bd}=6.8$, $^2J_{cd}=12.8$. H-a and H-b are geminal and H-c and H-d are geminal.

C.4. Summary of atropisomers of DHBT

We have demonstrated a preparative procedure for DHBT in methanol induced by Cu^{2+} under oxygen. The coupling condition is simple and the work-up is straightforward. The primary amino function of 5-HT is essential for a good yield under the experimental conditions. We hypothesize that Cu^{2+} ion coordinates to a 5-HT through the amino function, and that coupling occurs in the coordination sphere of the metal. The existence

of atropisomers of DHBT was supported by ^1H NMR spectroscopy. And DHBT atropisomers are also resolved using chiral capillary electrophoresis.

C.5. Experimental

C.5.1. Materials

Sigma-Aldrich Chemical Company supplied all chemicals unless otherwise noted. Water was purified with a Millipore Milli-Q ultrapure water purification system with an 18 M Ω -cm resistivity.

C.5.2. NMR Spectroscopy

^1H and ^{13}C NMR spectra were recorded with a Varian 300 MHz and Bruker 600 MHz instrument. Chemical shifts are reported in ppm relative to TMS as internal standard. A typical *in situ* ^1H NMR reaction is as follows; 4.5 mg (21.2 μmol , 1.0 eq.) of 5-HT $\cdot\text{HCl}$ was dissolved in 0.75 mL of methanol- d_4 in an NMR tube and neutralized by various amount of NaOH solution (5M in H_2O). The NMR tube was placed in the 300 MHz NMR spectrometer at 23 $^\circ\text{C}$ and the ^1H NMR spectrum of 5-HT prior to the reaction was obtained. 4.5 mg (26.4 μmol , 1.25 eq.) of $\text{CuCl}_2\cdot 2\text{H}_2\text{O}$ was then added into 5-HT solution in the NMR tube and the *in situ* ^1H NMR spectra were recorded over time.

C.5.3. Chiral Capillary Electrophoresis

Capillary electrophoresis was performed with an Agilent 3D Capillary Electrophoresis System using bare fused silica capillary (purchased from Polymicro Technologies, L.L.C.) (50 μm i.d., 32.5 cm total length, 24.0 cm to detector) under normal polarity (10 kV), and detection was by UV absorbance at 214 nm. Prior to first use, the capillary was primed for 2 min with 1 M NaOH solution and then for 2 min with 0.1 M NaOH solution. For each use, the capillary was preconditioned for 1 min using background electrolyte (BGE). BGE was 80 mM sodium taurodeoxycholate as chiral selector in 20 mM tris buffer. Samples (diluted 10 fold into 90:10 v/v milli-Q water/acetone solvent) were injected into the capillary under 50.0 mbar pressures for 3 seconds. At the end of each run, the capillary was post-conditioned with 0.1 M NaOH solution for 1 min and then with Milli-Q water for 1 min.

C.5.4. Synthesis and Purification

C.5.4.1. 5,5'-dihydroxy-4, 4'-bitryptamine (DHBT)·2HCl

To a stirred solution of serotonin hydrochloride (60mg, 0.282 mmol) in 5.0 mL methanol at room temperature, a solution of 5.0 M NaOH (56.4 μL , 0.282 mmol) was added. After 5 min, $\text{CuCl}_2 \cdot 2\text{H}_2\text{O}$ (60 mg, 0.352 mmol) in 5.0 mL methanol was added dropwise, and the mixture was reacted for 2.5 hours at ambient temperature without stirring but with swirling every 15 min. The mixture was vacuum filtered, and the solvent was evaporated off under vacuum flow. Purification was accomplished by Sephadex LH-

20 column chromatography (Column: 15 x 2.5 cm; mobile phase: H₂O: methanol (9:1, v/v), pH = 2.0 adjusted by 1 M HCl) at a flow of 10 mL·h⁻¹. The eluent was monitored with capillary electrophoresis at 214 nm using taurodeoxycholic acid as chiral selector. Eluent was removed by nitrogen flow to obtain a red solid. Isolated yield: 45mol %. ¹H NMR (300 MHz, D₂O) δ 7.50 (H-7, d, *J* = 9.0 Hz, 2H), 7.22 (H-2, s, 2H), 6.99 (H-6, d, *J* = 9.0 Hz, 2H), 2.00-2.65 (m, 8H). ¹³C NMR (75 MHz, D₂O) δ 146.8, 131.8, 126.4, 126.1, 112.6, 112.3, 111.7, 109.3, 39.6, 23.3. For mass spectral analysis, the product was recovered from D₂O. HRMS (ESI): calcd for C₂₀H₂₂DN₄O₂⁺ (M-HCl-Cl)⁺ 352.1883 found 352.1876, calcd for C₂₀H₂₁D₂N₄O₂⁺ (M-HCl-Cl)⁺ 353.1945 found 353.1938. (Figure C10 and C11).

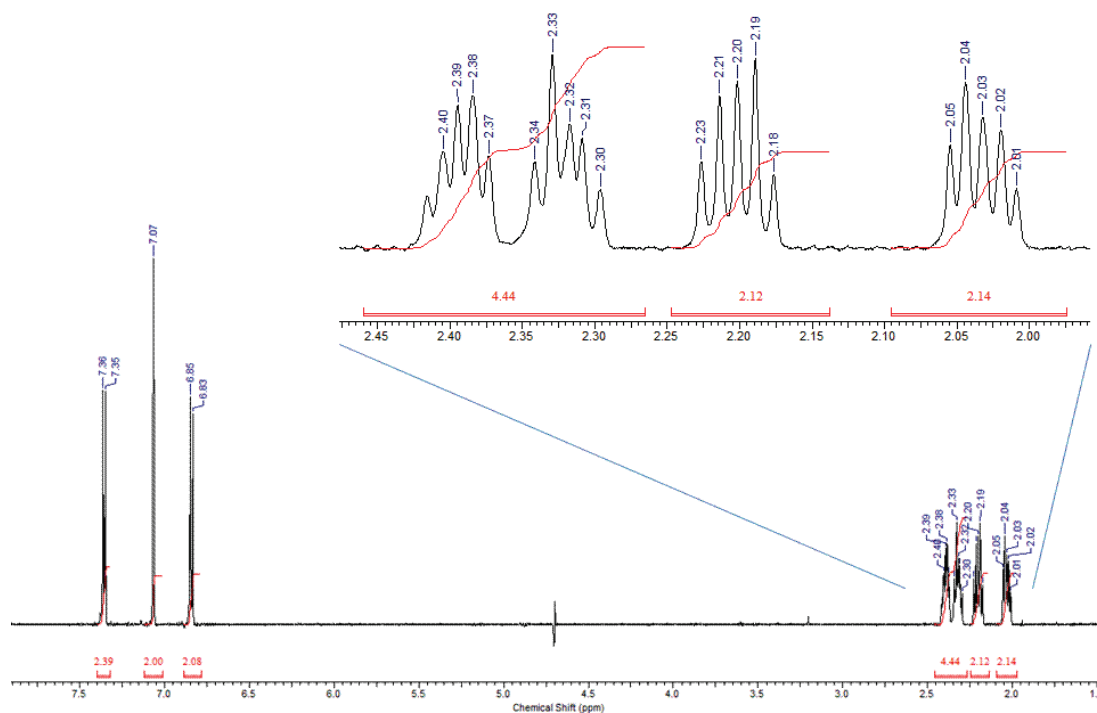


Figure C7. ¹H NMR spectrum of 5, 5'-dihydroxy-4, 4'-bitryptamine (DHBT) in D₂O; D₂O was depressed.

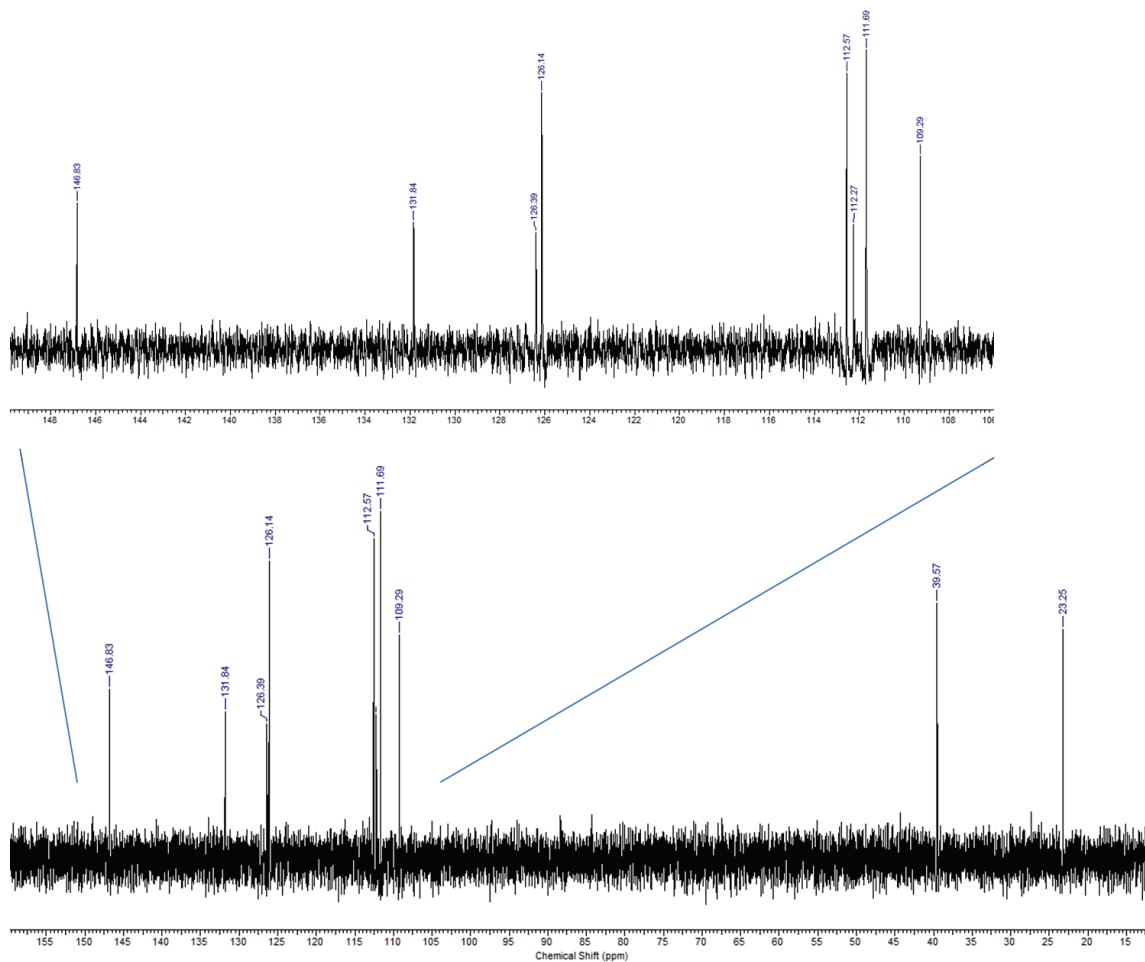


Figure C8. ^{13}C NMR spectrum of 5, 5'-dihydroxy-4, 4'-bitryptamine (DHBT) in D_2O .

C.5.4.2. Boc-protected 5-HT

To magnetically stirred suspension of 5-HT·HCl (425 mg, 2.0 mmol) in 6.0 ml H_2O and 2.0 ml THF, was added 1.0 equivalent of NaOH solution. Di-tert-butyl dicarbonate (480 mg, 2.2 mmol) was added at room temperature. After 6 h, the reaction mixture was concentrated under vacuum, and extracted by EtOAc (2 x 15 ml); the combined organic layers were dried over anhydrous Na_2SO_4 and removed by rotovaporization. Isolated

yield: 94%. ^1H NMR (300 MHz, CDCl_3) δ 8.20 (OH, br s, 1H), 7.13 (H-7, d, $J = 9.0$ Hz, 1H), 6.98 (H-4, dd, $J = 3.0$ Hz, 1H), 6.88 (H-2, br s, 1H), 6.79 (H-6, dd, $J = 9.0, 3.0$ Hz, 1H), 6.57 (N-H, br s, 1H), 4.76 (NH-COO, br s, 1H), 3.38 (CH_2 , t, $J = 6.0$ Hz, 2H), 2.79 (CH_2 , t, $J = 6.0$, 2H), 1.43 (Me_3 , s, 9H); ^{13}C NMR (75 MHz, CDCl_3) 156.35, 149.76, 131.48, 127.93, 123.16, 112.05, 111.99, 111.87, 103.22, 79.50, 40.65, 28.44, 25.76.

(Figure C12 and C13)

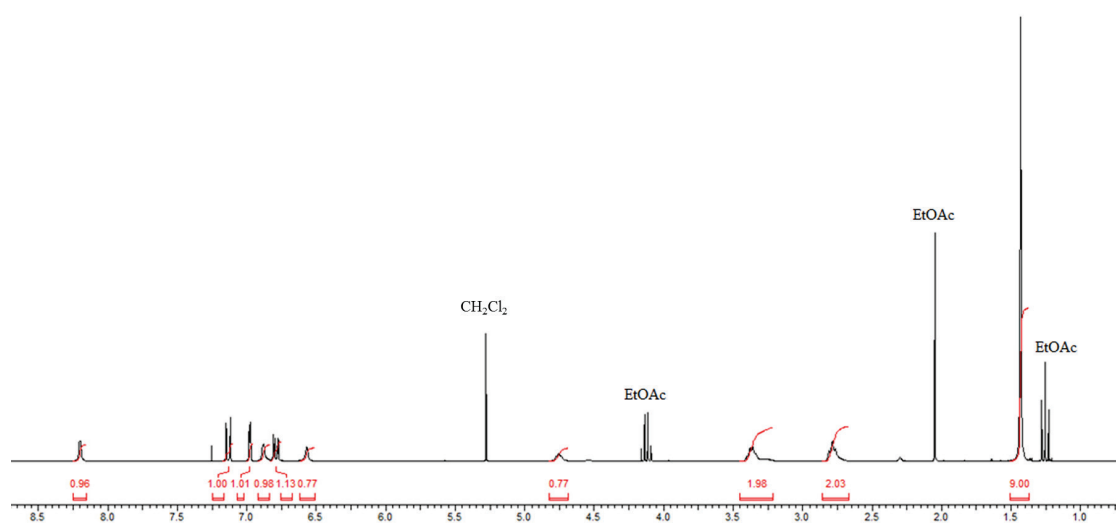


Figure C9. ^1H NMR spectrum of Boc-protected 5-HT.

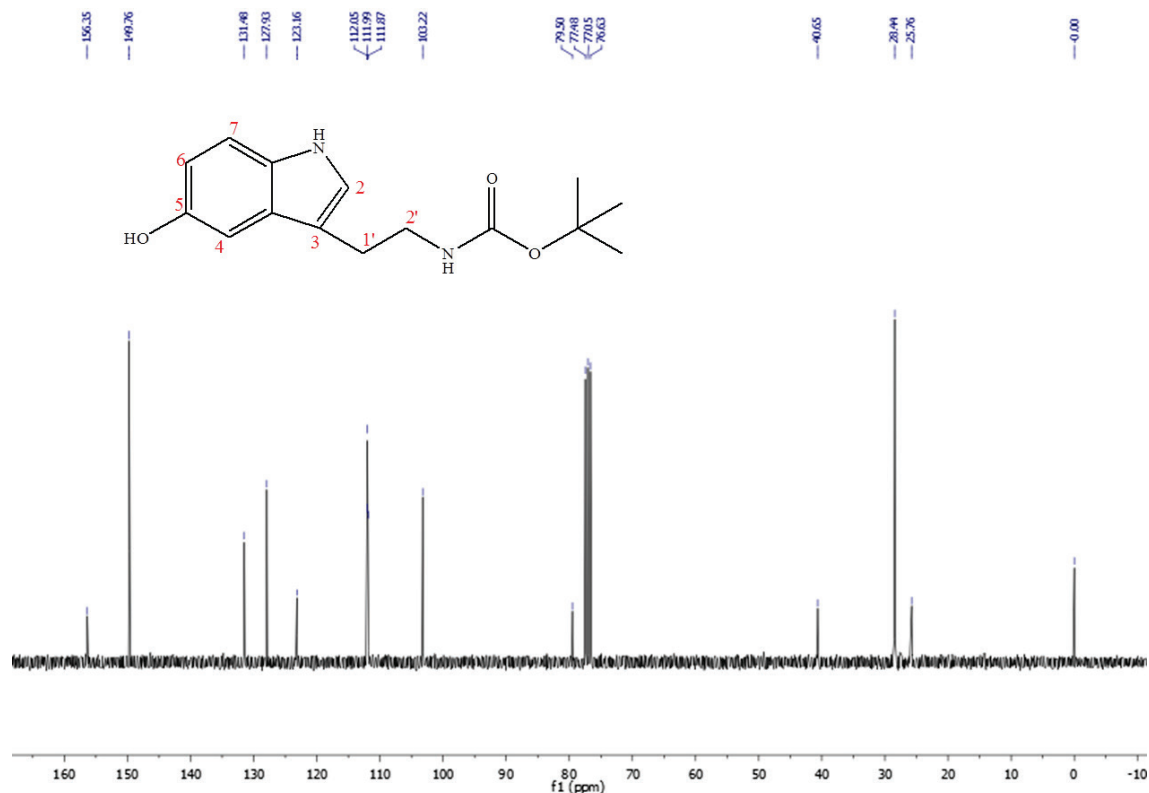


Figure C10. ¹³C NMR spectrum of Boc-protected 5-HT.

C.6. Calculations

We completed calculations on the DHBT using the Gaussian03 computational suite (Gaussian 03). Molecular geometries were optimized at the HF level of theory with the 3-21g basis set. Two separate calculations of DHBT were initiated in each isomeric form and a progression of dihedral angles (48 steps of 10 degrees) was explored using a relaxed potential energy surface (RPES) scan rotating between the two stereoisomers. For the RPES scans the basis was increased to 6-31g(d,p) in order to better capture interactions between the polar amine and hydroxyl groups.

C.7. Conclusion on atropisomers of DHBT

5-HT dimer, 5,5'-dihydroxy-4,4'-bitryptamine (DHBT), is potentially neurotoxic and contributes to neurodegenerative diseases. However, no further work has appeared on preparative scale synthesis of DHBT. This dissertation described a preparative scale synthesis of DHBT and studied the atropisomerism of DHBT, which is a type of stereoisomerism and results from sterically hindered rotation about a bond axis. The reaction was performed in methanol induced by Cu^{2+} under oxygen and monitored with ^1H NMR in Methol- d_4 and D_2O or capillary electrophoresis at 214 nm using taurodeoxycholic acid as chiral selector. After the reaction was completed, DHBT was purified by Sephadex LH-20 column chromatography and characterized by NMR and HRMS. The primary amino function of 5-HT is essential for good yield under the experimental conditions. A hypothesis is proposed in which Cu^{2+} ion coordinates to a 5-HT through the amino function, and that coupling occurs in the coordination sphere of the metal. HRMS shows the hydrogen exchange between D_2O and hydrogen of DHBT. Isolated DHBT atropisomers were also resolved using chiral capillary electrophoresis, which is consistent with ^1H NMR spectrum and computational simulation.

Reference

- Bringmann, G., Mortimer, A.J.P., Keller, P.A., Gresser, M.J., Garner, J. and Breuning, M. (2005). Atroposelective synthesis of axially chiral biaryl compounds. *Angew. Chem., Int. Ed.* 34: 5384-5427.
- Brownrigg, T.D., Theisen, C.S., Fibuch, E.E. and Seidler, N.W. (2011). Carnosine protects against the neurotoxic effects of a serotonin-derived melanoid. *Neurochem. Res.* 3: 467-475.
- Christie, G.H. and Kenner, J. (1922). LXXI.-The molecular configurations of polynuclear aromatic compounds. Part I. The resolution of γ -6 : 6[prime or minute]-dinitro- and 4 : 6 : 4[prime or minute] : 6[prime or minute]-tetranitro-diphenic acids into optically active components. *J. Chem. Soc. Trans.*
- Clayden, J., Moran, W.J., Edwards, P.J. and LaPlante, S.R. (2009). The Challenge of atropisomerism in drug discovery. *Angew. Chem., Int. Ed.* 35: 6398-6401.
- Eriksen, N., Martin, G.M. and Benditt, E.P. (1960). Oxidation of the indole nucleus of 5-hydroxytryptamine and the formation of pigments: isolation and partial characterization of a dimer of 5-hydroxytryptamine. *J. Biol. Chem.* 166:2-1667.
- Feringa, B. and Wynberg, H. (1977). Oxidative phenol coupling with cupric-amine complexes. *Tetrahedron Lett.* 50: 4447-4450.
- Feringa, B. and Wynberg, H. (1978). Biomimetic asymmetric oxidative coupling of phenols. *Bioorg. Chem.* 4: 397-408.
- Hassan, J., Sévignon, M., Gozzi, C., Schulz, E. and Lemaire, M. (2002). Aryl-aryl bond formation one century after the discovery of the Ullmann reaction. *Chem. Rev.* 5: 1359-1470.
- Heath, M.J.S. and Hen, R. (1995). Serotonin Receptors - Genetic Insights into Serotonin Function. *Curr. Biol.* 9: 997-999.
- Huether, G., Fettkotter, I., Keilhoff, G. and Wolf, G. (1997). Serotonin acts as a radical scavenger and is oxidized to a dimer during the respiratory burst of activated microglia. *J. Neurochem.* 5: 2096-2101.
- Huether, G., Reimer, A., Schmidt, F., Schuff-Werner, P. and Brudny, M.M. (1990). Oxidation of the indole nucleus of 5-hydroxytryptamine and formation of dimers in the presence of peroxidase and H₂O₂. *Amine Oxidases and Their Impact on Neurobiology.* P. Riederer and M. H. Youdim, Springer Vienna. 32: 249-257.
- Jones, C.E., Underwood, C.K., Coulson, E.J. and Taylor, P.J. (2007). Copper induced oxidation of serotonin: analysis of products and toxicity. *J. Neurochem.* 4: 1035-1043.
- LaPlante, S.R., Edwards, P.J., Fader, L.D., Jakalian, A. and Hucke, O. (2011). Revealing atropisomer axial chirality in drug discovery. *Chem. Med. Chem.* 3: 505-513.

LaPlante, S.R., Fader, L.D., Fandrick, K.R., Fandrick, D.R., Hucke, O., Kemper, R., Miller, S.P.F. and Edwards, P.J. (2011). Assessing atropisomer axial chirality in drug discovery and development. *J. Med. Chem.* 20: 7005-7022.

Lesch, K.-P., Bengel, D., Heils, A., Sabol, S.Z., Greenberg, B.D., Petri, S., Benjamin, J., Müller, C.R., Hamer, D.H. and Murphy, D.L. (1996). Association of anxiety-related traits with a polymorphism in the serotonin transporter gene regulatory region. *Science* 272: 1527-1531.

Noji, M., Nakajima, M. and Koga, K. (1994). A new catalytic system for aerobic oxidative coupling of 2-naphthol derivatives by the use of CuCl-amine complex: A practical synthesis of binaphthol derivatives. *Tetrahedron Lett.* 43: 7983-7984.

Oki, M. (1983). Recent advances in atropisomerism. *Top. Stereochem.* 1-81.

Roussel, C., Vanthuyne, N., Shineva, N., Boucekara, M. and Djafri, A. (2008). Atropisomerism in the 2-arylimino-N-(2-aryl)-thiazoline series. *Arkivoc* 28-41.

Sambeth, A., Riedel, W., Tillie, D., Blokland, A., Postma, A. and Schmitt, J. (2009). Memory impairments in humans after acute tryptophan depletion using a novel gelatin-based protein drink. *J. Psychopharmacology* 1: 56-64.

Smrčina, M., Lorenc, M., Hanuš, V. and Kočovský, P. (1991). A facile synthesis of 2-amino-2'-hydroxyl-1,1'-binaphthyl and 2,2'-diamino-1,1'-binaphthyl by oxidative coupling using copper (II) chloride. *Synlett* 4: 231-232.

Tobler, E., Lammerhofer, M., Mancini, G. and Lindner, W. (2001). On-column deracemization of an atropisomeric biphenyl by quinine-based stationary phase and determination of rotational energy barrier by enantioselective stopped-flow HPLC and CEC. *Chirality* 10: 641-647.

Walther, D.J., Peter, J.U., Bashammakh, S., Hortnagl, H., Voits, M., Fink, H. and Bader, M. (2003). Synthesis of serotonin by a second tryptophan hydroxylase isoform. *Science* 299: 76-76.

Woolley, D.W. and Shaw, E. (1954). A biochemical and pharmacological suggestion about certain mental disorders. *Proc. Natl. Acad. Sci. U. S. A.* 4: 228-231.

Wrona, M.Z. and Dryhurst, G. (1987). Oxidation chemistry of 5-hydroxytryptamine. 1. mechanism and products formed at micromolar concentrations. *J. Org. Chem.* 52: 2817-2825.

Wrona, M.Z. and Dryhurst, G. (1990). Electrochemical oxidation of 5-hydroxytryptamine in aqueous-solution at physiological Ph. *Bioorg. Chem.* 3: 291-317.

Wrona, M.Z. and Dryhurst, G. (1998). Oxidation of serotonin by superoxide radical: Implications to neurodegenerative brain disorders. *Chem. Res. Toxicol.* 6: 639-650.

Wrona, M.Z., Goyal, R.N., Turk, D.J., Blank, C.L. and Dryhurst, G. (1992). 5,5'-Dihydroxy-4,4'-bitryptamine - a potentially aberrant, neurotoxic metabolite of serotonin. *J. Neurochem.* 58: 1392-1398.